SYNCHRONIZED MEASUREMENTS AND APPLICATIONS DURING POWER SYSTEM DYNAMICS

Dawei Fan

Dissertation submitted to the faculty of the Virginia Polytechnic Institute and State University in partial fulfillment of the requirements for the degree of

Doctor of Philosophy
In
Electrical Engineering

Dr. Virgilio Centeno, Chair
Dr. Arun Phadke
Dr. Yilu Liu
Dr. Richard Conners
Dr. Werner Kohler

Feb. 1st, 2008
Blacksburg, Virginia

Keywords: synchronized measurement, frequency disturbance, dynamic condition, wide area measurement, out-of-step protection.

SYNCHRONIZED MEASUREMENTS AND APPLICATIONS DURING POWER SYSTEM DYNAMICS

by

Dawei Fan

(Abstract)

Synchronized phasor measurements during dynamics tend to be affected by prevailing system frequency. Some major blackouts in power systems are indeed featured with very large frequency disturbance. Quantitative study done in this dissertation shows that small frequency disturbance may lead to measurement errors, and large frequency disturbance may lead to wrong measurements as well as catastrophic results if applied in system protection and control. The purpose of this dissertation is to bring up this issue, point to some possible solutions and application examples.

A synchronized frequency measurement method, which has better dynamic performance, is proposed in this dissertation. Based on this accurate synchronized frequency, a phasor compensation algorithm is proposed to correct the errors due to frequency disturbance in legacy PMUs or as alternative frequency tracking algorithm in new PMUs. Phasor positioning and unbalance issues are also investigated in this dissertation. With these improved synchronized measurements, wide area protection and control can be achieved with higher reliability. As an application example, traditional preset out-of-step protection could be replaced by the adaptive out-of-step protection using wide area measurements. Real-time swing curve and real-time EEAC based adaptive out-of-step protection schemes are developed respectively in this dissertation. Numerical Simulations are performed for validation of the proposed concepts.

Acknowledgements

The completion of this dissertation is due in large part to Dr. Virgilio Centeno's guidance, encouragement and financial support during my PhD at Virginia Tech. Dr. Arun Phadke, Dr. Yilu Liu, Dr. Richard Conners, and Dr. Werner Kohler served as my PhD committee members and shared with me many of their insightful views. Likewise, Dr. Wei Li shared much of his time and thought in EEAC. Each of them is to be greatly thanked for giving me an open door and open mind.

Special thanks are given to my parents, sister and wife for their consistent consideration, support, and understanding. With you, I am able to overcome the rough patch and move forward.

Contents

List of Figures

List of Tables

Chapter 1
Introduction

Electric power is essential to modern society. Economic prosperity, national security, and standard of living depend on reliable electric power systems. As the environment becomes more regulated and energy becomes more deregulated, power systems are being operated closer to the stability limit nowadays. Environmental regulation requires a long and stringent process to site new generation, transmission and distribution. Increases in open access transactions, heavy loading, weak connections, hidden failure in protection, and other unexpected events may cause the system to lose balance and even lead to catastrophic failures. “Unless substantial amounts of capital are invested over the next several decades in new generation, transmission, and distribution facilities, service quality will degrade and costs will go up. These investments will involve new technologies that improve the existing electric system and possibly advanced technologies that could revolutionize the electric grid.” [1]

Time-synchronized measurement is thought to be one of such revolutionary technologies in power systems. Power systems are the largest manmade dynamic systems. They are highly nonlinear and involve complicated electromagnetic and electromechanical phenomena. To operate the systems reliably and economically, system conditions, as reflected on voltage phasors, have to be monitored. Traditionally, static state estimation is used to evaluate the steady-state conditions from power and voltage magnitude measurements. However, for dynamic applications, these measurements are time-skewed without a common time reference. With the development of microcomputer, synchronizing technology and communication, measurements can be made with a common time reference, usually GPS clock. As such, the precise comparison of two or more quantities is possible in time. These comparisons can be directly used to assess system conditions accurately, and improve system operation, control and planning. Currently applications of time-synchronized measurements are still not yet widely

investigated and implemented. It is estimated that increasing use of synchronized measurements, as promoted by the Eastern Interconnection Phasor Projects (EIPP) now known as the North American Synchrophasor Initiative (NASPI), and other initiatives in Department of Energy (DOE), will lead to increasing reliability and efficiency for power systems.

1.1 Review of Synchronized Measurements and Applications

Synchronized measurements are obtained from phasor measurement units (PMUs). Figure 1.1 shows the typical block diagram of PMUs. The power system voltage and current signals are converted to standard secondary levels by voltage and current transformers, and properly isolated and filtered by signal conditioning units. Synchronization can be achieved with equal results by two methods. a) The sampling pulses are synchronized to a GPS receiver guaranteeing that samples are taken at the same time in all devices with an error dictated by the ability of the sampling clock to phase lock to the 1PPS of a GPS receiver. b) The samples are time tagged precisely with respect to the GPS 1PPS and local sub-second time signals followed by the correct processing of the data samples and time tagging of the output data. Properly implemented, both of these methods produce estimated phasors that can be used for common synchronized data applications.

The following subsections review synchronized measurements and applications in both steady state and dynamic state.

1.1.1 Steady State

Steady state is a condition defined here as one where the frequency, magnitude, and phase angle of the observed signal are constant [2] . PMU algorithms, standards and applications almost all begin with the steady state.

Discrete Fourier transform (DFT) has found popular applications in digital relaying as well as phasor measurement. The first experimental PMU, based on DFT, was

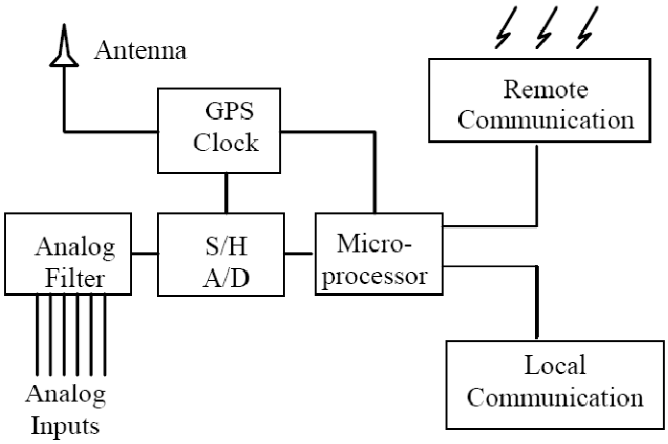

Figure 1.1 Block diagram of PMUs

developed and tested at Virginia Tech in 1988, and then was followed by the first commercial unit in 1991 and more commercial PMUs thereafter. Figure 1.2 shows the important events in PMU history. The first PMU and the first commercial PMU came up before the first standard, the IEEE Std. 1344-1995 Standard for Synchrophasors for Power Systems. These "Old PMUs" defined their phasors in terms of the nominal-frequency component of the signal. The phasor, $\mathbf{X} = X_m(f)e^{j\phi}$, measured by these units represents the magnitude and angle of the nominal frequency component (60 or 50 Hz) of an input signal $x(t) = X_m\cos(\omega t + \phi)$. In these PMUs as the system frequency deviates from the nominal, the nominal-frequency based DFT and fixed samples will lead to errors, so the measured phase angles and magnitudes cannot reflect the actual values. In 1995 the first standard for synchrophasor IEEE Std. 1344 was established, and has been evolving since then. The latest version is the IEEE Std. C37.118-2005, in which the phasors, $\mathbf{X} = X_m e^{j\phi}$, represent the actual magnitude and angle of the input signal $x(t) = X_m\cos(2\pi ft + \phi)$ as long as the system frequency is within a given range.

Figure 1.2 Timeline of PMU and standard development

Even though PMU standard have been revised several times for a period of more than ten years, the synchronized measurements in steady state are well established and standardized. The major steady-state applications include real-time monitoring, visualization, and state estimation. With time-synchronized measurements, dedicated fiber optic communication, and 2D/3D visualization, system operators could have better situation awareness. Likewise, synchronized measurements will lead to improved state estimation. Pure phasor measurements enable linear state estimation or state measurement. Combined with traditional P, Q and V measurements, a hybrid nonlinear state estimation is possible with improved accuracy. In more recent work, an alternative approach has been proposed where it is possible to retain the traditional state estimator software intact, and add the phasor measurements in a linear post-processing step. [4] [5] [6]

1.1.2 Dynamic State

In a dynamic state, signal frequency, magnitude, and phase angle are not constant. It is still quite an issue to implement synchronized measurements accurately under dynamic conditions. The IEEE C37.118-2005 Standard for Synchrophasors in Power Systems addresses the phasor definition and accuracy requirements in terms of Total Vector Error (TVE) for steady state conditions. However, the standard does not do so for the dynamic state. Some recommended dynamic tests are given in the annex of the standard. The major difficulty is that PMU algorithms, such as DFT, assume steady state or quasi steady state. The accuracy of synchronized measurement may still be acceptable for a slow dynamic process. But for those significant disturbances in power systems, using DFT to do synchronized measurement has to be done with care. Two aspects should be considered.

a) Window size. Signals in power systems normally contain noise due to the complicated electromagnetic interference. A/D conversion will introduce quantization errors as well. So the computed phasor has an uncertainty associated with them, which can be depicted as shown in Figure 1.3 [4] **.** The circle of uncertainty is inversely proportional to the square root of the data window [4]. In this regard, the longer data window for phasor computing is beneficial. But this long window may deteriorate the

dynamic performance as shown in Figure 1.4. For a frequency, magnitude or phase jump, the shorter window can minimize the affected measurements and follow the dynamics more quickly. Therefore, a balance has to be made between the pros and cons. Appropriate filters and high-resolution A/D are helpful to limit the adverse effect of noise. Thus, a short window, such as one-cycle window, could achieve both high certainty and excellent dynamic performance.

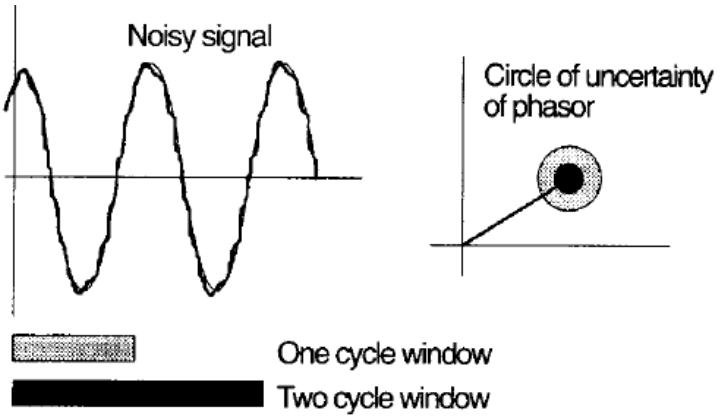

Figure 1.3 Data window and uncertainty in phasor estimation

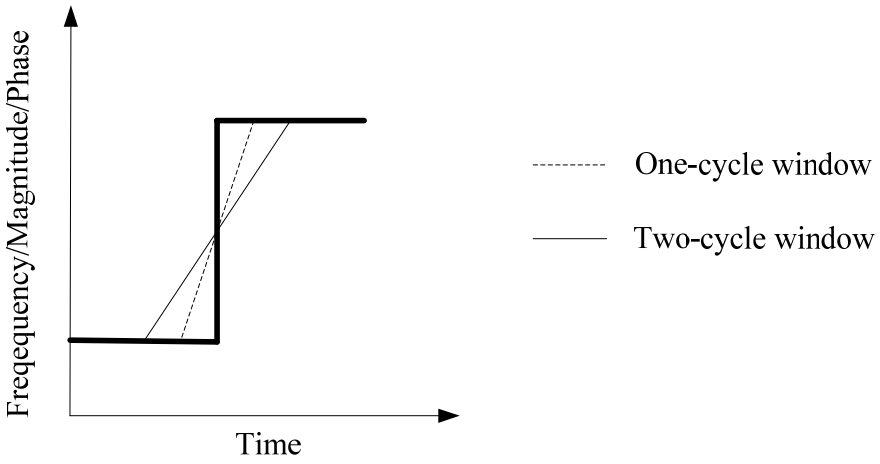

Figure 1.4 Data window and step response in phasor estimation

b) DFT leakage effect [7] [8] [9] [10] . This problem arises because of limited length of the signal or inappropriate sampling frequency which is not integer multiples of the fundamental component. The net effect is a distortion of the spectrum. There is a

spreading or leakage of the spectral components away from the correct frequency, resulting in an undesirable modification of the total spectrum. The sampling frequency can be designed to be integer multiples of the nominal frequency in power systems. But power system dynamics involves a great deal of load generation disturbances as well as frequency disturbances. How to deal with the variable frequency, how to minimize or eliminate the leakage effect, and how to obtain accurate synchronized measurements during dynamics remain to be under investigation.

Though the synchronized measurements in dynamic state have not been standardized yet, the applications in dynamic state are thought to be the most valuable. Simultaneous measurement sets derived from synchronized phasors provide a vastly improved method for tracking power system dynamic phenomena for improved power system monitoring, protection, operation, and control [11] - [28] . Synchronized measurements provide operators a system-wide dynamic picture, and these dynamic data could be used for system model validation in transient stability studies. Synchronized measurements provide the first real possibility of providing a dynamic state estimator. By maintaining a continuous stream of phasor data from the substations to the control center, a state vector that can follow the system dynamics can be constructed. With synchronized measurements, real-time monitoring and prediction of stability is possible, which offer a unique opportunity of improving the response of protection and control systems to an evolving power swing. The high speed synchronized measurements offer an improved feed-back control, such as controlling power system stabilizer (PSS), HVDC terminals and FACTS devices. Adaptive relaying and system integrity protective schemes (SIPS) will greatly benefit from the synchronized measurements. Besides, synchronized measurements can also be used to improve the performance of under frequency load shedding, fault location, and so on.

1.2 Motivation and Objective

The current trend of increased use of wide area measurement devices is expected to result in a more efficient and reliable operation in power systems. As stated before, synchronized measurements and applications in steady state are relatively mature.

However, synchronized measurements in dynamic state remain unstandardized though there is an increasing demand for dynamic applications. “The problem with including transient performance requirements comes in stating requirements that are measurable, can be uniformly applied, and are not unduly restrictive on implementations. This is still an emerging technology and applying anticipated performance requirements could hamper development. Harmonizing a common set of dynamic performance requirements should be undertaken once the range of implementations and measurement applications has been more fully explored. At this time, dynamic performance under transient conditions should be specified and verified by the users to meet their application needs.” [2]

The motivation of this work arises with the fact that synchronized phasor measurements during dynamic conditions tend to be affected by prevailing system frequency. Some major blackouts in power systems have shown that very large frequency variations are possible. Quantitative study presented in this dissertation shows that small frequency disturbance may lead to measurement errors, and large frequency disturbance may lead to wrong measurements as well as catastrophic results if applied in system protection and control. The objective of this work is to clearly bring up this issue, analyze it, suggest solutions and illustrate them with application examples. It is also the author’s hope that this work could be beneficial to the standardization and application of synchronized measurements in dynamic conditions.

1.3 Outline of the Dissertation

This dissertation is organized as follows.

Chapter 1, Introduction, reviews the synchronized measurements and applications in both steady and dynamic states, presents the motivation and objective of this dissertation as well as the outline.

Chapter 2, Synchronized Frequency Measurements under Dynamics, reviews frequency measurement techniques, and then proposes a synchronized frequency measurement method, which has better dynamic performance. The least-square application in frequency estimation is also investigated.

Chapter 3, Synchronized Phasor Measurements under Dynamics, proposes a phasor compensation algorithm based on accurate synchronized frequency, to correct the errors due to frequency disturbance. Phasor positioning and unbalance issues are also investigated in details.

Chapter 4, General Applications, classifies the application scenarios of synchronized measurements under dynamics. Two scenarios for applications are introduced and analyzed. One scenario is where small frequency disturbance happens. The other one is where big frequency disturbance happens.

Chapter 5, Adaptive Out-of-Step Protection Using Wide Area Measurements, takes out-of-step protection as an example to demonstrate how synchronized measurements help realize adaptive out-of-step protection. Real-time swing curve and real-time extended equal area criteria (EEAC) based adaptive out-of-step protection schemes are developed respectively in this dissertation. Numerical simulations are performed for validation of the proposed concepts.

Chapter 6, Conclusions and Future Work, summarizes the conclusions of this work. A brief recommendation of the future work is also included.

Chapter 2
Synchronized Frequency Measurements under Dynamics

Frequency is an important parameter for the monitoring and control of power systems. It is well known that any unbalance between generation and load is faithfully reflected by a change in the operating frequency. In well regulated systems any significant variation from nominal frequency jeopardizes the efficient and safe operation of the system forcing generator governors, under/over frequency relays, and other devices to take corrective actions intended to bring the frequency back to the nominal values as soon as possible. The current trend of increased use of wide area measurement devices is expected to result in a more efficient and reliable use of these corrective actions for system-wide dynamic conditions. This type of applications requires accurate phasor and frequency information from multiple synchronized devices to provide a valid picture of the dynamic behavior of the system.

The IEEE C37.118-2005 Standard for Synchrophasors in Power Systems addresses the phasor definition and accuracy requirements in terms of Total Vector Error (TVE) for steady state conditions [2] . To accurately measure the phasors under rapid frequency changes, the standard annex C assumes that the PMU has accurate frequency estimation at the center of the window, but the standard does not define accuracy requirements for the frequency as it does for phasors. This chapter reviews the frequency measurement techniques in power systems, and then proposes a method to accurately measure frequency under frequency-dynamic conditions. One of the applications is to accurately measure that frequency at the center of the window. Furthermore, the lease-square application in frequency estimation is also investigated.

2.1 Frequency Measurements in Power Systems

Various techniques have been developed to measure power system frequency, including modified zero crossing technique [32] , level crossing technique [33] , least square technique [34] [35] , Kalman filter technique [36] [37] , leakage effect technique [38] , and phasor-based technique [39] [40] [41] . These algorithms are mostly developed based on the fixed-frequency model, and mainly used to measure the steady-state frequency. For use in wide area application dynamic frequency or instantaneous frequency is more useful to describe the behavior of the system. It is commonly accepted in signal processing that instantaneous frequency is defined as the derivative of the phase angles of the signals [42] . For a frequency modulated signal $x(t) = X\cos[\phi(t)]$, where X represents the magnitude and ϕ represents the cumulative phase angles, instantaneous frequency is calculated as $f(t) = \frac{1}{2\pi}\frac{d\phi}{dt}$. Reference [43] proposes a phase control loop to measure the dynamic frequency, and reference [32] uses polynomial fitting combined with phasor-based technique to get instantaneous frequency.

Of the different techniques used to measure frequency the phasor-based technique is much closer to the definition of instantaneous frequency. The basic idea in reference [39] [40] [41] is to calculate the positive sequence voltage phasor for a balanced system operating at off-nominal frequency, while still use the nominal frequency based DFT and samples. Though the calculated phasor is not accurate, it is found that the phase angle change in this phasor is a function of steady-state frequency deviation. All the phase angle changes in this chapter mean the difference of phase angles of the same signal at different times. Therefore, actual frequency can be estimated by the inaccurate phasors.

2.2 Synchronized Frequency Measurements

This section analyzes the phasor-based frequency measurement algorithm considering the effect of dynamic frequency on the algorithm. A new method is presented that improves the dynamic performance of the phasor-based frequency measurement and

synchronizes it to the correct time tag. This time-tagged instantaneous frequency could be called synchronized frequency.

In the following subsections, first a theoretical analysis of the phasor-based frequency measurement technique considering the effect of dynamically changing frequency is provided to serve as the basis of the proposed method, and then simulation results are shown to verify the effectiveness of the proposed method. Finally, a laboratory experiment is described and comparisons are made between the frequency measured by the proposed method and the frequency given by two synchrophasor standard compliant commercial PMUs.

2.2.1 Theoretical Analysis

This subsection analyzes what the nominal frequency based DFT measures when the frequency is changing, i.e., to get a mathematical expression of the measured phasors for a given changing frequency which is assumed linear within each phasor and frequency calculation window. By checking these calculated phasors it is expected to find a relationship between the phase angle changes and dynamic frequency. All the phasors calculated here are for frequency measurement, and cannot be reported as synchrophasors directly. Once the frequency is measured accurately, the actual synchrophasors can be obtained, for example, by doing frequency based compensation.

It is an issue where to put the calculated phasors within the data window. We put the phasor at the beginning of the data window initially. After this we will expand our analysis by putting the phasors anywhere else within the window. So we'll cover all possible cases.

Now consider three phase balanced inputs at angular frequency ω. The three time functions for the phase quantities are given by

$$x_a(t) = X_m \cos(\omega t + \varphi) = \sqrt{2}\,\mathrm{Re}\left(\mathbf{X}e^{j\omega t}\right) \tag{2.1}$$

$$x_b(t) = X_m \cos(\omega t + \varphi - 2\pi/3) = \sqrt{2}\,\mathrm{Re}\left(\mathbf{X}\alpha^2 e^{j\omega t}\right) \tag{2.2}$$

$$x_c(t) = X_m \cos(\omega t + \varphi - 4\pi/3) = \sqrt{2}\,\mathrm{Re}\left(\mathbf{X}\alpha e^{j\omega t}\right) \tag{2.3}$$

where $\mathbf{X} = \left(X_m/\sqrt{2}\right)e^{j\varphi}$, $\alpha = e^{j\frac{2\pi}{3}}$.

If the angular frequency is no longer a constant, the three time functions for the phase quantities are given by

$$x_a(t) = \sqrt{2}\,\mathrm{Re}\left(\mathbf{X}e^{j\int_0^t \omega dt}\right) \tag{2.4}$$

$$x_b(t) = \sqrt{2}\,\mathrm{Re}\left(\mathbf{X}\alpha^2 e^{j\int_0^t \omega dt}\right) \tag{2.5}$$

$$x_c(t) = \sqrt{2}\,\mathrm{Re}\left(\mathbf{X}\alpha e^{j\int_0^t \omega dt}\right). \tag{2.6}$$

The above phase quantities (2.4), (2.5) and (2.6) can be expressed with the help of Euler's formula as follows

$$x_a(t) = \sqrt{2}\frac{1}{2}\left(\mathbf{X}e^{j\int_0^t \omega dt} + \mathbf{X}^* e^{-j\int_0^t \omega dt}\right) \tag{2.7}$$

$$x_b(t) = \sqrt{2}\frac{1}{2}\left(\mathbf{X}\alpha^2 e^{j\int_0^t \omega dt} + \mathbf{X}^*\alpha e^{-j\int_0^t \omega dt}\right) \tag{2.8}$$

$$x_c(t) = \sqrt{2}\frac{1}{2}\left(\mathbf{X}\alpha e^{j\int_0^t \omega dt} + \mathbf{X}^*\alpha^2 e^{-j\int_0^t \omega dt}\right). \tag{2.9}$$

Assume the above phase quantities (2.7), (2.8) and (2.9) are sampled N (integer number) times per full cycle of the nominal frequency waveform. In the following formula deduction, we always use this nominal frequency based samples. Nominal frequency f_N, angular frequency $\omega_N = 2\pi f_N$, and sampling period $\Delta t = \frac{1}{Nf_N} = \frac{2\pi}{N\omega_N}$. Then the discrete sample sets are as follows

$$x_{a,k} = \sqrt{2}\frac{1}{2}\left(\mathbf{X}e^{j\int_0^{k\Delta t} \omega dt} + \mathbf{X}^* e^{-j\int_0^{k\Delta t} \omega dt}\right) \tag{2.10}$$

$$x_{b,k} = \sqrt{2}\frac{1}{2}\left(\mathbf{X}\alpha^2 e^{j\int_0^{k\Delta t} \omega dt} + \mathbf{X}^*\alpha e^{-j\int_0^{k\Delta t} \omega dt}\right) \tag{2.11}$$

$$x_{c,k} = \sqrt{2}\frac{1}{2}\left(\mathbf{X}\alpha e^{j\int_0^{k\Delta t} \omega dt} + \mathbf{X}^*\alpha^2 e^{-j\int_0^{k\Delta t} \omega dt}\right) \tag{2.12}$$

where $k = 0, 1, 2, \cdots\cdots$.

Now we can calculate the phasor at the r^{th} sample with DFT algorithm for the data window starting from the r^{th} sample. The calculated phasors are put at the first sample of the windows, so we have

$$\mathbf{X}_a^{(r)} = \frac{1}{\sqrt{2}}\frac{2}{N}\sum_{k=r}^{r+N-1} x_{a,k} e^{-jk\omega_N \Delta t}$$
$$= \frac{1}{N}\sum_{k=r}^{r+N-1}\left(\mathbf{X}e^{j\int_0^{k\Delta t}\omega dt} + \mathbf{X}^* e^{-j\int_0^{k\Delta t}\omega dt}\right)e^{-jk\omega_N \Delta t} \tag{2.13}$$

$$\mathbf{X}_b^{(r)} = \frac{1}{\sqrt{2}}\frac{2}{N}\sum_{k=r}^{r+N-1} x_{b,k} e^{-jk\omega_N \Delta t}$$
$$= \frac{1}{N}\sum_{k=r}^{r+N-1}\left(\mathbf{X}\alpha^2 e^{j\int_0^{k\Delta t}\omega dt} + \mathbf{X}^* \alpha e^{-j\int_0^{k\Delta t}\omega dt}\right)e^{-jk\omega_N \Delta t} \tag{2.14}$$

$$\mathbf{X}_c^{(r)} = \frac{1}{\sqrt{2}}\frac{2}{N}\sum_{k=r}^{r+N-1} x_{c,k} e^{-jk\omega_N \Delta t}$$
$$= \frac{1}{N}\sum_{k=r}^{r+N-1}\left(\mathbf{X}\alpha e^{j\int_0^{k\Delta t}\omega dt} + \mathbf{X}^* \alpha^2 e^{-j\int_0^{k\Delta t}\omega dt}\right)e^{-jk\omega_N \Delta t} . \tag{2.15}$$

Equation (2.13), (2.14), and (2.15) use the nominal frequency based DFT and samples to calculate the phasors as done in reference [41] . Of course, these phasors cannot reflect the actual values unless actual frequency based DFT and samples are used. Besides, the phase angles are referenced to a phasor rotating at nominal angular frequency since we are not doing summation from 0 to $(N-1)$. This makes the phase angle changes divided by time to be a function of frequency deviation instead of frequency, which is helpful to reduce the calculation errors in real applications. Then the positive sequence component is calculated as

$$\mathbf{X}_1^{(r)} = \frac{1}{3}\left[\mathbf{X}_a^{(r)} + \alpha\mathbf{X}_b^{(r)} + \alpha^2\mathbf{X}_c^{(r)}\right]$$
$$= \frac{1}{3N}\sum_{k=r}^{r+N-1}\left[\begin{array}{l}\mathbf{X}e^{j\int_0^{k\Delta t}\omega dt}(1+\alpha\alpha^2+\alpha\alpha^2) \\ +\mathbf{X}^* e^{-j\int_0^{k\Delta t}\omega dt}(1+\alpha^2+\alpha^2\alpha^2)\end{array}\right]e^{-jk\omega_N \Delta t} \tag{2.16}$$

Recognizing that $1+\alpha\alpha^2+\alpha\alpha^2 = 3$ and $1+\alpha^2+\alpha^2\alpha^2 = 0$, equation (2.16) can be simplified as

$$\mathbf{X}_1^{(r)} = \frac{1}{N}\sum_{k=r}^{r+N-1}\mathbf{X}e^{j\int_0^{k\Delta t}\omega dt}e^{-jk\omega_N \Delta t} \tag{2.17}$$

Now the frequency needs to be defined as a function of time in order to perform the integration. For a linearized frequency within the phasor and frequency calculation

window, define ω_r as the instantaneous angular frequency at the r^{th} sampling point. Then $\omega_r = \omega_0 + r\omega_d = \omega_0 + \frac{\omega_d}{\Delta t}t$, where ω_0 is the instantaneous angular frequency at the initial sampling point, ω_d is the frequency increment between two consecutive samples, and $(\omega_d / \Delta t)$ is the rate of change of frequency. Thus

$$\begin{aligned}\int_0^{k\Delta t} \omega dt &= \int_0^{k\Delta t} (\omega_0 + \frac{\omega_d}{\Delta t}t)dt = \int_0^{k\Delta t} \omega_0 dt + \int_0^{k\Delta t} \frac{\omega_d}{\Delta t}t dt \\ &= k\omega_0\Delta t + \frac{\omega_d}{\Delta t}\frac{(k\Delta t)^2}{2} = k\omega_0\Delta t + \frac{k^2}{2}\omega_d\Delta t\end{aligned} \tag{2.18}$$

Substituting equation (2.18) into equation (2.17), and expressing frequency deviation as $\Delta\omega_r = \omega_r - \omega_N$, we obtain

$$\begin{aligned}\mathbf{X}_1^{(r)} &= \frac{1}{N}\sum_{k=r}^{r+N-1} \mathbf{X} e^{j(k\omega_0\Delta t + \frac{k^2}{2}\omega_d\Delta t)} e^{-jk\omega_N\Delta t} \\ &= \frac{1}{N}\sum_{k=r}^{r+N-1} \mathbf{X} e^{j\left[k(\omega_0-\omega_N)\Delta t + \frac{k^2}{2}\omega_d\Delta t\right]} \\ &= \frac{1}{N}\sum_{k=r}^{r+N-1} \mathbf{X} e^{j(k\Delta\omega_0\Delta t + \frac{k^2}{2}\omega_d\Delta t)} \\ &= \frac{\mathbf{X}}{N}\sum_{k=r}^{r+N-1} Z\end{aligned} \tag{2.19}$$

where $Z = e^{j(k\Delta\omega_0\Delta t + \frac{k^2}{2}\omega_d\Delta t)}$.

When ω_d is zero, equation (2.19) can be simplified using geometric series, which is the basis of the steady-state frequency measurement. But when ω_d is non-zero, equation (2.19) has to be simplified to a single phasor expression for ease of analysis. Linearization of Z within each phasor calculation window can be used to facilitate the summation. The real and imaginary parts of Z as a function of k are plotted in Figure 2.1 and Figure 2.2 for $f_N = 60$ Hz, $\omega_d = 0.0001$ Hz, N=24, and $\Delta t = 0.000694$. The rate of change of frequency is 0.1441 Hz/s. The two plots shows that the smaller the frequency deviation, the more precise the linearization. Take the first order Taylor series expansion

of Z centered around $k = r + \frac{N-1}{2}$, to obtain

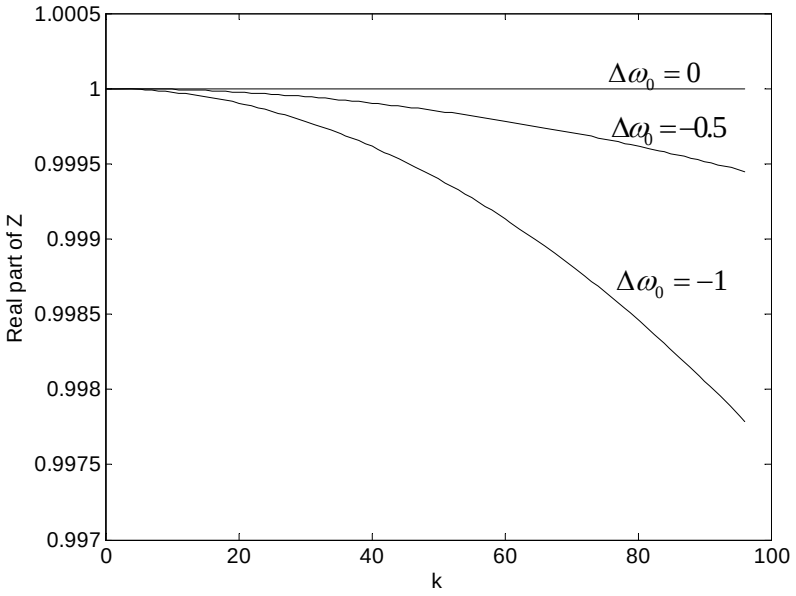

Figure 2.1 Real part of z as a function of k

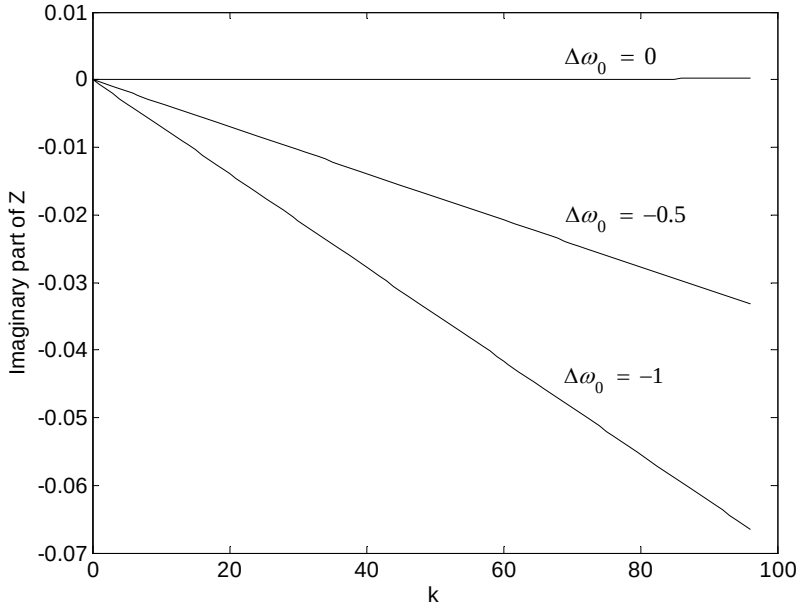

Figure 2.2 Imaginary part of z as a function of k

$$Z \approx e^{j\left[\left(r+\frac{N-1}{2}\right)\Delta\omega_0\Delta t+\frac{\omega_d}{2}\left(r+\frac{N-1}{2}\right)^2\Delta t\right]}+e^{j\left[\left(r+\frac{N-1}{2}\right)\Delta\omega_0\Delta t+\frac{\omega_d}{2}\left(r+\frac{N-1}{2}\right)^2\Delta t\right]}$$

$$*\, j\left[\left(r+\frac{N-1}{2}\right)\Delta\omega_0\Delta t+\frac{\omega_d}{2}\left(r+\frac{N-1}{2}\right)^2\Delta t\right]*\left(k-r-\frac{N-1}{2}\right).$$

Recognizing that $\sum_{k=r}^{r+N-1}\left(k-r-\frac{N-1}{2}\right)=0$, then

$$\sum_{k=r}^{r+N-1} Z = Ne^{j\left[\left(r+\frac{N-1}{2}\right)\Delta\omega_0\Delta t+\frac{\omega_d}{2}\left(r+\frac{N-1}{2}\right)^2\Delta t\right]}. \tag{2.20}$$

So equation (19) can be simplified as

$$\mathbf{X}_1^{(r)} = \mathbf{X}e^{j\left[\left(r+\frac{N-1}{2}\right)\Delta\omega_0\Delta t+\frac{\omega_d}{2}\left(r+\frac{N-1}{2}\right)^2\Delta t\right]}. \tag{2.21}$$

Equation (2.21) shows the calculated phasor at the r^{th} sample given the initial phase φ and linearly changing frequency. For any off-nominal frequency, this phasor rotates on the complex plane if the observation interval is an integer multiple of the nominal power system cycle as stated in the IEEE C37.118-2005. The phase angles at the r^{th} and $(r+M)^{th}$ samples can be calculated using

$$\varphi_1^{(r)} = \varphi+\left(r+\frac{N-1}{2}\right)\Delta\omega_0\Delta t+\frac{\omega_d}{2}(r+\frac{N-1}{2})^2\Delta t$$

$$\varphi_1^{(r+M)} = \varphi+\left(r+M+\frac{N-1}{2}\right)\Delta\omega_0\Delta t+\frac{\omega_d}{2}(r+M+\frac{N-1}{2})^2\Delta t\,.$$

The difference between these two phase angles is

$$\begin{aligned}\varphi_1^{(r+M)}-\varphi_1^{(r)} &= \varphi+\left(r+M+\frac{N-1}{2}\right)\Delta\omega_0\Delta t+\frac{\omega_d}{2}(r+M+\frac{N-1}{2})^2\Delta t\\ &\quad-\left[\varphi+\left(r+\frac{N-1}{2}\right)\Delta\omega_0\Delta t+\frac{\omega_d}{2}(r+\frac{N-1}{2})^2\Delta t\right]\\ &= M\Delta\omega_0\Delta t+\frac{\omega_d}{2}\left[(r+M+\frac{N-1}{2})^2-(r+\frac{N-1}{2})^2\right]\Delta t\\ &= M\Delta\omega_0\Delta t+\frac{\omega_d}{2}M(2r+M+N-1)\Delta t\end{aligned}.$$

So that

$$\begin{aligned}\frac{\varphi_1^{(r+M)}-\varphi_1^{(r)}}{M\Delta t} &= \Delta\omega_0+\frac{\omega_d}{2}(2r+M+N-1)\\ &= \Delta\omega_0+\left(r+\frac{M+N-1}{2}\right)\omega_d\end{aligned} \tag{2.22}$$

Equation (2.22) shows that the phase angle change in the calculated phasor is a function of dynamic frequency. According to the assumption $\omega_r=\omega_0+r\omega_d$, $\Delta\omega_r=\Delta\omega_0+r\omega_d$ also holds. Thus equation (2.22) can be rewritten as

$$\frac{\varphi_1^{(r+M)}-\varphi_1^{(r)}}{M\Delta t}=\Delta\omega_{r+\frac{M+N-1}{2}} \tag{2.23}$$

where N is the size of the data window for phasor calculation, and M is the size of the data window for frequency calculation.

Equation (2.23) shows that the frequency deviation, which is obtained from the calculated phasors at the r^{th} and $(r+M)^{th}$ samples, actually corresponds to the instantaneous frequency deviation at samples $\left(r+\frac{M+N-1}{2}\right)$ or at time $(r+\frac{M+N-1}{2})\Delta t$.

Above analysis assumes that the calculated phasors are put at the first sample of the window. Now consider a more general case and put the calculated phasors at the m th sample of the data window. Then the phasors can be obtained by multiplying equation (2.13), (2.14) and (2.15) by $e^{j2\pi m/N}$, respectively. Similarly, equation (2.21) should also be multiplied by $e^{j2\pi m/N}$ if repeat the formula deduction. Finally, the subtraction of phase angles will cancel this item, and we get the exactly same phase angle changes and frequency deviation as equation (2.22). The derived frequency deviation still represents the one at sample $\left(r+\frac{M+N-1}{2}\right)$ or at time $(r+\frac{M+N-1}{2})\Delta t$.

2.2.2 Proposed method

With the sample series shown in Figure 2.3, equation (2.23) can be rewritten based on the above analysis

$$\frac{\varphi_1^{(D-E)}-\varphi_1^{(A-B)}}{M\Delta t}=\Delta\omega_{r+\frac{M+N-1}{2}}. \tag{2. 24}$$

Normally we make r to be zero. So

$$\frac{\varphi_1^{(D-E)} - \varphi_1^{(A-B)}}{M\Delta t} = \Delta\omega_{\frac{M+N-1}{2}}. \tag{2.25}$$

Equation (2.25) shows that the calculated frequency deviation, which is obtained from the phasors calculated from windows A-B and D-E, actually corresponds to the instantaneous frequency deviation at sample $\left(\frac{M+N-1}{2}\right)$ or at time $\left(\frac{M+N-1}{2}\right)\Delta t$ no matter where the phasors are put within the window. The phasors are calculated with nominal frequency based DFT and samples. Therefore, the phasor-based frequency measurement could be improved to have a better dynamic performance. Though a linearly changing frequency is assumed in the theoretical analysis, non-linearly changing frequency can also be measured accurately since the frequency can be linearized within each data window between sample 0 and sample $(M+N-1)$. This is a reasonable assumption since power system frequency changes very slowly during such a short time period even during dynamic conditions.

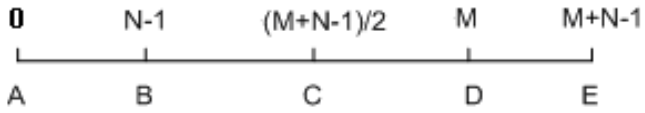

Figure 2.3 Sample series

The proposed method assigns the correct time to the calculated frequency and can be realized based on the traditional method. First, nominal frequency based DFT and samples are used to calculate the phasor $\mathbf{X}_1^0$ with the window from sample 0 to $(N-1)$, and phasor $\mathbf{X}_1^M$ with the window from sample M to $(M+N-1)$; second, equation (2.25) is used to calculate the angular frequency deviation $\Delta\omega_t$ and frequency $f_t = f_N + \frac{\Delta\omega_t}{2\pi}$; third, the calculated frequency is assigned as the instantaneous frequency at sampling point $\left(\frac{M+N-1}{2}\right)$, or at time $\left(\frac{M+N-1}{2}\right)\Delta t$.

The above analysis assumes that automation devices are designed to sample N times per full cycle of the power system nominal frequency. If this condition cannot be satisfied, the proposed method still works well. For example, the power system nominal

frequency is 60Hz, while the devices sample N times per full cycle of 61Hz. Then f_N =61Hz should be used for all the equations. The cost to do so is that calculated phasors are not accurate and have to be corrected even though power systems operate at nominal frequency. Furthermore, to obtain the accurate phasors and frequency, some devices may use re-sampling and iteration, and some others may perform hardware adjustment of sampling periods. The proposed method just uses nominal frequency based DFT and fixed samples to accurately measure frequency. It is fast and easy to implement.

2.2.3 Simulation Verification

In the simulation, take N=24, M=72 and $\frac{M+N-1}{2}=47.5$. For convenience we set $\frac{M+N-1}{2}=47$.

2.2.3.1 Linearly changing frequency

Generate a three-phase signal

$$\begin{cases} v_a(t) = \sqrt{2}V\cos(2\pi ft + \varphi) \\ v_b(t) = \sqrt{2}V\cos(2\pi ft + \varphi - 2\pi/3) \\ v_c(t) = \sqrt{2}V\cos(2\pi ft + \varphi + 2\pi/3) \end{cases}$$

with frequency

$$f = \begin{cases} 60 & 0 \le t < 1 \\ 60 - \dfrac{t-1}{6} & 1 \le t < 7 \\ 59 & 7 \le t \le 8 \end{cases}$$

as shown in Figure 2.4.

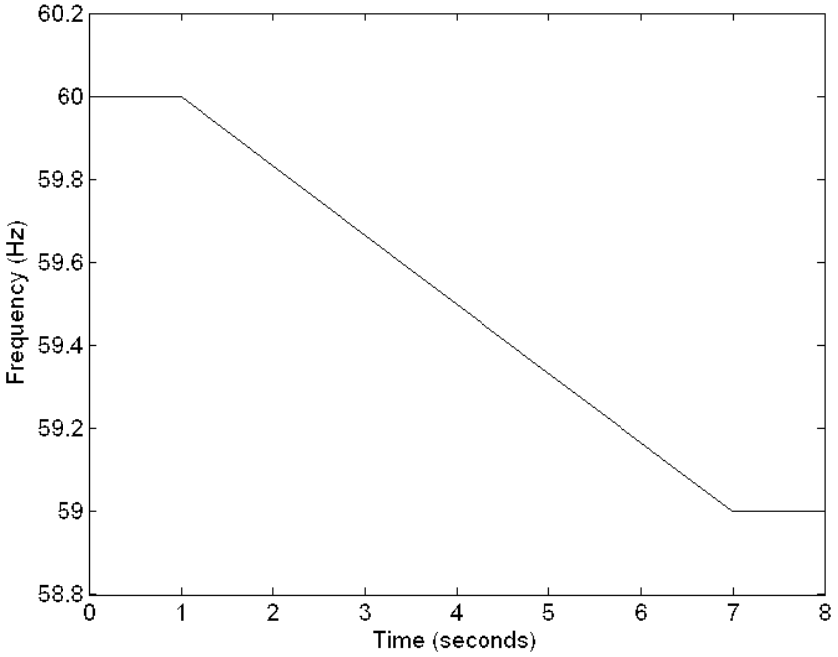

Figure 2.4 Linearly changing frequency

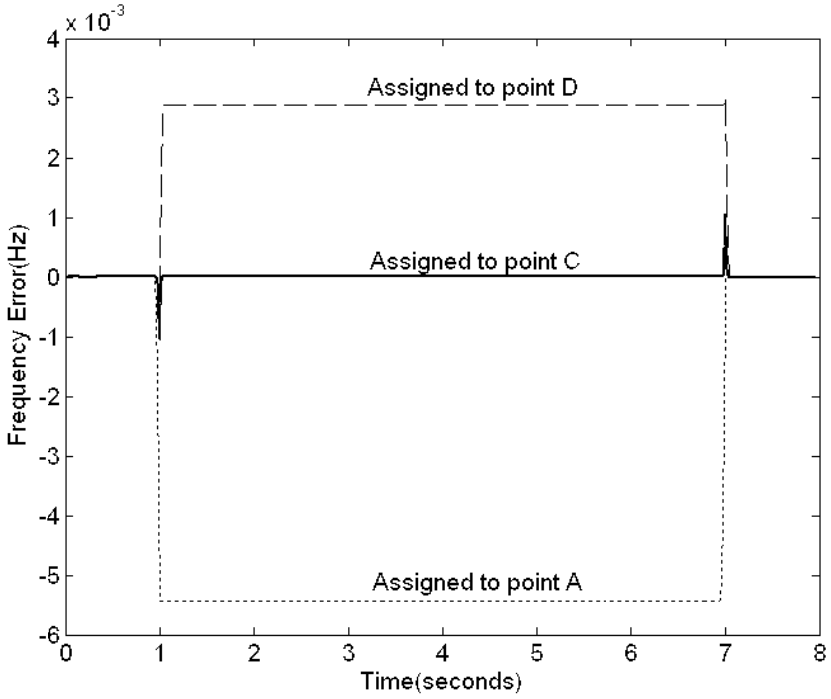

Figure 2.5 Errors between measured and actual frequency when frequency is assigned to different points

The proposed method is applied to the signals to perform the frequency calculations. The frequency is then computed and assigned to the appropriate instant of time which should be time point C as shown in Figure 2.3. Some algorithms not intended for dynamic frequency measurement assume that the frequency is constant within the data window, so the calculated frequency can be assigned to any point within the window. For comparison, we also select time point A and D to assign the calculated frequency, and we refer it as the traditional frequency measurement algorithm for ease of quoting.

As shown in Figure 2.5, traditional phasor-based frequency algorithm has a very good steady-state performance, but it has bigger errors during dynamic conditions. However, the measurement errors of the proposed method are almost zero anywhere except for the spikes where frequency changes very quickly.

2.2.3.2 Non-linearly changing frequency

Generate the similar three-phase signals with frequency

$$f = \begin{cases} 60 & when \quad 0 \le t < 1 \\ 60 + \sin\left[2\pi(t-1)\Big/ 4.8 - \pi\right] & when \quad 1 \le t < 7 \\ 59 & when \quad 7 \le t \le 8 \end{cases}$$

as shown in Figure 2.6.

The proposed method is applied to the signals to perform the frequency calculations. The frequency is then computed and assigned to the appropriate instant of time which should be time point C as shown in Figure 2.3. For comparison, we also select time point A and D to assign the calculated frequency, and we refer it as the traditional frequency measurement algorithm for ease of quoting. As shown in Figure 2.7, traditional phasor-based frequency method has much bigger errors under non-linearly changing frequency. The measurement errors of the proposed method are greatly reduced to almost zero except for spikes where frequency changes dramatically.

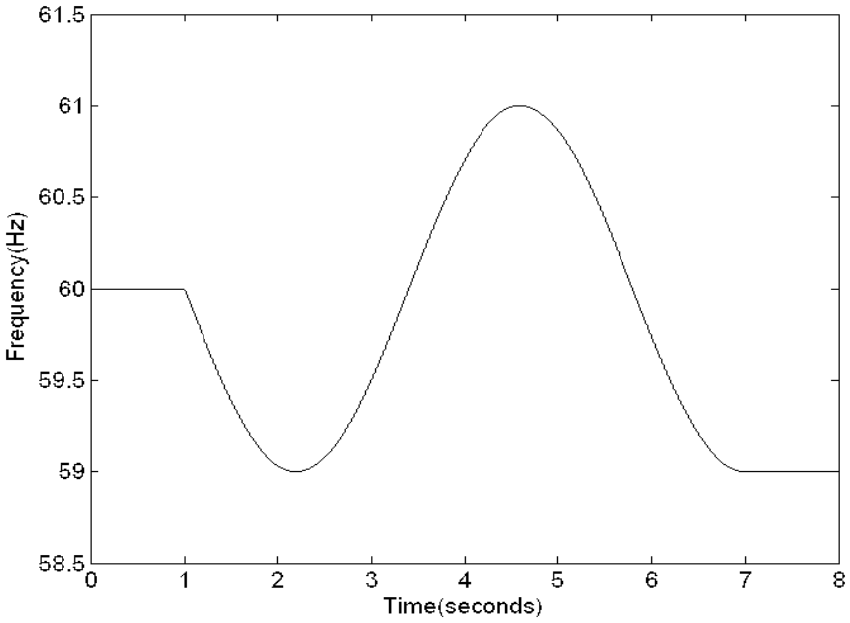

Figure 2.6 Non-linearly changing frequency

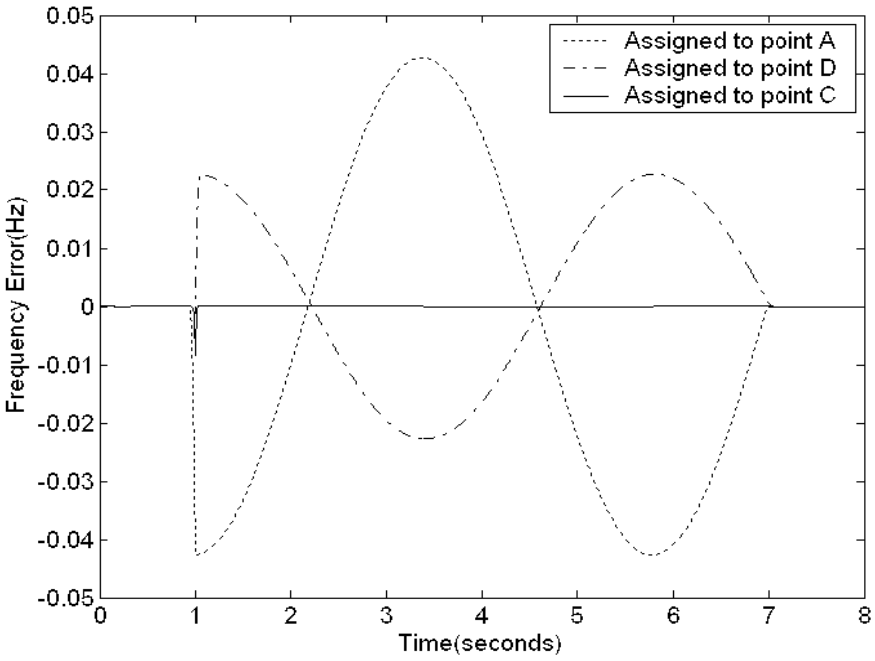

Figure 2.7 Errors between measured and actual frequency when frequency is assigned to different points

2.2.3.3 Frequency Estimation

The main purpose of this part is that the frequency derived from our algorithm in most cases corresponds to a time different than the reporting time of the synchrophasors as required by the IEEE C37.118-2005. Therefore, before attaching the frequency to a time tagged synchrophasors we must estimate the frequency to agree with the reported time tags. For this purpose we introduce a simple linear estimation of the frequency at required time tags based on the derived frequency. It is better to do it in the least square sense, which we will expand in next section. In the following simulations, we assume time point D is the reporting time. To obtain this value, previous calculated frequency and the rate of change of frequency $\omega_d / \Delta t$ are used to estimate the frequency. Figure 2.8 and Figure 2.9 show the estimation errors for linear and non-linearly changing frequency, respectively.

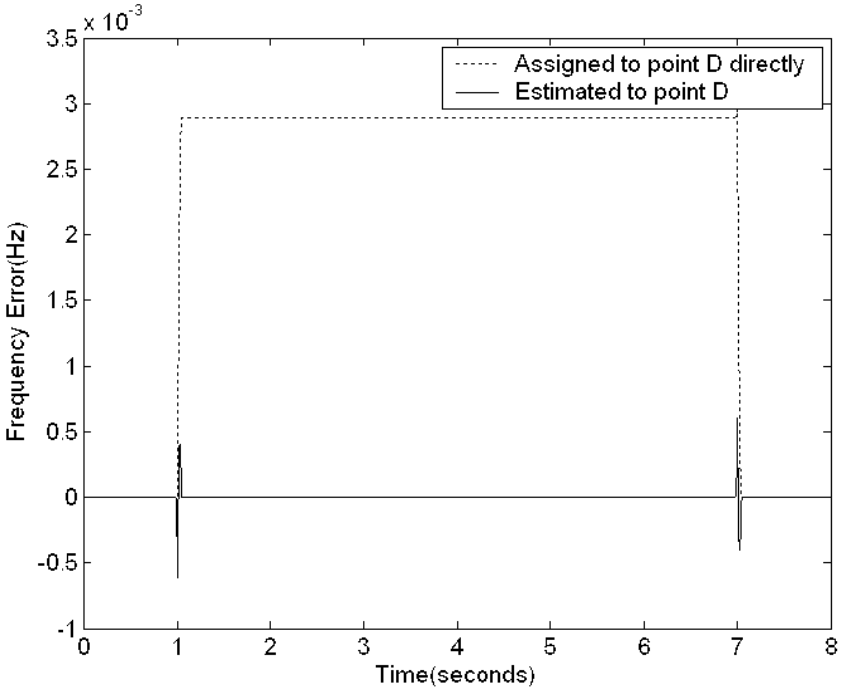

Figure 2.8 Errors between measured and actual frequency (Linearly changing frequency)

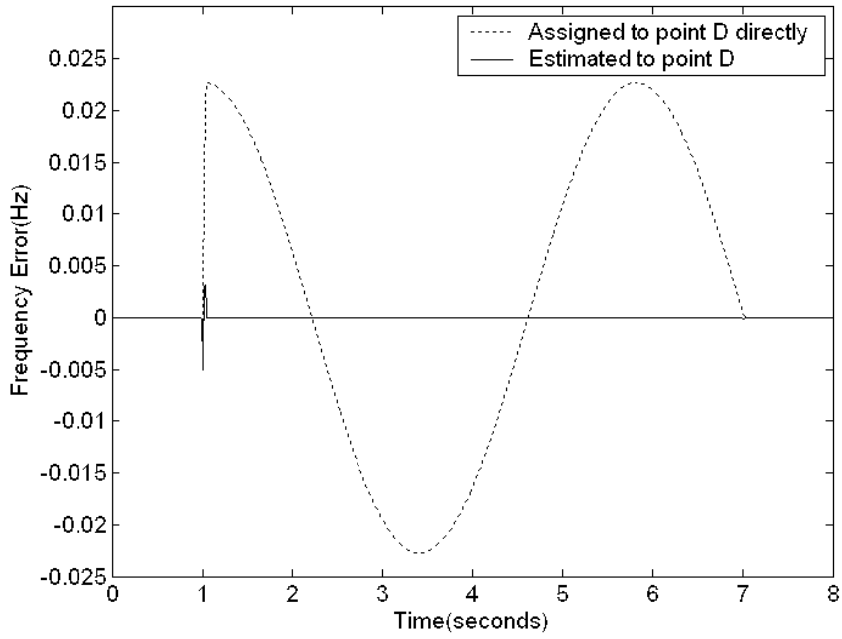

Figure 2.9 Errors between measured and actual frequency (Non-linearly changing frequency)

2.2.3.4 Step Frequency

The response of different methods to a 60-59Hz step frequency was also investigated. Figure 2.10 shows the simulation results for a frequency step. It has a better response when frequency is assigned to time C. The estimated frequency for point D is always affected by the previous trend. To have a steep frequency response, the size of the data window can be reduced.

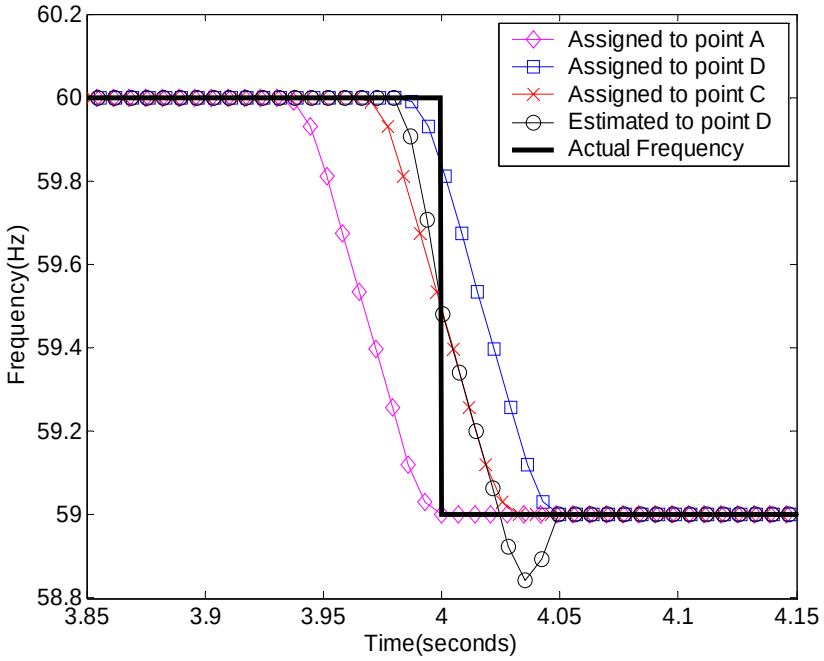

Figure 2.10 Step frequency test

2.2.4 Laboratory Experiment

A laboratory experiment was performed to compare the frequency measured by the proposed method with those measured by two commercial phasor measurement units (PMUs). The experiment setup is shown in Figure 2.11. PMU A and B sense the same three-phase voltage and binary outputs generated by a precise signal source. All synchrophasors, event data and system information are collected by the computer. And one of the PMUs provides the original sample data, which are used to calculate the frequency by the proposed method.

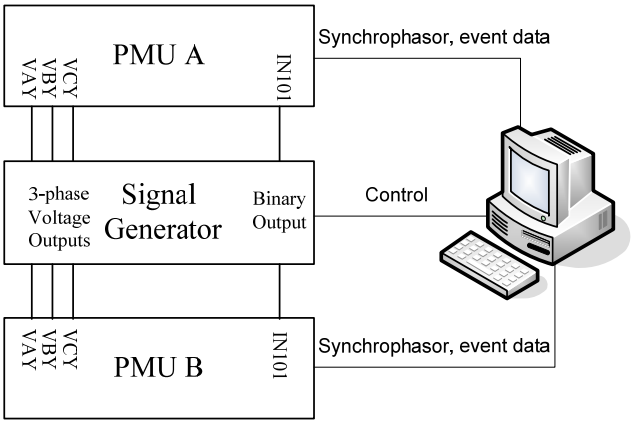

Figure 2.11 Experiment setup

Figure 2.12 shows the comparison of all the measured frequency in the laboratory experiment. The actual frequency generated by the signal source is time-tagged to 1 millisecond through a detailed study of the signal generators. The frequency of PMU A and B is extracted from the synchrophasor data. Compared with others, the measured frequency by the proposed method is the closest to the actual frequency.

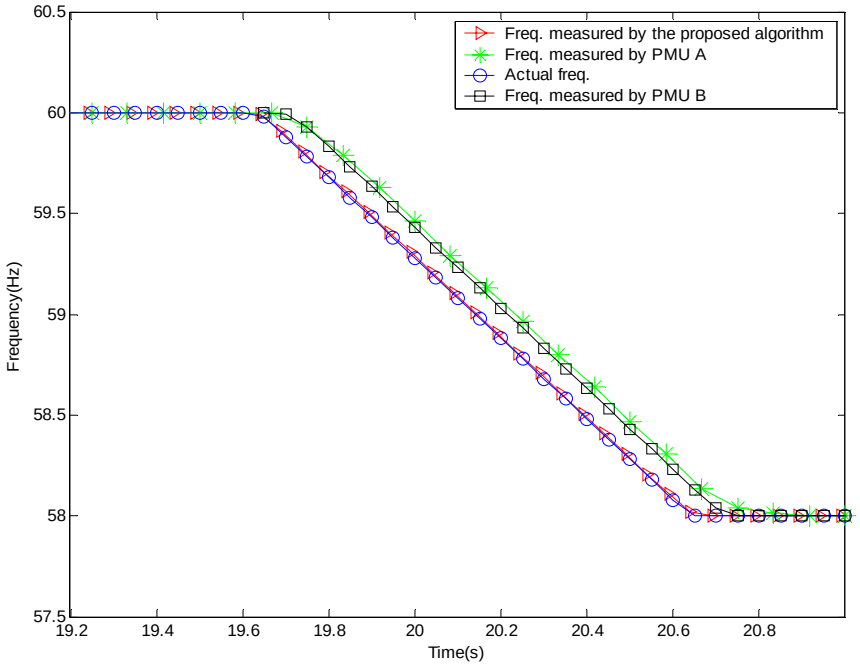

Figure 2.12 Comparison of measured frequency in the laboratory experiment

2.3 Least-Squares Applications in Phasor-Based Synchronized Frequency Measurements

Frequency can be computed as the phase angle difference divided by the time window as shown in Figure 2.13. Since the samples are inexact due to random and system errors, the estimates obtained for phasors and frequency are also inexact. Least-squares (LS) estimation is good at reducing the effects of random errors. It is also helpful to get the continuous frequency values from the spaced values by doing curve fitting in the least-squares sense. Furthermore, it is also helpful to improve the dynamic performance. As show in Figure 2.13, average frequency tends to be close to the instantaneous frequency when the time window shrinks.

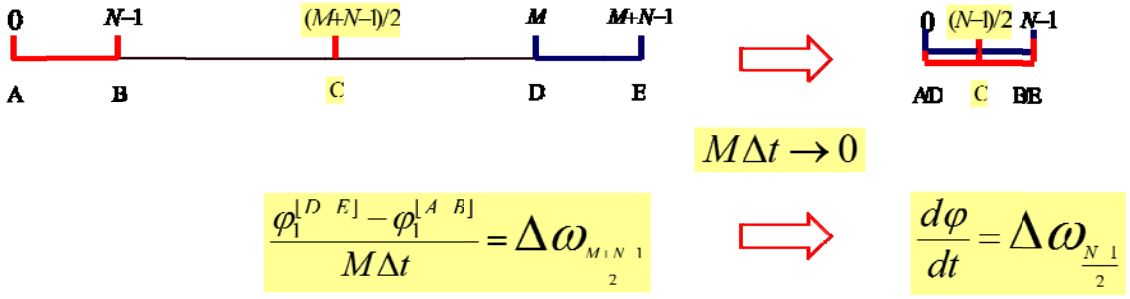

Figure 2.13 Phasor-based synchronized frequency measurements

Assuming the samples are only contaminated by random errors, this section investigates the applications of least-squares estimation in phasor-based synchronized frequency measurements. First, LS estimation is discussed for the synchronized frequency measurement with DFT error-free phasors. The DFT errors considered in this paper mainly come from the fact that nominal frequency based samples and DFT are used when system frequency deviates from the nominal values. Second, LS estimation for the traditional synchronized frequency measurements is reviewed [39] [40] [41] [44] . Third, LS estimation for the proposed synchronized frequency measurements (section 2.2 and reference [30] with DFT error-affected phasors is developed. Finally, the performance of these methods is illustrated on several scenarios by computer simulations.

2.3.1 LS Estimation for Synchronized Frequency Measurements with DFT Error-Free Phasors

In this subsection, we assume the obtained phasors are only affected by random sample errors, and no DFT errors involved. DFT errors associated with off-nominal frequency can be corrected by doing adaptive sampling, re-sampling and iterative calculation, or compensation. Therefore, we assume the obtained phasors are perfect given perfect samples.

LS estimation for synchronized frequency measurement with DFT error-free phasors is quite straightforward. Assume an *n-th* degree polynomial to model the cumulative phase angles as a function of time

$$\varphi(t) = a_0 + a_1 t + a_2 t^2 + \cdots + a_n t^n . \tag{2.26}$$

With a set of DFT error-free phase angle measurements $\varphi_r \{r = 1, 2, \cdots, m\}$ obtained at multiples of t_p, we have

$$\begin{aligned}
&\varphi_1 = a_0 + a_1 t_p + a_2 {t_p}^2 + \cdots + a_n {t_p}^n \\
&\varphi_2 = a_0 + a_1 \left(2t_p\right) + a_2 \left(2t_p\right)^2 + \cdots + a_n \left(2t_p\right)^n \\
&\cdots\cdots\cdots\cdots \\
&\varphi_m = a_0 + a_1 \left(mt_p\right) + a_2 \left(mt_p\right)^2 + \cdots + a_n \left(mt_p\right)^n
\end{aligned} \quad . \tag{2.27}$$

Rewrite equation (2.27) in matrix notation

$$\begin{bmatrix} \varphi_1 \\ \varphi_2 \\ \vdots \\ \varphi_m \end{bmatrix} = \begin{bmatrix} 1 & t_p & \cdots & \left(t_p\right)^n \\ 1 & 2t_p & \cdots & \left(2t_p\right)^n \\ \vdots & \vdots & \ddots & \vdots \\ 1 & mt_p & \cdots & \left(mt_p\right)^n \end{bmatrix} \begin{bmatrix} a_0 \\ a_1 \\ \vdots \\ a_n \end{bmatrix} \quad or \tag{2.28}$$

$$\boldsymbol{\varphi} = \mathbf{H}\mathbf{A}$$

where $\boldsymbol{\varphi} = \begin{bmatrix} \varphi_1 & \varphi_2 & \cdots & \varphi_m \end{bmatrix}^T$, $\mathbf{A} = \begin{bmatrix} a_0 & a_1 & \cdots & a_n \end{bmatrix}^T$, and

$$\mathbf{H} = \begin{bmatrix} 1 & t_p & \cdots & \left(t_p\right)^n \\ 1 & 2t_p & \cdots & \left(2t_p\right)^n \\ \vdots & \vdots & \ddots & \vdots \\ 1 & mt_p & \cdots & \left(mt_p\right)^n \end{bmatrix}.$$

Then the coefficient matrix can be computed by the least-squares formula

$$\mathbf{A} = \left[\mathbf{H}^T\mathbf{H}\right]^{-1}\mathbf{H}^T\boldsymbol{\varphi}\,. \tag{2.29}$$

$\left[\mathbf{H}^T\mathbf{H}\right]^{-1}\mathbf{H}^T$ can be calculated off-line. Then the instantaneous frequency at time t is calculated by definition

$$f(t) = \frac{1}{2\pi}\frac{d\varphi}{dt} = \frac{1}{2\pi}\left(a_1 + 2a_2 t + \cdots + na_n t^{n-1}\right). \tag{2.30}$$

The rate of change of frequency at time t is calculated as

$$f'(t) = \frac{1}{2\pi}\frac{d^2\varphi}{dt^2} = \frac{1}{2\pi}\left[2a_2 + \cdots + n(n-1)a_n t^{n-2}\right]. \tag{2.31}$$

For simplicity, second or third degree polynomial could be taken as fitting models.

2.3.2 LS Estimation for Traditional Synchronized Frequency Measurements with DFT Error-Affected Phasors

Under off-nominal frequency conditions, phasors computed from nominal frequency based DFT and sampling rate contain errors. But these DFT error-affected phasors can still be used to obtain frequency accurately.

Assuming an off-nominal but fixed angular frequency ω within the DFT window, the balanced three-phase signals are

$$\begin{aligned} x_a(t) &= X_m\cos(\omega t + \varphi) = \sqrt{2}\,\mathrm{Re}\left(\mathbf{X}e^{j\omega t}\right) \\ x_b(t) &= X_m\cos(\omega t + \varphi - 2\pi/3) = \sqrt{2}\,\mathrm{Re}\left(\mathbf{X}\alpha^2 e^{j\omega t}\right). \\ x_c(t) &= X_m\cos(\omega t + \varphi - 4\pi/3) = \sqrt{2}\,\mathrm{Re}\left(\mathbf{X}\alpha e^{j\omega t}\right) \end{aligned} \tag{2.32}$$

where $\mathbf{X} = \left(X_m/\sqrt{2}\right)e^{j\varphi}$, $\alpha = e^{j\frac{2\pi}{3}}$, φ represents the initial phase. The above phase quantities are sampled N times per full cycle of the nominal frequency f_N, so the sampling period is $\Delta t = \frac{1}{Nf_N} = \frac{2\pi}{N\omega_N}$. With the window beginning from the *r-th* sample, perform the nominal frequency-based one-cycle DFT recursively for each phase, and obtain the positive-sequence component phasors as

$$\mathbf{X}_1^r = \mathbf{X}\frac{\sin\frac{N\Delta\omega\Delta t}{2}}{N\sin\frac{\Delta\omega\Delta t}{2}}\exp\left[j\left(r + \frac{N-1}{2}\right)\Delta\omega\Delta t\right] \tag{2.33}$$

where $\Delta\omega = \omega - \omega_N$. Equation (2.33) shows the calculated phasor placed at the *r-th* sample. The derivative of this calculated phase angle with respect to time is

$$\frac{d\left[\varphi + \left(r + \frac{N-1}{2}\right)\Delta\omega\Delta t\right]}{dt} = \frac{d\left(\Delta\omega t\right)}{dt} = \Delta\omega . \tag{2.34}$$

Though the calculated phasor in equation (2.33) contains DFT errors, it is found in equation (2.34) that the derivative of this phase angle is the actual value of frequency deviation. The result is frequency deviation instead of frequency is because the DFT is performed recursively and the calculated phasor is actually referenced to the synchronous frame.

Take a set of calculated phase angles, and perform the least-squares curve fitting with a second degree polynomial model. Then the coefficients are computed as

$$\begin{bmatrix} a_0 \\ a_1 \\ a_2 \end{bmatrix} = \left[\mathbf{H}^T\mathbf{H}\right]^{-1}\mathbf{H}^T\begin{bmatrix} \varphi_1 \\ \varphi_2 \\ \vdots \\ \varphi_m \end{bmatrix}. \tag{2.35}$$

Instantaneous frequency at time t is calculated as

$$f(t) = f_N + \frac{1}{2\pi}\left(a_1 + 2a_2 t\right). \tag{2.36}$$

The rate of change of frequency at time t is calculated as

$$f'(t) = \frac{2a_2}{2\pi}. \tag{2.37}$$

Given fixed frequency and three-phase balanced model, this method performs very well, and the DFT errors in phasors actually don't affect the frequency. For a slowly changing frequency, this algorithm also performs well.

2.3.3 LS Estimation for Proposed Synchronized Frequency Measurements with DFT Error-Affected Phasors

As discussed in section 2.2, proposed synchronized frequency measurements in this work have better dynamic performance compared with the traditional method. So in this subsection, LS estimation for the proposed synchronized frequency measurement method is developed.

With linearized instead of fixed angular frequency within the window, three-phase signals

$$\begin{aligned} x_a(t) &= \sqrt{2}\,\mathrm{Re}\left(\mathbf{X} e^{j\int_0^t \omega dt} \right) \\ x_b(t) &= \sqrt{2}\,\mathrm{Re}\left(\mathbf{X}\alpha^2 e^{j\int_0^t \omega dt} \right) \\ x_c(t) &= \sqrt{2}\,\mathrm{Re}\left(\mathbf{X}\alpha e^{j\int_0^t \omega dt} \right) \end{aligned} \tag{2.38}$$

where $\mathbf{X} = \left(X_m / \sqrt{2} \right) e^{j\varphi}$ and $\alpha = e^{j\frac{2\pi}{3}}$, are also sampled N times per full cycle of the nominal frequency f_N. Equation (2.21) shows the calculated phasor placed at the *r-th* sample given the initial phase φ and linearly changing frequency. The time derivative of the phase angle is calculated as

$$\frac{d\varphi_1^{(r)}}{dt} = \Delta\omega_{r+\frac{N-1}{2}} \ . \tag{2.39}$$

Equation (2.39) further shows that the time derivative of the obtained phase angle placed at the *r-th* sample does not calculate the instantaneous frequency at the *r-th* sample because of the effect of the DFT errors, but it reflects the instantaneous frequency deviation at sample $\left(r + \frac{N-1}{2} \right)$ or at time $\left(r + \frac{N-1}{2} \right)\Delta t$. And this conclusion can be extended to cases in which the calculated phasors are placed anywhere within the windows, and the obtained instantaneous frequency deviation still reflects the values at sample $\left(r + \frac{N-1}{2} \right)$ or at time $\left(r + \frac{N-1}{2} \right)\Delta t$.

Take a set of calculated phase angles, and perform the least-squares curve fitting with a third degree polynomial model. Then the coefficients are computed as

$$\begin{bmatrix} a_0 \\ a_1 \\ a_2 \\ a_4 \end{bmatrix} = \left[\mathbf{H}^T \mathbf{H} \right]^{-1} \mathbf{H}^T \begin{bmatrix} \varphi_1 \\ \varphi_2 \\ \vdots \\ \varphi_m \end{bmatrix}. \tag{2.40}$$

If the calculated phasors are placed at the beginning of the window, frequency is

calculated as

$$f\left(t+\frac{N-1}{2}\Delta t\right)=f_N+\frac{1}{2\pi}\left(a_1+2a_2t+3a_3t^2\right). \tag{2.41}$$

The rate of change of frequency is calculated as

$$f'\left(t+\frac{N-1}{2}\Delta t\right)=\frac{2a_2+6a_3t}{2\pi}\ . \tag{2.42}$$

If the calculated phasors are placed at the center of the window, frequency is then calculated as

$$f(t)=f_N+\frac{1}{2\pi}\left(a_1+2a_2t+3a_3t^2\right). \tag{2.43}$$

The rate of change of frequency is calculated as

$$f'(t)=\frac{2a_2+6a_3t}{2\pi}\ . \tag{2.44}$$

If the calculated phasors are placed at the end of the window, frequency is then calculated as

$$f\left(t-\frac{N-1}{2}\Delta t\right)=f_N+\frac{1}{2\pi}\left(a_1+2a_2t+3a_3t^2\right). \tag{2.45}$$

The rate of change of frequency is calculated as

$$f'\left(t-\frac{N-1}{2}\Delta t\right)=\frac{2a_2+6a_3t}{2\pi}\ . \tag{2.46}$$

The above three phasor positioning methods will get the same results. But it is better to put the calculated phasors at the center of the window so that the frequency can be obtained directly without shift.

2.3.4 Simulations and Discussions

In the simulations, three-phase balanced signals are generated

$$\begin{cases} v_a(t)=\sqrt{2}V\cos(2\pi ft+\varphi)+\varepsilon_a \\ v_b(t)=\sqrt{2}V\cos(2\pi ft+\varphi-2\pi/3)+\varepsilon_b \\ v_c(t)=\sqrt{2}V\cos(2\pi ft+\varphi+2\pi/3)+\varepsilon_c \end{cases} \tag{2.47}$$

with frequency shown in Figure 2.14. ε_a, ε_b and ε_c are independent random variables which follow Gaussian distribution with zero mean and σ standard deviation. The

frequency of segment A-B stays at 60Hz, the frequency of segment B-C changes faster than the frequency of segment C-D, and the frequency of segment D-E stays at 59.8Hz.The signals are sampled 24 times per full cycle of 60Hz waveform, i.e. the sampling rate is 1440Hz.

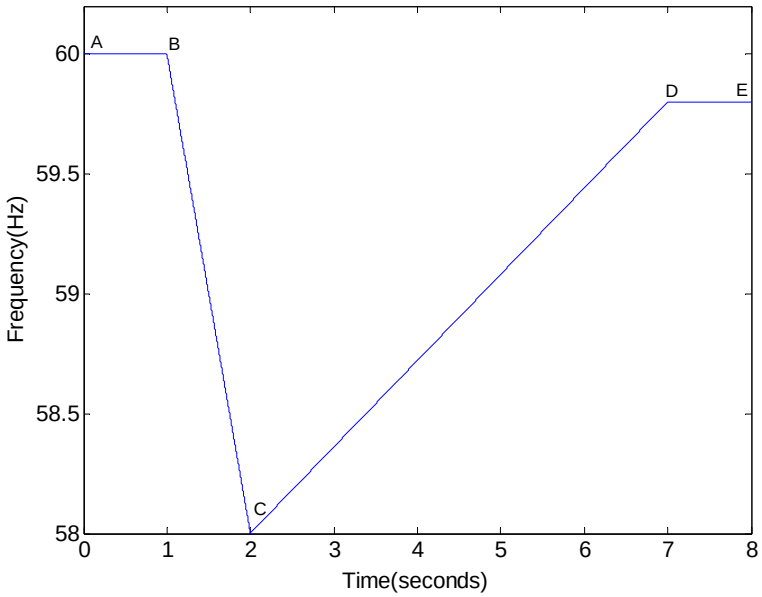

Figure 2.14 Actual frequency

From Figure 2.15 and Figure 2.16, we can see the phasor-based synchronized frequency measurement is sensitive to random sample errors, but LS estimation can suppress these errors. Figure 2.17 and Figure 2.18 show the performance of traditional method and proposed method without any disturbance in the samples. With fixed frequency in segments A-B and D-E, both of them perform very well, and the errors are almost zero. With slowly changing frequency in segment C-D, traditional method has small errors, but errors in proposed method are close to zero. With fast changing frequency in segment B-C, traditional method has big errors, but errors in proposed method are still close to zero. Spikes occur where frequency changes dramatically.

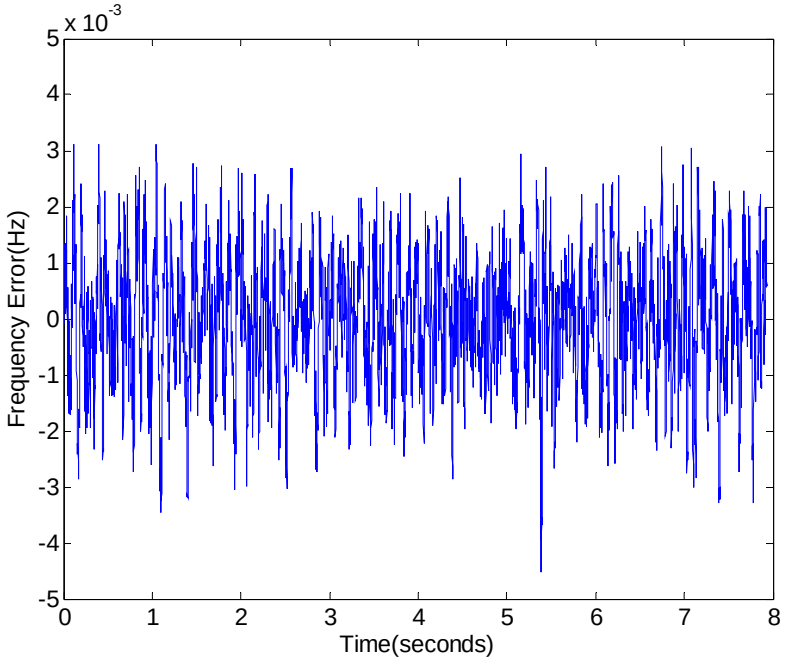

Figure 2.15 Errors between the actual and measured frequency without LS estimation (DFT error free phasors, 24 points per window, one-cycle DFT, $\sigma = 0.002V$)

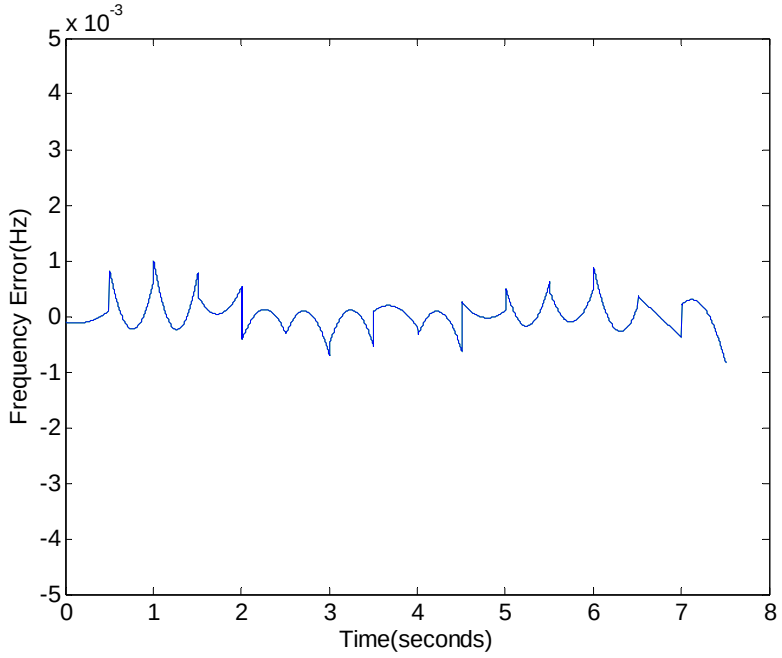

Figure 2.16 Errors between the actual and LS estimated frequency (30 LS windows, 24 points per window, third degree polynomial, one-cycle DFT, $\sigma = 0.002V$)

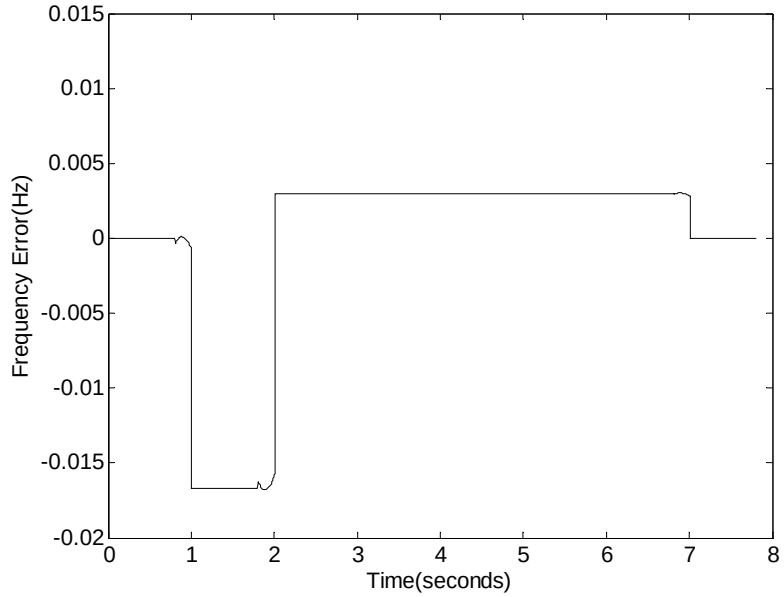

Figure 2.17 Errors between the actual and LS estimated frequency with traditional method (12 LS windows, 24 points per window, third degree polynomial, one-cycle DFT, $\sigma = 0$)

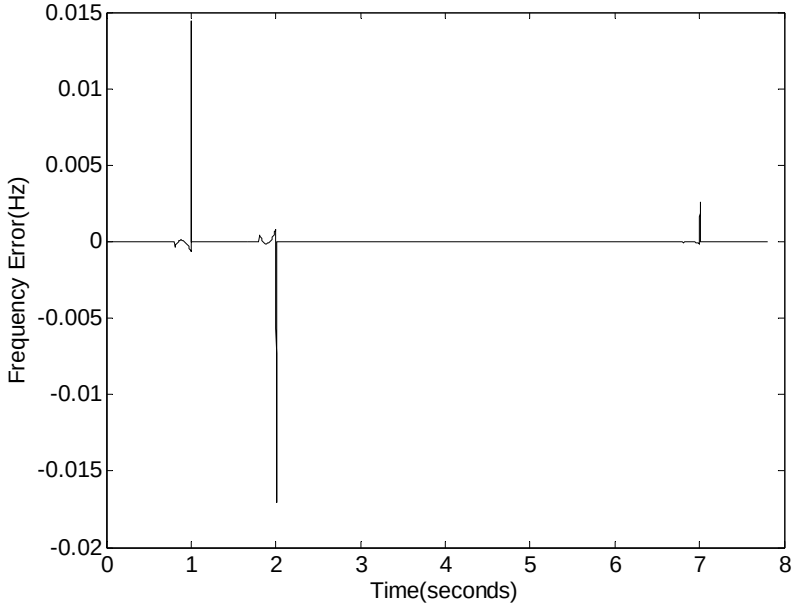

Figure 2.18 Errors between the actual and LS estimated frequency with proposed method (12 LS windows, 24 points per window, third degree polynomial, one-cycle DFT, $\sigma = 0$)

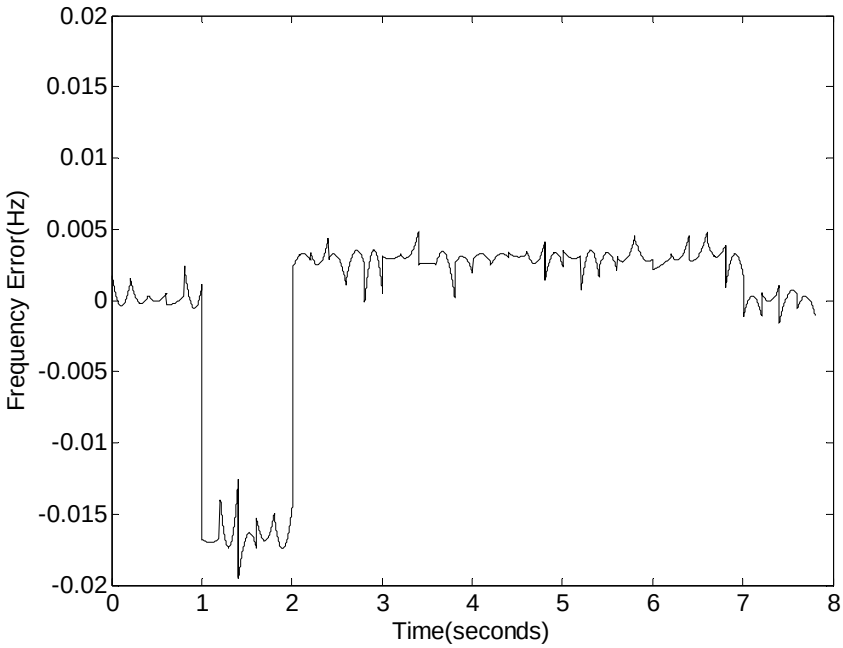

Figure 2.19 Errors between the actual and LS estimated frequency with traditional method (12 LS windows, 24 points per window, third degree polynomial, one-cycle DFT, $\sigma = 0.002V$)

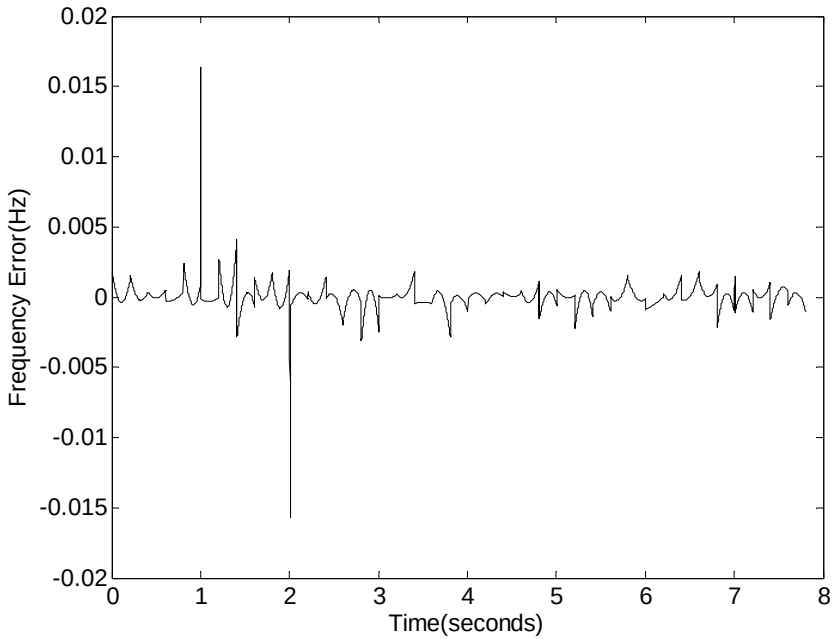

Figure 2.20 Errors between the actual and LS estimated frequency with proposed method (12 LS windows, 24 points per window, third degree polynomial, one-cycle DFT, $\sigma = 0.002V$)

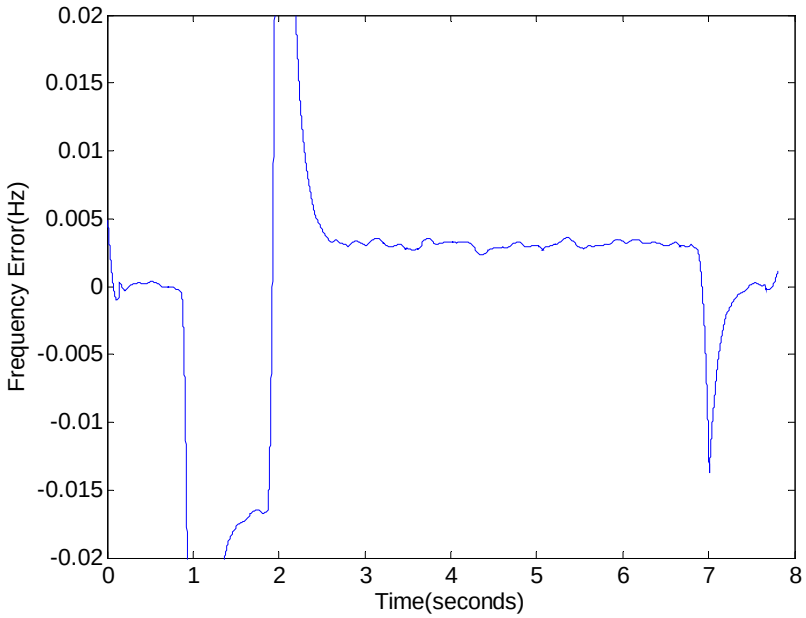

(a) Traditional method

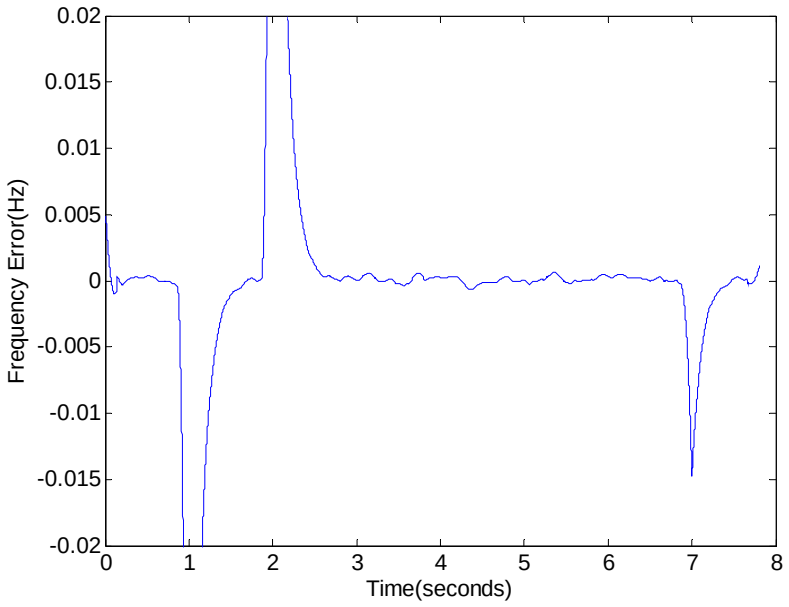

(b) Proposed method

Figure 2.21 Errors between the actual and LS estimated frequency (12 LS windows, 24 points per window, third degree polynomial, one-cycle DFT, $\sigma = 0.002V$, 16-cycle average filter)

Figure 2.19 and Figure 2.20 show the performance of traditional method and proposed method with standard deviation equal to $0.002V$ in the samples. With fixed frequency in segments A-B and D-E, both perform well, and the means of the errors are closes to zero. With slowly changing frequency in segment C-D, the mean of errors in traditional method is 0.003, while the mean of errors in proposed method is close to zero. With fast changing frequency in segment B-C, the mean of errors in traditional method is 0.016, while the mean of errors in proposed method is close to zero. Proposed method performs better when frequency changes very quickly. If a more smooth frequency is desired, another filter could be used to smooth the obtained frequency. For example, Figure 2.21 shows the results with a 16-cycle average filter. The frequency is much smoother, but the long window deteriorates the dynamic performance.

Chapter 3
Synchronized Phasor Measurements under Dynamics

As stated in Chapter 1, window sizes and leakage effects due to frequency dynamics are two major aspects that may affect the accuracy of synchronized measurements. Window sizes have been discussed in some sections in Chapter 1 and Chapter 2. An accurate synchronized frequency measurement technique is proposed in Chapter 2. This chapter discusses how to use measured frequency to eliminate the leakage effects and obtain accurate synchronized phasor measurements under frequency dynamics.

This chapter reviews some techniques that can be used to obtain accurate synchronized phasor measurements and proposes a frequency based phasor compensation method. This method can be used by those legacy PMUs to do post correction, or by those new PMUs as alternative frequency-tracking algorithm. Phasor positioning is another issue affecting the dynamic measurement performance, which is also studied in detail. Some unbalance issues are investigated in this chapter as well.

3.1 Techniques for Accurate Synchrophasor Measurements under Dynamics

This section reviews several techniques for accurate synchrophasor measurements under frequency dynamics.

3.1.1 Variable Sampling Rates

Fixed sampling rates are vulnerable to the leakage effects when frequency changes. The measured frequency can be used to adjust the sampling rate on line [45] [46] , to make the sampling frequency an integer multiple of the fundamental component. Figure 3.1 shows the block diagram of a variable sampling-rate system. Properly conditioned signals are sampled and held for A/D conversion. CPUs estimate the system frequency from the obtained samples, and use it to online adjust the sampling rates.

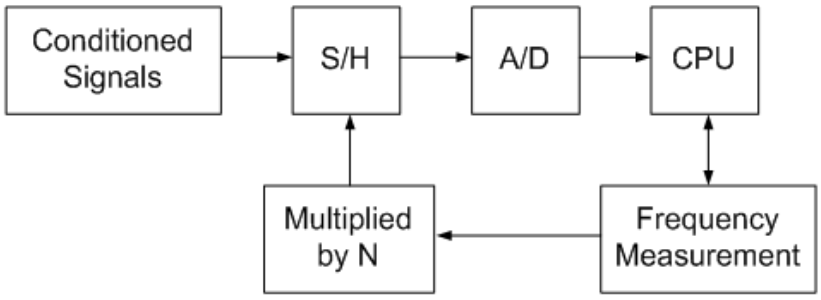

Figure 3.1 Block diagram of variable sampling-rate system

The sampling rates in this technique are adapted to the prevailing system frequency. Though there is delay in frequency calculation, it is very small. But this technique is not friendly for digital fault recording. Traditionally, digital fault recorders (DFRs) acquire data at fixed sampling rate to provide voltage and current oscillography and harmonic analysis. It is also not suitable for phasor reporting since the IEEE Std. C37.118-2005 requires reporting synchronized phasors at multiples of nominal period. With variable sampling rates, a rate-conversion method is required to meet the above requirements. Furthermore, measured frequency spikes have to be used with care.

3.1.2 Re-sampling

Figure 3.2 shows a re-sampling scheme. Conditioned signals are sampled at fixed sampling rates, the obtained samples are stored in a data base, and then these data can be re-sampled according to the measured system frequency. [48]

The advantages of this technique include adapted sampling rates, suitable for digital fault recording and phasor reporting. Disadvantages are that frequency spikes may

lead to wrong sampling and interpolation model may not consider harmonics. For example, the blue line in Figure 3.3 is the actual signal with harmonics, but the interpolation model is based on the fundamental component, which is shown by the red line causing re-sampling errors in the presence of harmonics.

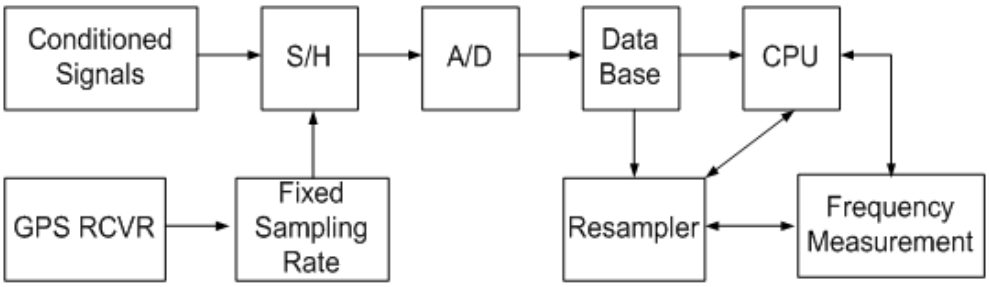

Figure 3.2 Re-sampling scheme

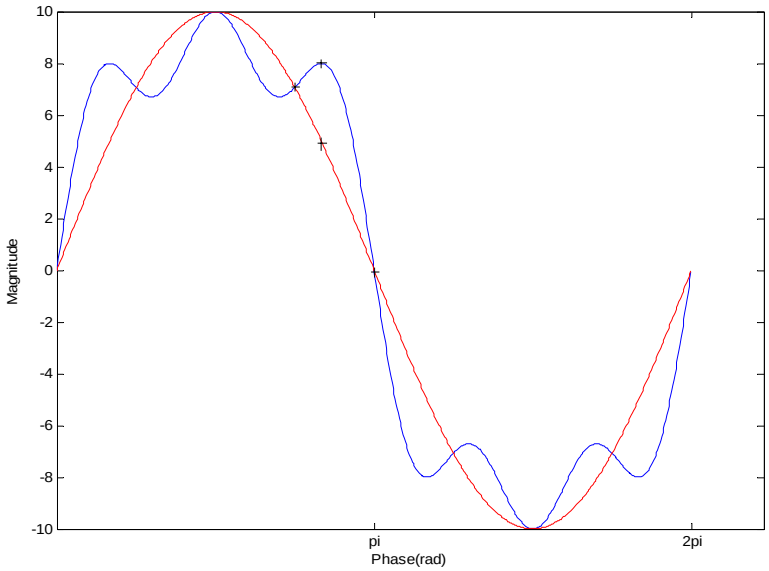

Figure 3.3 Re-sampling errors

3.1.3 Variable Data Windows

Instead of changing the sampling rates or intervals, the length of the window used could be changed to adapt to the system frequency [47] . As shown in Figure 3.4, sampling interval is fixed, but the number of points used for DFT calculation could be

changed. For example, for a sampling rate of 14400Hz, the number of samples used for DFT can be selected according to the system frequency as shown in Table 3.1.

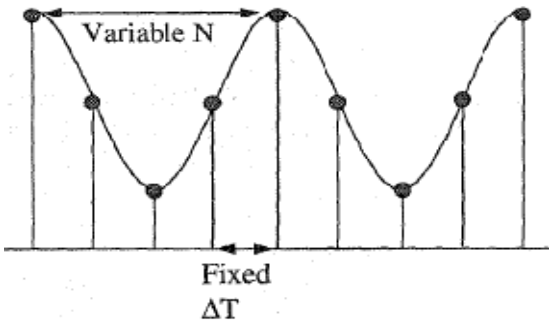

Figure 3.4 Variable data window

Table 3.1 Number of samples used

Number of samples	System frequency (Hz)
238	60.5042
239	60.2510
240	60.0000
241	59.7510
242	59.5041

The sampling rates can be easily adapted to some extent, and it is suitable for digital fault recording and phasor reporting. However, the sampling rates are adapted only at certain values of frequency. A much higher sampling frequency is required to obtain better performance.

3.2 Frequency Based Phasor Compensation

Adaptive sampling or re-sampling can help obtain accurate synchronized phasor

measurements during dynamics. In this section, a frequency based phasor compensation method with fixed sampling is proposed to obtain accurate synchronized phasor measurements during dynamics. This method can be used by those legacy PMUs to do post correction, or by those new PMUs as alternative frequency-tracking algorithm.

3.2.1 Proposed Method

Assuming an off-nominal but fixed angular frequency ω within the window, the balanced three-phase signals are

$$\begin{aligned} x_a(t) &= X_m \cos(\omega t + \varphi) = \sqrt{2}\,\mathrm{Re}\left(\mathbf{X}e^{j\omega t}\right) \\ x_b(t) &= X_m \cos(\omega t + \varphi - 2\pi/3) = \sqrt{2}\,\mathrm{Re}\left(\mathbf{X}\alpha^2 e^{j\omega t}\right) \\ x_c(t) &= X_m \cos(\omega t + \varphi - 4\pi/3) = \sqrt{2}\,\mathrm{Re}\left(\mathbf{X}\alpha e^{j\omega t}\right) \end{aligned} \quad (3.1)$$

where $\mathbf{X} = \left(X_m/\sqrt{2}\right)e^{j\varphi}$, $\alpha = e^{j\frac{2\pi}{3}}$, φ represents the initial phase. The phase quantities can be expressed with the help of Euler's formula

$$\begin{aligned} x_a(t) &= \sqrt{2}\frac{1}{2}(\mathbf{X}e^{j\omega t} + \mathbf{X}^* e^{-j\omega t}) \\ x_b(t) &= \sqrt{2}\frac{1}{2}(\mathbf{X}\alpha^2 e^{j\omega t} + \mathbf{X}^* \cdot \alpha \cdot e^{-j\omega t}) \\ x_c(t) &= \sqrt{2}\frac{1}{2}(\mathbf{X}\alpha \cdot e^{j\omega t} + \mathbf{X}^* \cdot \alpha^2 \cdot e^{-j\omega t}) \end{aligned} \quad (3.2)$$

The above phase quantities are sampled N times per full cycle of the nominal frequency f_N, so the sampling period is $\Delta t = \frac{1}{Nf_N} = \frac{2\pi}{N\omega_N}$. Then the discrete sample sets are as follows

$$\begin{aligned} x_{a,k} &= \sqrt{2}\frac{1}{2}\left(\mathbf{X}e^{jk\omega\Delta t} + \mathbf{X}^* e^{-jk\omega\Delta t}\right) \\ x_{b,k} &= \sqrt{2}\frac{1}{2}\left(\mathbf{X}\alpha^2 e^{jk\omega\Delta t} + \mathbf{X}^*\alpha e^{-jk\omega\Delta t}\right) \\ x_{c,k} &= \sqrt{2}\frac{1}{2}\left(\mathbf{X}\alpha e^{jk\omega\Delta t} + \mathbf{X}^*\alpha^2 e^{-jk\omega\Delta t}\right) \end{aligned} \quad (3.3)$$

With the data window, perform the nominal frequency-based one-cycle DFT for each phase

$$\begin{aligned}\mathbf{X}_a &= \frac{1}{\sqrt{2}}\frac{2}{N}\sum_{k=0}^{N-1} x_{a,k}\, e^{-jk\omega_N \Delta t} \\ \mathbf{X}_b &= \frac{1}{\sqrt{2}}\frac{2}{N}\sum_{k=0}^{N-1} x_{b,k}\, e^{-jk\omega_N \Delta t} \\ \mathbf{X}_c &= \frac{1}{\sqrt{2}}\frac{2}{N}\sum_{k=0}^{N-1} x_{c,k}\, e^{-jk\omega_N \Delta t}\end{aligned} \quad . \tag{3.4}$$

The positive-sequence component phasors can be calculated as

$$\begin{aligned}\mathbf{X}_1 &= \frac{1}{3}(\mathbf{X}_a + \alpha\mathbf{X}_{b+}\alpha^2\mathbf{X}_c) \\ &= \frac{1}{3N}\sum_{k=0}^{N-1}\Big[\left(\mathbf{X}e^{jk\omega\Delta t} + \mathbf{X}^* e^{-jk\omega\Delta t}\right) + \alpha\left(\mathbf{X}\alpha^2 e^{jk\omega\Delta t} + \mathbf{X}^*\alpha e^{-jk\omega\Delta t}\right) \\ &\qquad + \alpha^2\left(\mathbf{X}\alpha e^{jk\omega\Delta t} + \mathbf{X}^*\alpha^2 e^{-jk\omega\Delta t}\right)\Big]e^{-jk\omega_N\Delta t} \\ &= \frac{1}{N}\sum_{k=0}^{N-1}\mathbf{X}e^{jk\omega\Delta t}e^{-jk\omega_N\Delta t} \\ &= \frac{1}{N}\sum_{k=0}^{N-1}\mathbf{X}e^{jk\Delta\omega\Delta t} \\ &= \mathbf{X}\frac{\sin\frac{N\Delta\omega\Delta t}{2}}{N\sin\frac{\Delta\omega\Delta t}{2}}\exp\left(j\frac{N-1}{2}\Delta\omega\Delta t\right)\end{aligned} \tag{3.5}$$

where $\Delta\omega = \omega - \omega_N$. Equation (3.5) shows the calculated phasor placed at the beginning of the window. The calculated phasor is

$$\varphi_{measured} = \varphi + \frac{N-1}{2}\Delta\omega\Delta t \tag{3.6}$$

$$X_{measured} = X \frac{\sin\frac{N\Delta\omega\Delta t}{2}}{N \sin\frac{\Delta\omega\Delta t}{2}} \tag{3.7}$$

and the actual phasor is

$$\varphi_{actual} = \varphi \tag{3.8}$$

$$X_{actual} = X \tag{3.9}$$

Equations (3.6) - (3.9) can be used to develop a phasor compensation method. So

$$\varphi_{actual} = \varphi_{measured} - \frac{N-1}{2}\Delta\omega\Delta t \tag{3.10}$$

$$X_{actual} = X_{measured} \frac{N \sin\frac{\Delta\omega\Delta t}{2}}{\sin\frac{N\Delta\omega\Delta t}{2}} \tag{3.11}$$

In the above analysis, a fixed frequency is assumed within the data window. In practice, if the frequency is changing, we can use the frequency at the center of window. Actually the frequency change within one data window is very small in real power systems.

3.2.2 Simulation Verification

Three phase balanced signals are generated with the dynamic frequency shown as in Figure 3.5. The signals are sampled 24 times per full cycle of 60Hz waveform. One-cycle DFT is performed to calculate the phasors, and then those phasors are compensated with the proposed method. Phase shift, magnitude attenuation and TVE are all computed to demonstrate how the proposed compensation method improves the dynamic performance of synchronized phasor measurements during dynamic conditions. Although the TVE is defined in terms of steady state in the synchrophasor standard, here we also calculate it for the dynamic state to see how it is affected.

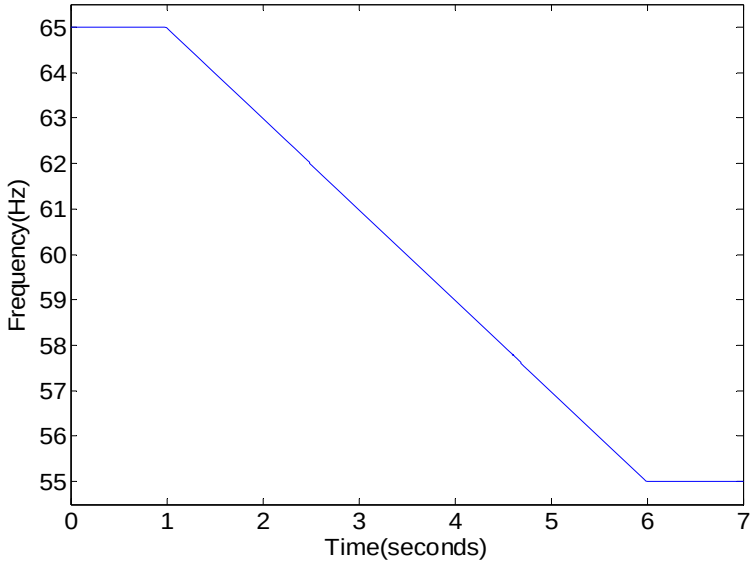

Figure 3.5 Linearly changing dynamic frequency for generated three phase signals

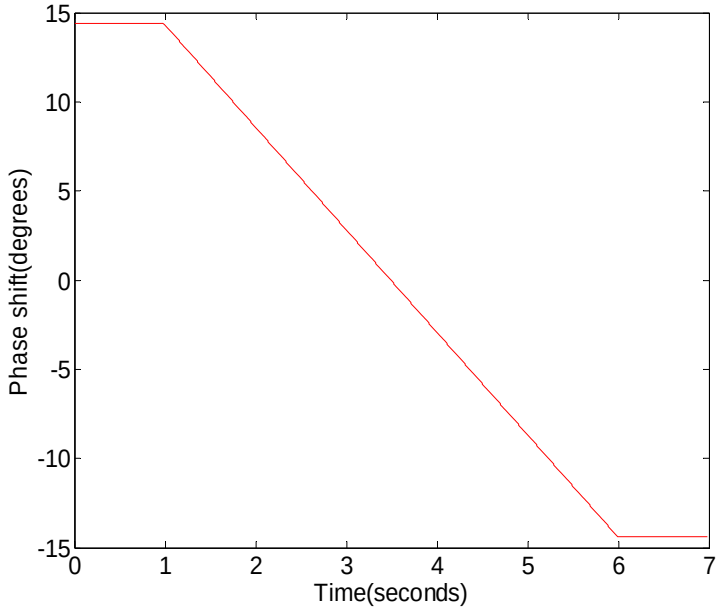

Figure 3.6 Phase shift (w/o compensation, phasor at beginning of window)

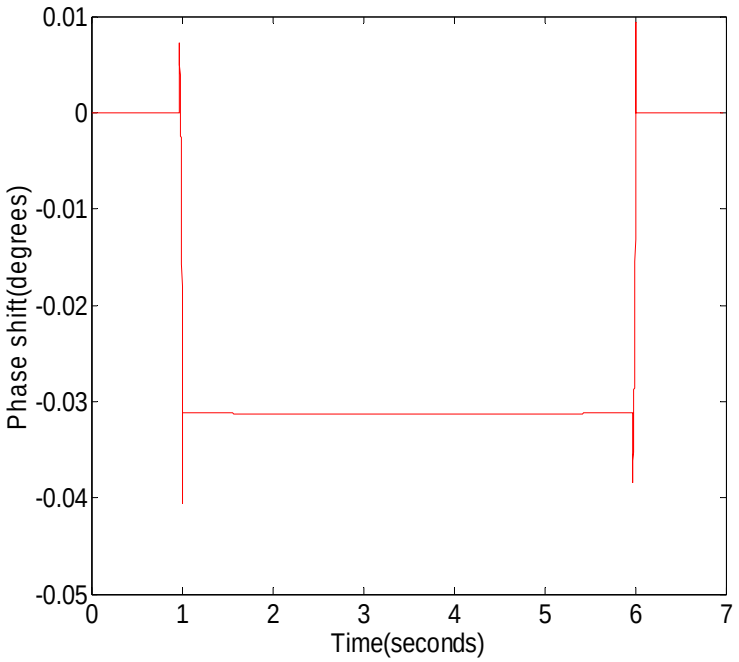

Figure 3.7 Phase shift (w/ compensation, phasor at beginning of window)

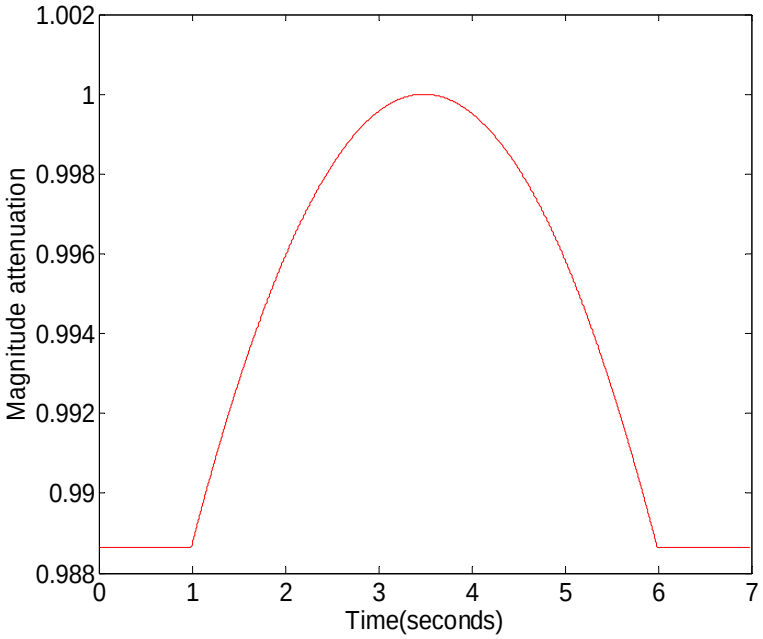

Figure 3.8 Magnitude attenuation (w/o compensation, phasor at beginning of window)

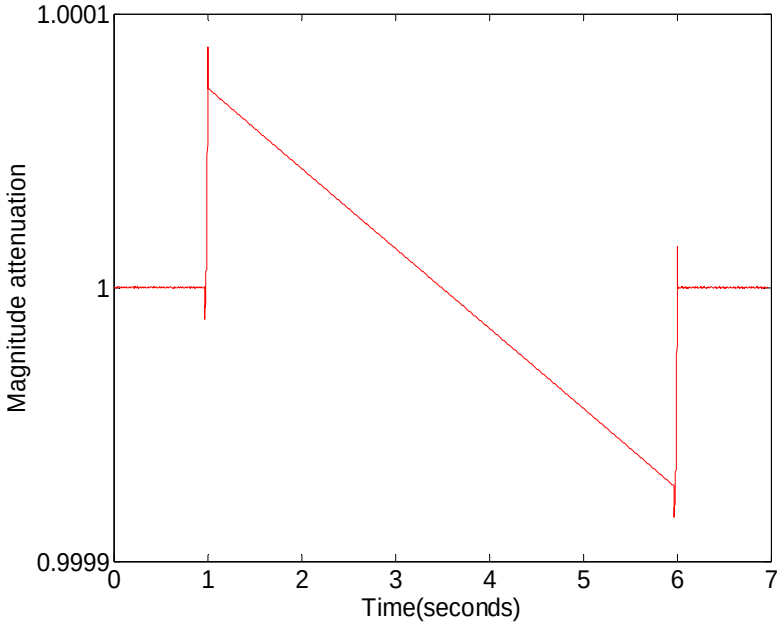

Figure 3.9 Magnitude attenuation (w/ compensation, phasor at beginning of window)

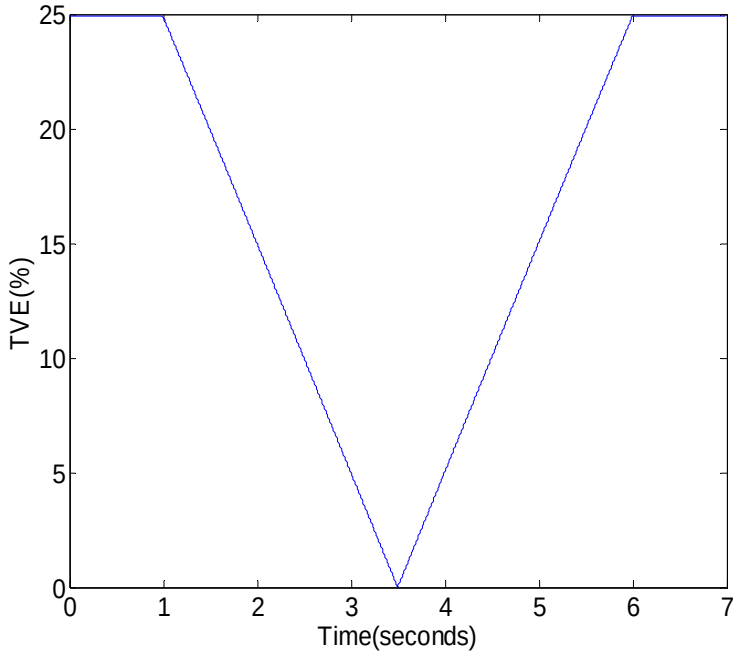

Figure 3.10 TVE (w/o compensation, phasor at beginning of window)

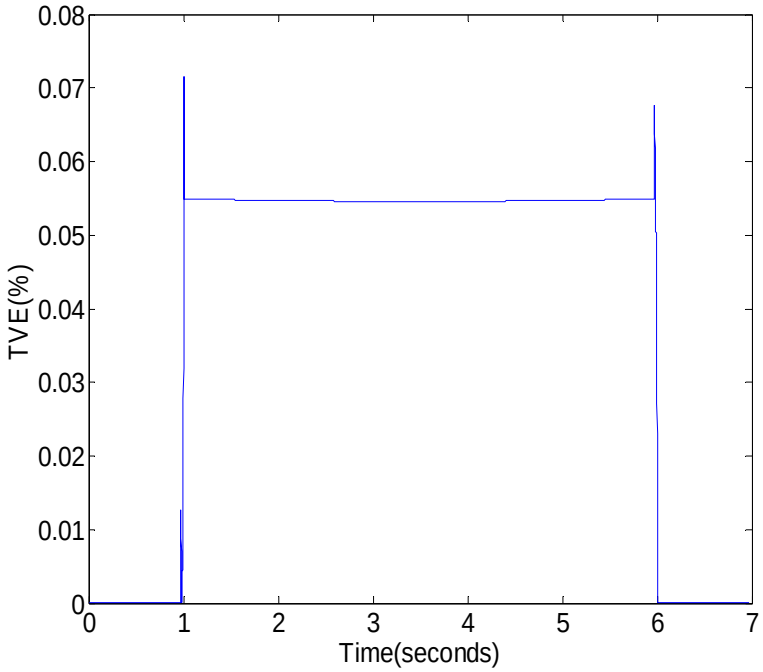

Figure 3.11 TVE (w/ compensation, phasor at beginning of window)

As shown in Figure 3.6 through Figure 3.11, we can see that the phase shift and TVE are greatly reduced. Magnitude attenuation is not so significant with frequency dynamics, but it is still reduced with compensation.

3.3 Effects of Phasor Positioning

Synchronized phasor measurements are the estimation of the phasor representation of a sinusoidal signal at a particular instant of time. The process of making a phasor estimate will require sampling the waveform over some interval of time which can lead to some confusion as to which time within that window is the correct timetag for the phasor. This section investigates the effects of phasor positioning on measurements during dynamics.

IEEE Std. 1344-1995 assigns the timetag to the last sample in the window. Some researchers argues that it should be positioned at the center or beginning of the window. Consequently, the IEEE C37.118-2005 defines the timetag at the time of the theoretical phasor that the estimated phasor represents. There is different group delay with different

positioning. Regardless of the group delay, all positioning should produce the same measurement for the steady state with nominal frequency. Otherwise, positioning may lead to phasor measurements errors when frequency is changing. Consider the same simulation case as in section 3.2, now we calculate the phasor at the center of the window instead. Phase shift, magnitude attenuation and TVE are obtained and plotted as shown in Figure 3.12, Figure 3.13 and Figure 3.14. Compared with Figure 3.6, Figure 3.8 and Figure 3.10 where phasor are positioned at the beginning of the window, we can see magnitude attenuation does not change much, but the phase shift and TVE are reduced greatly even without any compensation.

With the calculated phasor placed at point m of the window (*0~N-1*) as shown in Figure 3.15, we could derive the general form of the calculated phasor based on the analysis in section 3.2.

$$\mathbf{X}_1 = X\frac{\sin\frac{N\Delta\omega\Delta t}{2}}{N\sin\frac{\Delta\omega\Delta t}{2}}\exp\left(j\frac{N-1}{2}\Delta\omega\Delta t + j\omega_N m\Delta t\right) \tag{3.12}$$

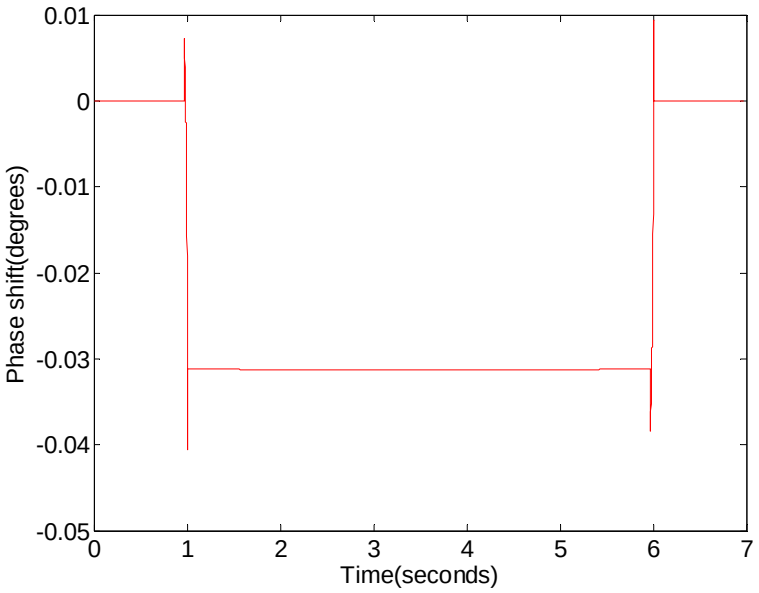

Figure 3.12 Phase shift (w/o compensation, phasor at center of window)

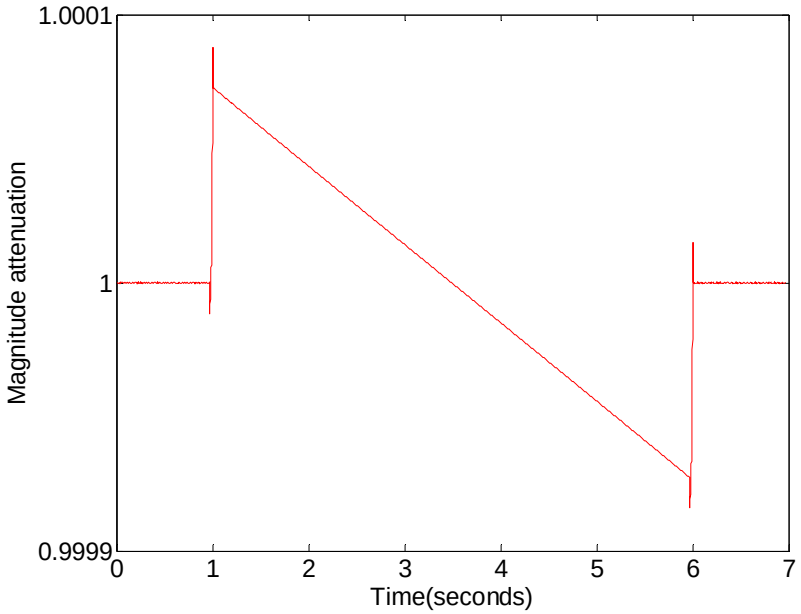

Figure 3.13 Magnitude attenuation (w/o compensation, phasor at center of window)

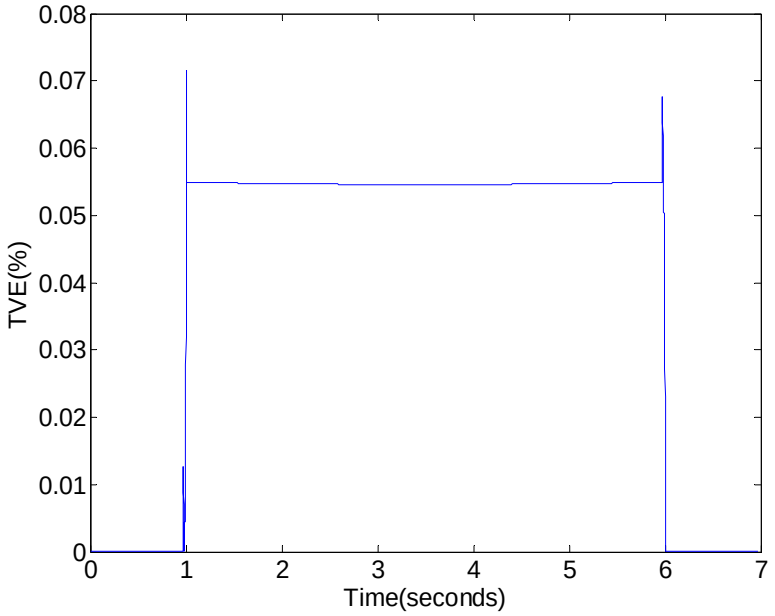

Figure 3.14 TVE (w/o compensation, phasor at center of window)

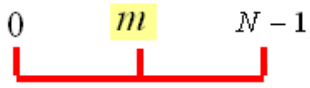

Figure 3.15 Phasor positioning

Compare the actual phase angles with those calculated using equation (3.12), phase errors with different positioning can be derived analytically as shown in Table 3.2. We can see that the phase errors are the same but with different sign when the phasors are placed at the beginning and end. The errors are the smallest when the phasors are placed at the center of the window, which explains the simulation results. Even though there are small errors with phasor placed at the center of the window, we can still perform compensation based on the measured frequency and the errors shown in Table 3.2. Considering the same simulation case as in section 3.2, phasors are calculated for the center of the window, and then compensated. Phase shift, magnitude attenuation and TVE are obtained and plotted as shown in Figure 3.16, Figure 3.17 and Figure 3.18. We can see that the phase shift, magnitude attenuation and TVE are all reduced close to zero.

Table 3.2 Errors with different phasor positioning

Phasor Position	Beginning m=0	Center m=N/2	End m=N-1
Phase Error	$-\frac{N-1}{2}\Delta\omega\Delta t$	$\frac{1}{2}\Delta\omega\Delta t$	$\frac{N-1}{2}\Delta\omega\Delta t$

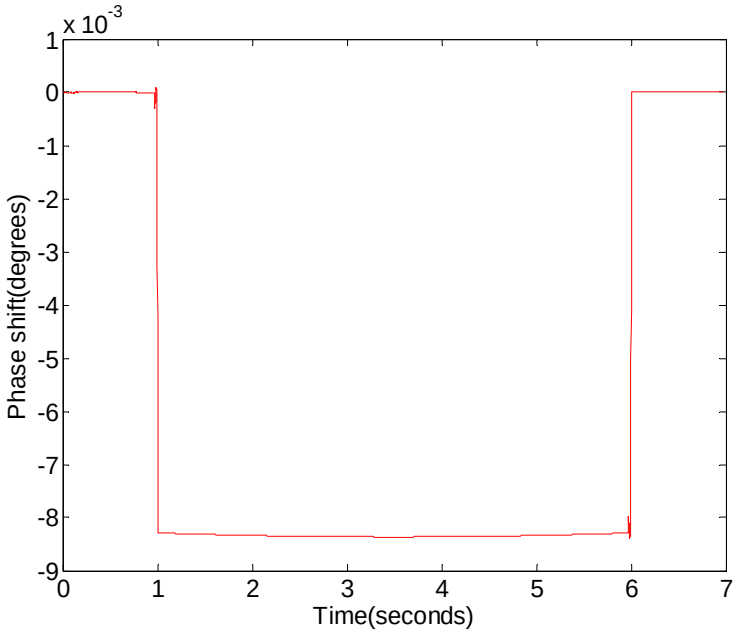

Figure 3.16 Phase shift (w/ compensation, phasor at center of window)

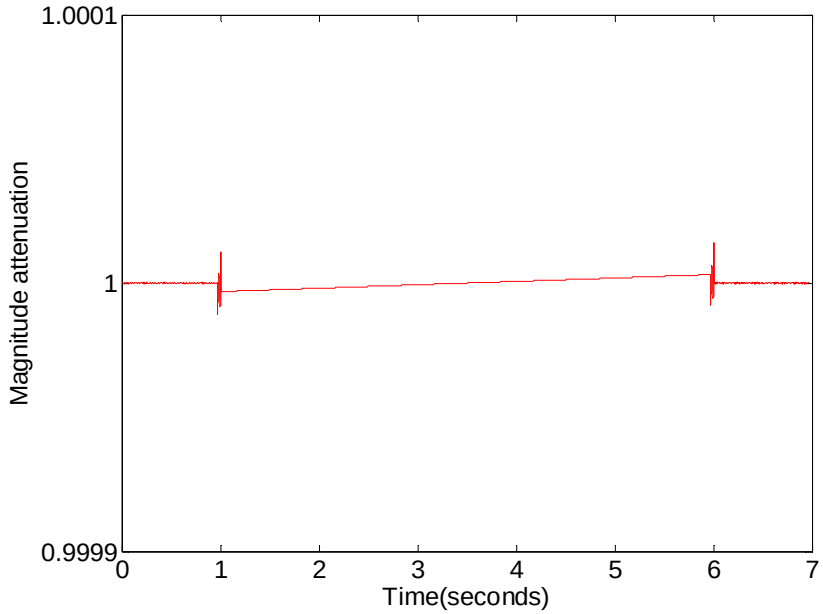

Figure 3.17 Magnitude attenuation (w/ compensation, phasor at center of window)

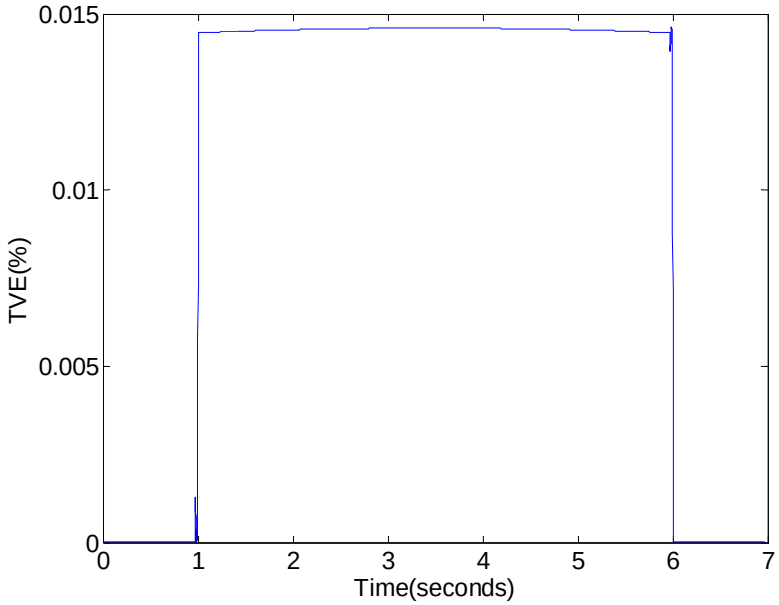

Figure 3.18 TVE (w/ compensation, phasor at center of window)

3.4 Unbalance Issues

Power systems are designed to operate with balanced conditions, but there are always unbalanced conditions due to uneven distribution of single-phase loads or unbalanced faults. All previous analysis is based on three-phase balanced systems. In this section, we explore the effect of unbalanced signals on the phasor and frequency estimation.

Assume three-phase unbalanced signals as shown in equation (3.13) with the frequency as shown in Figure 3.19.

$$\begin{aligned} V_a(t) &= V_m \cos(2\pi f t + \varphi) \\ V_b(t) &= V_m \cos(2\pi f t + \varphi - 2\pi/3) \\ V_c(t) &= 0.9V_m \cos(2\pi f t + \varphi + 2\pi/3) \end{aligned} \tag{3.13}$$

Applying the synchronized frequency measurement method proposed in section 2.2, the errors between actual and measurement frequency are computed and shown in Figure 3.20. Neglecting the two big spikes caused by dramatic frequency change, we can see oscillation in the frequency measurement. The oscillation for fixed off-nominal frequency is constant as shown in Figure 3.21, while the oscillation for changing frequency changes

as shown in Figure 3.22. The oscillation frequency is around 120 Hz.

If the system is not balanced, equation (3.5) can be rewritten as

$$\begin{aligned}\mathbf{X}_1 &= \frac{1}{3}(\mathbf{X}_a + \alpha\mathbf{X}_{b+}\alpha^2\mathbf{X}_c)\\ &= \frac{1}{3N}\sum_{k=0}^{N-1}\Big[\left(\mathbf{X}_{\mathrm{a}}e^{\mathrm{jk}\omega\Delta\mathrm{t}} + \mathbf{X}_{\mathrm{a}}{}^{*}e^{-\mathrm{jk}\omega\Delta\mathrm{t}}\right) + \alpha\left(\mathbf{X}_{\mathrm{b}}e^{\mathrm{jk}\omega\Delta\mathrm{t}} + \mathbf{X}_{\mathrm{b}}{}^{*}e^{-\mathrm{jk}\omega\Delta\mathrm{t}}\right)\\ &\qquad + \alpha^2\left(\mathbf{X}_{\mathrm{c}}e^{\mathrm{jk}\omega\Delta\mathrm{t}} + \mathbf{X}_{\mathrm{c}}{}^{*}e^{-\mathrm{jk}\omega\Delta\mathrm{t}}\right)\Big]e^{-\mathrm{jk}\omega_{\mathrm{N}}\Delta\mathrm{t}}\\ &= \frac{1}{3N}\sum_{k=0}^{N-1}\Big[(\mathbf{X}_{\mathrm{a}} + \alpha\mathbf{X}_{\mathrm{b}} + \alpha^2\mathbf{X}_{\mathrm{c}})e^{\mathrm{jk}\omega\Delta\mathrm{t}}\\ &\qquad + \left(\mathbf{X}_{\mathrm{a}}{}^{*} + \alpha\mathbf{X}_{\mathrm{b}}{}^{*} + \alpha^2\mathbf{X}_{\mathrm{c}}{}^{*}\right)e^{\mathrm{jk}\omega\Delta\mathrm{t}}\Big]e^{-\mathrm{jk}\omega_{\mathrm{N}}\Delta\mathrm{t}}\\ &= \frac{1}{N}\sum_{k=0}^{N-1}\left[\mathbf{X}_{1\mathrm{actual}}e^{\mathrm{jk}(\omega-\omega_{\mathrm{N}})\Delta\mathrm{t}} + \mathbf{X}^{*}_{2\mathrm{actual}}e^{-\mathrm{jk}(\omega+\omega_{\mathrm{N}})\Delta\mathrm{t}}\right]\end{aligned} \tag{3.14}$$

where $\mathbf{X}_{1\mathrm{actual}}$ is the actual positive sequence value and $\mathbf{X}^{*}_{2\mathrm{actual}}$ is the actual negative sequence value. When system is balanced, $\mathbf{X}^{*}_{2\mathrm{actual}}$ is zero. However, when system is unbalanced, $\mathbf{X}^{*}_{2\mathrm{actual}}$ is not zero, and this component is multiplied by a vector whose frequency is $(\omega + \omega_{\mathrm{N}})$. This explains why frequency measurements oscillate at around 120Hz when system is not balanced. At off-nominal frequency, the positive and negative sequence components of the input signals create false negative and positive sequence components respectively, which introduce errors in the estimate of the positive and negative sequence components. Zero sequence component alone makes error contribution to the zero sequence estimate. [50] [51]

Knowing the origin of the oscillation, filters can be designed to minimize this effect. For example, an average filter could be applied [50] . The least-squares estimation introduced in section 2.3 also has ability of averaging. Least-square estimation can be used to minimize the oscillation with a window size selected to be multiples of 1/120 s. Figure 3.23 shows the errors obtained when the least-squares estimation is performed as described. Compared with the results without LS estimation as shown in Figure 3.20, LS

estimation minimize the oscillation greatly and the errors are very close to zero except for the spikes which is mainly caused by dramatic frequency change.

With the frequency oscillation minimized, we can now perform the frequency based phasor compensation proposed in section 3.2. Figure 3.24, Figure 3.25 and Figure 3.26 show the phase shift, magnitude attenuation and TVE, respectively. The biggest phase shift is below 0.2 degrees, and the magnitude attenuation is within 0.15%. Although unbalance together with frequency dynamics make the synchronized measurements much more complicated, the errors can still be maintained within reasonable range with the methods described in this work.

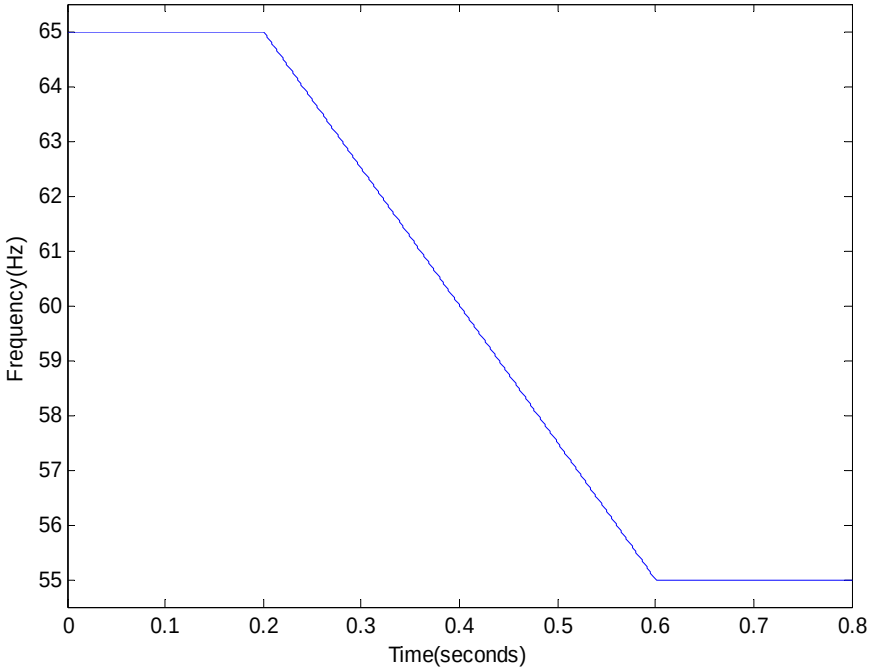

Figure 3.19 Actual frequency for three-phase unbalanced signals

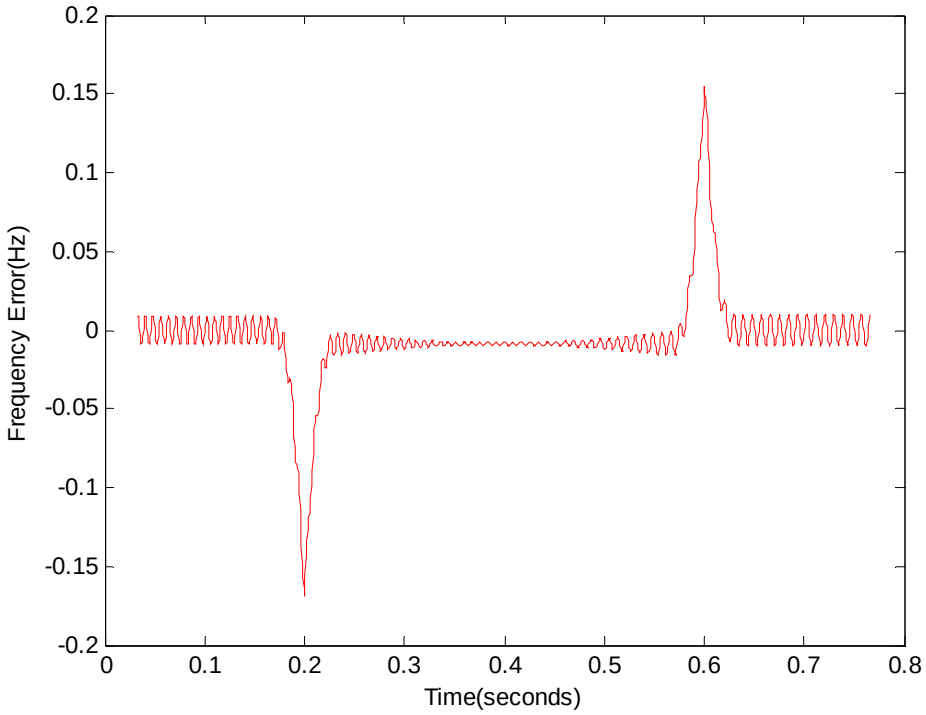

Figure 3.20 Frequency errors for unbalanced signals

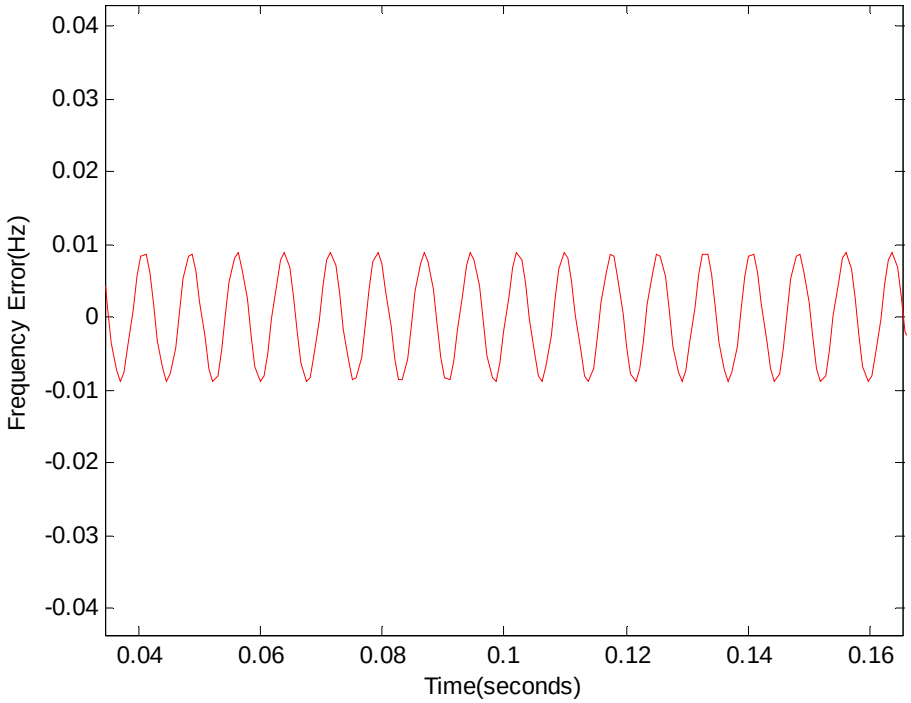

Figure 3.21 Frequency errors for unbalanced signals with frequency at 65Hz

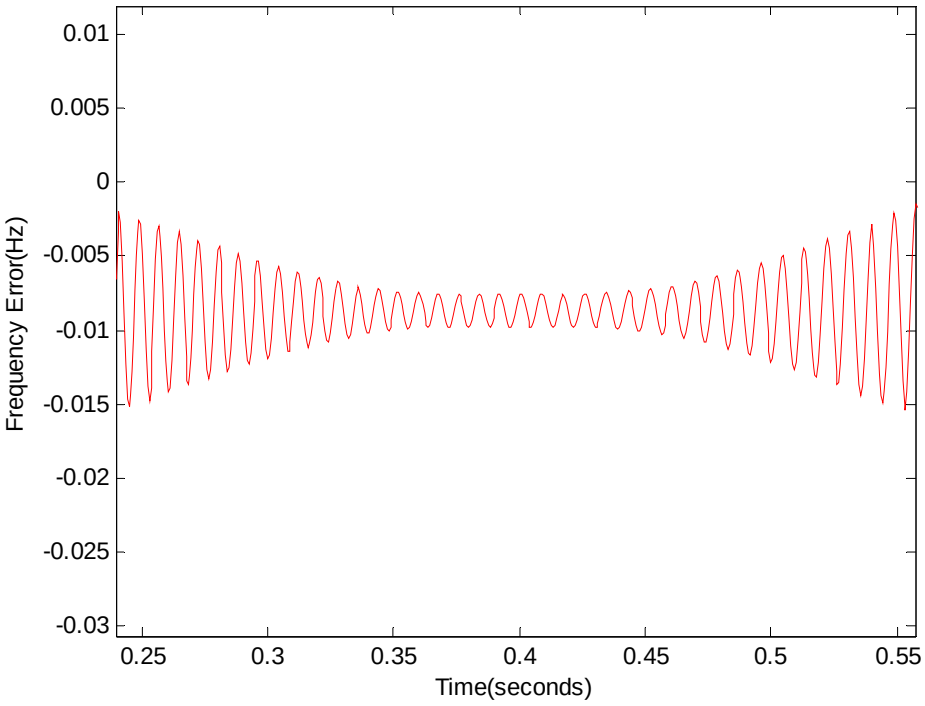

Figure 3.22 Frequency errors for unbalanced signals with changing frequency

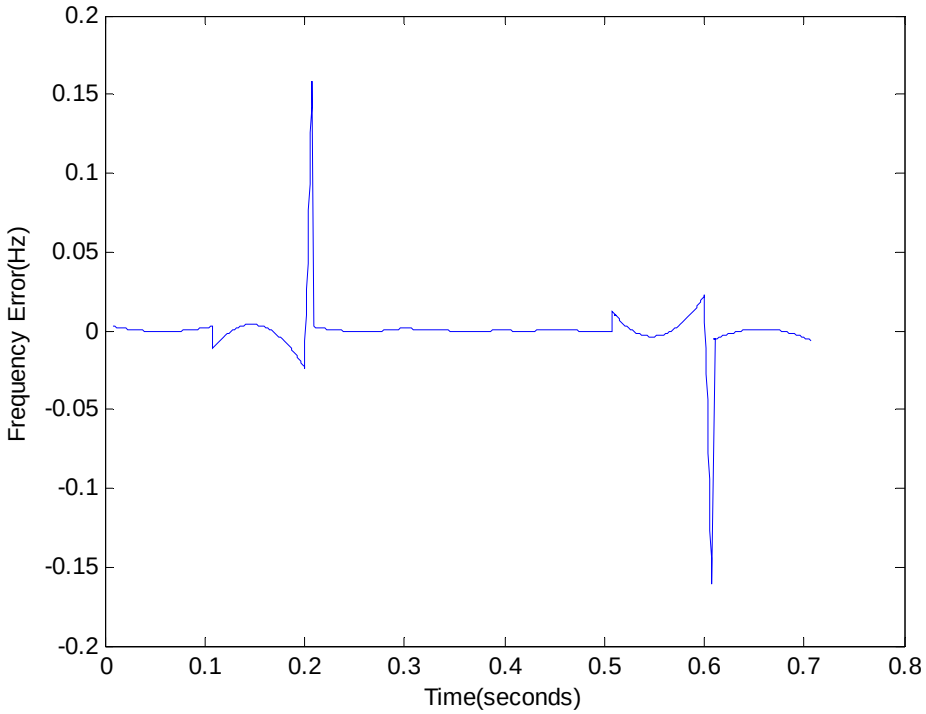

Figure 3.23 Frequency errors with LS estimation

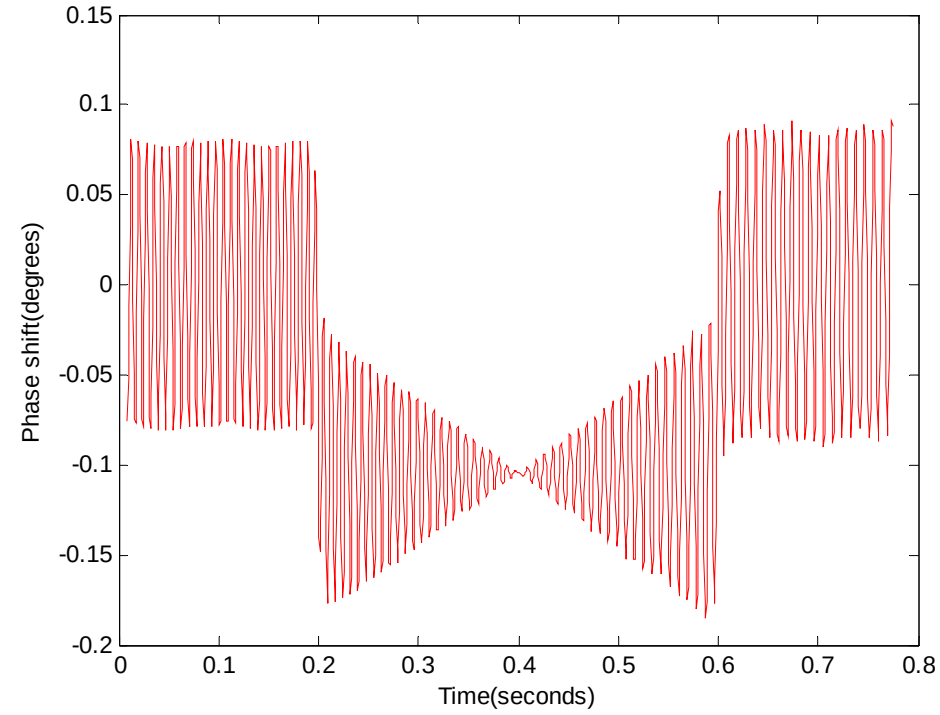

Figure 3.24 Phase shift for unbalanced signals

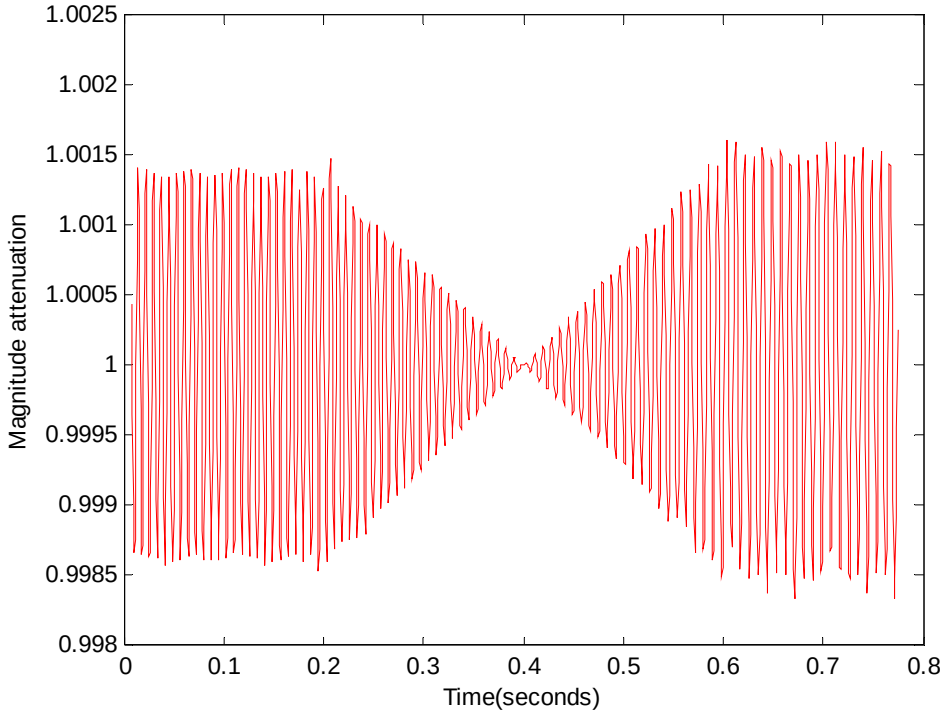

Figure 3.25 Magnitude attenuation for unbalanced signals

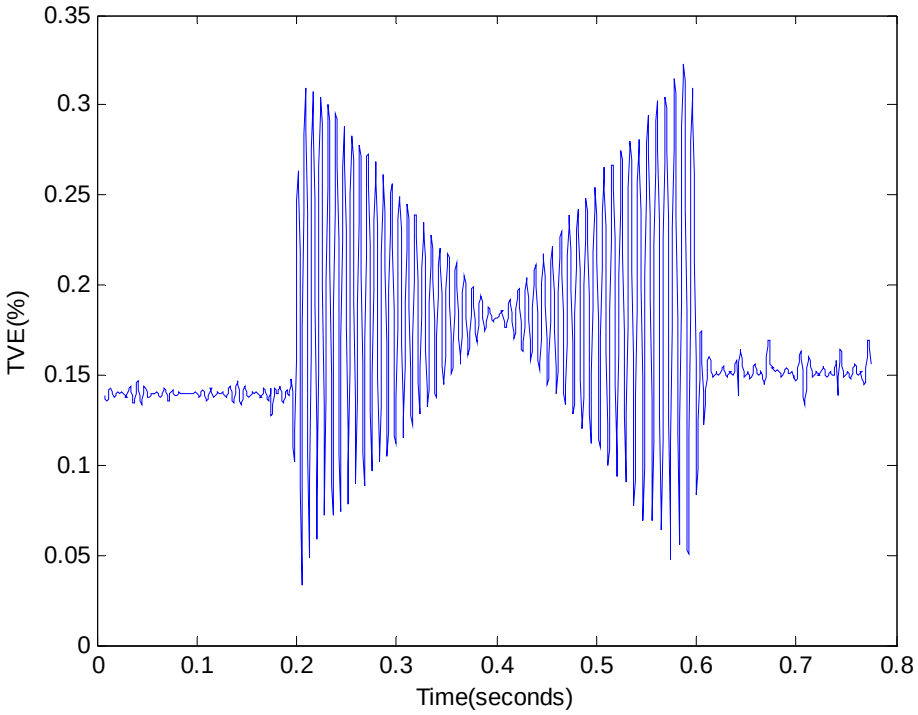

Figure 3.26 TVE for unbalanced signals

Chapter 4
General Applications

The past few years have witnessed an increased interest in synchronized measurements in power systems. The state-of-the-art technology permits monitoring, analyzing and controlling the system on a scale not previously possible. North American SynchroPhasor Initiative (NASPI, previously EIPP) leads the efforts of implementation and application of synchronized measurements in power systems. This increased interest has resulted in increased attention on the dynamic performance of synchronized measurements to make sure different hardware and different algorithms yield functionally the same measurements.

The previous chapters of this dissertation focus on the effects of algorithms on dynamic performance of synchronized measurements. Some key problems of synchronized measurements under dynamic conditions are analyzed, and corresponding solutions are proposed. Improved synchronized measurements guarantee an accurate observation of the system states. This chapter will point to some general applications of synchronized measurements under dynamic conditions. Since it is not practical to enumerate every possible application, in this chapter, only two general scenarios for applications are introduced and analyzed. One scenario is the effects of small frequency disturbances; the other is the effects of large frequency disturbances in synchronized measurements. Chapter 5 will point the application to a very detailed topic — out-of-step protection.

4.1 Power System Frequency Dynamics

The frequency of a power system is dependent on the electrical angular velocity of synchronous generators. The combined inertia of the generator and prime mover is accelerated by the unbalance in the applied torques. Hence, the swing equation is

$$J\frac{d\omega_m}{dt} = T_a = T_m - T_e \tag{4.1}$$

where

J : combined moment of inertia of generator and turbine

ω_m: angular velocity of the rotor in mechanical rad/s

T_m: mechanical torque

T_e: electromagnetic torque

T_a: accelerating torque

Multiplying both sides of above equation by angular velocity ω_m gives

$$J\omega_m\frac{d\omega_m}{dt} = \omega_m(T_m - T_e) = P_m - P_e \tag{4.2}$$

The above equation can be normalized in terms of per unit inertia constant H, defined as the kinetic energy in watt-seconds at rated speed divided by the apparent power base S_{base}. Using ω_{nm} to denote the nominal angular velocity in mechanical rad/s, the inertia constant is

$$H = \frac{J{\omega_{nm}}^2}{2S_{base}} \tag{4.3}$$

The moment of inertia in terms of H is

$$J = \frac{2HS_{base}}{{\omega_{nm}}^2} \tag{4.4}$$

Substituting equation (4.4) in equation (4.2) gives

$$\frac{2HS_{base}}{{\omega_{nm}}^2}\omega_m\frac{d\omega_m}{dt} = P_m - P_e \tag{4.5}$$

Noting that

$$\omega_m = \frac{\omega}{p} \tag{4.6}$$

and

$$\omega_{nm} = \frac{\omega_n}{p} \tag{4.7}$$

where

p : number of poles

ω_n: nominal angular velocity of the rotor in electrical rad/s

ω: angular velocity of the rotor in electrical rad/s

Equation (4.5) can be rearranged as

$$\frac{2HS_{base}}{{\omega_n}^2}\omega\frac{d\omega}{dt} = P_m - P_e \tag{4.8}$$

Thus frequency f can be solved from the following differential equation

$$\omega\frac{d\omega}{dt} = \frac{{\omega_n}^2(P_m - P_e)}{2HS_{base}} \tag{4.9}$$

If the right side of equation (4.9) is constant, frequency can be solved analytically as

$$\omega = \sqrt{\frac{{\omega_n}^2(P_m - P_e)}{HS_{base}}t + \omega_0} \tag{4.10}$$

where ω_0 is the angular frequency at t=0. Therefore, the frequency will decrease continuously when mechanical power is less than electromagnetic power. However, there are some frequency-dependent loads in real systems where P_e is not constant, and can be express as a function of frequency. Normally, P_e decreases when frequency drops. Thus, when generation decreases, frequency may still stabilize at some level due to the load adjustment. Furthermore, the interaction of generator governors, exciters, automatic generation control (AGC), and dynamic load make equation (4.9) much more complicated requiring it to be solved by numeric iteration techniques.

Failure to match generation to demand causes the frequency of an AC power system to increase or decrease. Random small variations in frequency are normal, as loads come on and off and generators modify their output to follow the demand changes. However, large deviations in frequency may happen due to unexpected events.

4.2 Scenarios with Small Frequency Disturbance

In light of the frequency differential equation, any load-generation unbalance will cause frequency disturbance. The severity of the unbalance determines how big the frequency disturbance is. This section discusses the application scenarios with small frequency disturbance.

Small frequency disturbance means either small frequency deviation or small rate of change of frequency. Power systems are dynamic systems, and there are many expected and unexpected events which could cause slight change in the power flow. Control actions will try to bring the system to an acceptable state. This process involves small frequency disturbance, which can lead to errors in synchronized measurements.

Using the one-cycle DFT, Figure 4.1, Figure 4.2 and Figure 4.3 show the phase shift, magnitude attenuation and TVE with different frequency values. Figure 4.4 shows the frequency measurement errors with different rate of change of frequency. It has to be pointed out that the size of frequency calculation window and positioning will affect these errors. Here we use six-cycle window and assign the frequency at the beginning of the window. From these figures, we can see the errors could be very small with small frequency disturbance. Furthermore, the methods proposed in chapter 2 and 3 can still eliminate or reduce these small errors and improve the precision of synchronized measurements.

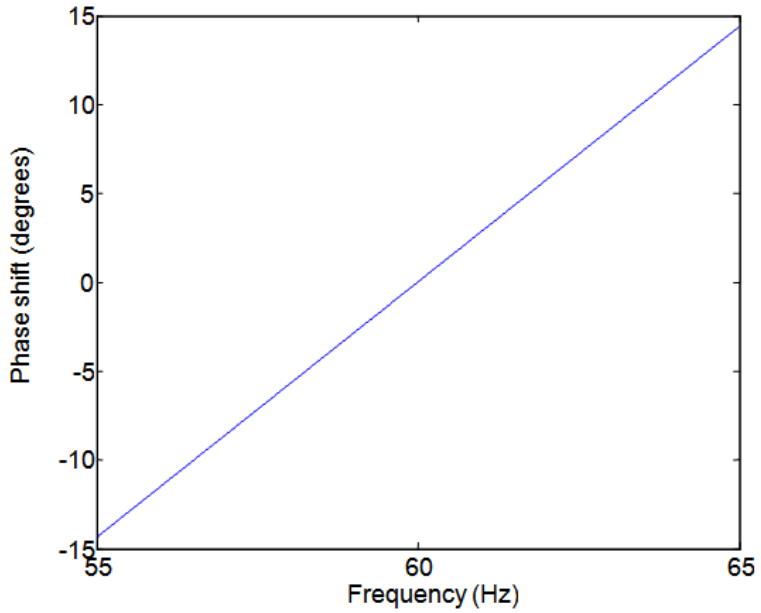

Figure 4.1 Phase shift vs. frequency

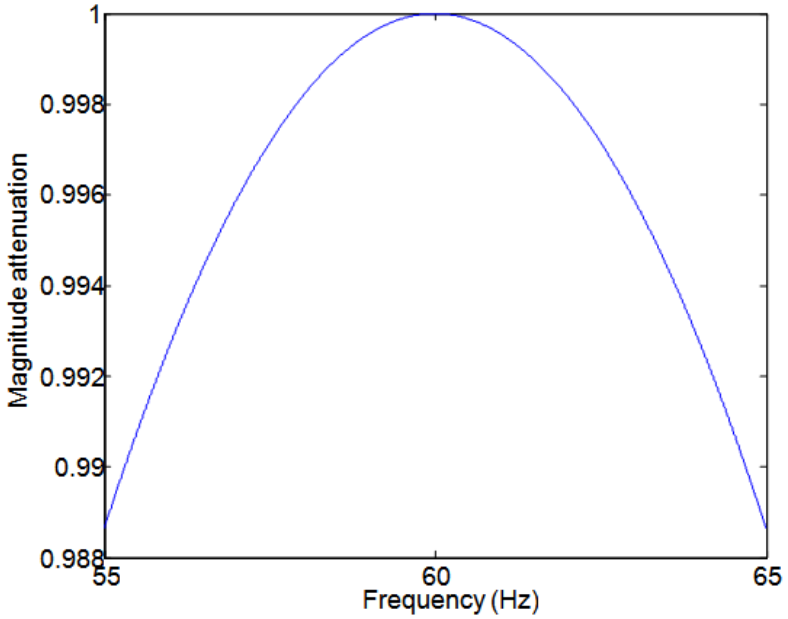

Figure 4.2 Magnitude attenuation vs. frequency

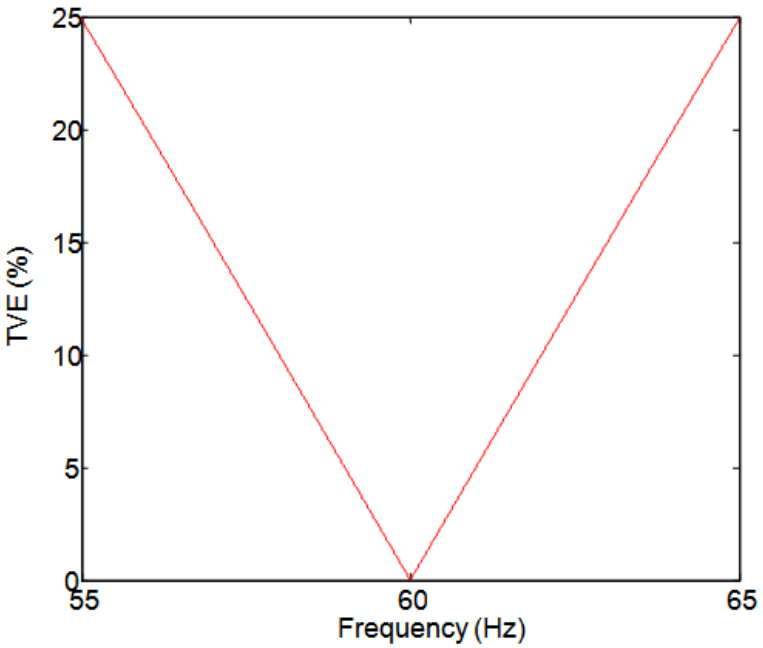

Figure 4.3 TVE vs. frequency

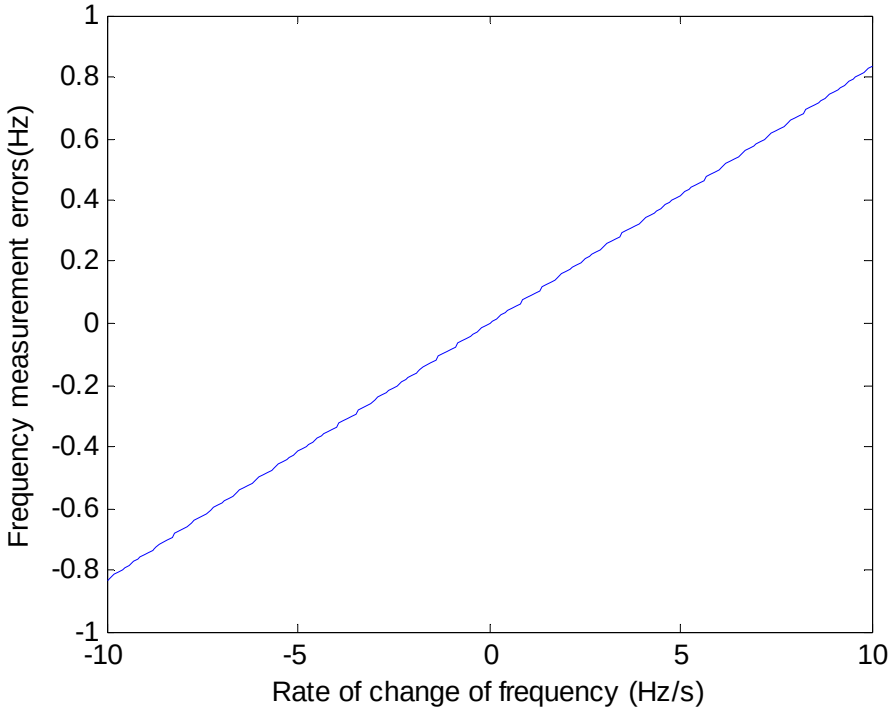

Figure 4.4 Frequency measurement errors vs. rate of change of frequency

4.3 Scenarios with Large Frequency Disturbance

This section discusses the application scenarios with large frequency disturbance. Large frequency disturbance could be either big frequency deviation or big rate of change of frequency. Severe load-generation unbalance, cascading events, or controlled islanding may lead to very large frequency disturbance. Some major blackouts in power systems are indeed featured with very large frequency disturbance. Figures 4.1 through 4.4 do show that large frequency disturbance may lead to wrong measurements. The following parts of this section will give some real and simulated examples where large frequency disturbance happens.

4.3.1 2003 US-Canada Blackout

The US-Canada blackout of August 14, 2003 affected approximately 50 million people in eight US states and two Canadian provinces. Roughly 63 GW of load was interrupted, which equates to approximately 11% of the total load served in the Eastern Interconnection of the North American system. During this event, over 400 transmission lines and 531 generating units at 261 power plants tripped. It is now evident that a series of events in northern Ohio that began earlier in the day resulted in a rapid succession of severe power swings, voltage depression, and frequency oscillations. [58] [59] [60]

After the New York grid separated with NJ, NE, and Ontario grid, the system frequency underwent large change. The highest recorded frequency is about 63Hz, and the lowest around 57Hz. In reality the frequency in east New York was at free fall. Although the rate of change of frequency is not so large, the frequency deviation is extremely large. Under this situation, synchronized measurements may contain large leakage errors if there is no appropriate technique applied to correct them. Those methods proposed in previous chapters can help obtain accurate synchronized measurements under these extreme circumstances. A true picture of the system state reflected by accurate measurements is indispensable to record, analyze, and even mitigate the blackouts.

4.3.2 Mexican Blackout

At the local time of 06:27:35 on January 1, 2004, undamped inter-area oscillations

were observed throughout the northern portions of the Mexican interconnected system (MIS). These oscillations involved severe frequency, voltage, and power changes throughout the northern systems and resulted in load shedding and the disconnection of major equipment. Power oscillations were in the order of 300 MW on some major interconnections and continued for several minutes before damping out. The events that initiated the oscillations included a failed temporary interconnection of the Northwest regional system to the MIS through a 230-kV line. Prior to this temporary interconnection, the Northwestern system operated as an electrical island. After the tie line was connected, undamped inter-area oscillations were observed throughout the system. These were in the order of 250 MW in the main interconnection and continued for some minutes before damping out. As a consequence, protective relays operated, tripping about 140MWof load and three generating units in order to compensate for the imbalance caused by system oscillations. The line was finally disconnected. [62]

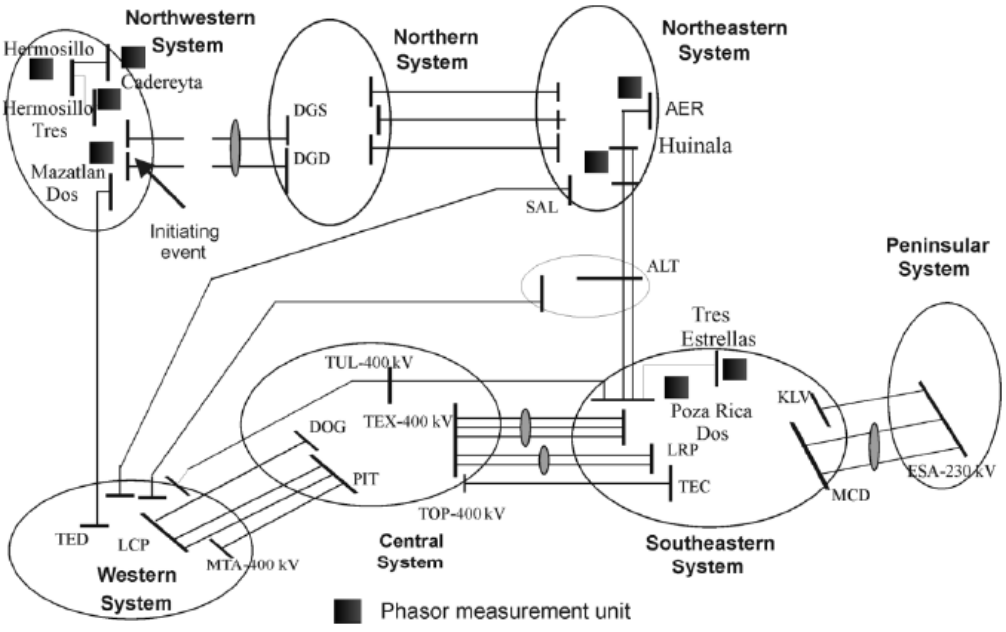

Figure 4.5 Mexican interconnected system

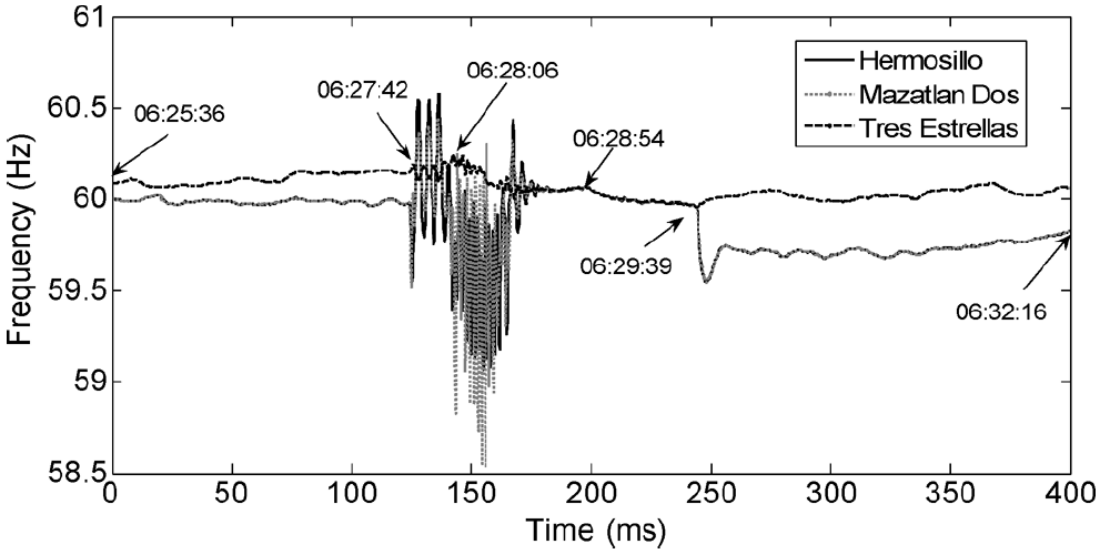

Figure 4.6 Time traces of recorded frequencies

Figure 4.6 shows the recorded frequency disturbance. We do not know whether this frequency measurement is perfect or not, but most frequency measurement units have good performance during quasi steady state. The system states within (180-230 ms) and (280-330 ms) are relatively steady. But the frequency difference between the two states is very large. Based on this analysis, we could conclude there is a large rate of change of frequency around 250 ms. As stated before, big rate of change of frequency will also lead to errors in synchronized measurements. So correction techniques have to be applied to obtain better measurements during dynamics.

4.3.3 Simulated Case

Synchronized measurements cannot reflect the actual system state with severe dynamics, and may lead to catastrophic results if applied in system protection and control at that moment. This subsection gives an example simulated in PSS/E. The test system, as shown in Figure 4.7, has the generation and load listed in Table 4.1 and Table 4.2. Generator-102, which is an important generator for the system real power support, is tripped to produce the disturbance. The dynamic data from PSS/E simulations are outputted to a text data file, which is read into Matlab and reprocessed.

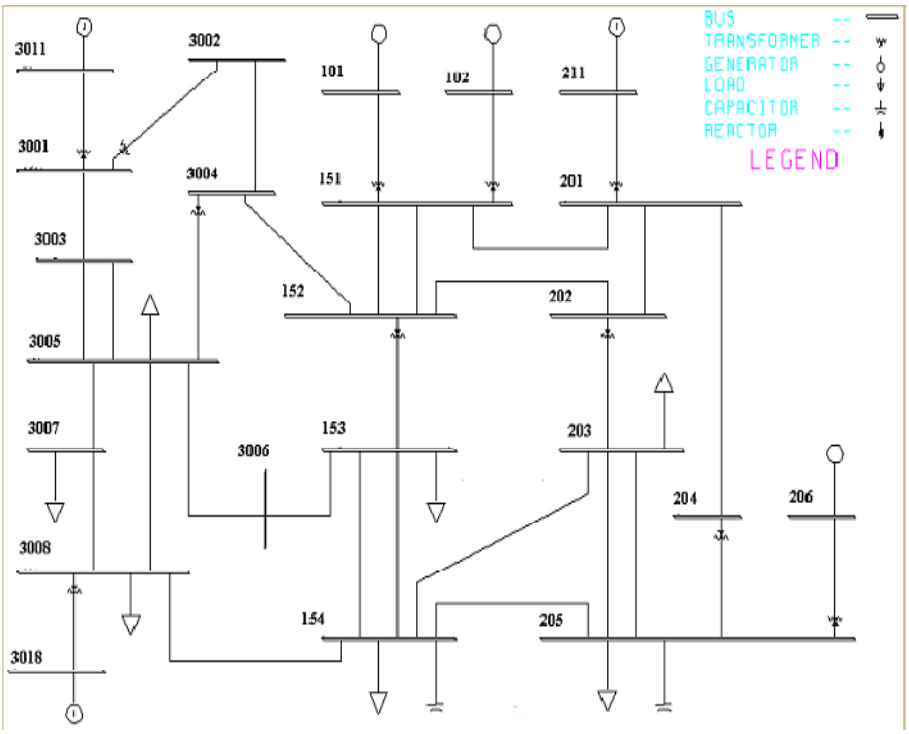

Figure 4.7 Test system

Table 4.1 Generation power outputs

Gen Bus No.	P_G (MW)	P_G%	Q_G (MVAR)	Q_G%
101	753	23.1	81	8.4
102	753	23.1	87	9
206	800	24.6	600	62.2
211	600	18.4	17	1.8
3011	258	7.9	104	10.8
3018	100	3.1	80	8.3

Table 4.2 Load injection

Load Bus No.	P_L (MW)	P_L %	Q_L (MVAR)	Q_L %
153	200	6.3	100	5.1
154	1000	31.3	800	41
203	300	9.4	150	7.7
205	1200	37.5	700	35.9
3005	100	3.1	50	2.6
3007	200	6.3	75	3.8
3008	200	6.3	75	3.8

When Generator-102 (753MW, 23.1%) is tripped at 0.3 second, the system undergoes real power deficiency, and the real power reserve of other generators is not enough to meet this shortage. The frequencies at bus 101 and 3011, shown in Figure 4.8, will both decrease and then stabilize around at 55.31Hz. The two frequency curves are almost the same, so they overlap. Figure 4.9 shows the actual relative phase angles between bus 101 and bus 3011. After the disturbance, the phase angle oscillates for a period of time, and then stabilizes at a new value.

Suppose a PMU with perfect measurements, is installed at bus 101. The phasors measured by this PMU always reflect the actual values even though the system frequency deviates from the nominal values. Another PMU without any correction for frequency dynamics is installed at bus 3011. The phasors measured by this PMU cannot reflect the actual values when system frequency deviates from the nominal value because nominal frequency based DFT and fixed samples are still used. Take the data from PSS/E, and we can perform calculations and simulate the above two PMUs in Matlab. Figure 4.10 shows the measured and actual relative phase angles between bus 101 and 3011. We can see that the measured value cannot reflect the actual value during the dynamics, and the measured value increases gradually. The system undergoes a stable oscillation and attains a new steady state, but the measured relative phase angle shows an unstable oscillation. Out-of-step protection may take false action, and we have to deal with it with caution.

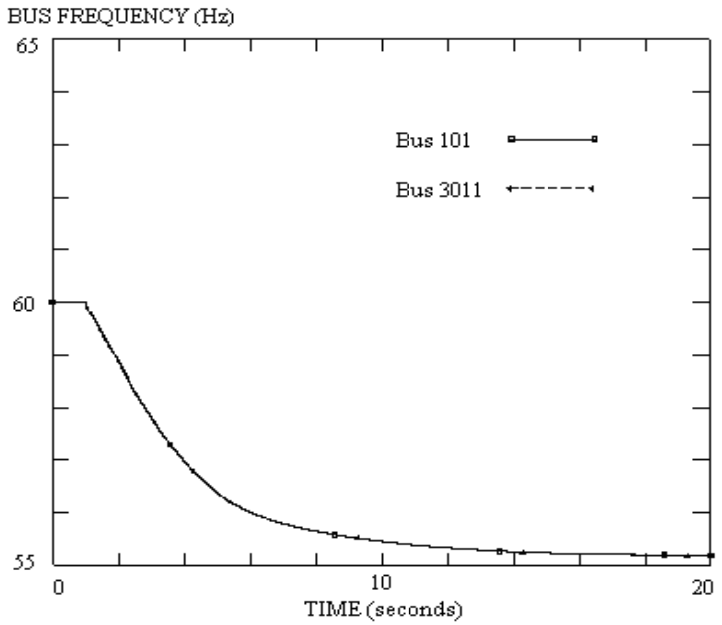

Figure 4.8 Frequency response

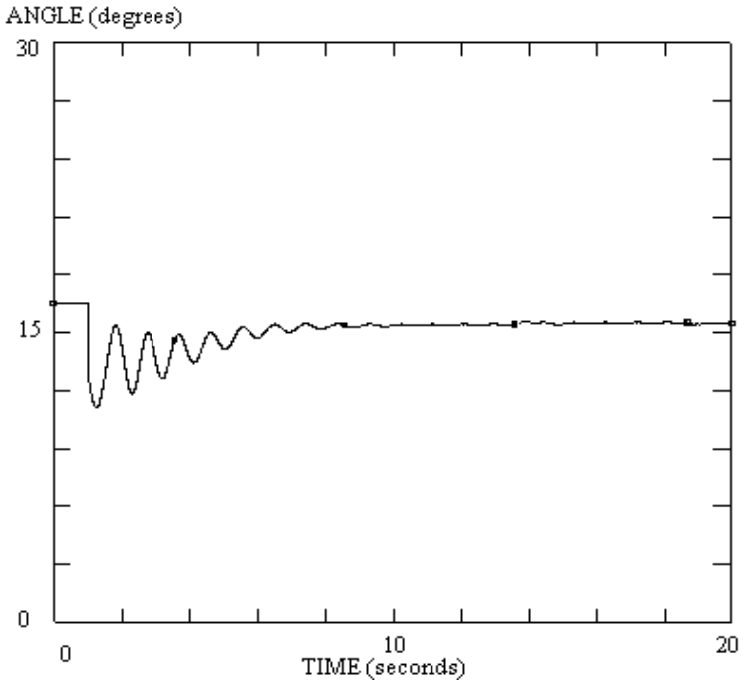

Figure 4.9 Actual relative phase angle between bus 101 and 3011

Applying the correction method proposed in previous chapters, we can get the corrected relative phase angles as shown in Figure 4.11. During the dynamic process, the corrected relative phase angle can almost follow the actual value except for the initial jumps where the disturbance occurs suddenly.

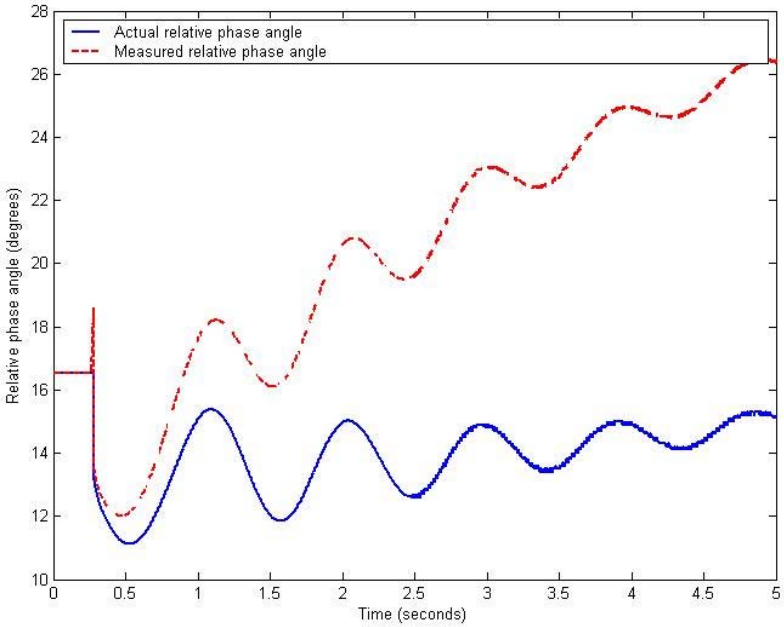

Figure 4.10 Relative phase angle dynamics after tripping Gen. 102

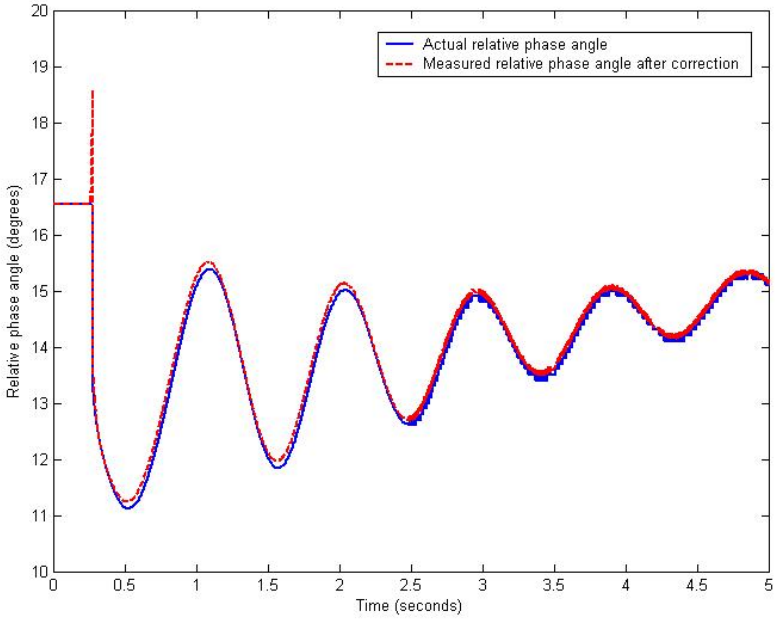

Figure 4.11 Relative phase angle dynamics after tripping Gen. 102 with compensation

Chapter 5
Adaptive Out-of-Step Protection Using Wide Area Measurements

Power system faults, line switching, generator tripping, load rejection and connection of large amount of load result in sudden changes in electromagnetic power. The generator governors cannot respond to this change quickly, and the prime movers cannot adjust the output without limits allowing us to assume that for the time window under consideration the mechanical power input to generators remains relatively constant. The unbalance between mechanical and electromagnetic powers causes oscillations in machine rotor angles and power flow swings. Depending on the severity of the disturbance and the actions of power system controls, the system may attain a new operating equilibrium point experiencing what is referred to as a stable power swing. Sever disturbances may cause large excursion of generator rotor angles, large swings of power flow, large fluctuation of voltage and current and even loss of synchronism. Large power swings, stable or unstable, can lead to device damage as well as inappropriate relay operation, which will cause more disturbance and possibly cascading outages and power blackouts. Therefore, power swings have to be monitored for safe operation of bulk power systems. Preventive control actions could be taken to mitigate severe power swings. Furthermore, emergency control actions, such as out-of-step (OOS) protection, could be taken to separate the system into several islands to prevent the propagation of severe disturbance and limit load outage.

This chapter takes out-of-step protection as an application example of using synchronized measurements under dynamic conditions. It reviews the existing out-of-step protection schemes. Then adaptive out-of-step protection with wide area measurements is developed. Two schemes are investigated to detect the out-of-step condition. One is based on the swing curves, and the other is based on real-time extended equal area

criteria (EEAC). Both of them require identifying the groups of coherent generators, so coherency identification is also introduced in this chapter.

5.1 Out-of-Step Protection Review

Many techniques have been proposed to detect out-of-step condition [63] - [87] . This section discusses a number of major power-swing detection methods used for out-of-step protection. It covers traditional detection methods based on the rate of change of impedance or resistance and newer methods used in microprocessor-based relays.

5.1.1 Apparent Impedance Based Out-of-Step Protection

Impedance relays are initially used to implement out-of-step protection. Normally voltage and current phasors measured locally are used to compute the apparent impedance.

5.1.1.1 Apparent Impedance during Power Swings

For a simple two-source power system as shown in Figure 5.1, an impedance relay is installed at bus A.

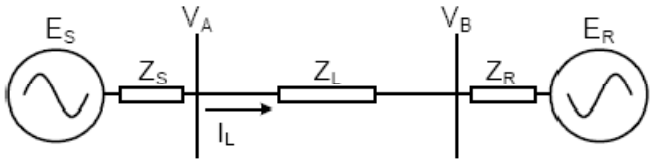

Figure 5.1 Two-generator power system

The apparent impedance measured at bus A is

$$Z = \frac{V_A}{I_L} = \frac{E_S(Z_S + Z_L + Z_R)}{E_S - E_R} - Z_S \tag{5.1}$$

Assuming that E_S has a phase advance of δ over E_R and that the ratio of the two source voltage magnitude $E_s/E_R = k$, we would then have

$$\frac{E_S}{E_S - E_R} = \frac{k(\cos\delta + j\sin\delta)}{k(\cos\delta + j\sin\delta) - 1} \tag{5.2}$$

For the particular case where the magnitudes are equal, we have k=1. Equation (5.1) can be expressed as

$$Z = \frac{V_A}{I_L} = \frac{(Z_S + Z_L + Z_R)}{2}\left(1 - cot\frac{\delta}{2}\right) - Z_S \qquad (5.3)$$

The trajectory of the measured impedance in equation (5.3) during a power swing when the angle between the two source voltages varies corresponds to the straight line that intersects the segment A to B at its middle point as shown in Figure 5.2 (a). This point is called the electrical center of the swing. The angle between the two segments that connect P to points A and B is equal to the angle δ. When the angle δ reaches the value of 180 degrees, the impedance is precisely at the location of the electrical center. It can be seen that the impedance trajectory during a power swing will cross any relay characteristic that covers the line, provided the electrical center falls inside the line. In situations where k, the ratio of the sources magnitudes, is not one, it can be demonstrated that the impedance trajectory will be like those curves as shown in Figure 5.2 (b). [64]

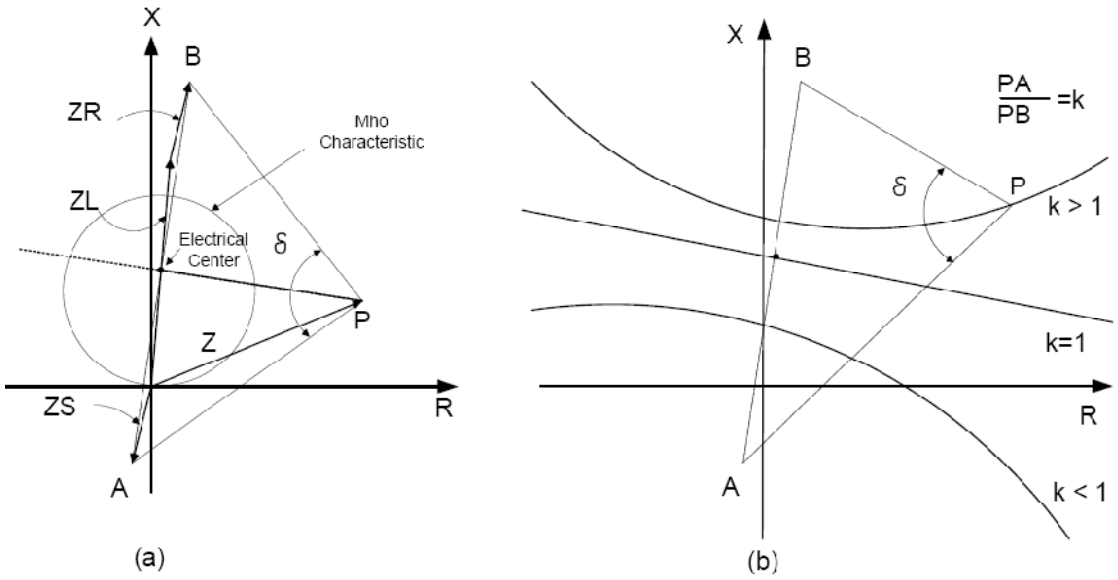

Figure 5.2 Impedance trajectory during power swings

5.1.1.2 Apparent Impedance Based OOS Protection Implementation

Conventional out-of-step protection schemes are based mostly on measuring the

positive-sequence impedance at the relay location. During normal system operating conditions, the measured impedance is the load impedance, and its locus is away from the distance relay protection characteristics. When a fault occurs, the measured impedance moves immediately from the load impedance location to the location that represents the fault on the impedance plane. During a system swing, the measured impedance moves slowly on the impedance plane, and the rate of impedance change is determined by the slip frequency of an equivalent two-source system. Therefore, difference between impedance rate of change can be used to differentiate between a fault and a swing.

To accomplish this, two concentric impedance circles or blinders, shown in Figure 5.3, are used. If the measured impedance enters the outer zone, a timer starts. If it enters the inner zone before timer runs out, a fault is declared. If it enters the inner zone after timer runs out, an unstable power swing is declared. If it never enters the inner zone, a stable power swing is declared. [64]

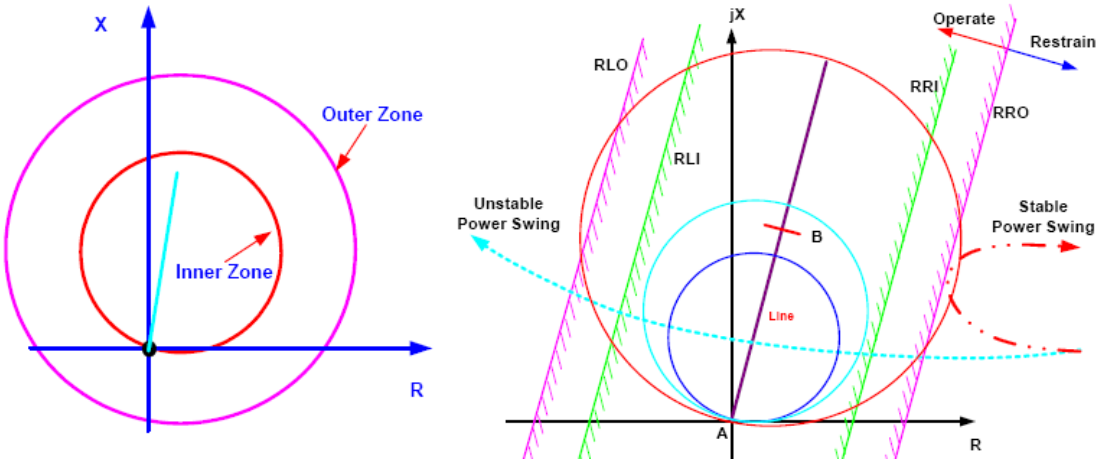

Figure 5.3 Out-of-step relay

Although it is easy to use local measurements to implement out-of-step protection, there are many limitations for out-of-step protection based on apparent impedance. The settings obtained from simulations become outdated once the conditions assumed for simulations become outdated. Real disturbances are different from those used in simulations, and incorrect operation tends to exacerbate out-of-step problem.

5.1.2 R-Rdot Out-of-Step Protection

An out-of-step relay described in references [85] [86] was applied in the US Pacific NW-SW 500 kV AC Intertie. This scheme was augmented with the rate of change of apparent resistance and it was termed as the R-Rdot scheme.

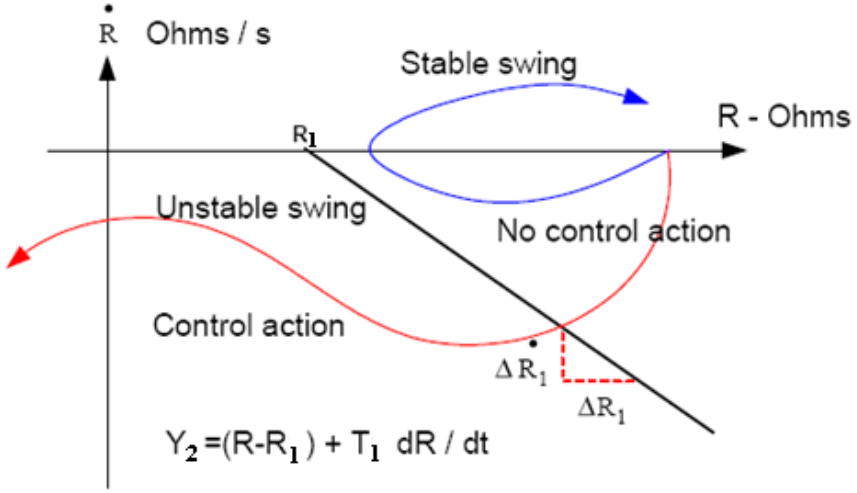

Figure 5.4 R-Rdot scheme

The above characteristic of the R-Rdot relay can be best visualized in the R-Rdot phase-plane shown in Figure 5.4. The R-Rdot relay develops an output when the power-swing trajectory crosses a "switching line" in the R-Rdot plane. Switching line Y_2 is a straight line having slope T_1 in the R-Rdot plane. System separation is initiated when output Y_2 becomes negative. For low separation rates (small dR/dt) the performance of the R-Rdot scheme is similar to the conventional apparent impedance based out-of-step relaying schemes. However, higher separation rates dR/dt would cause a larger negative value of Y_2 and will initiate tripping much earlier. In the actual implementation, the relay uses a piecewise linear characteristic.

Although R-Rdot scheme can initiate an earlier decision, it still uses apparent impedance, and still has those limitations for apparent impedance based out-of-step schemes.

5.1.3 Swing-Center Voltage and Its Rate of Change

Swing-center voltage (SCV) is defined as the voltage at the location of a two-

source equivalent system where the voltage value is zero when the angles between the two sources are 180 degrees apart. When a two-source system loses stability after some disturbance, the angle difference of the two sources will increase as a function of time. Figure 5.5 illustrates the voltage phasor diagram of a general two-source system. An approximation of the SCV can be obtained through the use of locally available quantities as follows

$$\text{SCV} \cong |V_s| cos\varphi \tag{5.4}$$

where $|V_s|$ is the magnitude of locally measured voltage, and φ is the angle difference between local voltage and current. For a homogeneous system with the system impedance angle θ close to 90 degrees, this approximates well the magnitude of the swing-center voltage. For the purpose of power-swing detection, the rate of change of the SCV provides the main information of system swings since swing center voltage is a function of δ. Similarly, real power is also a function of δ , so real power and its rate of change can also be used to do out-of-step detection.

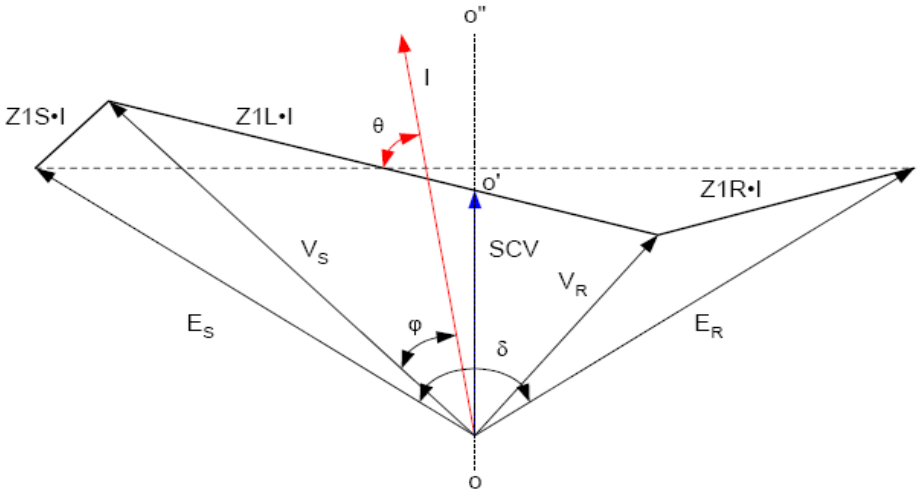

Figure 5.5 Voltage phasor diagram of a two-source system

5.1.4 Frequency Based Out-of-Step Protection

A recent paper proposed a very new idea to use angular frequency and its rate of change to detect the out-of-step condition [87] . When a disturbance occurs in one machine infinite bus (OMIB) system, the power angle swings in the sequence as shown in Figure 5.6 and Figure 5.7. The swings in angular frequency and its acceleration

coordinates are also drawn in those two figures. Table 5.1 shows the relationships between power angle swings and operation points. The difference of the swing curve in the coordinate of angular frequency and its rate of change can be used to differentiate between stable swings and unstable swings. A problem with this scheme is to determine the angular frequency ω_0, especially if there is load generation unbalance, where ω_0 is no longer constant.

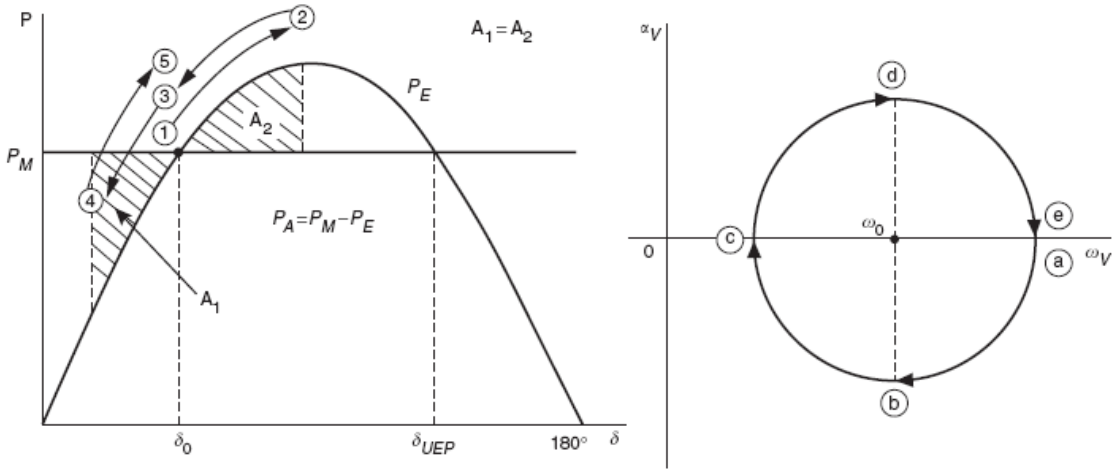

Figure 5.6 Stable case

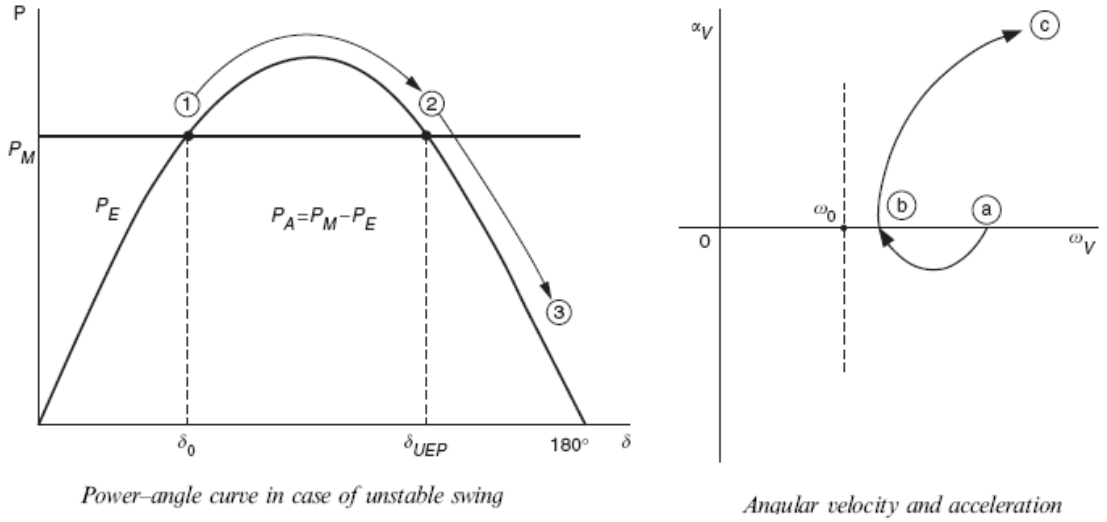

Figure 5.7 Unstable case

Table 5.1 Relationships between location and operation point

Conditions	Curves	Location of operation point					Ref.
Stable swing	P–δ	①	②	③	④	⑤	Figure 5.6
	α_V–ω_V	ⓐ	ⓑ	ⓒ	ⓓ	ⓔ	
Unstable swing	P–δ	①	②	③	–	–	Figure 5.7
	α_V–ω_V	ⓐ	ⓑ	ⓒ	–	–	

5.1.5 Synchronized Phasors Based Out-of-Step Protection

With the advent of PMUs, measurement of the phase angle of bus voltages at different locations can be accomplished. The measured bus angles can be transmitted through fast communication system, which leads to the development of special protection systems for out-of-step relaying.

Two approaches have been described in the literature to implement synchrophasor-based out-of-step protection [67] - [69] . To the extent that a two-machine system equivalent can represent a network, one approach consists of synchronous measurement of the phase angle between the voltages behind the transient reactance of the two machines. When a disturbance occurs, the new phase angle between the two machines is computed and the equal area algorithm is implemented in real time to determine whether the new point of operation is stable. A second approach consists of measuring the positive sequence phasors at two or more strategically located buses. During a disturbance, the phase angle between the signal pairs is computed in real time, and a predictive algorithm is used to establish whether the disturbance will be stable.

5.2 Coherency Identification

The adaptive out-of-step protection with wide area measurements, developed later in this chapter, requires identifying the groups of coherent generators. This section will discuss the techniques of coherency identification.

5.2.1 Review

Coherency identification originates from transient stability analysis. A portion of the system, called study system, is of interest. The rest of the system is called the external system. Due to the dimension of the interconnected systems, it is impossible or uneconomical to represent the entire system model in detail. A reduced order approximate model of the external or unimportant systems is used for transient stability studies. Modern dynamic equivalencing of large power systems is typically done in two stages. In the first stage, coherent machines are identified**.** In the second stage, an aggregate network is constructed and an equivalent machine is obtained for each coherent group of machines. An important step in deriving coherency-based dynamic equivalents is to identify the coherent groups of generators. Earlier work in this area required a full-time nonlinear simulation of the whole power system [88] . Obviously, the amount of computation needed may be prohibitively large when several studies have to be made to assess coherency in relation to fault locations. To avoid detailed stability studies, many techniques to identify coherency have been proposed. References [90] - [92] derive a simplified and linearized power system model for coherency identification. The coherent groups are identified by processing the approximate swing curves obtained by solving a set of linear equations. References [95] - [100] use the concept of slow coherency. The assumption of this method is that the areas within a dynamic network are weakly connected. Under this assumption, the dynamic network exhibits two time-scales. The slow time-scale behavior can be captured by the aggregate model which represents the motions between the areas, and the fast time-scale behavior can be captured by the local models which represent the motions within the individual areas. The slow coherency is nearly independent of the severity and location of disturbances. References [101] [102]

use spectrum analysis to identify coherency. Some references also use artificial intelligence to do coherency identification [103] .

5.2.2 Coherency Identification Using Wide Area Measurements

Many of the coherency identifying techniques require off-line analysis, or/and have strong assumptions. With wide area measurements transmitted to the system control center in real time, system states can be much more accurately monitored than simulation analysis, and the measured synchronized phasors can be used to identify coherent groups of generators in real time. Swing curves directly reflect the dynamic behavior of generators. After a disturbance, some generators will swing together exhibiting coherency. Though complicated pattern recognition techniques could be used, closeness of generator rotor angles is more suitable for real-time implementation of coherency identification. An intuitive way to do this is to rank the rotor angles, and use certain tolerance rules to group generators. In this subsection, we will develop a coherency identification technique using the slope of the swing curves.

The basic idea of this method is to obtain all generator angles in a study system, apply curve fitting in the least-squares sense with linear model y=a+bx, and then use the slope b to identify coherency when any angle is bigger than a threshold value (for example 120 degrees). Figure 5.8 shows the flowchart of the described method. This method will produce similar results with the method using rotor angle differences except that oscillation effects can be mitigated by linear curve fitting.

To demonstrate this method, a 127-bus WSCC test system, as shown in Figure 5.9 and Figure 5.10, was simulated in PSS/E. The detailed power flow and dynamic data can be found in Appendix B. We have simulated 18 fault scenarios including stable, first swing unstable and multi-swing unstable cases. For each case, we apply the proposed method. The effects of window type, window size, and angle reference are also studied and compared. One case in each category is shown below.

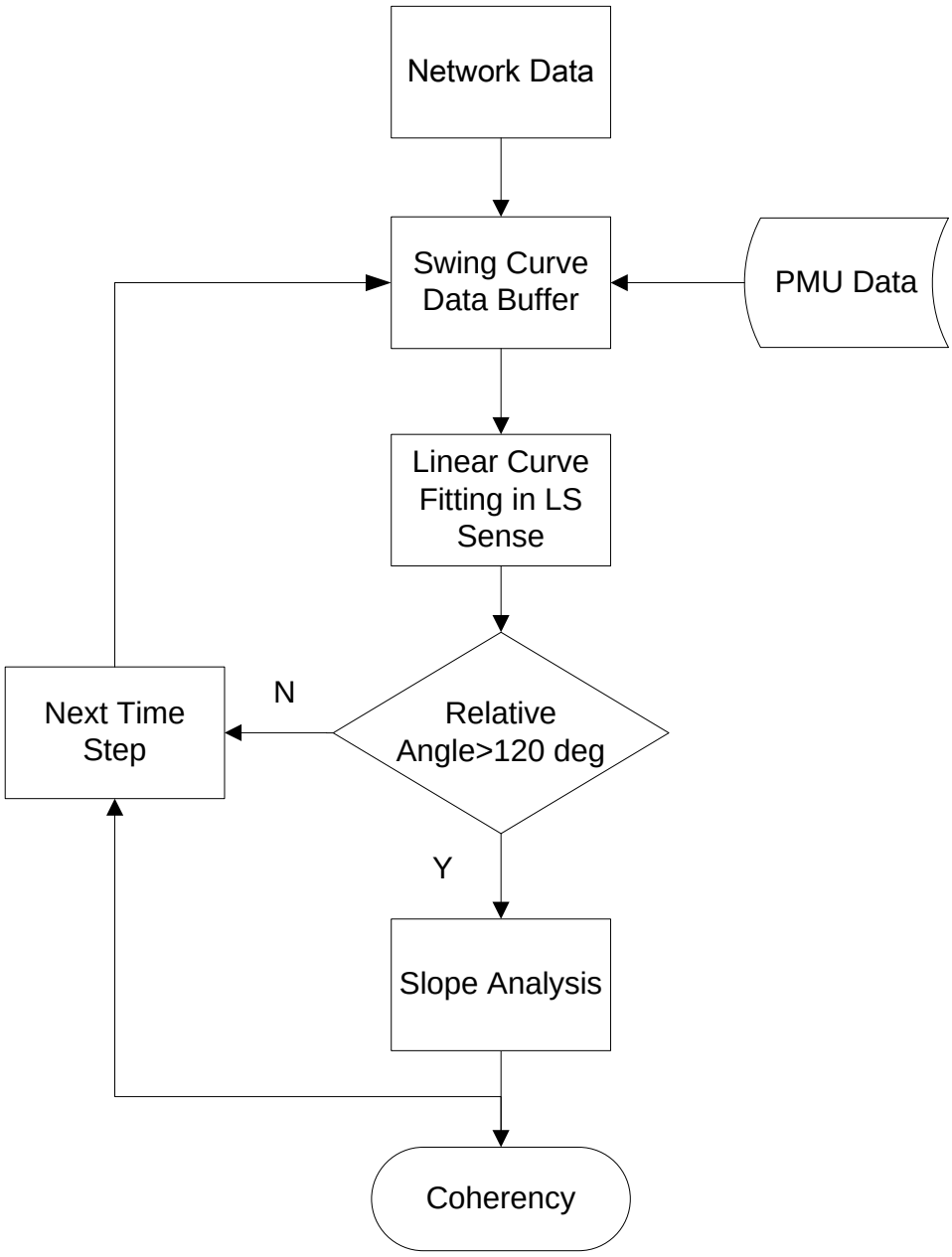

Figure 5.8 Coherency identification

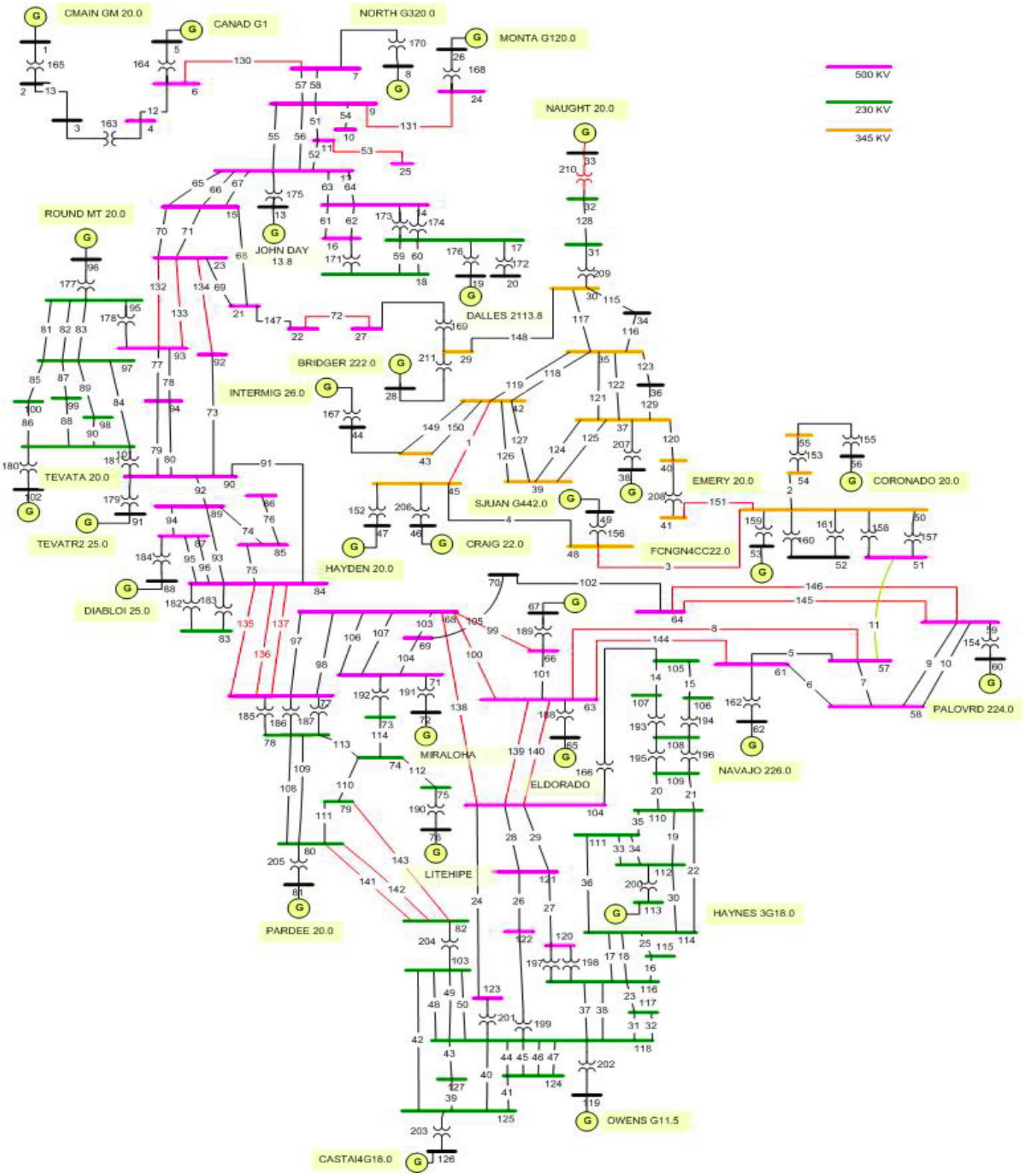

Figure 5.9 127-bus WSCC system

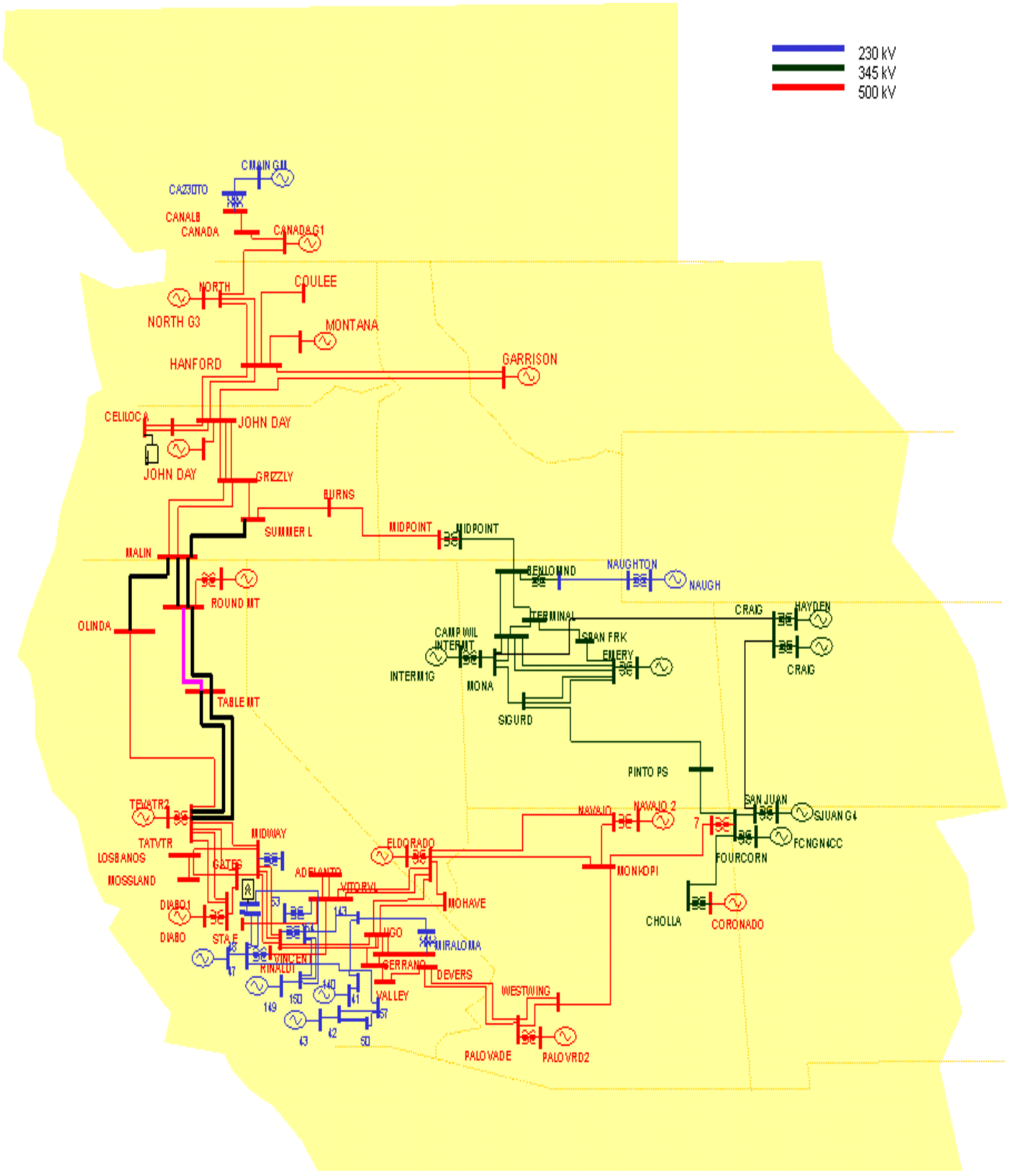

Figure 5.10 127-bus WSCC system with geographical information

5.2.2.1 Stable Case

A three-phase fault is created between Devers and Palovade (bus 64-bus 59, CK1) as shown in Figure 5.11. The fault begins at 0.05s, and the transmission line is tripped at 0.35s. All generator rotor angles are monitored and plotted. Figure 5.12 shows the rotor angles with John Day as reference, and Figure 5.13 shows the angles with their initial steady-state values as reference. Although the system swings after the fault, it is still a stable case. There is no angle difference between consecutive swing curves bigger than a 120 degrees threshold value, so the proposed method is not triggered to calculate and compare the slope.

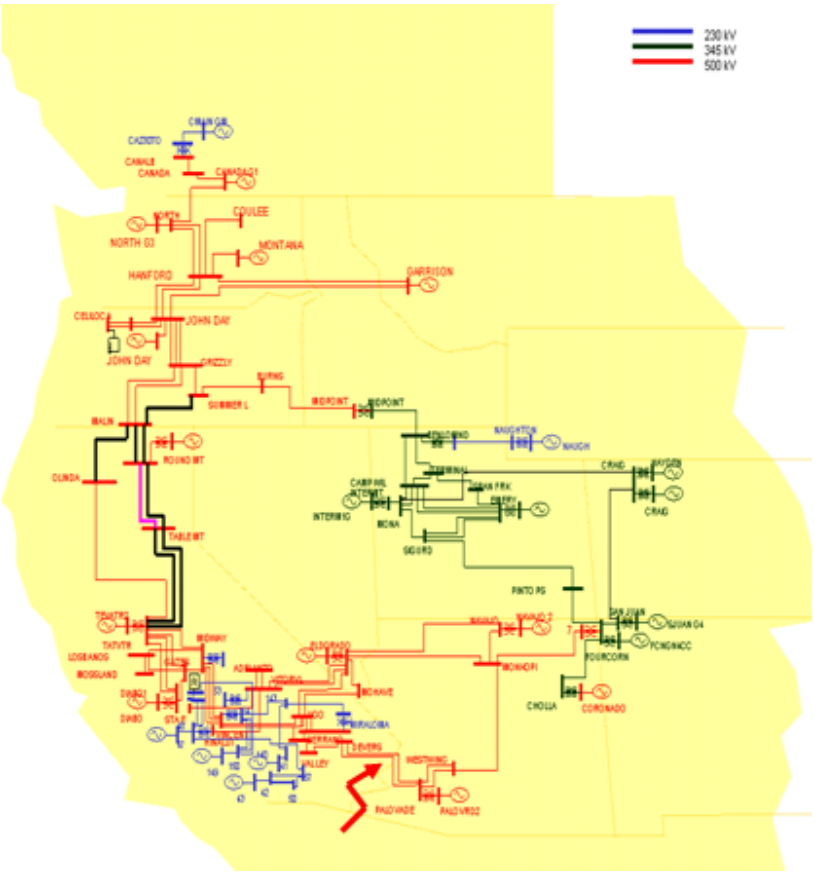

Figure 5.11 Three-phase fault between Devers and Palovade

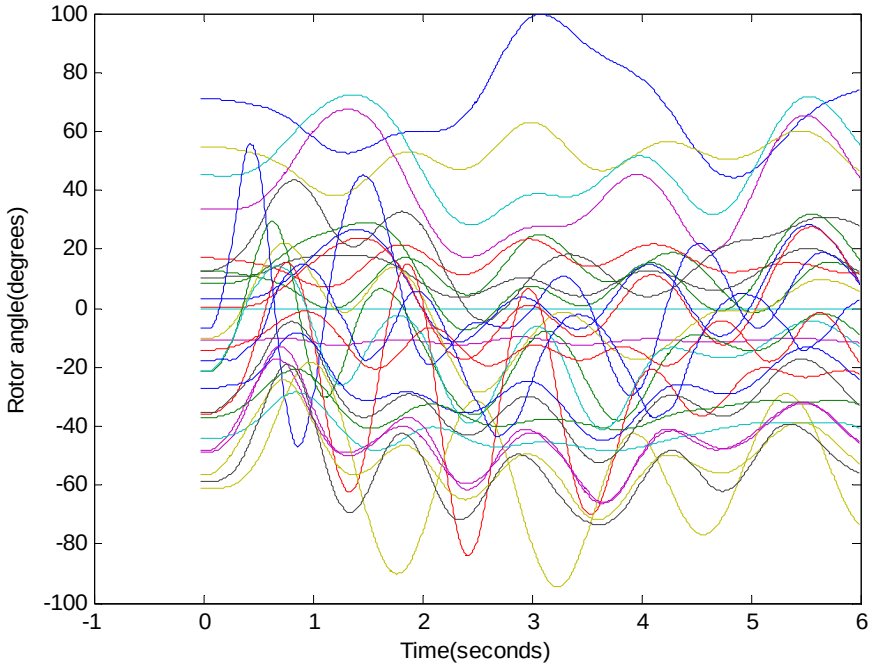

Figure 5.12 Rotor angles referenced to John Day

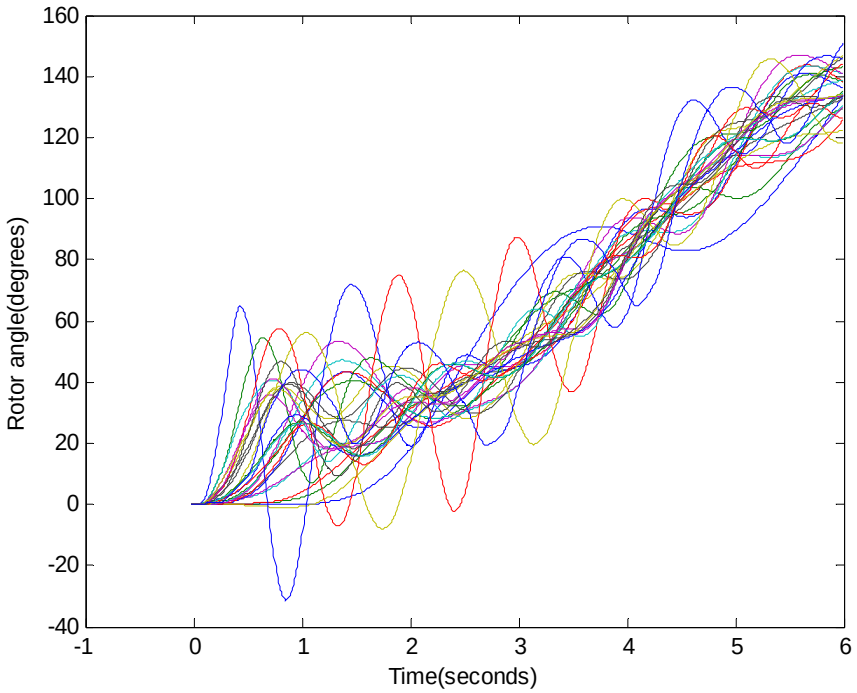

Figure 5.13 Rotor angles referenced to their initial values

5.2.2.2 First-Swing Unstable Case

A three-phase fault is created between Westwin and Navajo (bus 58-bus 61, CK1) as shown in Figure 5.14. The fault begins at 0.05s, and the transmission line is tripped at 0.35s. All generator rotor angles are monitored and plotted. Figure 5.15 shows the rotor angles with John Day as reference, and Figure 5.16 shows the angles with their initial steady-state values as reference. From the swing curves, we can determine that it is a first-swing unstable case. One group of generators goes out of step against the rest. The proposed method is triggered when any angle difference is bigger than 120 degrees. Figure 5.17 and Figure 5.18 show the calculated slope with growing window. Figure 5.19 shows the slope with sliding window. All of them can be used to identify the coherent groups.

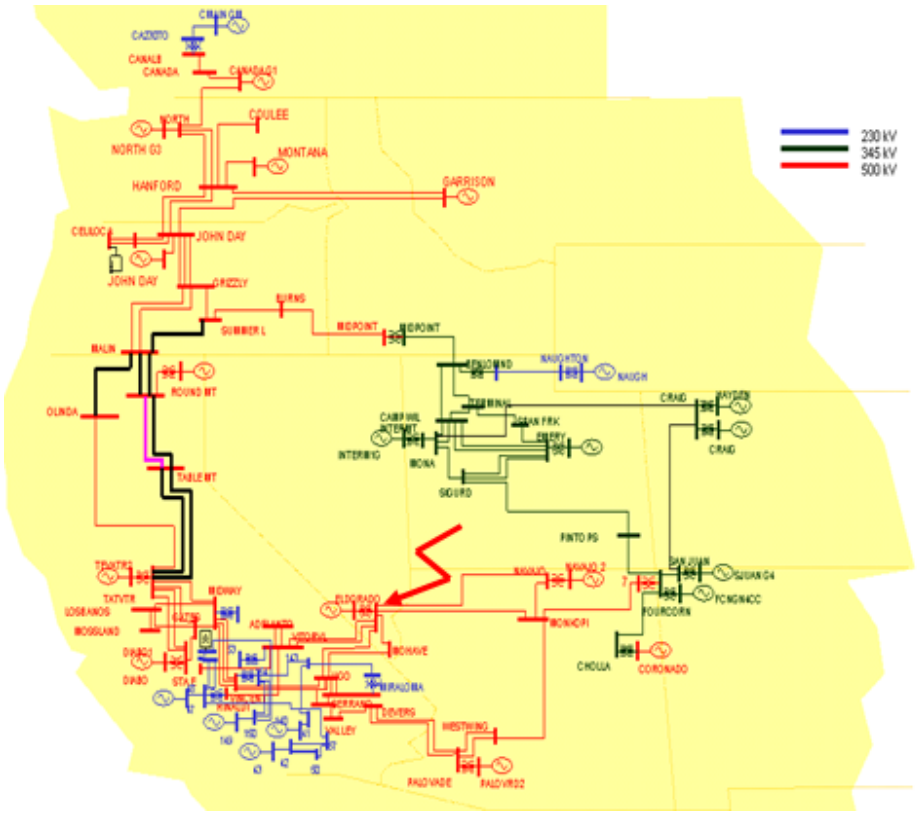

Figure 5.14 Three-phase fault between Westwin and Navajo

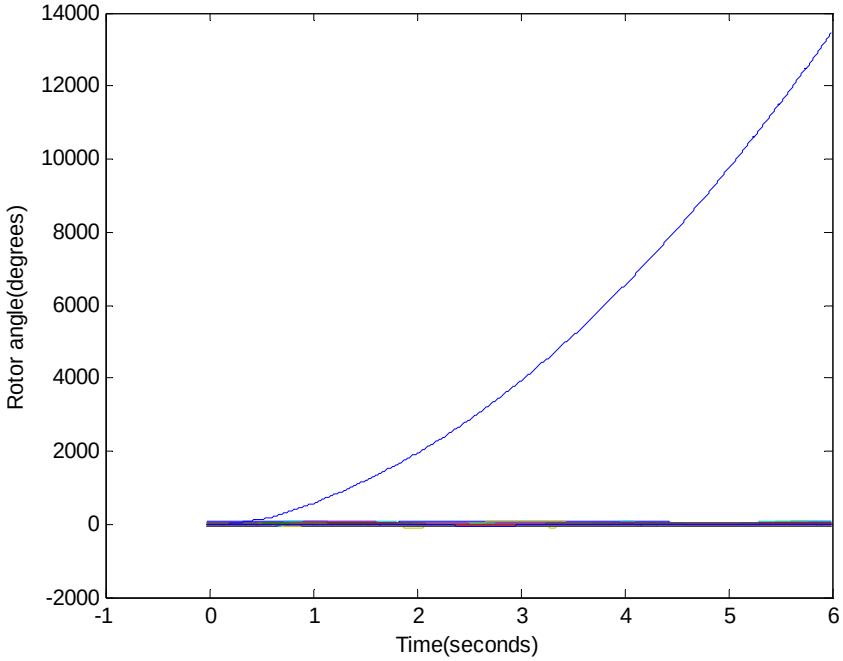

Figure 5.15 Rotor angles referenced to John Day

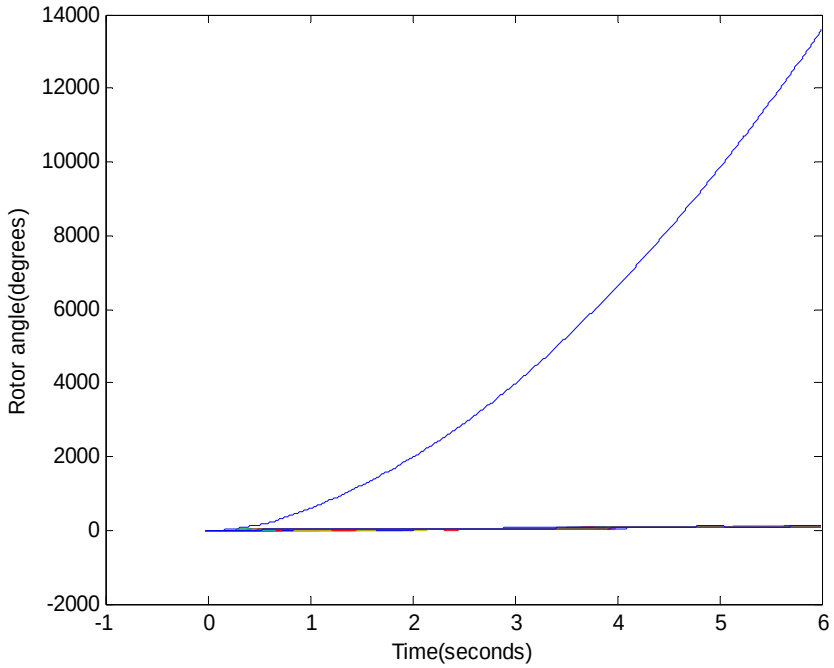

Figure 5.16 Rotor angles referenced to their initial values

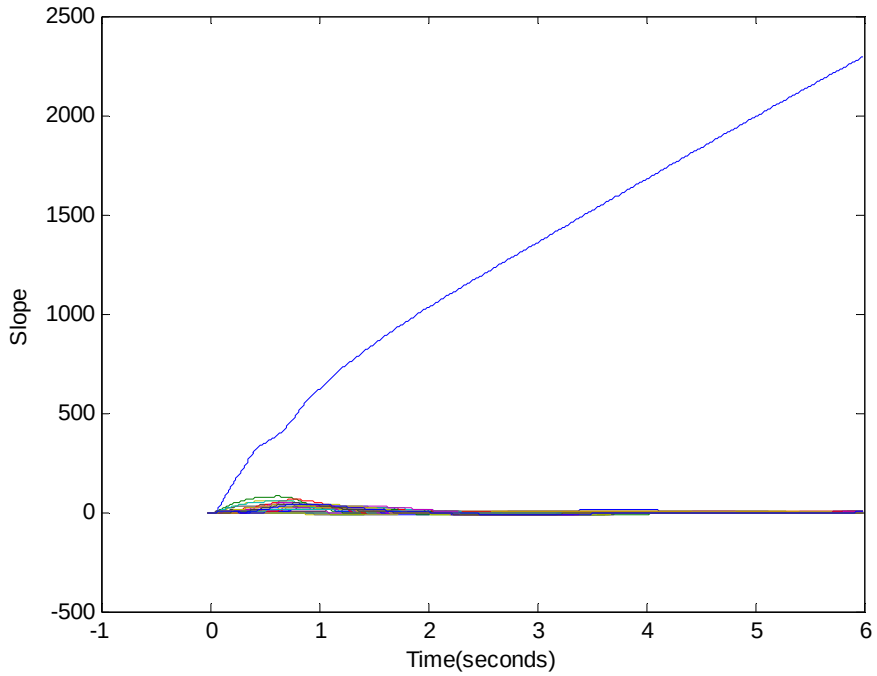

Figure 5.17 Slope of rotor angles referenced to John Day (w/ growing window)

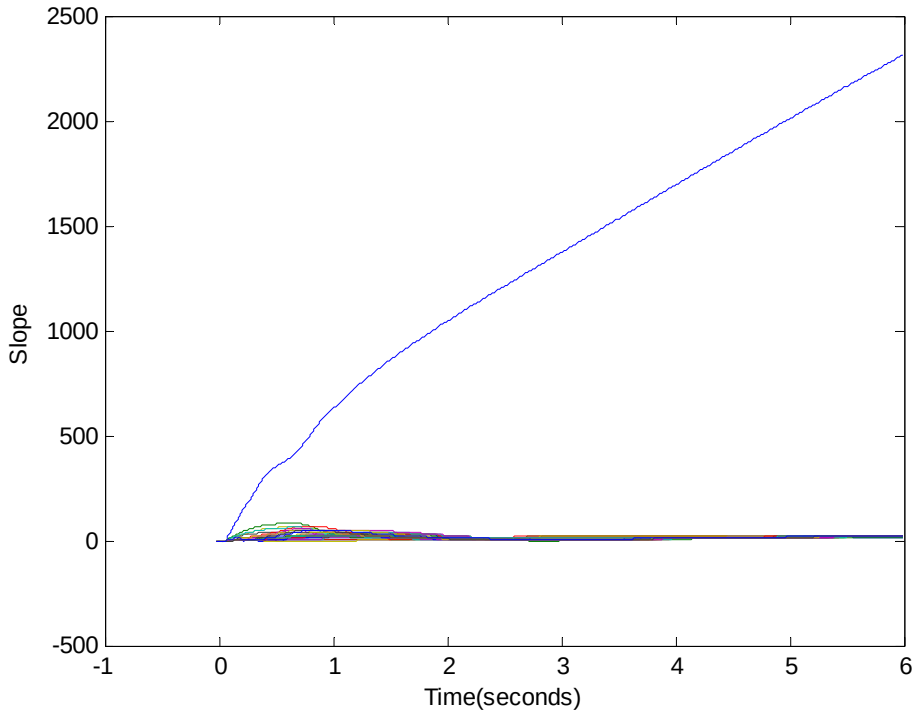

Figure 5.18 Slope of rotor angles referenced to initial values (w/ growing window)

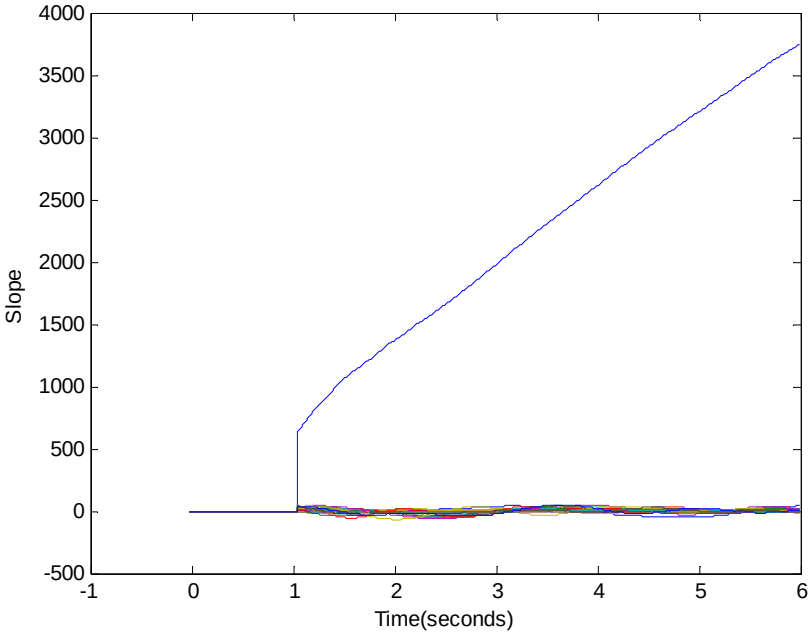

(a) One-second window

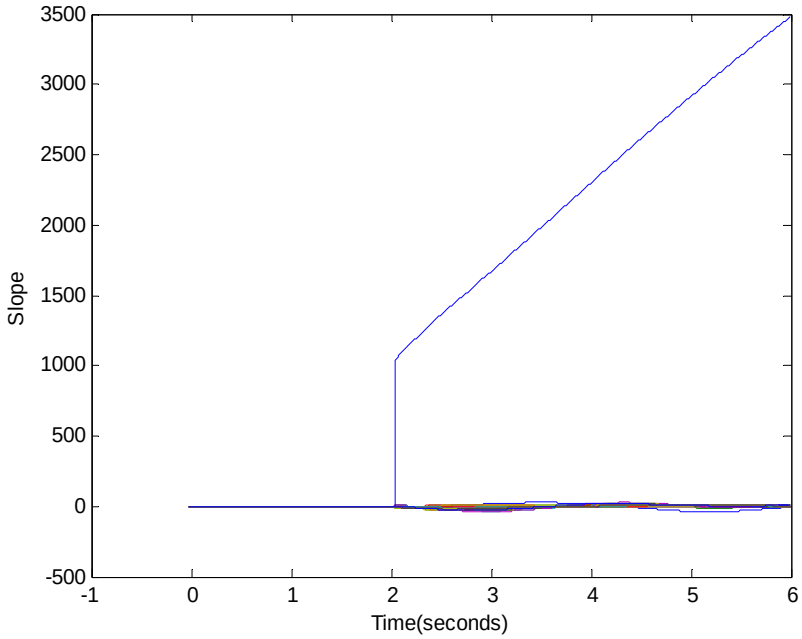

(b) Two-second window

Figure 5.19 Slope of rotor angles referenced to John Day (w/ sliding window)

5.2.2.3 Multi-Swing Unstable Case

A three-phase fault is created between Malin and Olinda (bus 23-bus 92) as shown in Figure 5.20. The fault begins at 0.05s, and the transmission line is tripped at 0.35s. All generator rotor angles are monitored and plotted. Figure 5.21 shows the rotor angles with John Day as reference, and Figure 5.22 shows the angles with their initial steady-state values as reference. From the swing curves, we can determine that it is a multi-swing unstable case. Two or more groups of generators go out of step against each other. The proposed method is triggered when any angle difference is bigger than 120 degrees. Figure 5.23 and Figure 5.24 show the calculated slope with growing window. Figure 5.25 shows the slope with sliding window. The growing window is greatly affected by the initial oscillation, while the sliding window can stay away from the initial oscillation. In addition, the sliding window gives a bigger slope compared with the growing window. According to the calculated slope, we can divide the system into two groups. If needed, further separation can be obtained.

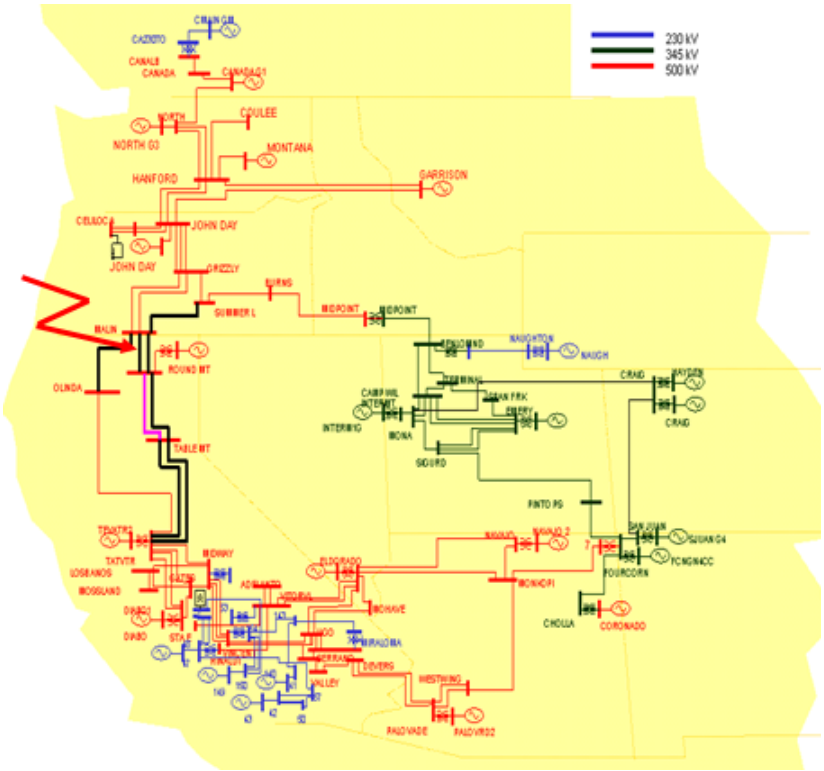

Figure 5.20 Three-phase fault between Malin and Olinda

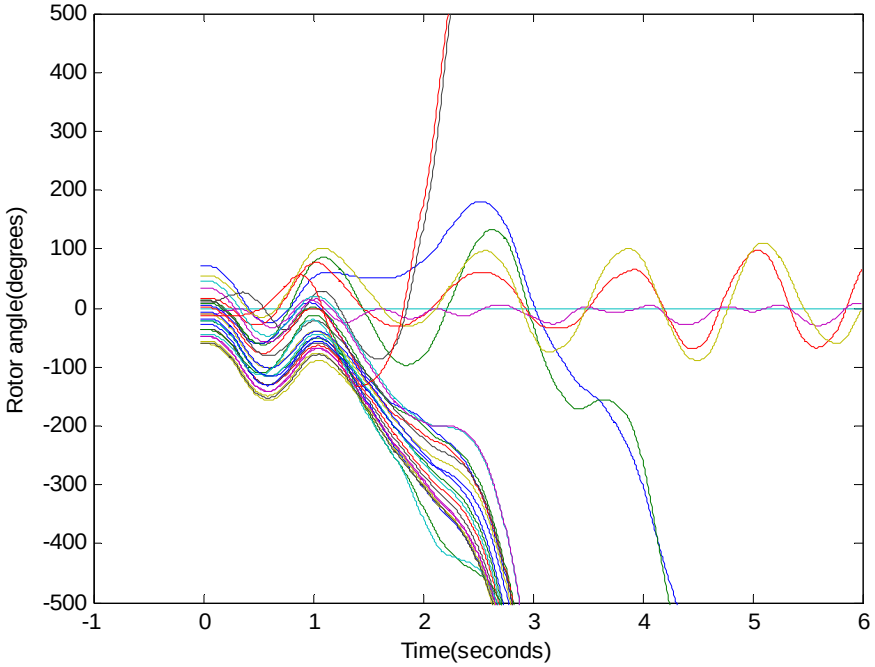

Figure 5.21 Rotor angles referenced to John Day

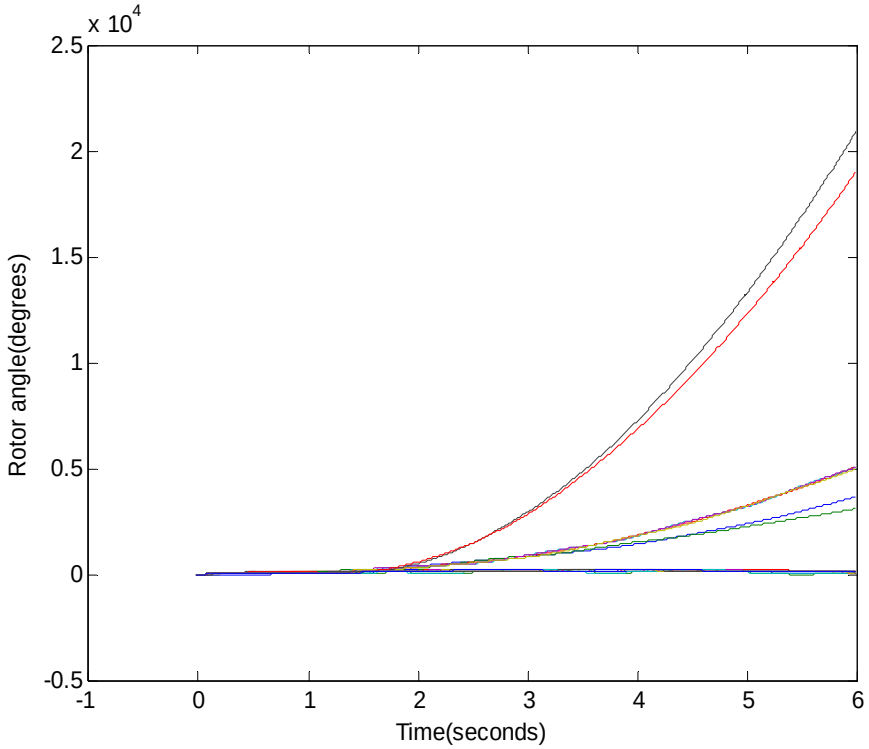

Figure 5.22 Rotor angles referenced to their initial values

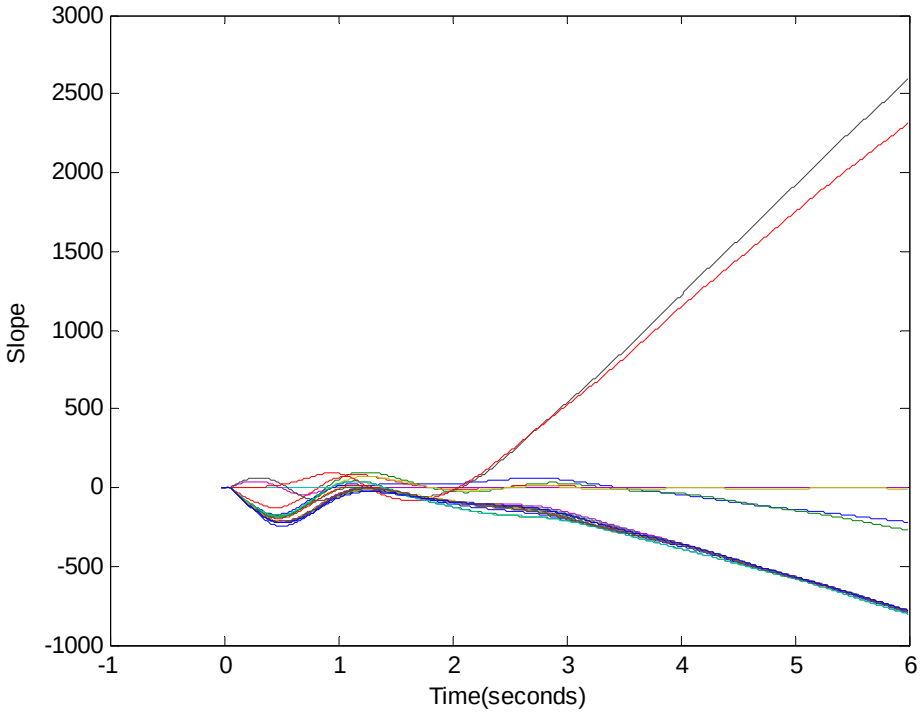

Figure 5.23 Slope of rotor angles referenced to John Day (w/ growing window)

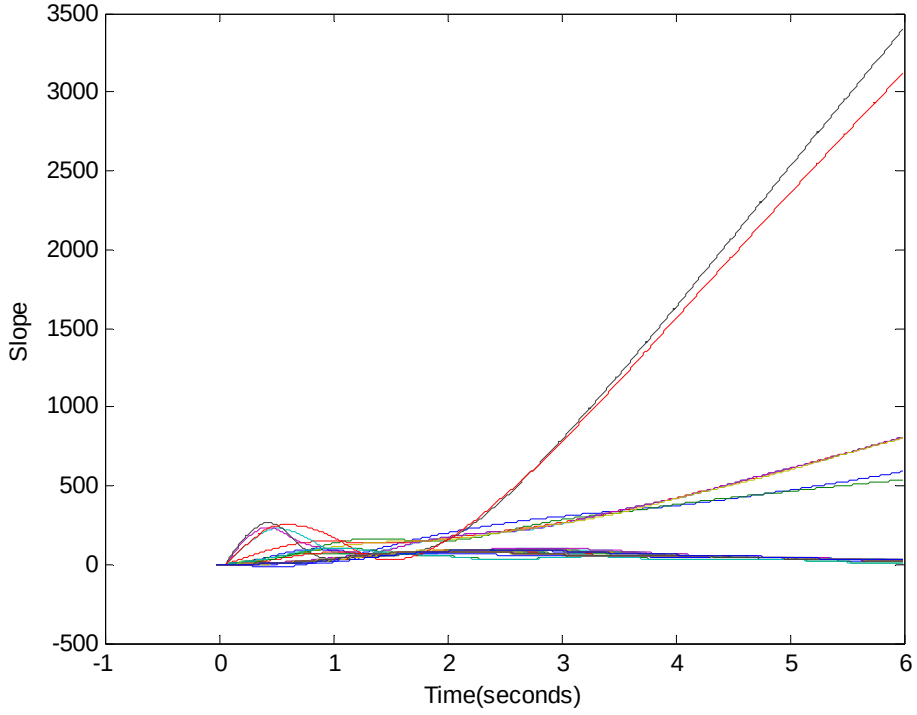

Figure 5.24 Slope of rotor angles referenced to initial values (w/ growing window)

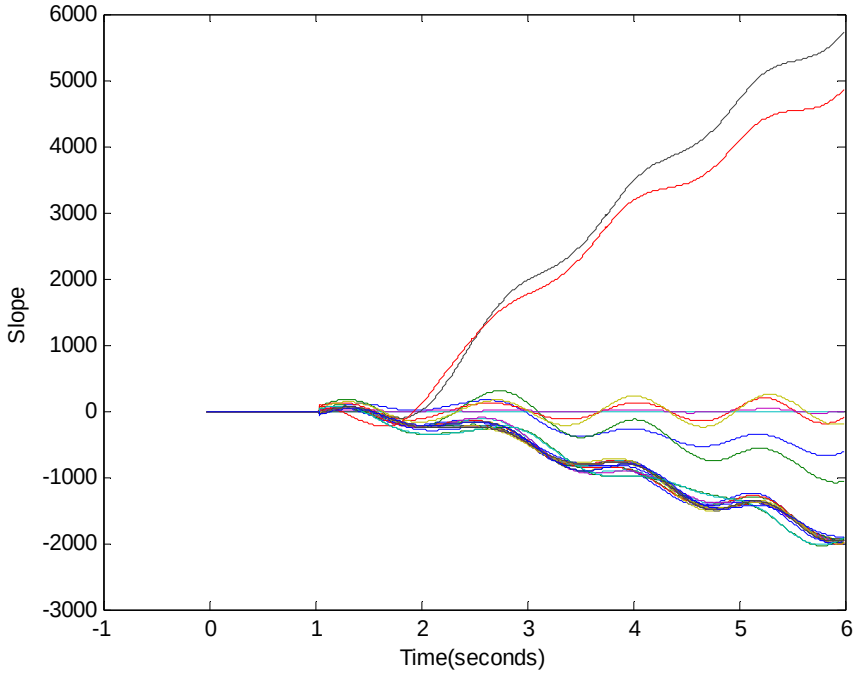

(a) One-second window

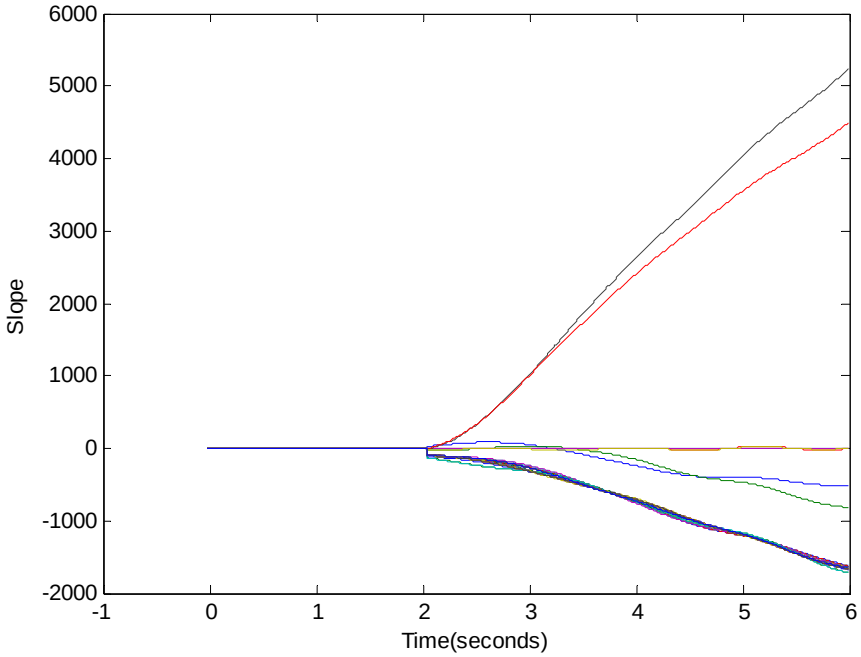

(b) Two-second window

Figure 5.25 Slope of rotor angles referenced to John Day (w/ sliding window)

From above simulations, using initial angle values does not help much. Growing window is faster for the first-swing unstable case. Compared with growing window, sliding windows is helpful to stay away from the initial oscillation, and provide larger slope values. It is more reliable though the long window will delay detection. In addition, when to start a growing window may not be easy to decide in reality.

5.3 Real-Time Swing Curve Based OOS Protection

The traditional stability analysis depends on time-domain simulations, which tends to be confined to offline studies based on extensive computation. Synchronized phasor measurements offer a unique opportunity of improving stability analysis. The progress of system transients can be monitored in real time with the help of wide-area synchronized measurements. The system trajectories up to the present time are observable directly. Therefore, out-of-step decision can be made directly based on real-time swing curves. Compared with those methods using indirect information such as apparent impedance, swing center voltage, real power transfer or frequency, this real-time swing curve based out-of-step protection scheme is more reliable since it adapts to the prevailing system conditions.

This section focuses on the development of real-time swing curve based out-of-step protection. The procedures are as follows

- Identify coherency with wide area measurements
- Calculate equivalent center of angle (COA) for each group of coherent generators
- Determine stability or instability based on the COA difference

Coherency identification can be done with the technique introduced in section 5.2. It can be implemented online with wide area measurements, and the results always reflect the latest system coherency characteristics. With the system coherency information, the center of angle of each group of coherent generators can be computed with the rotor angles weighted by inertia coefficients as shown by equation (5.5).

$$\delta_{COA} = \sum_{i \in S} (\delta_i M_i) \Big/ \sum_{i \in S} M_i \tag{5.5}$$

Then the differences among COAs can be compared with a given threshold value to determine stability. If the difference is bigger than the threshold value, unstable condition is declared, and out-of-step relays can be used to separate those identified coherent groups. Of course, load generation balance and ease of circuit separation have to be considered in practice. This controlled islanding scheme will help minimize the spreading of severe disturbance in wide areas, prevent blackouts, maintain operation in each island with reduced reliability, and facilitate system restoration.

An example is given below to demonstrate the implementation of this proposed method. We still use the WSCC test system described earlier. A three-phase fault is created between Grizzly and Malin (bus 15 - bus 23, CK1) as shown in Figure 5.26. The fault begins at 0.05s, and the transmission line is tripped at 0.35s. Figure 5.27 shows the response of rotor angles. From the swing curves, we can determine it is an unstable case. Applying the coherency identification, two groups, leading and lagging groups, are identified as shown in Figure 5.27. The leading group, which is mainly composed of the generators in the north of WSCC, goes out of step against the lagging group. The equivalent COAs of leading and lagging groups are computed and plotted in Figure 5.28. Figure 5.29 shows the angle difference between the two COAs. When the out-of-step decision is made depends how large the threshold value is. For example, if the threshold value is 180 degrees, the time reaching this is around 1.1 second. Due to the strong nonlinearity and complicated control actions in power systems, rotor angles may swing back even beyond 180 degrees. So larger threshold will make more reliable decision, but involve longer time delay.

To make an earlier out-of-step decision, reference [4] proposes to predict the swing curve. “The time track of state variables and several of their derivatives are available over an observation window, so it seems possible that the outcome of the swing for a future time interval can be calculated with relatively good, simplified models. It seems probable that predictions of up to a second in the future can be made with reasonable confidence. With this prediction capability, useful protection and control decisions can be made to change the course of the transient if that seems desirable.”

References [104] [105] propose a new technique of determining first swing stability limit of a power system through checking the existence of peaks of rotor angles of the severely disturbed generators in the post-fault period. The existence of peaks is checked by observing the roots of time derivatives of rotor angles of these generators expressed through truncated Taylor series expansions. However, how to deal with multi-swing stability with this method requires more efforts.

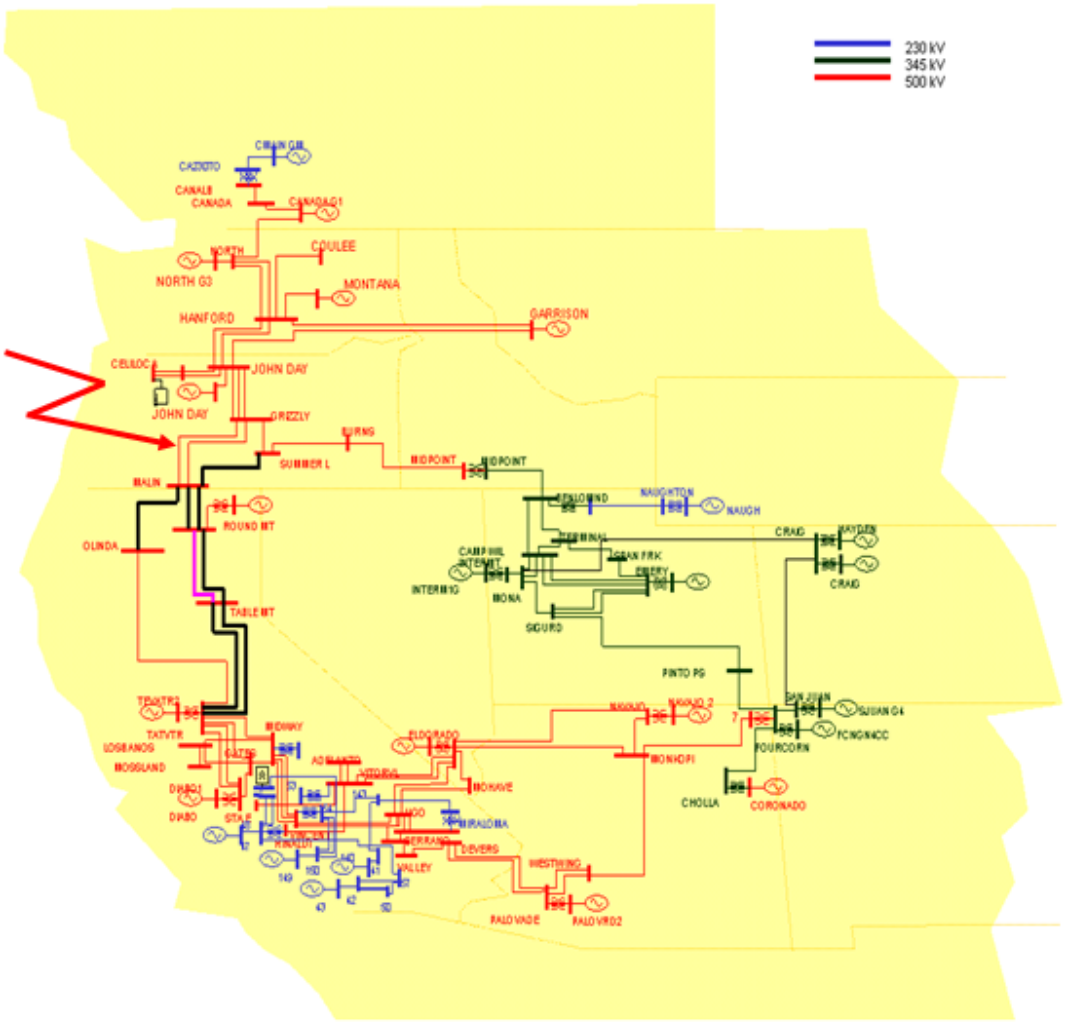

Figure 5.26 Three-phase fault between Grizzly and Malin

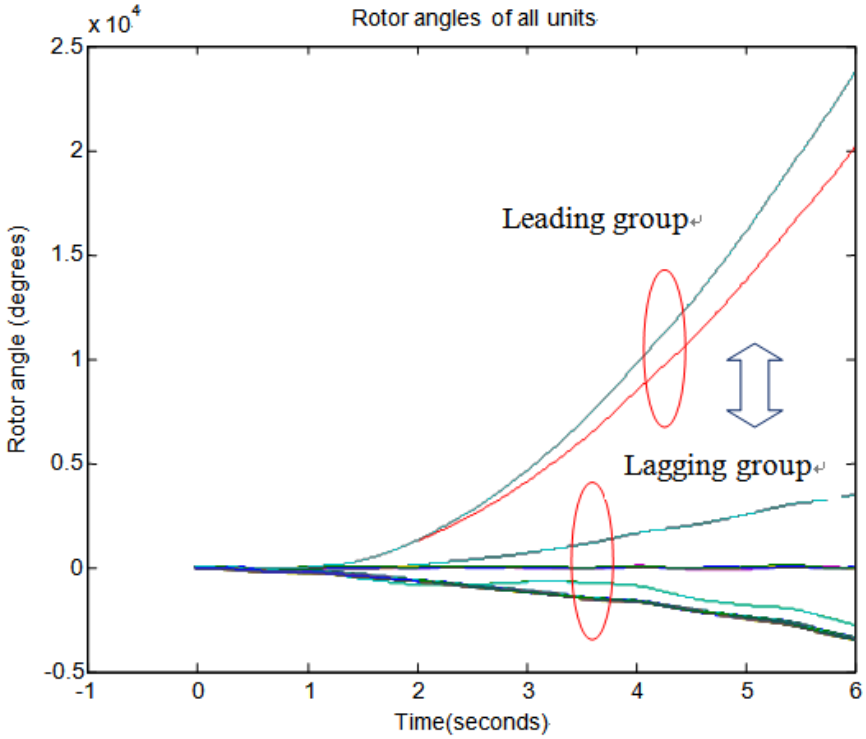

Figure 5.27 Rotor angles and coherent groups

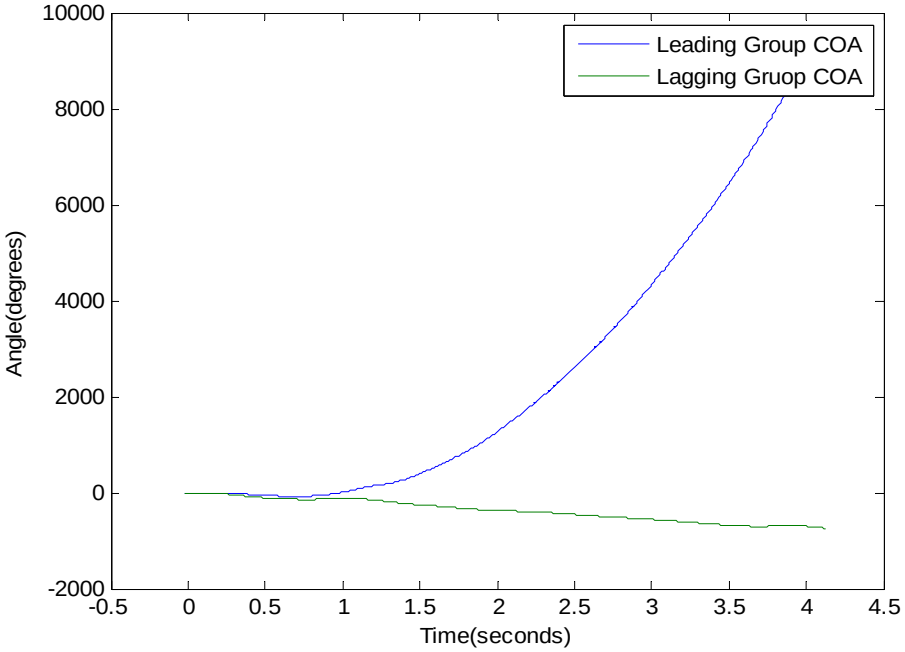

Figure 5.28 Equivalent COA

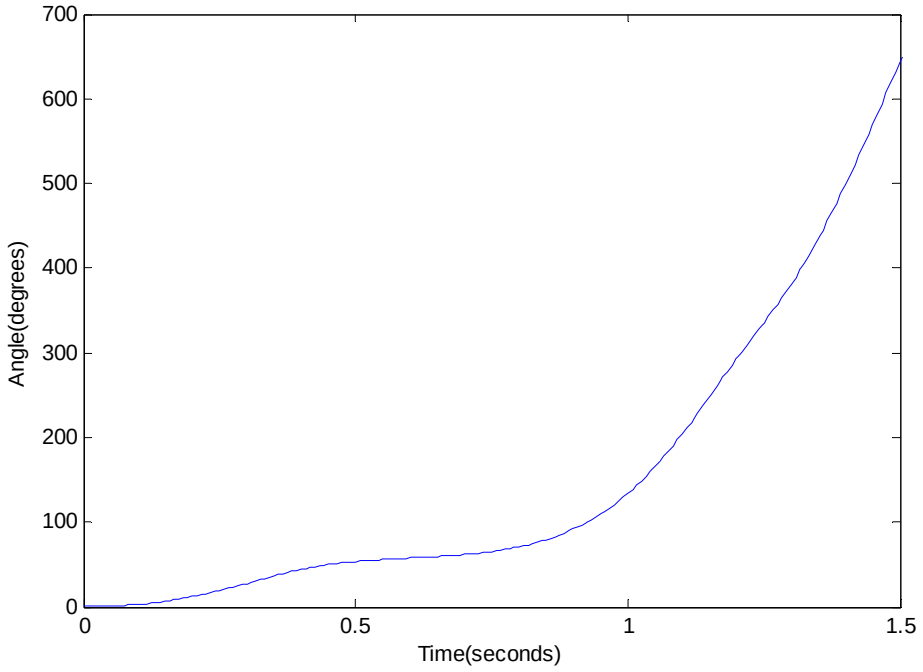

Figure 5.29 Difference between leading and lagging COAs

5.4 Real-Time EEAC based OOS Protection

Stability problems may not happen frequently, but their impact can be enormous. The most common tool for transient stability analysis is the time domain dynamic simulation, which involves a great deal of numerical integration. Transient energy function methods, based on Lyapunov's direct method, are much faster than full-scale time-domain simulations, and thus more suitable for on-line studies. They also have the advantage to provide a stability index. The main idea of the direct methods is to use a Lyapunov-type function to compute the region of stability around the post disturbance equilibrium point of the system. The boundary of the region of stability allows the assessment of the stability qualitatively and quantitatively via the computation of critical clearing time, critical energy and stability margin. Implementation of the transient energy function includes the lowest energy unstable equilibrium point method, the potential energy boundary surface method (PEBS), and the boundary-controlling unstable

equilibrium point method (BCU). Extended equal area criterion method (EEAC) is also associated with the Lyapunov's direct method. A similar approach referred to as generalized equal area criterion (GEAC) is also proposed by some researchers. [117]

This section investigates the use of real-time EEAC to implement adaptive out-of-step protection. A brief introduction of the equal area criteria (EAC) and EEAC is given. Real-time EEAC based out-of-step protection scheme is then developed with an example demonstration.

5.4.1 EAC Principles

This subsection provides the basics of EAC for a one-machine infinite-bus (OMIB) system. The dynamics of the machine in classical model are expressed as

$$\frac{d\delta}{dt} = \omega \tag{5.6}$$

$$M\frac{d\omega}{dt} = (P_m - P_e) \equiv P_a \tag{5.7}$$

where

δ: machine rotor angle in synchronous frame

ω: machine angular velocity in synchronous frame

P_e: output electromagnetic power

P_m: input mechanical power

P_a: net accelerating power

M : inertia coefficient

Eliminating dt by combining equations (5.6) and (5.7), the relationship between $d\omega$ and $d\delta$ can be written as

$$M\omega d\omega = (P_m - P_e)d\delta \tag{5.8}$$

The system is initially operating in steady state and the corresponding system states are $\delta = \delta_0$ and $\omega = 0$. After a fault, the rotor angle increases and reaches a maximum value and then starts decreasing. The system states at the maximum angle point are $\delta = \delta_m$ and $\omega = 0$. Integration of equation (5.8) from pre-fault operating point to the maximum angle

point provides

$$\int_{\omega=0}^{\omega=0} M\omega\, d\omega = \int_{\delta_o}^{\delta_m} (P_m - P_e)\, d\delta \quad . \tag{5.9}$$

Equation (5.9) can be expressed as

$$0 = \int_{\delta_o}^{\delta_c} \left(P_m - P_e^f\right) d\delta + \int_{\delta_c}^{\delta_m} \left(P_m - P_e^p\right) d\delta \tag{5.10}$$

where δ_c is the machine angle at fault clearing and superscripts " *f* " and " *p* " represent faulted and post-fault conditions, respectively. The above equation can be rewritten as

$$\int_{\delta_o}^{\delta_c} \left(P_m - P_e^f\right) d\delta = \int_{\delta_c}^{\delta_m} \left(P_e^p - P_m\right) d\delta \Rightarrow A_a = A_d \quad . \tag{5.11}$$

Equation (5.11) represents the well-known EAC.

5.4.2 EEAC Introduction

EEAC was initially developed by Xue and Pavella. The implementation of EEAC involves the transformation of a multi-machine system to a two-machine system, and further to an equivalent OMIB system. Thus the equal area criteria can be applied to a multi-machine system. Dealing with the multi-machine system as OMIB equivalent system relies on the observation that the loss of synchronism of a multi-machine power system originates from the separation of its machines into two groups, which are replaced by a two-machine system and then by an OMIB equivalent. [106] - [116]

The swing equation of the *kth* machine in a multi-machine system can be expressed as

$$M_k \ddot{\delta}_k = P_{mk}(t) - P_{ek}(t) \tag{5.12}$$

The multi-machine system can be divided into two coherent groups following a contingency. One belongs to group S, and the other belongs to group A. The summations of swing equation in each group are

$$\sum_{i \in S} M_i \ddot{\delta}_i = \sum_{i \in s} P_{mi} - \sum_{i \in s} P_{ei} \tag{5.13}$$

$$\sum_{j \in A} M_j \ddot{\delta}_j = \sum_{j \in A} P_{mj} - \sum_{j \in A} P_{ej} \tag{5.14}$$

.

Equations (5.13) and (5.14) can be written as

$$M_s \ddot{\delta}_s = P_{ms} - P_{es} \tag{5.15}$$

$$M_a \ddot{\delta}_a = P_{ma} - P_{ea} \tag{5.16}$$

where

$$\delta_s = \sum_{i \in S} M_i \delta_i / \sum_{i \in S} M_i$$

$$\delta_a = \sum_{j \in A} M_j \delta_j / \sum_{j \in A} M_j$$

$$M_s = \sum_{i \in S} M_i$$

$$M_a = \sum_{j \in A} M_j$$

$$\mathrm{P_{ms}} = \sum_{\mathrm{i \in S}} \mathrm{P_{mi}}$$

$$\mathrm{P_{es}} = \sum_{\mathrm{i \in S}} \mathrm{P_{ei}}$$

$$P_{ma} = \sum_{j \in A} P_{mj}$$

$$P_{ea} = \sum_{j \in A} P_{ej}$$

Then, the equivalent OMIB is obtained as

$$M\ddot{\delta} = P_m - P_e \tag{5.17}$$

where

$$M = \frac{M_s M_a}{M_s + M_a}$$

$$\delta = \delta_s - \delta_a$$

$$P_m = \frac{M_a P_{ms} - M_s P_{ma}}{M_s + M_a}$$

$$P_e = \frac{M_a P_{es} - M_s P_{ea}}{M_s + M_a}$$

With the equivalent OMIB, EAC can be used to for stability analysis. EEAC can be used in fault screening in contingency analysis, early termination of time-domain simulation, calculating stability indices, and sensitivity analysis. Table 5.2 is obtained from a PSERC report, which surveys the applications of online dynamic security assessment (DSA). It can be seen from Table 5.2 that the DSA with EEAC method is used by many utilities.

Table 5.2 Online DSA survey (PSERC)

Vendors	Areva T&D	Bigwood Systems	Powertech Labs Inc.	Siemens EMIS	University of Liege, Belgium	V&R Energy System Research Inc.
Methodology	Full Scale Time Domain Simulation Extended Equal Area Criterion	Full Scale Time Domain Simulation Transient Energy Function Method	Other : SIME (for Single-Machine Equivalent)	Full Scale Time Domain Simulation	Full Scale Time Domain Simulation Transient Energy Function Method	Hybrid Version (Full time domain with EEAC)
Customers	On-line licnesees (all may not have tools installed yet) ERCOT Entergy BPA ATC TVA Southern Company Services MAIN MISO GuangXi Electric Company Approximately 45 entities (commercial and educational) are using the same tools for off-line Analysis.	Tokyo Electric Power Company, ABB-NM (ABB is a BSI software reseller: BSI's DSA application is integrated sold as an option in their Ranger EMS), CFE (the National Power Company of Mexico), and Commonwealth Edison	Test facilities have been set-up at HTSO (Hellenic Transmission System Operator) and at CESI with remote connection to GRTN (Italy)	None	The function was installed at NSP (now XCEL Energy). The tool was demonstrated to the industry. However, the tool is no longer	Voltage stability has been delivered to the following utilities: ENTERGY, MISO, ATC, BPA and ESB Ireland. Transient stability has been delivered to ERCOT. Voltage and transient stability has been delivered to ERCOT and is scheduled for delivery to TVA

5.4.3 Real-Time EEAC Based OOS Protection Implementation

"Hybrid methods that combine time-domain transient simulation and some transient energy function method (included EEAC) have evolved as a natural extension combining the advantages of the time domain simulations with the benefits that can be obtained by the use of an energy function method (like the computation of stability margins and other indices and limits etc). These hybrid approaches have become a very active area of research and many hybrid implementations have been proposed and tested." "Hybrid methods combining the accuracy of time-domain simulation and the advantages of an energy function method are currently the state of the art in on-line transient stability assessment (TSA) applications." [117]

With enough wide-area synchrophasor measurements, the system states are directly observable. The measurements are similar to the results of time-domain simulations except that the measurements are a truly accurate picture of the system states. In this sense, a hybrid methods that combine wide area measurements and direct methods for stability analysis is much better for online stability applications. This subsection discusses how to use wide-area synchrophasor measurements to develop the real-time EEAC based out-of-step protection scheme.

Figure 5.30 shows the flowchart of the real-time EEAC based out-of-step detection scheme. With PMU data and network data collected in the system control center, online coherency analysis is performed continuously. If there is only one coherent group, it means that the system is operating in steady state or just with small disturbance. There is no need to separate the system, and the main program should go back to the beginning. If more than one coherent group is identified, the system has the possibility of losing stability. OMIB equivalencing is performed, and EAC is applied to determine the system stability. Pure direct methods for transient stability analysis stop time-domain simulation at some time, and then analyze based on classical model or some other assumptions. One striking difference of using synchrophasors for real-time EEAC based out-of-step protection is that measured system states are always used. The latest system responses are considered in every step, which is more accurate than those assumptions.

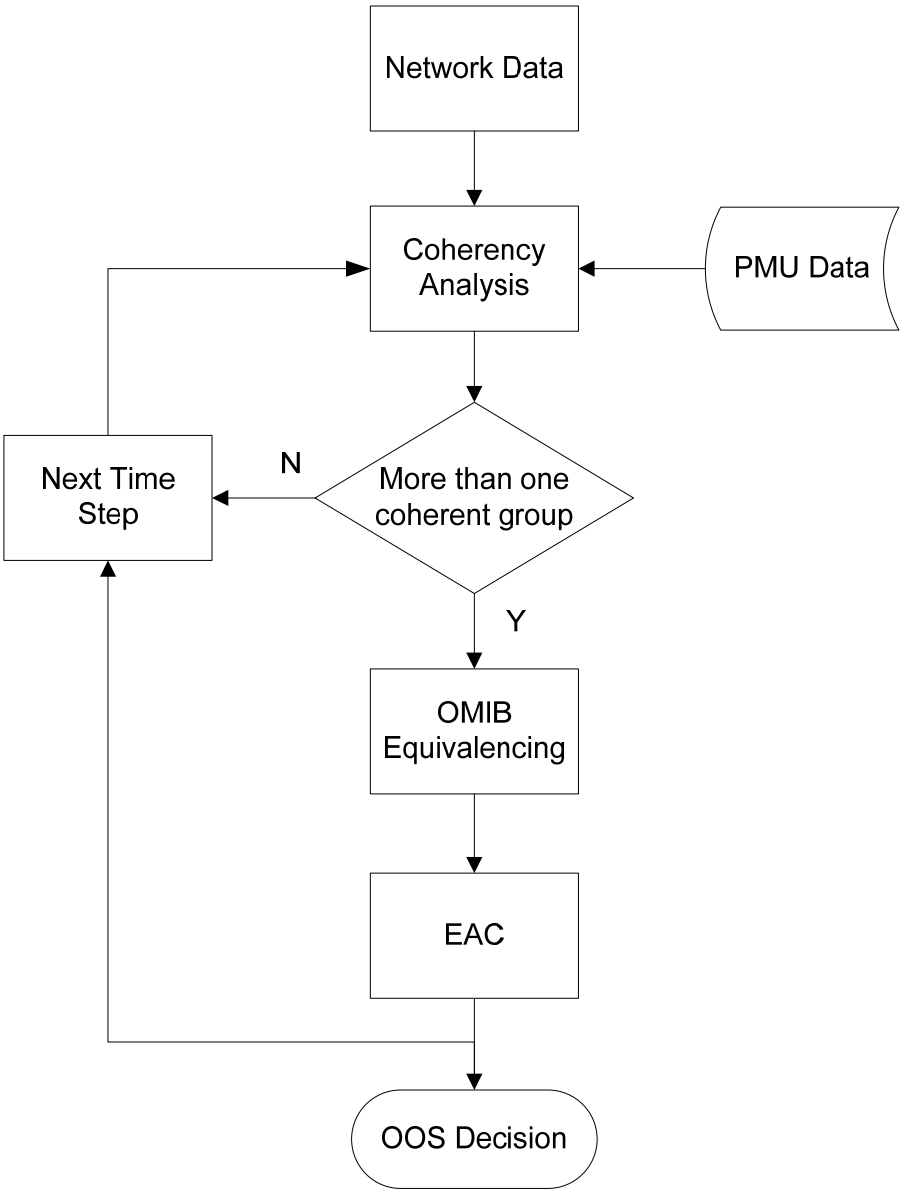

Figure 5.30 Real-time EEAC based OOS detection scheme

5.4.3.1 Example A

Here an example is given to demonstrate the proposed real-time EEAC based out-of-step protection. We use the same WSCC simulation case as in section 5.3. A three-phase fault is created between Grizzly and Malin (bus 15 - bus 23, CK1) as shown in Figure 5.26. The fault begins at 0.05s, and the transmission line is tripped at 0.35s. Figure

5.27 shows the response of rotor angles. Applying the coherency identification, two groups, leading and lagging groups, are identified as shown in Figure 5.27. The leading group, which is mainly composed of the generators in the north of WSCC, goes out of step against the lagging group. Figure 5.31 shows the generator electromagnetic power outputs. The mechanical power inputs to each generator are roughly held constant due to the large time constants of generator governors. Applying the synchrophasor based EEAC, the equivalent OMIB electromagnetic and mechanical power are shown in Figure 5.32 and Figure 5.33, and the power angle curves are shown in Figure 5.34 and Figure 5.35. Figure 5.36 shows the OMIB rotor angle, and Figure 5.37 shows the OMIB stability index calculated as decelerating area subtracted by accelerating area.

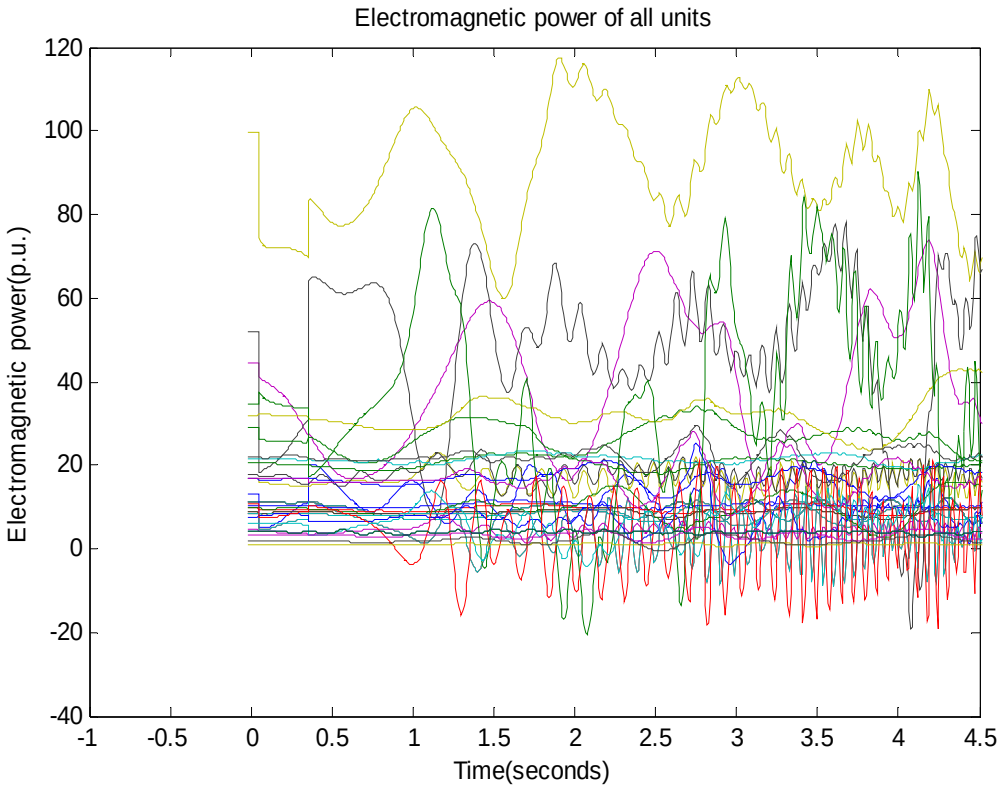

Figure 5.31 Electromagnetic power output of all generators

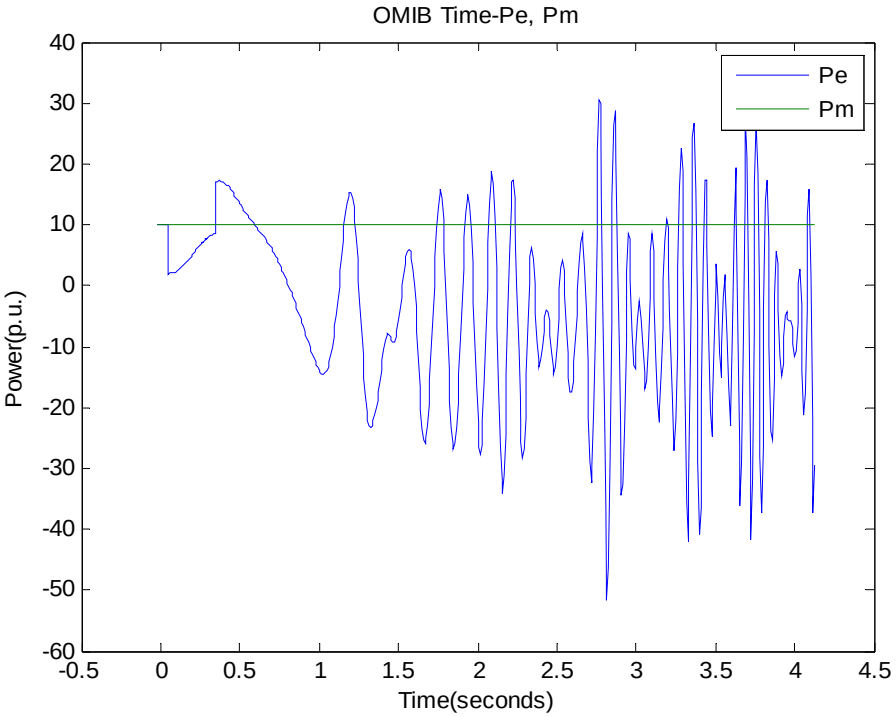

Figure 5.32 Power vs. time curve of OMIB system

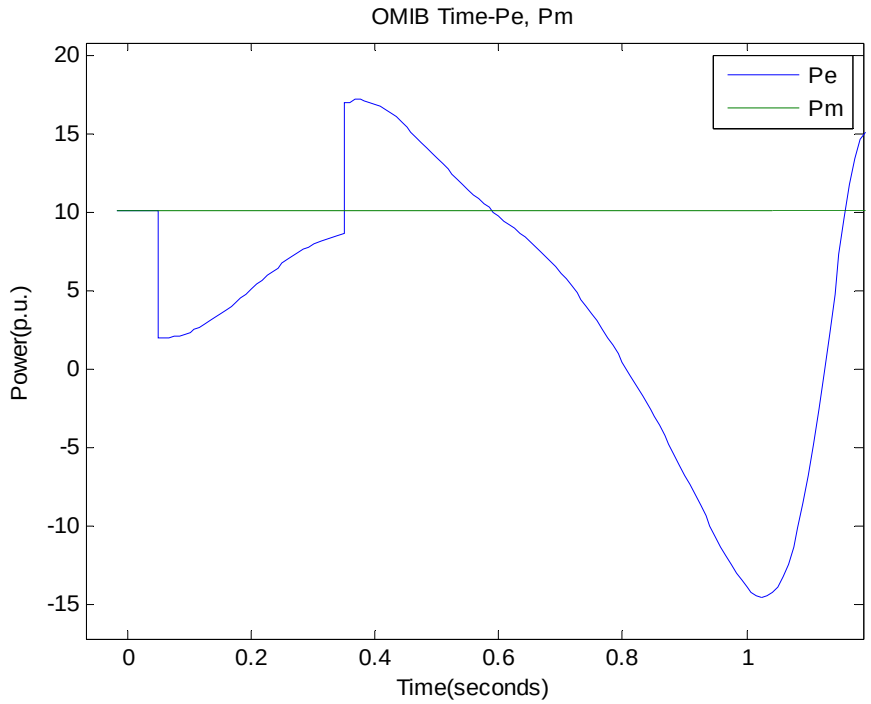

Figure 5.33 Power vs. time curve of OMIB system (enlarged)

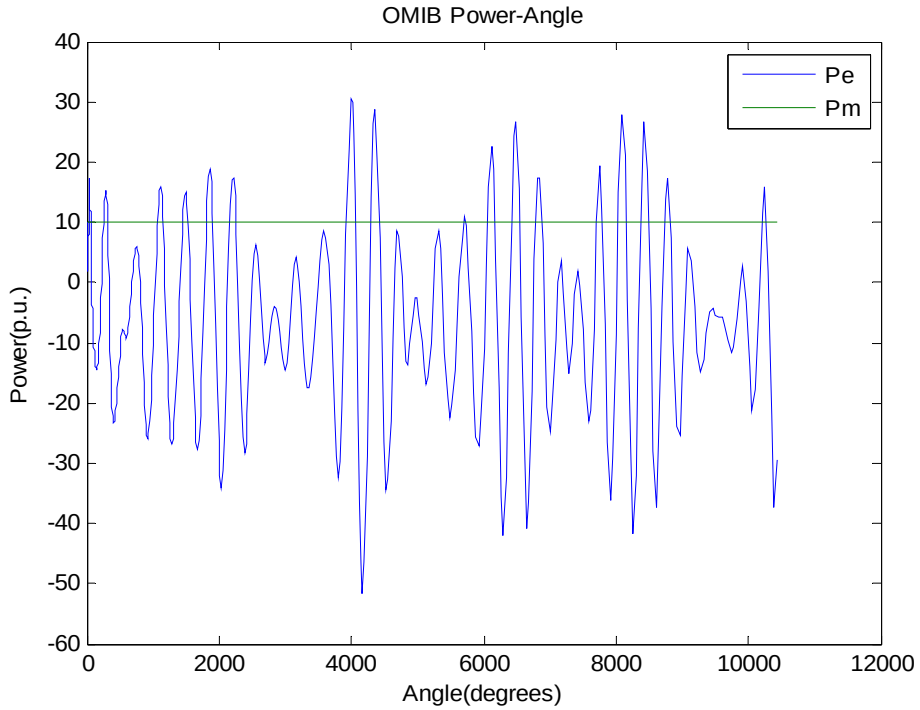

Figure 5.34 Power vs. angle curve of OMIB system

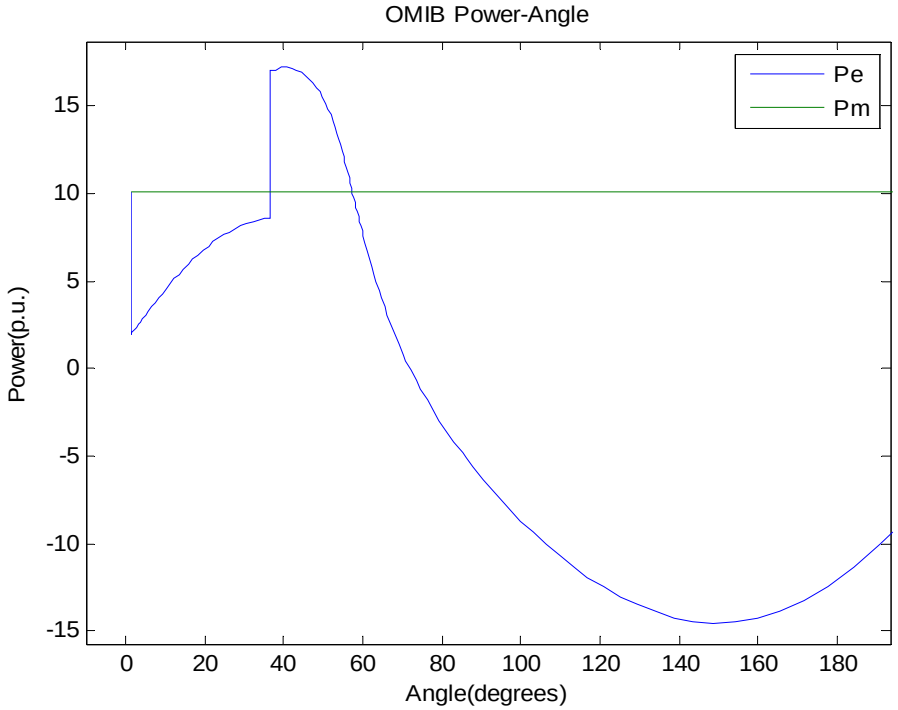

Figure 5.35 Power vs. angle curve of OMIB system (enlarged)

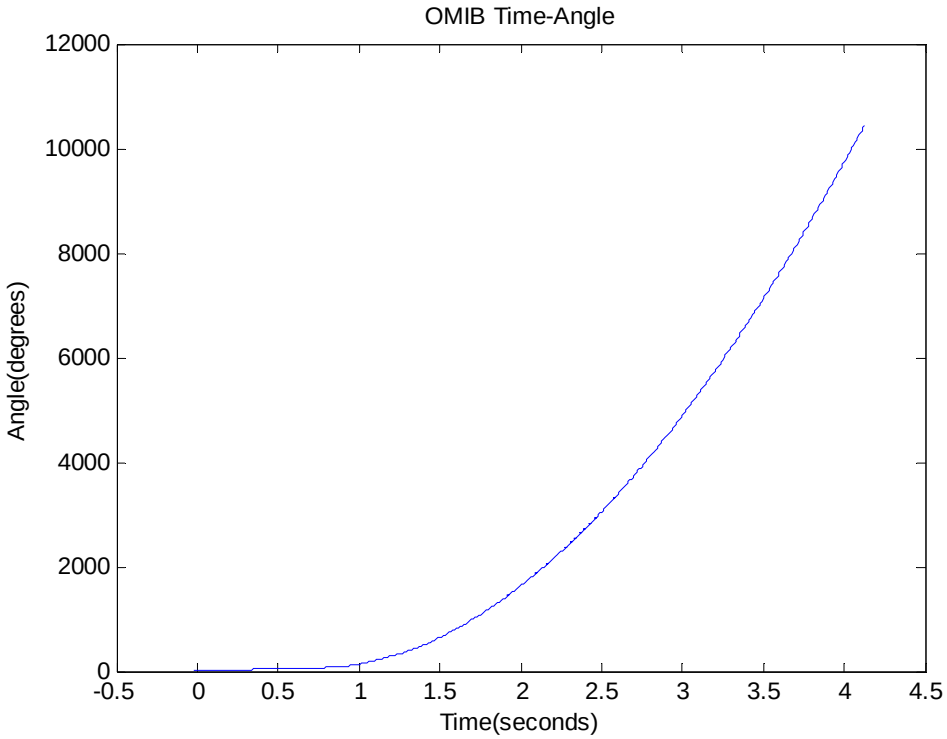

Figure 5.36 Rotor angle of OMIB system

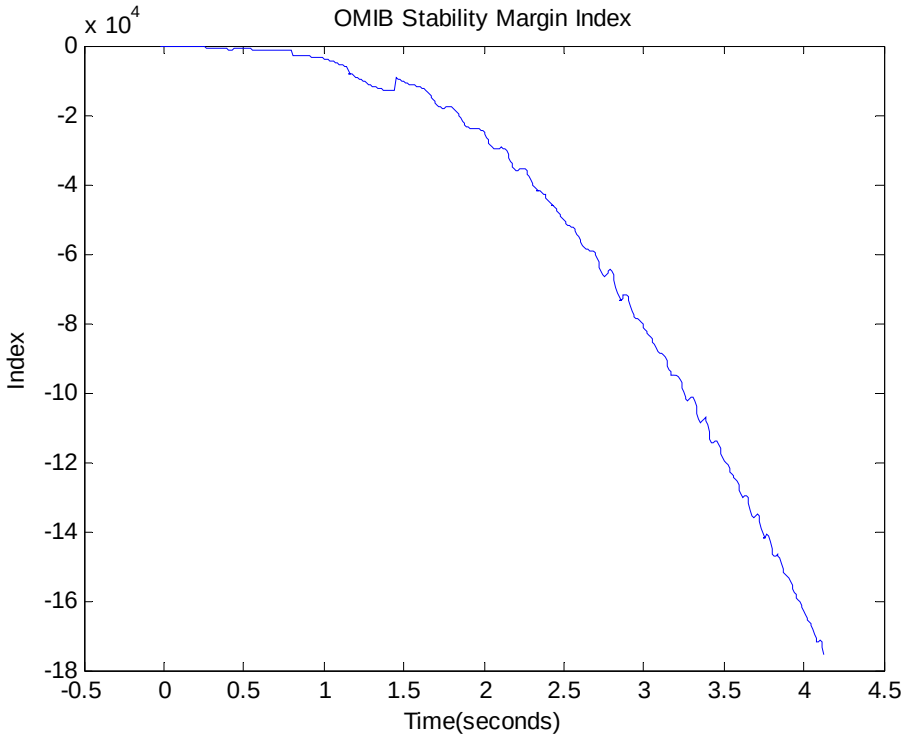

Figure 5.37 Stability index of OMIB system

From the OMIB equivalent quantities, we can see that the equivalent machine accelerates after the fault, and it begins to decelerate after the fault is cleared. The two segments of the power angle curve are roughly sinusoidal. In terms of the first-swing stability, it is fair enough to declare an unstable case around 0.6 s. To make a more reliable decision, it is better to check the stability index. A larger threshold value for the stability index will make a more reliable out-of-step decision. An alternative is to use the trend of stability index, which is also very reliable. If the stability index continuously goes negative, it means that the control actions cannot bring system back, and the rotor angles continue to separate.

5.4.3.2 Example B

Here another example is given to demonstrate the proposed real-time EEAC based out-of-step protection. We use the same simulation case as in subsection 5.2.2.3, which is a multi-swing unstable case. A three-phase fault is applied between Malin and Olinda (bus 23-bus 92) as shown in Figure 5.20. The fault begins at 0.05s, and the transmission line is tripped at 0.35s. Figure 5.38 shows the rotor angles referenced to John Day. Applying the coherency identification, two groups, leading and lagging groups, are identified as shown in Figure 5.39. The leading group goes out of step against the lagging group. Figure 5.40 shows the generator electromagnetic power outputs. The mechanical power inputs to each generator are roughly held constant due to the large time constants of generator governors. Applying the synchrophasor based EEAC, the equivalent OMIB electromagnetic and mechanical powers are shown in Figure 5.41. Figure 5.42 shows the OMIB rotor angle, and Figure 5.43 shows the OMIB stability index calculated as decelerating area subtracted by accelerating area.

After the disturbance, all generators swing together until around 1.8 s. The OMIB equivalent power curve shows that the first accelerating area is smaller than the first decelerating area, so it is first-swing stable. But in the long run, it is multi-swing unstable. We can determine this by checking the stability margin. In Figure 5.43, the beginning of this curve is fairly flat, but it goes negative continuously from 1.8 s on. Therefore, the multi-swing instability can be declared with this out-of-step protection using real-time EEAC and wide-area synchrophasor measurements.

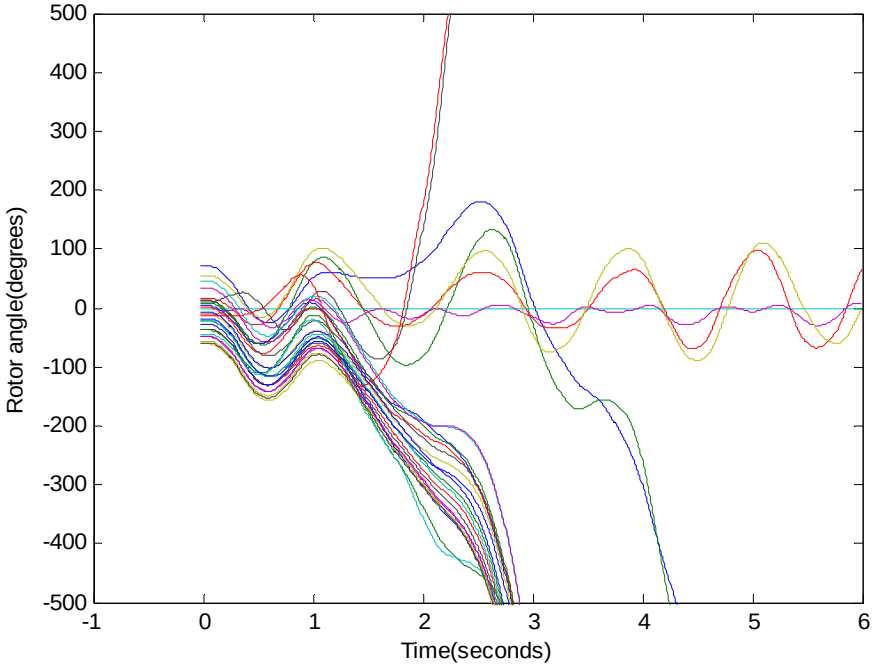

Figure 5.38 Rotor angles referenced to John Day

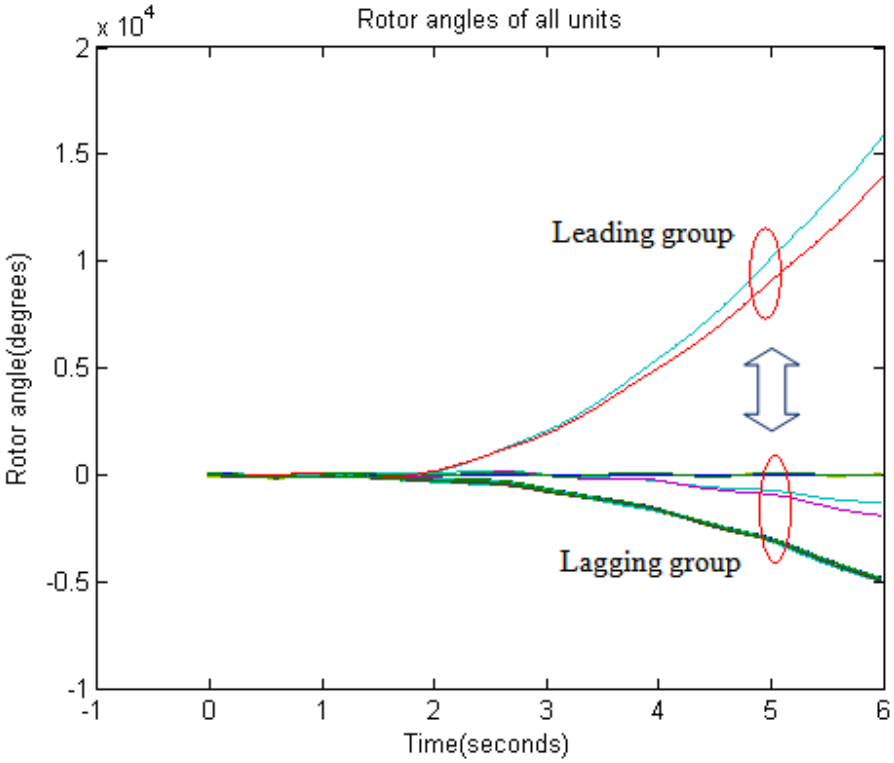

Figure 5.39 Coherent groups

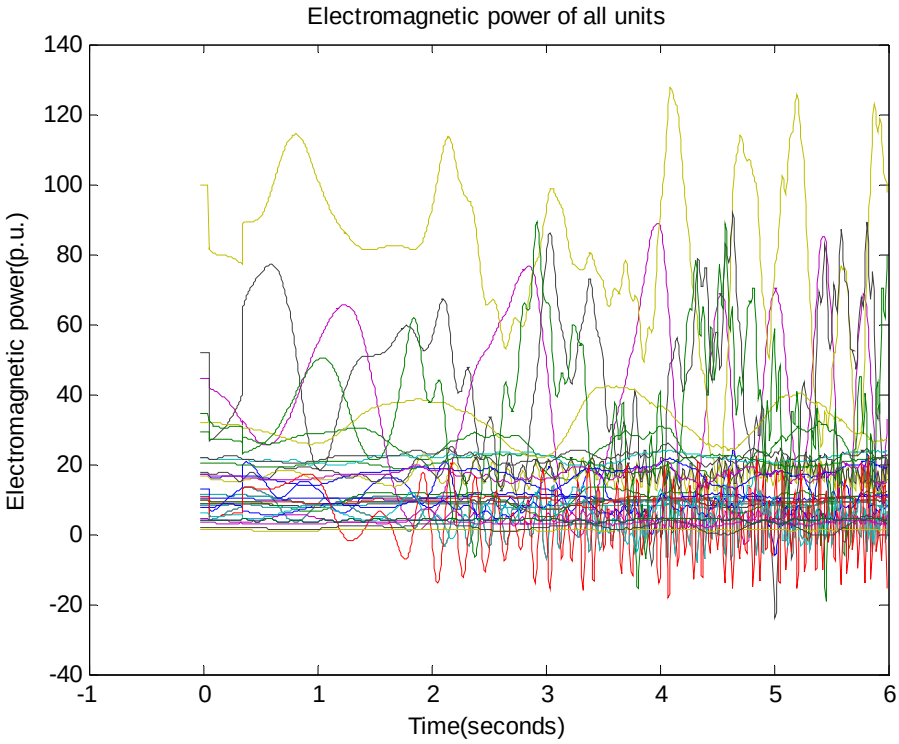

Figure 5.40 Electromagnetic power output of all generators

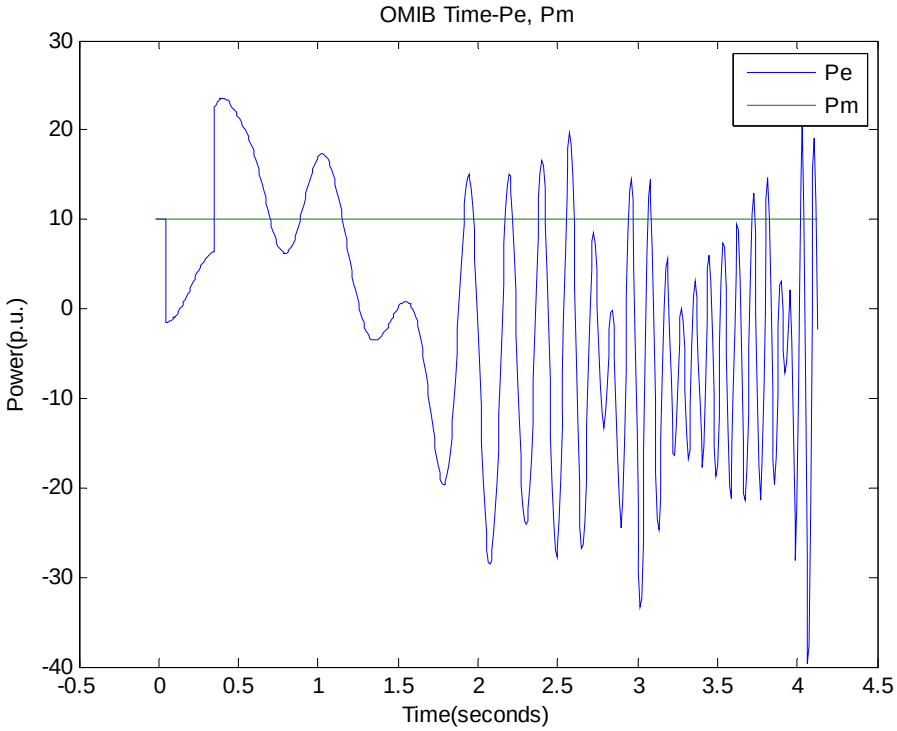

Figure 5.41 Power vs. time curve of OMIB system

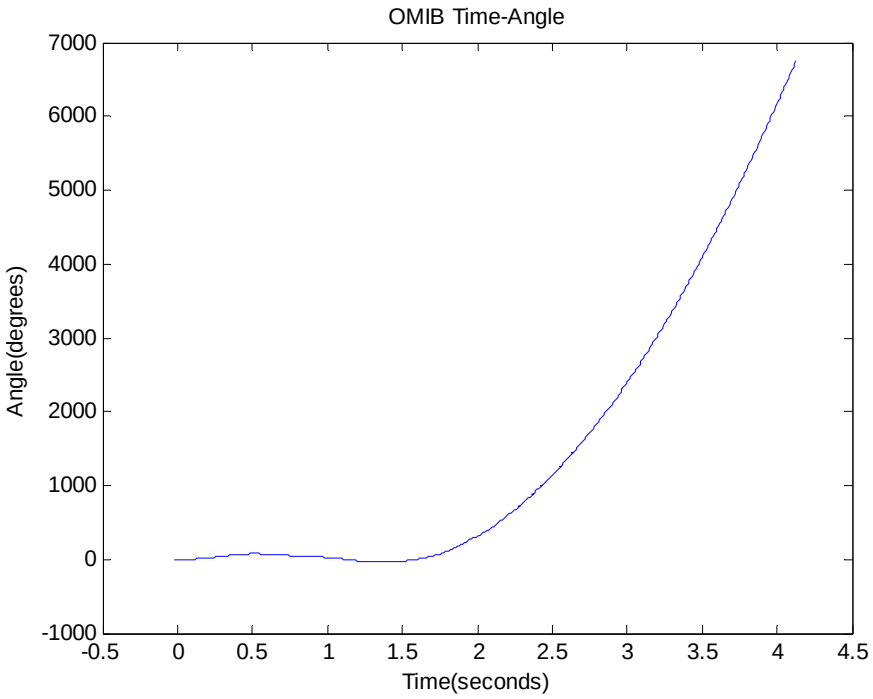

Figure 5.42 Rotor angle of OMIB system

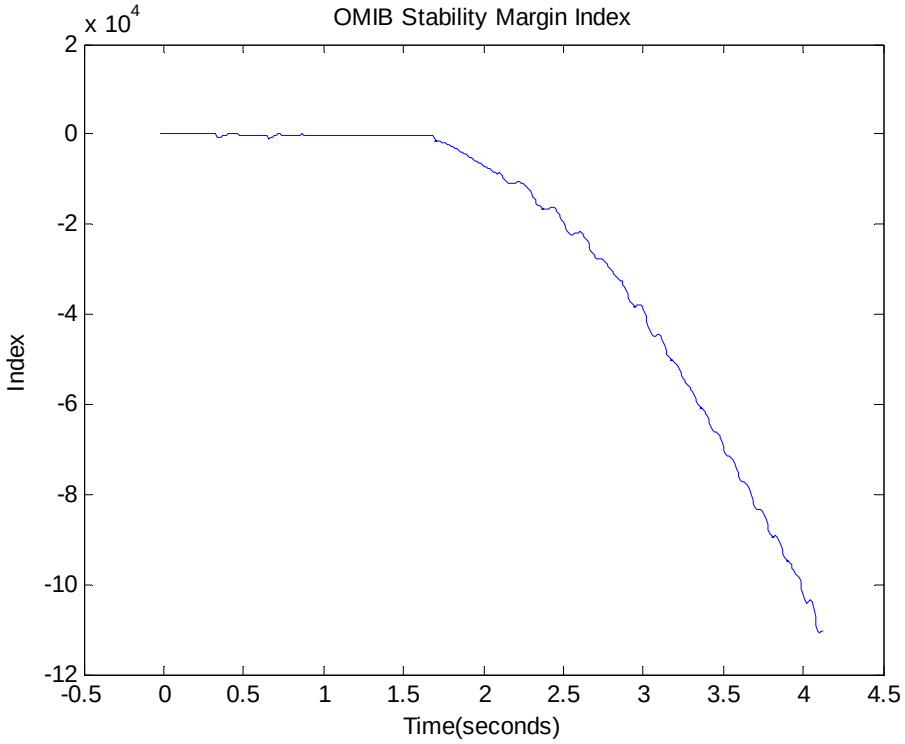

Figure 5.43 Stability index of OMIB system

Although real-time EEAC based out-of-step protection is supposed to be faster and more reliable, EEAC is criticized for its two-group separation assumption. We believe it is hard to find exact two-group separation in real power systems and multi-group separation may occur. However, the multi-group separation may not occur at the same time. So the multi-group separation can be handled with several two-group separations occurring at different time. Even though the multi-group separation happens exactly at the same time, the severity of the separation is not the same. So we can process the most severe two-group separation first. This strategy can be termed as cascading out-of-step protection scheme, or cascading controlled islanding. For example, the system is composed of three coherent groups: A, B and C. After a disturbance, the three groups are all oscillating. A separates with B and C first, or A separates more at the same time, we should disconnect group A from the system, and make it to be an island. Now the system is composed of B and C. If it stabilizes, we can leave it alone. If not, we can do controlled islanding again.

Chapter 6
Conclusions and Future Work

Recently occurrence of catastrophic failures in power systems seems to be more frequent. The usual scenario of such events is that the power system is in a stressed state. Faults on critical facilities will lead to unanticipated tripping of system components. Once the N-1 rules, according to which the system is designed, are violated, catastrophic failures or blackouts may occur. To avoid this, better system awareness is extremely important. The electric power system is mathematically represented as a multidimensional nonlinear dynamic system. To obtain the system state variables accurately and quickly is the prerequisite for any control actions taken to operate the system reliably and economically. The current trend of increased use of wide-area synchronized measurements is expected to result in a more efficient and reliable operation in power systems. The very important part of this work is to investigate the performance of synchronized measurements when systems involve dynamics, and then point to some possible solutions and application scenarios.

This chapter summarizes the conclusions drawn from previous chapters, and also recommends some possible future work in the studied areas.

6.1 Conclusions

The following conclusions have been established with supporting theory, analysis, verification and comparison.

First, synchronized measurements under system dynamics are analyzed qualitatively and quantitatively. Window sizes of DFT have to be selected appropriately to balance noise suppressing and dynamic performance. A short window (one-cycle in our study) with well-tuned filters can achieve both high certainty and excellent dynamic

performance. The leakage effect of DFT due to frequency disturbance in power systems is a major issue affecting the accuracy of synchronized measurements. The errors of synchronized measurements with nominal frequency based sampling rate and nominal frequency based DFT are simulated when frequency is disturbed. The larger the frequency disturbance, the less accurate the measurements.

Second, theoretical analysis is performed to explain above errors in synchronized measurements analytically. Based on it, methods to correct the errors are developed. A phasor-based synchronized frequency measurement is proposed, which has better dynamic performance when frequency changes quickly. Numerical simulation results verify its effectiveness under different dynamic conditions. The performance of the proposed method is also compared to frequency measurements obtained from commercial PMUs. The results show a better performance of the proposed method when compared to the actual signal. Furthermore, a synchronized frequency based phasor compensation technique is proposed with simulation verification to correct the phasor errors due to frequency disturbance. It can be easily used by already installed legacy PMUs based on nominal frequency (60Hz) algorithms. And it is also a very good alternative technique for frequency tracking in future PMUs.

Third, lease-square estimation, phasor positioning, and unbalance issue in synchronized measurements are also investigated theoretically and numerically. Least-square estimation helps suppresses the effect of random sample errors, and obtain continuous frequency values to improve dynamic performance. In steady states with nominal frequency, different phasor positioning will not make any difference. Otherwise, this is not true. Theoretical analysis and simulations in this work show that it is better to place the calculated phasor at the center of the window to reduce the errors due to frequency disturbance. When desired, these small errors can still be compensated. Performance of synchronized measurements under unbalance conditions in power systems is simulated and analyzed. When system is unbalanced, the measured frequency oscillates at around two times of the system nominal frequency. Knowing this, an average filter can be used to mitigate it. Actually, the least-square estimation discussed in this work also has the similar averaging effect. Although unbalance together with frequency dynamics make the synchronized measurements much more complicated, the

measurement errors, shown by simulations, can still be maintained within reasonable range with the methods proposed in this work.

Fourth, general application scenarios of the previous proposed methods in this work are categorized. In the scenarios with small frequency disturbance, the proposed methods are helpful to provide better accuracy. In the scenarios with large frequency disturbance, the large errors or wrong measurements, which could lead to wrong control actions when applied, can be corrected with the proposed methods. A test power system is simulated dynamically to show the large errors, and the effectiveness of the proposed correction.

Fifth, as a detailed application example, adaptive out-of-step protection using wide area measurements is studied. Two schemes are developed to detect the out-of-step condition. One is based on the real time swing curves directly, and the other on real-time EEAC. Both of them require identifying the groups of coherent generators, so a coherency identification technique suitable for online applications is also developed. The developed schemes are tested on the 127-bus WSCC system. Both of them can detect, online, the out-of-step condition in an early stage of the disturbance. These results of coherency identification provide valuable information for the controlled islanding scheme.

6.2 Future Work

Synchronized measurements have continually developed over the past two decades. The steady-state measurements have been standardized through the IEEE Std. C37.118. The measurement requirements for dynamic states have not been established yet. Instead, some dynamic measurement requirements are suggested in the annex of IEEE Std. C37. 118. The Power System Relaying Committee (PSRC) is currently working to put some requirements on dynamic frequency and synchrophasor measurements. Harmonizing a common set of dynamic performance requirements should be undertaken once the range of implementations and measurement applications has been more fully explored. As such, a systematic investigation on every aspect of dynamic measurements is necessary for all possible applications. In terms of measurement techniques and digital algorithms, there is already a very good choice of algorithms, and

most of the remaining work depends on the power engineer. What should be the benchmark tests for dynamic conditions? What should be the allowed errors for specific applications? Furthermore, it will be of great importance to create a library of recorded transient data from real system disturbance to be used for selecting and testing appropriate algorithms and associated parameters.

Applications of wide-area synchronized measurements in power systems will revolutionize the way of system monitoring, protection and control. Out-of-step protection or transient stability is one of the best dynamic application areas. With the advent of PMUs, measurement of the phase angle of bus voltages at different locations can now be accomplished and the progress of system transients can be monitored in real time. The system trajectories up to the present time are observable directly. Therefore, out-of-step decision can be made directly based on real-time swing curves. One possible future work is to study system separation with more than two coherent groups. An equivalent COA for each coherent group is calculated and the difference among them is monitored to detect out-of-step conditions. This method is straightforward, but it requires a large threshold values for reliable decisions, and involves longer time delay. An improvement of this method is to predict the swing curves. This is performed in reference [105] to determine the first-swing stability by checking for the existence of peaks of rotor angles of the severely disturbed generators in the post-fault period. Therefore, another possible future work is to use predicted swing curves to determine multi-swing stability. This is possible since the measured phasor data are monitored continuously. The prediction with a sliding window will stay away from the first several stable swings, and approach the unstable one. Direct methods for transient stability analysis depend on many simplifications and assumptions. However, the hybrid methods, which combine the advantages of direct methods and wide-area measurements, have the potential to relax those restrictions on accuracy and are another promising area for future work.

Historically, synchronously connected AC systems won out over the DC systems. Nowadays, stability in AC systems becomes a more prominent issue driven by competitive energy markets. Some prospects for future power systems advocate the use of superconducting transmission, and some others consider more utilization of DC transmission. However, the reality is that the current stressed system condition will

remain for a long time. The transient stability assessment and control rely on the analysis of power systems represented as multi-dimensional nonlinear differential equations. Due to the limitations in nonlinear control theory, current applications in transient stability depend heavily on time-domain simulations. The maturity of wide-area synchrophasor measurement will lead to a more reliable and efficient transient stability assessment as well as transient stability control with wide-area feedback.

References

[1] United States Department of Energy, “Grid 2030: a national vision for electricity’s second 100 years”, July 2003.

[2] C37.118-2005 IEEE Standard for Synchrophasors for Power System, prepared by the IEEE Power System Relaying Committee of the Power Engineering Society.

[3] IEEE Std. 1344-1995(R2001) Standard for Synchronphasors for Power Systems, prepared by the IEEE Power System Relaying Committee of the Power Engineering Society.

[4] A. G. Phadke, "Synchronized phasor measurements in power systems," Computer Applications in Power, IEEE, vol. 6, pp. 10-15, 1993.

[5] A. G. Phadke, "Synchronized phasor measurements-a historical overview," presented at Transmission and Distribution Conference and Exhibition 2002: Asia Pacific. IEEE PES, 2002.

[6] A. G. Phadke and J. S. Thorp, "History and applications of phasor measurments," presented at Power Systems Conference and Exposition, IEEE PES, 2006.

[7] K. Prabhu and J. Agrawal, "Selection of data windows for digital signal processing," presented at Acoustics, Speech, and Signal Processing, IEEE International Conference on ICASSP '78, 1978.

[8] H. Xue and R. Yang, "Optimal interpolating windowed discrete Fourier transform algorithms for harmonic analysis in power systems," Generation, Transmission and Distribution, IEE Proceedings-, vol. 150, pp. 583-587, 2003.

[9] D. Agrez, "Improving phase estimation with leakage minimization," Instrumentation and Measurement, IEEE Transactions on, vol. 54, pp. 1347-1353, 2005.

[10] D. Agrez, "Active Power Estimation in the Non-coherent Sampling: A Comparative Study," presented at Instrumentation and Measurement Technology Conference, 2005. IMTC 2005. Proceedings of the IEEE, 2005.

[11] M. Begovic, D. Novosel, D. Karlsson, C. Henville, and G. Michel, "Wide-area protection and emergency control," Proceedings of the IEEE, vol. 93, pp. 876-891, 2005.

[12] M. G. Adamiak, A. P. Apostolov, M. M. Begovic, C. F. Henville, K. E. Martin, G. L. Michel, A. G. Phadke, and J. S. Thorp, "Wide Area Protection-Technology and Infrastructures," Power Delivery, IEEE Transactions on, vol. 21, pp. 601-609, 2006.

[13] M. G. Adamiak, D. Novosel, B. Kasztenny, V. Madani, J. Sykes, and A. G. Phadke, "Wide Area Protection and Control - Today and Tomorrow," presented at PES TD 2005/2006, 2006.

[14] X. Jian, W. Fushuan, C. Y. Chung, and K. P. Wong, "Wide-Area Protection and its Applications - A Bibliographical Survey," presented at Power Systems Conference and Exposition, 2006.

[15] R. Moxley, "Practical Application of Synchronized Phasor Measurement," presented at Power Systems Conference: Advanced Metering, Protection, Control, Communication, and Distributed Resources, 2006. PS '06, 2006.

[16] G. Benmouyal, E. O. Schweitzer, and A. Guzman, "Synchronized phasor measurement in protective relays for protection, control, and analysis of electric power systems," presented at Protective Relay Engineers, 2004 57th Annual Conference for, 2004.

[17] G. Benmouyal, E. O. Schweitzer, and A. Guzman, "Synchronized phasor measurement in protective relays for protection, control, and analysis of electric power systems," presented at Developments in Power System Protection, 2004. Eighth IEE International Conference on, 2004.

[18] M. Yong, "Phasor measurement applications in China," presented at Transmission and Distribution Conference and Exhibition 2002: Asia Pacific. IEEE/PES, 2002.

[19] L. Chih-Wen, S. Mu-chun, T. Shuenn-Shing, and W. Yi-Jen, "Application of a novel fuzzy neural network to real-time transient stability swings prediction based on synchronized phasor measurements," IEEE Transactions on Power Systems,, vol. 14, pp. 685-692, 1999.

[20] Q. Yang, T. Bi, and J. Wu, "WAMS Implementation in China and the Challenges for Bulk Power System Protection," presented at Power Engineering Society General Meeting, 2007. IEEE, 2007.

[21] N. Niglye, F. S. Peritore, R. D. Soper, C. Anderson, R. Moxley, and A. Guzman, "Considerations for the Application of Synchrophasors to Predict Voltage

Instability," presented at Power Systems Conference: Advanced Metering, Protection, Control, Communication, and Distributed Resources, 2006. PS '06, 2006.

[22] J. Y. Cai, H. Zhenyu, J. Hauer, and K. Martin, "Current Status and Experience of WAMS Implementation in North America," presented at Transmission and Distribution Conference and Exhibition: Asia and Pacific, 2005 IEEE/PES, 2005.

[23] G. Yanfeng, N. Schulz, and A. Guzman, "Synchrophasor-Based Real-Time Voltage Stability Index," presented at Power Systems Conference and Exposition, 2006. PSCE '06. 2006 IEEE PES, 2006.

[24] D. Karlsson, L. Broski, and S. Ganesan, "Maximizing power system stability through wide area protection," presented at Protective Relay Engineers, 2004 57th Annual Conference for, 2004.

[25] J. Izykowski, E. Rosolowski, M. M. Saha, M. Fulczyk, and P. Balcerek, "A Fault-Location Method for Application With Current Differential Relays of Three-Terminal Lines," Power Delivery, IEEE Transactions on, vol. 22, pp. 2099-2107, 2007.

[26] Y. Chi-Shan, L. Chih-Wen, Y. Sun-Li, and J. Joe-Air, "A new PMU-based fault location algorithm for series compensated lines," Power Delivery, IEEE Transactions on, vol. 17, pp. 33-46, 2002.

[27] G. Zhang, P. Hirsch, and S. Lee, "Wide Area Frequency Visualization using Smart Client Technology," presented at Power Engineering Society General Meeting, 2007. IEEE, 2007.

[28] H. Zhenyu, M. Kosterev, R. Guttromson, and T. Nguyen, "Model validation with hybrid dynamic simulation," presented at Power Engineering Society General Meeting, 2006. IEEE, 2006.

[29] A. G. Phadke, B. Pickett, M. Adamiak, M. Begovic, G. Benmouyal, R. O. Burnett, Jr., T. W. Cease, J. Goossens, D. J. Hansen, M. Kezunovic, L. L. Mankoff, P. G. McLaren, G. Michel, R. J. Murphy, J. Nordstrom, M. S. Sachdev, H. S. Smith, J. S. Thorp, M. Trotignon, T. C. Wang, and M. A. Xavier, "Synchronized sampling and phasor measurements for relaying and control," Power Delivery, IEEE Transactions on, vol. 9, pp. 442-452, 1994.

[30] D. Fan and V. Centeno, "Phasor-Based Synchronized Frequency Measurement in Power Systems," Power Delivery, IEEE Transactions on, vol. 22, pp. 2010-2016, 2007.

[31] D. Fan, V. Centeno, and H. Zhang, "Aspects on Relative Phase Angle Measurement," presented at IEEE Power Engineering Society General Meeting, 2007.

[32] M.M. Begovic, P.M. Djuric, S. Dunlap, A.G. Phadke, “Frequency tracking in power networks in the presence of harmonics”, IEEE Trans. on Power Delivery, Vol.8, no. 2, pp. 480-486, Apr. 1993.

[33] C.T. Nguyen, K. Srinivasan, “A new technique for rapid tracking of frequency deviations based on level crossing”, IEEE Trans. on PAS, Vol. PAS-103, No. 8, Aug. 1984, pp. 2230-2236.

[34] M.S Sachdev, M.M. Giray, “A least error squares technique for determining power system frequency”, IEEE Trans. on PAS, Vol. PAS-104, No. 2, February 1985, pp. 437-443.

[35] M.M. Giray, M.S. Sachdev, “Off-normal frequency measurements in electric power systems”, IEEE Trans. on Power Delivery, Vol. 4, No.3, July 1989, pp.1573-1578.

[36] A.A. Girgis, R.G. Brown, “Application of Kalman filter in computer relaying”, IEEE Trans. on PAS, Vol. PAS-100, No. 7, July 1981, pp.3387-3395.

[37] A.A. Girgis, T.L. Hwang, “Optimal estimation of voltage phasors and frequency deviation using linear and non-linear Kalman filtering: theory and limiations”, IEEE Trans. on PAS, Vol. PAS-103, No. 10, Oct. 1984, pp.2943-2951.

[38] A.A. Girgis, F.M. Ham, “A new FFT-based digital frequency relay for load shedding”, IEEE Trans. on PAS, Vol. PAS-101, No. 2, February 1982, pp. 433-439.

[39] A.G. Phadke, J.S. Thorp, M.G. Adamiak, “A new measurement technique for tracking voltage phasors, local frequency, and rate of change of frequency”, IEEE Trans. on PAS, Vol. PAS-102 No. 5, May 1983, pp 1025-1038.

[40] Jian Chen, “Accurate frequency estimation with phasor angles”, master thesis, Virginia Polytechnic Institute and State University, 1994.

[41] A. G. Phadke, J.S. Thorp, Computer relaying for power systems (book), Research study press Ltd., 1988.

[42] B.C. Lovell, R.C. Williamson, B. Boashash, “The relationship between instantaneous frequency and time-frequency representations”, IEEE Trans. on Signal Processing, Volume 41, Issue 3, March 1993 Page(s):1458 – 1461.

[43] V. Eckhardt, P. Hippe, G. Hosemann, “Dynamic measuring of frequency and frequency oscillation in multiphase power systems”, IEEE Trans. on Power Delivery, Vol.4, No. 1, January 1989, pp.95-102.

[44] A. G. Phadke, J.S. Thorp, “Improved control and protection of power systems through synchronized phasor measurements” (book chapter), Control and dynamic systems, Vol. 43, pp 335-376, Academic Press Inc., 1991.

[45] G. Benmouyal, “An adaptive sampling-interval generator for digital relaying”, IEEE Trans. on Power Delivery, Vol. 4, No. 3, July 1989.

[46] Dawei Fan, Chengxue Zhang, *etc*., “Adaptive data acquisition of power system based on microcontroller”, Relay, Vol. 29, No. 10, Oct. 2001.

[47] David Hart, Damir Novosel, Yi Hu, Bob Smith, Mike Egolf, “A new frequency tracking and phasor estimation algorithm for generator protection”, IEEE Trans. on Power Delivery, Vol 12, No. 3, July 1997.

[48] Jian Chen, “Accurate frequency estimation with phasor angles”, master thesis, Virginia Polytechnic Institute and State University, 1994.

[49] A. von Jouanne and B. Banerjee, "Assessment of voltage unbalance," Power Delivery, IEEE Transactions on, vol. 16, pp. 782-790, 2001.

[50] A. G. Phadke, “Aspects of phasor measurement processes”, research report performed for Bonneville Power Administration, March 2003.

[51] A. G. Phadke, comments on Dawei Fan’s PhD preliminary examination, December 2007.

[52] P. Kurdur, Power system stability and control (book), McGraw-Hill, 1994.

[53] Steven J. Chapman, Electric Machinery and Power System Fundamental (book), McGraw-Hill, New York, 2002.

[54] A. E. Fitagerald, Charles Kingsley, Jr., Stephen D. Umans, Electric Machinery (book), McGraw-Hill.

[55] J. Duncan Glover, Mulukutla S. Sarma, Power System Analysis and Design (book), Brooks/Cole Thomson Learning.

[56] Simon Haykin, Barry Van Veen, Signals and Systems (book), John Wiley & Sons, Inc. 1999.

[57] Alan V. Oppenheim, Ronald W. Schafer, Discrete-Time Signal Processing (book), Prentice Hall, New Jersey, 1989.

[58] U.S.-Canada Power System Outage Task Force, Final Report on the August 14, 2003 Blackout in the United States and Canada: Causes and Recommendations.， April 2004, available online http://www.nerc.com.

[59] New York ISO, Final Report on the August 14, 2003 Blackout, February 2005.

[60] P. Pourbeik, P. S. Kundur, and C. W. Taylor, "The anatomy of a power grid blackout - Root causes and dynamics of recent major blackouts," *Power and Energy Magazine, IEEE,* vol. 4, pp. 22-29, 2006.

[61] S. H. Horowitz and A. G. Phadke, “Boosting immunity to blackouts,” *IEEE Power Energy Mag.*, pp. 47–53, Sep./Oct. 2003.

[62] A. R. Messina, V. Vittal, D. Ruiz-Vega, and G. Enriquez-Harper, "Interpretation and Visualization of Wide-Area PMU Measurements Using Hilbert Analysis," *IEEE Transactions on Power Systems,*, vol. 21, pp. 1763-1771, 2006.

[63] "Out of step relaying for generators working group report," Power Apparatus and Systems, IEEE Transactions on, vol. 96, pp. 1556-1564, 1977.

[64] "Power swing and out-of-step considerations on transmission lines," IEEE PSRC WG D6, 2005.

[65] A. Y. Abdelaziz, M. R. Irving, M. M. Mansour, A. M. El-Arabaty, and A. I. Nosseir, "Adaptive protection strategies for detecting power system out-of-step conditions using neural networks," Generation, Transmission and Distribution, IEE Proceedings-, vol. 145, pp. 387-394, 1998.

[66] R. O. Burnett, Jr., M. M. Butts, T. W. Cease, V. Centeno, G. Michel, R. J. Murphy, and A. G. Phadke, "Synchronized phasor measurements of a power system event," IEEE Transactions on Power Systems,, vol. 9, pp. 1643-1650, 1994.

[67] V. Centeno, J. de la Ree, A. G. Phadke, G. Michel, R. J. Murphy, and R. O. Burnett, Jr., "Adaptive out-of-step relaying using phasor measurement techniques," Computer Applications in Power, IEEE, vol. 6, pp. 12-17, 1993.

[68] V. Centeno, A. G. Phadke, A. Edris, J. Benton, M. Gaudi, and G. Michel, "An adaptive out-of-step relay [for power system protection]," IEEE Transactions on Power Delivery, vol. 12, pp. 61-71, 1997.

[69] J. S. Thorp, A. G. Phadke, S. H. Horowitz, M. M. Begovic, “Some Applications of Phasor Measurements to Adaptive Protection”, IEEE Transactions on Power Systems, Vol. 3, No. May 1988.

[70] C. L. Chang, A. S. Liu, and C. T. Huang, "Oscillatory stability analysis using real-time measured data," IEEE Transactions on Power Systems,, vol. 8, pp. 823-829, 1993.

[71] C. L. Clemans, L. W. Lloyd, W. R. Roemish, and F. R. Schleif, "An Acceleration Relay for Power Systems," IEEE Transactions on Power Apparatus and Systems, vol. PAS-90, pp. 1150-1154, 1971.

[72] C. L. Clemans and W. R. Roemish, "A Power Rate Relay for System Applications," IEEE Transactions on Power Apparatus and Systems, vol. PAS-92, pp. 122-126, 1973.

[73] A. A. Daoud, G. G. Karady, and R. A. Amin, "A new fast-learning algorithm for predicting power system stability," Power Engineering Society winter meeting, 2001.

[74] T. Minakawa, M. Sato, Y. Ichikawa, and Y. Ishihara, "A new method for detecting loss of synchronism using power and current measured on a line," Power Delivery, IEEE Transactions on, vol. 14, pp. 68-73, 1999.

[75] P. J. Moore and A. T. Johns, "New method of power swing blocking for digital distance protection," Generation, Transmission and Distribution, IEE Proceedings-, vol. 143, pp. 19-26, 1996.

[76] Y. Morioka, K. Tomiyama, H. Arima, K. Sawai, K. Omata, T. Matsushima, K. Takagi, A. Ishibashi, and H. Saito, "System separation equipment to minimize power system instability using generator's angular-velocity measurements," Power Delivery, IEEE Transactions on, vol. 8, pp. 941-947, 1993.

[77] P. O'Shea, "The use of sliding spectral windows for parameter estimation in power system disturbance monitoring," IEEE Transactions on Power Systems,, vol. 15, pp. 1261-1267, 2000.

[78] K. R. Padiyar and S. Krishna, "Online detection of loss of synchronism using energy function criterion," Power Delivery, IEEE Transactions on, vol. 21, pp. 46-55, 2006.

[79] K. K. P. Poon and K. C. Lee, "Analysis of transient stability swings in large interconnected power systems by Fourier transformation," IEEE Transactions on Power Systems,, vol. 3, pp. 1573-1581, 1988.

[80] M. A. Redfern and M. J. Checkfield, "A new pole slipping protection algorithm for dispersed storage and generation using the equal area criterion," Power Delivery, IEEE Transactions on, vol. 10, pp. 194-202, 1995.

[81] W. R. Roemish and E. T. Wall, "A New Synchronous Generator Out-of-Step Relay Scheme Part II Complete Version," IEEE Transactions on Power Apparatus and Systems, vol. PAS-104, pp. 572-582, 1985.

[82] W. R. Roemish and E. T. Wall, "A New Synchronous Generator Out-of Step Relay Scheme Part I Abbreviated Version," IEEE Transactions on Power Apparatus and Systems, vol. PAS-104, pp. 562-571, 1985.

[83] F. R. Schleif, L. W. Lloyd, R. W. World, and W. B. Gish, "A Swing Relay for the East-West Intertie," IEEE Transactions on Power Apparatus and Systems, vol. PAS-88, pp. 821-825, 1969.

[84] C. A. Stigers, C. S. Woods, J. R. Smith, and R. D. Setterstrom, "The acceleration trend relay for generator stabilization at Colstrip," Power Delivery, IEEE Transactions on, vol. 12, pp. 1074-1081, 1997.

[85] C. W. Taylor, J. M. Haner, L. A. Hill, W. A. Mittelstadt, and R. L. Cresap, "A New Out-of-Step Relay with Rate of Change of Apparent Resistance Augmentation," IEEE Transactions on Power Apparatus and Systems, vol. PAS-102, pp. 631-639, 1983.

[86] J.M. Haner, T.D. Laughlin, and C.W. Taylor, “Experience with the R-Rdot Out-of-Step Relay,” IEEE Transactions on Power Delivery, Vol. 1, No. 2, pp. 35-39, April 1986.

[87] K. H. So, J. Y. Heo, C. H. Kim, R. K. Aggarwal, and K. B. Song, "Out-of-step detection algorithm using frequency deviation of voltage," *Generation, Transmission & Distribution, IET*, vol. 1, pp. 119-126, 2007.

[88] A. CHANG and M. M. ADIBI, "Power System Dynamic Equivalents," IEEE Transactions on Power Apparatus and Systems, vol. 89, pp. 1737-1744, 1970.

[89] S. T. Y. Lee and F. C. Schweppe, "Distance Measures and Coherency Recognition for Transient Stability Equivalents," IEEE Transactions on Power Apparatus and Systems, vol. PAS-92, pp. 1550-1557, 1973.

[90] R. Podmore, "Identification of Coherent Generators for Dynamic Equivalents," IEEE Transactions on Power Apparatus and Systems, vol. PAS-97, pp. 1344-1354, 1978.

[91] R. Podmore, "A Comprehensive Program For Computing Coherency-based Dynamic Equivalents," Power Industry Computer Applications Conference, 1979. PICA-79.

[92] J. C. Giri, "Coherency Reduction in the EPRI Stability Program," IEEE Transactions on Power Apparatus and Systems, vol. PAS-102, pp. 1285-1293, 1983.

[93] R. Nath, S. S. Lamba, and K. S. Prakasa Rao, "Coherency Based System Decomposition into Study and External Areas Using Weak Coupling," IEEE Transactions on Power Apparatus and Systems, vol. PAS-104, pp. 1443-1449, 1985.

[94] R. J. Newell, M. D. Risan, L. Allen, I. S. Rao, and D. L. Stuehm, "Utility Experience with Coherency-Based Dynamic Equivalents Of Very Large Systems," IEEE Transactions on Power Apparatus and Systems, vol. PAS-104, pp. 3056-3063, 1985.

[95] M. Parsa and J. Toyoda, "Slow-coherency based composite mode oscillatory stabilization by means of a hybrid PSS," IEEE Transactions on Power Systems,, vol. 4, pp. 1499-1506, 1989.

[96] S. B. Yusof, G. J. Rogers, and R. T. H. Alden, "Slow coherency based network partitioning including load buses," IEEE Transactions on Power Systems,, vol. 8, pp. 1375-1382, 1993.

[97] J. H. Chow, R. Galarza, P. Accari, and W. W. Price, "Inertial and slow coherency aggregation algorithms for power system dynamic model reduction," IEEE Transactions on Power Systems,, vol. 10, pp. 680-685, 1995.

[98] J. H. Chow, Time-Scale Modeling of Dynamic Networks with Applicationsto Power Systems. New York: Springer-Verlag, 1982, vol. 46.

[99] H. You, V. Vittal, and W. Xiaoming, "Slow coherency-based islanding," IEEE Transactions on Power Systems,, vol. 19, pp. 483-491, 2004.

[100] B. Yang, V. Vittal, and G. T. Heydt, "Slow-Coherency-Based Controlled Islanding: A Demonstration of the Approach on the August 14, 2003 Blackout Scenario," IEEE Transactions on Power Systems,, vol. 21, pp. 1840-1847, 2006.

[101] K. L. Lo, Z. Z. Qi, and D. Xiao, "Identification of coherent generators by spectrum analysis," Generation, Transmission and Distribution, IEE Proceedings-, vol. 142, pp. 367-371, 1995.

[102] M. Jonsson, M. Begovic, and J. Daalder, "A new method suitable for real-time generator coherency determination," IEEE Transactions on Power Systems, vol. 19, pp. 1473-1482, 2004.

[103] W. Mang-Hui and C. Hong-Chan, "Novel clustering method for coherency identification using an artificial neural network," IEEE Transactions on Power Systems,, vol. 9, pp. 2056-2062, 1994.

[104] M. H. Haque and A. H. M. A. Rahim, "An efficient method of identifying coherent generators using Taylor series expansion," IEEE Transactions on Power Systems,, vol. 3, pp. 1112-1118, 1988.

[105] Haque, M.H. and Rahim, A.H.M.A., “Determination of First Swing Stability limits of Multimachine Systems through Taylor Series Expansion”, *IEEE Proc. C*, 1989, **136**, (6), pp 373-379.

[106] Y. Xue, L. Wehenkel, R. Belhomme, P. A. R. P. Rousseaux, M. A. P. M. Pavella, E. A. E. E. Euxibie, B. A. H. B. Heilbronn, and J. F. A. L. J. F. Lesigne, "Extended equal area criterion revisited," IEEE Transactions on Power Systems, vol. 7, pp. 1012-1022, 1992.

[107] Y. Xue, T. Van Custem, and M. Ribbens-Pavella, "Extended equal area criterion justifications, generalizations, applications," IEEE Transactions on Power Systems, vol. 4, pp. 44-52, 1989.

[108] M. Pavella, D. Ernst, D. Ruiz-Vega Transient stability of power systems: a unified approach to assessment and control (book), Kluwer Academic Publishers, Boston, 2000.

[109] M. Pavella, P.G. Mruthy, Transient stability of power systems: theory and practice (book), Wiley, New York, 1994.

[110] Y. Xue, “A critical comparison of various methods for transient stability assessment (1)”, Automation of Electric Power Systems, vol 25, No. 11, 2001.

[111] Y. Xue, “A critical comparison of various methods for transient stability assessment (2)”, Automation of Electric Power Systems, vol 25, No. 11, 2001.

[112] Y. Xue, “A critical comparison of various methods for transient stability assessment (3)”, Automation of Electric Power Systems, vol 25, No. 11, 2001.

[113] Y. Xue, “A critical comparison of various methods for transient stability assessment (4)”, Automation of Electric Power Systems, vol 25, No. 11, 2001.

[114] Y. Xue, “Space-time cooperative framework for defending blackouts (1)”, Automation of Electric Power Systems, vol 30, No. 1, 2006.

[115] Y. Xue, “Space-time cooperative framework for defending blackouts (2)”, Automation of Electric Power Systems, vol 30, No. 2, 2006.

[116] Y. Xue, “Space-time cooperative framework for defending blackouts (3)”, Automation of Electric Power Systems, vol 30, No. 3, 2006.

[117] PSERC project team, “On-Line Transient Stability Assessment Scoping Study”, PSERC publication, February, 2005.

[118] Virginia Tech project plan, “Advanced protection systems using wide area measurements”, March 2006.

Appendix A

23-Bus PSS/E Test System

A.1 Power Flow Data in PSS/E Format

```
0,   100.00          / PSS/E-30.0    TUE, MAY 11 2004  13:26
PSS/E PROGRAM APPLICATION GUIDE EXAMPLE
BASE CASE INCLUDING SEQUENCE DATA
   101,'NUC-A       ',  21.6000,2,     0.000,     0.000,   1,  77,1.02000,  16.5465,  11
   102,'NUC-B       ',  21.6000,2,     0.000,     0.000,   1,  77,1.02000,  16.5465,  11
   151,'NUCPANT     ', 500.0000,1,     0.000,  -600.000,   1,   1,1.01190,  10.8887,   1
   152,'MID500      ', 500.0000,1,     0.000,     0.000,   1,   1,1.01707,  -1.1152,   1
   153,'MID230      ', 230.0000,1,     0.000,     0.000,   1,   1,0.99300,  -3.2357,   1
   154,'DOWNTN      ', 230.0000,1,     0.000,   300.000,   1,   1,0.93892,  -9.8857,   1
   201,'HYDRO       ', 500.0000,1,     0.000,   300.000,   2,   2,1.04000,   6.1599,  22
   202,'EAST500     ', 500.0000,1,     0.000,     0.000,   2,   2,1.00879,  -1.3172,   2
   203,'EAST230     ', 230.0000,1,     0.000,    50.000,   2,   2,0.96651,  -6.9180,   2
   204,'SUB500      ', 500.0000,1,     0.000,     0.000,   2,   2,0.97873,  -3.7331,   2
   205,'SUB230      ', 230.0000,1,     0.000,   300.000,   2,   2,0.94902,  -9.1798,   2
   206,'URBGEN      ',  18.0000,2,     0.000,     0.000,   2,   2,1.02361,  -2.9699,  22
   211,'HYDRO_G     ',  20.0000,2,     0.000,     0.000,   2,   2,1.04042,  12.9204,  22
  3001,'MINE        ', 230.0000,1,     0.000,     0.000,   5,   5,1.02979,  -1.3728,  55
  3002,'E. MINE     ', 500.0000,1,     0.000,     0.000,   5,   5,1.02791,  -1.8253,   5
  3003,'S. MINE     ', 230.0000,1,     0.000,     0.000,   5,   5,1.02333,  -2.2538,   5
  3004,'WEST        ', 500.0000,1,     0.000,     0.000,   5,   5,1.01647,  -3.4289,   5
  3005,'WEST        ', 230.0000,1,     0.000,     0.000,   5,   5,0.99478,  -5.1800,   5
  3006,'UPTOWN      ', 230.0000,1,     0.000,     0.000,   5,   5,0.99404,  -3.7921,   5
  3007,'RURAL       ', 230.0000,1,     0.000,     0.000,   5,   5,0.96370,  -8.5380,   5
  3008,'CATDOG      ', 230.0000,1,     0.000,     0.000,   5,   5,0.95861,  -9.0489,  55
  3011,'MINE_G      ',  13.8000,3,     0.000,     0.000,   5,   5,1.04000,   0.0000,  55
  3018,'CATDOG_G    ',  13.8000,2,     0.000,     0.000,   5,   5,1.02177,  -4.0804,  55
0 / END OF BUS DATA, BEGIN LOAD DATA
   153,'1 ',1,   1,   1,   200.000,   100.000,     0.000,     0.000,     0.000,     0.000,   1
   154,'1 ',1,   2,   1,   600.000,   450.000,     0.000,     0.000,     0.000,     0.000,   1
   154,'2 ',1,   2,   1,   400.000,   350.000,     0.000,     0.000,     0.000,     0.000, 100
```

203,'1 ',1, 2, 2, 300.000, 150.000, 0.000, 0.000, 0.000, 0.000, 2
205,'1 ',1, 2, 2, 1200.000, 700.000, 0.000, 0.000, 0.000, 0.000, 2
3005,'1 ',1, 5, 5, 100.000, 50.000, 0.000, 0.000, 0.000, 0.000, 5
3007,'1 ',1, 5, 5, 200.000, 75.000, 0.000, 0.000, 0.000, 0.000, 5
3008,'1 ',1, 5, 5, 200.000, 75.000, 0.000, 0.000, 0.000, 0.000, 5
0 / END OF LOAD DATA, BEGIN GENERATOR DATA
101,'1 ', 750.000, 81.194, 600.000, -100.000,1.02000, 0, 900.000, 0.01000, 0.30000, 0.00000, 0.00000,1.00000,1, 100.0, 810.000, 0.000, 11,0.6667, 1,0.3333
102,'1 ', 750.000, 81.194, 600.000, -100.000,1.02000, 0, 900.000, 0.01000, 0.30000, 0.00000, 0.00000,1.00000,1, 100.0, 810.000, 0.000, 11,0.6667, 1,0.3333
206,'1 ', 800.000, 600.000, 600.000, 0.000,0.98000, 205, 1000.000, 0.01000, 0.25000, 0.00000, 0.00000,1.00000,1, 100.0, 900.000, 0.000, 2,0.4000, 22,0.6000
211,'1 ', 600.000, 17.750, 400.000, -100.000,1.04000, 201, 725.000, 0.01000, 0.26000, 0.00000, 0.00000,1.00000,1, 100.0, 616.250, 0.000, 2,0.4000, 22,0.6000
3011,'1 ', 258.657, 104.042, 600.000, -100.000,1.04000, 0, 1000.000, 0.01000, 0.35000, 0.00000, 0.00000,1.00000,1, 100.0, 900.000, 0.000, 55,0.3846, 5,0.3077, 22,0.2308, 11,0.0769
3018,'1 ', 100.000, 80.000, 80.000, 0.000,1.02000, 3008, 130.000, 0.01000, 0.35000, 0.00000, 0.00000,1.00000,1, 100.0, 117.000, 0.000, 55,0.5556, 5,0.4444
0 / END OF GENERATOR DATA, BEGIN BRANCH DATA
151, 152,'1 ', 0.00260, 0.04600, 3.50000, 1200.00, 1300.00, 1.00, 0.00000, 0.00000, 0.00000, 0.00000,1, 0.00, 1,1.0000
151, 152,'2 ', 0.00260, 0.04600, 3.50000, 1200.00, 1300.00, 1.00, 0.00000, 0.00000, 0.00000, 0.00000,1, 0.00, 1,1.0000
151, 201,'1 ', 0.00100, 0.01500, 1.20000, 1200.00, 1300.00, 1.00, 0.00000, 0.00000, 0.00000, 0.00000,1, 0.00, 1,1.0000
152, -202,'1 ', 0.00080, 0.01000, 0.95000, 1200.00, 1300.00, 1.00, 0.00000, 0.00000, 0.00000, 0.00000,1, 0.00, 1,1.0000
152, 3004,'1 ', 0.00300, 0.03000, 2.50000, 0.00, 0.00, 1.00, 0.00000, 0.00000, 0.00000, 0.00000,1, 0.00, 1,1.0000
153, 154,'1 ', 0.00500, 0.04500, 0.10000, 300.00, 350.00, 1.00, 0.00000, 0.00000, 0.00000, 0.00000,1, 0.00, 1,0.7500, 100,0.2500
153, 154,'2 ', 0.00600, 0.05400, 0.15000, 300.00, 350.00, 1.00, 0.00000, 0.00000, 0.00000, 0.00000,1, 0.00, 1,1.0000
153, 3006,'1 ', 0.00100, 0.01200, 0.03000, 0.00, 0.00, 1.00, 0.00000, 0.00000, 0.00000, 0.00000,1, 0.00, 1,1.0000
154, 203,'1 ', 0.00400, 0.04000, 0.10000, 200.00, 250.00, 1.00, 0.00000, 0.00000, 0.00000, 0.00000,1, 0.00, 1,1.0000

154, 205,'1 ', 0.00033, 0.00333, 0.09000, 600.00, 660.00, 1.00, 0.00000, 0.00000, 0.00000, 0.00000,1, 0.00, 1,1.0000

154, 3008,'1 ', 0.00270, 0.02200, 0.30000, 400.00, 440.00, 1.00, 0.00000, 0.00000, 0.00000, 0.00000,1, 0.00, 1,1.0000

201, 202,'1 ', 0.00200, 0.02500, 2.00000, 1200.00, 1300.00, 1.00, 0.00000, 0.00000, 0.00000, 0.00000,1, 0.00, 22,1.0000

201, 204,'1 ', 0.00300, 0.03000, 2.50000, 1200.00, 1300.00, 1.00, 0.00000, 0.00000, 0.00000, 0.00000,1, 0.00, 22,1.0000

203, -205,'1 ', 0.00500, 0.04500, 0.08000, 200.00, 250.00, 1.00, 0.00000, 0.00000, 0.00000, 0.00000,1, 0.00, 2,1.0000

203, -205,'2 ', 0.00500, 0.04500, 0.08000, 200.00, 250.00, 1.00, 0.00000, 0.00000, 0.00000, 0.00000,1, 0.00, 2,1.0000

3001, 3003,'1 ', 0.00000, 0.00800, 0.00000, 0.00, 0.00, 1.00, 0.00000, 0.00000, 0.00000, 0.00000,1, 0.00, 55,1.0000

3002, 3004,'1 ', 0.00600, 0.05400, 0.09000, 0.00, 0.00, 1.00, 0.00000, 0.00000, 0.00000, 0.00000,1, 0.00, 5,1.0000

3003, 3005,'1 ', 0.00600, 0.05400, 0.09000, 0.00, 0.00, 1.00, 0.00000, 0.00000, 0.00000, 0.00000,1, 0.00, 5,1.0000

3003, 3005,'2 ', 0.00600, 0.05400, 0.09000, 0.00, 0.00, 1.00, 0.00000, 0.00000, 0.00000, 0.00000,1, 0.00, 5,1.0000

3005, 3006,'1 ', 0.00350, 0.03000, 0.07000, 0.00, 0.00, 1.00, 0.00000, 0.00000, 0.00000, 0.00000,1, 0.00, 5,1.0000

3005, 3007,'1 ', 0.00300, 0.02500, 0.06000, 0.00, 0.00, 1.00, 0.00000, 0.00000, 0.00000, 0.00000,1, 0.00, 5,1.0000

3005, 3008,'1 ', 0.00600, 0.05000, 0.12000, 0.00, 0.00, 1.00, 0.00000, 0.00000, 0.00000, 0.00000,1, 0.00, 5,1.0000

3007, 3008,'1 ', 0.00300, 0.02500, 0.06000, 0.00, 0.00, 1.00, 0.00000, 0.00000, 0.00000, 0.00000,1, 0.00, 5,1.0000

0 / END OF BRANCH DATA, BEGIN TRANSFORMER DATA

151, 101, 0,'1 ',1,1,1, 0.00000, 0.00000,2,' ',1, 1,1.0000 0.00030, 0.01360, 100.00 1.00000, 0.000, 0.000, 1250.00, 1350.00, 1750.00, 0, 0, 1.10000, 0.90000, 1.10000, 0.90000, 5, 0, 0.00000, 0.00000 1.00000, 0.000

151, 102, 0,'1 ',1,1,1, 0.00000, 0.00000,2,' ',1, 1,1.0000 0.00030, 0.01360, 100.00 1.00000, 0.000, 0.000, 1250.00, 1350.00, 1750.00, 0, 0, 1.10000, 0.90000, 1.10000, 0.90000, 5, 0, 0.00000, 0.00000 1.00000, 0.000

152, 153, 0,'1 ',1,1,1, 0.00000, 0.00000,2,' ',1, 1,1.0000 0.00000, 0.00500, 100.00
1.01000, 0.000, 0.000, 2500.00, 3000.00, 3500.00, 1, 154, 1.05000, 0.95000, 1.00000, 0.98000, 33, 0,
0.00000, 0.00000 1.00000, 0.000
201, 211, 0,'1 ',1,1,1, 0.00000, 0.00000,2,' ',1, 22,1.0000 0.00070, 0.02125, 100.00
1.00000, 0.000, 0.000, 800.00, 1000.00, 1120.00, 0, 201, 1.10000, 0.90000, 1.05000, 0.95000, 5, 0,
0.00000, 0.00000
1.00000, 0.000
202, 203, 0,'1 ',1,1,1, 0.00000, 0.00000,2,' ',1, 2,1.0000 0.00040, 0.01625, 100.00
1.00000, 0.000, 0.000, 800.00, 1040.00, 1200.00, 3, 0,30.00000,-30.0000,555.0000,545.0000, 33, 0,
0.00000, 0.00000 1.00000, 0.000
204, 205, 0,'1 ',1,1,1, 0.00000, 0.00000,2,' ',1, 2,1.0000 0.00030, 0.01500, 100.00
1.00000, 0.000, 0.000, 800.00, 1040.00, 1200.00, 1, 205, 1.05000, 0.95000, 1.00000, 0.98000, 33, 0,
0.00000, 0.00000 1.00000, 0.000
205, 206, 0,'1 ',1,1,1, 0.00000, 0.00000,2,' ',1, 2,1.0000 0.00026, 0.01333, 100.00
1.00000, 0.000, 0.000, 900.00, 1080.00, 1350.00, 0, 0, 1.10000, 0.90000, 1.10000, 0.90000, 5, 0,
0.00000, 0.00000 1.00000, 0.000
3001, 3002, 0,'1 ',1,1,1, 0.00000, 0.00000,1,' ',1, 55,1.0000 0.00030, 0.01500, 100.00
1.00000, 0.000, 0.000, 800.00, 1040.00, 1200.00, 0, 0, 1.10000, 0.90000, 1.05000, 0.95000, 33, 0,
0.00000, 0.00000 1.00000, 0.000
3001, 3011, 0,'1 ',1,1,1, 0.00000, 0.00000,2,' ',1, 55,1.0000 0.00020, 0.01000, 100.00
1.00000, 0.000, 0.000, 1300.00, 1560.00, 1820.00, 0, 0, 1.10000, 0.90000, 1.05000, 0.95000, 5, 0,
0.00000, 0.00000 1.00000, 0.000
3004, 3005, 0,'1 ',1,1,1, 0.00000, 0.00000,1,' ',1, 5,1.0000 0.00040, 0.01625, 100.00
1.00000, 0.000, 0.000, 800.00, 1040.00, 1200.00, 0, 0, 1.10000, 0.90000, 1.05000, 0.95000, 33, 0,
0.00000, 0.00000 1.00000, 0.000
3008, 3018, 0,'1 ',1,1,1, 0.00000, 0.00000,2,' ',1, 55,1.0000 0.00021, 0.08500, 100.00
1.00000, 0.000, 0.000, 150.00, 200.00, 250.00, 0, 0, 1.10000, 0.90000, 1.05000, 0.95000, 5, 0,
0.00000, 0.00000 1.00000, 0.000
0 / END OF TRANSFORMER DATA, BEGIN AREA DATA
1, 101, 250.000, 10.000,'FLAPCO '
2, 206, -100.000, 10.000,'LIGHTCO '
5, 3011, -150.000, 10.000,'WORLD '
0 / END OF AREA DATA, BEGIN TWO-TERMINAL DC DATA
0 / END OF TWO-TERMINAL DC DATA, BEGIN VSC DC LINE DATA
0 / END OF VSC DC LINE DATA, BEGIN SWITCHED SHUNT DATA
0 / END OF SWITCHED SHUNT DATA, BEGIN IMPEDANCE CORRECTION DATA
0 / END OF IMPEDANCE CORRECTION DATA, BEGIN MULTI-TERMINAL DC DATA

```
0 / END OF MULTI-TERMINAL DC DATA, BEGIN MULTI-SECTION LINE DATA
  201,    205,'&1',   204
 3005,  -3008,'&1',  3007
0 / END OF MULTI-SECTION LINE DATA, BEGIN ZONE DATA
  1,'FIRST       '
  2,'SECOND      '
  5,'FIFTH       '
 77,'PLANT       '
0 / END OF ZONE DATA, BEGIN INTER-AREA TRANSFER DATA
  1,   2,'A',    70.00
  1,   2,'B',    30.00
  1,   5,'A',   100.00
  1,   5,'B',    50.00
0 / END OF INTER-AREA TRANSFER DATA, BEGIN OWNER DATA
  1,'TRAN 1      '
  2,'TRAN 2      '
  5,'TRAN 5      '
 11,'GEN 1       '
 22,'GEN 2       '
 55,'GEN 5       '
100,'NO BUSES    '
0 / END OF OWNER DATA, BEGIN FACTS DEVICE DATA
0 / END OF FACTS DEVICE DAT
```

A.2 Dynamic Data in PSS/E Format

```
  101 'GENROU'  1     6.5000      0.60000E-01  0.20000      0.50000E-01
        4.0000       0.0000       1.8000       1.7500       0.60000
       0.80000      0.30000      0.15000      0.90000E-01  0.38000    /
  101 'IEEET1'  1     0.0000       400.00      0.40000E-01   7.3000
       -7.3000       1.0000      0.80000      0.30000E-01   1.0000
        0.0000       2.4700      0.35000E-01   4.5000      0.47000    /
  101 'TGOV1'   1    0.50000E-01  0.50000E-01   1.0500       0.30000
        1.0000       1.0000       0.0000    /
  102 'GENROU'  1     6.5000      0.60000E-01  0.20000      0.50000E-01
        4.0000       0.0000       1.8000       1.7500       0.60000
       0.80000      0.30000      0.15000      0.90000E-01  0.38000    /
```

```
102 'IEEET1'  1     0.0000       400.00      0.40000E-01   7.3000
     -7.3000       1.0000      0.80000      0.30000E-01   1.0000
      0.0000       2.4700      0.35000E-01   4.5000      0.47000    /
102 'TGOV1'   1    0.50000E-01  0.50000E-01   1.0500      0.30000
      1.0000       1.0000       0.0000    /
206 'GENROU'  1     4.5000      0.70000E-01  0.15000      0.50000E-01
      2.5000       0.0000       1.4000       1.3500      0.50000
     0.70000      0.25000      0.10000      0.90000E-01  0.38000    /
206 'IEEET1'  1     0.0000       40.000      0.60000E-01   2.1000
     -2.1000       0.0000      0.50000      0.80000E-01  0.80000
      0.0000       2.4700      0.35000E-01   3.5000      0.60000    /
206 'TGOV1'   1    0.50000E-01  0.50000E-01   0.9000      0.30000
      3.0000       9.0000       0.0000    /
211 'GENSAL'  1     5.0000      0.50000E-01  0.20000       5.0000
      0.0000       1.0000      0.75000      0.40000      0.26000
     0.10000      0.11000      0.62000    /
211 'SCRX'    1    0.10000       10.000       200.00      0.50000E-01
     -5.0000       5.0000       1.0000       10.000    /
211 'HYGOV'   1    0.50000E-01  0.30000       5.0000      0.50000E-01
     0.50000      0.20000       1.0000       0.0000       1.2500
      1.2000      0.50000      0.80000E-01/
3011 'GENROU'  1     5.0000      0.60000E-01  0.20000      0.60000E-01
      3.0000       0.0000       1.6000       1.5500      0.70000
     0.85000      0.35000      0.20000      0.90000E-01  0.38000    /
3011 'SEXS'    1    0.10000       10.000       100.00      0.10000
      0.0000       4.0000    /
3018 'GENROU'  1     5.0000      0.60000E-01  0.20000      0.60000E-01
      3.0000       0.0000       1.6000       1.5500      0.70000
     0.85000      0.35000      0.20000      0.90000E-01  0.38000    /
3018 'SEXS'    1    0.10000       10.000       100.00      0.10000
      0.0000       4.0000    /
```

Appendix B
WSCC 127-Bus System

The WSCC 127-Bus system was generated base on the WSCC 179-Bus system. The WSCC 127-bus system consists of 127 buses, 37 generators, and 211 transmission lines. The transmission lines and buses were significantly reduced; however, the amounts of load and generation were kept essentially the same.

B.1 Power Flow Data in PSS/E Format

```
0  100.0
This is a converted PF for WSCC 127 bus system from PSF
by Shu-Jen Steven Tsai Virginia Tech
    1 'CMAIN GM'   20.00 2      .000      .000   1    1 1.02000    67.7953
    2 'CA230   '  230.00 1      .000      .000   1    1 1.00114    62.8741
    3 'CA230TO '  230.00 1      .000      .000   1    1  .97855    53.8252
    4 'CANALB  '  500.00 1      .000      .000   1    1 1.07861    49.2363
    5 'CANAD G1'   20.00 2      .000      .000   1    1 1.00000    24.7373
    6 'CANADA  '  500.00 1      .000      .000   1    1 1.03634    20.9467
    7 'NORTH   '  500.00 1      .000   1200.000   1    1 1.04994    12.1080
    8 'NORTH G3'   20.00 2      .000      .000   1    1 1.00000    26.5866
    9 'HANFORD '  500.00 1      .000    550.000   1    1 1.04947     .2255
   10 'COULEE  '  500.00 1      .000      .000   1    1 1.07001     .1643
   11 'GARRISON'  500.00 1      .000      .000   1    1 1.03706   -12.1586
   12 'JOHN DAY'  500.00 1      .000   1019.350   1    1 1.08284   -11.1230
   13 'JOHN DAY'   13.80 3      .000      .000   1    1 1.00000     .0000
   14 'BIG EDDY'  500.00 1      .000      .000   1    1 1.08920   -13.3097
   15 'GRIZZLY '  500.00 1    -9.290   -560.290   1    1 1.06740   -17.1476
   16 'CELILOCA'  500.00 1      .000    462.000   1    1 1.08965   -13.4177
   17 'BIG EDDY'  230.00 1      .000    576.850   1    1 1.06592   -14.5698
   18 'CELILO  '  230.00 1      .000    792.000   1    1 1.06159   -15.0759
   19 'DALLES21'   13.80 2      .000      .000   1    1 1.05500    -7.9399
   20 'BIG EDDY'  115.00 1      .000      .000   1    1 1.06864   -16.9324
   21 'SUMMER L'  500.00 1      .280    116.380   1    1 1.05818   -18.2347
```

22 'BURNS2 ' 500.00 1 1156.740 -2375.410 1 1 .98437 -6.6864
23 'MALIN ' 500.00 1 7.990 -86.310 1 1 1.05433 -23.3443
24 'MONTANA ' 500.00 1 .000 .000 1 1 1.04928 48.2014
25 'COLSTRP ' 500.00 1 .000 .000 1 1 1.07840 -1.3597
26 'MONTA G1' 20.00 2 .000 .000 1 1 1.00000 56.5938
27 'MIDPOINT' 500.00 1 -1093.340 -220.000 1 1 1.06195 -5.2003
28 'BRIDGER2' 22.00 2 .000 .000 1 1 1.00900 2.4592
29 'MIDPOINT' 345.00 1 .000 -870.000 1 1 .99845 -1.5730
30 'BENLOMND' 345.00 1 .000 .000 1 1 1.04464 -3.3955
31 'BENLOMND' 230.00 1 .000 .000 1 1 1.04624 -3.9611
32 'NAUGHTON' 230.00 1 .000 .000 1 1 1.04453 .6117
33 'NAUGHT ' 20.00 2 .000 .000 1 1 1.00000 3.4114
34 'TERMINAL' 345.00 1 .000 .000 1 1 1.03911 -3.4234
35 'CAMP WIL' 345.00 1 .000 -60.000 1 1 1.04289 -2.4188
36 'SPAN FRK' 345.00 1 .000 .000 1 1 1.03514 -1.0947
37 'EMERY ' 345.00 1 .000 -220.000 1 1 1.03705 4.8870
38 'EMERY ' 20.00 2 .000 .000 1 1 1.05000 9.6024
39 'SIGURD ' 345.00 1 .000 -50.000 1 1 1.05190 -.5483
40 'PINTO ' 345.00 1 .000 -18.000 1 1 1.04044 -1.4058
41 'PINTO PS' 345.00 1 .000 .000 1 1 1.03679 -2.4445
42 'MONA ' 345.00 1 .000 .000 1 1 1.05596 -2.0100
43 'INTERMT ' 345.00 1 .000 430.000 1 1 1.05257 -4.3689
44 'INTERM1G' 26.00 2 .000 .000 1 1 1.05000 .2784
45 'CRAIG ' 345.00 1 .000 .000 1 1 .97518 16.2724
46 'CRAIG ' 22.00 2 .000 .000 1 1 .95000 23.5505
47 'HAYDEN ' 20.00 2 .000 .000 1 1 1.00000 33.7268
48 'SAN JUAN' 345.00 1 .000 390.000 1 1 1.03559 -3.8776
49 'SJUAN G4' 22.00 2 .000 .000 1 1 1.00000 -.8903
50 'FOURCORN' 345.00 1 .000 -155.000 1 1 1.00914 -4.6906
51 'FOURCORN' 500.00 1 .580 -113.000 1 1 1.06814 -7.9071
52 'FOURCORN' 230.00 1 .000 .000 1 1 1.00726 -5.2340
53 'FCNGN4CC' 22.00 2 .000 .000 1 1 1.00000 2.2268
54 'CHOLLA ' 345.00 1 .000 .000 1 1 .97744 -16.9635
55 'CORONADO' 500.00 1 .000 .000 1 1 .97947 -26.1777
56 'CORONADO' 20.00 1 .000 .000 1 1 1.04000 -19.6621
5699 'CORONADOEX' 20.00 2 .000 .000 1 1 1.04000 -19.6621
57 'MOENKOPI' 500.00 1 -.580 -370.700 1 1 1.06734 -24.8561

58 'WESTWING' 500.00 1 .000 -427.000 1 1 1.05593 -29.5931
59 'PALOVRDE' 500.00 1 .000 -146.000 1 1 1.04856 -29.6428
60 'PALOVRD2' 24.00 2 .000 .000 1 1 .96000 -21.7160
61 'NAVAJO ' 500.00 1 .000 -190.000 1 1 1.07205 -23.9373
62 'NAVAJO 2' 26.00 2 .000 .000 1 1 1.00000 -17.8134
63 'ELDORADO' 500.00 1 .000 -319.000 1 1 1.05122 -33.0973
64 'DEVERS ' 500.00 1 .000 .000 1 1 1.03539 -43.5235
65 'ELDORADO' 20.00 2 .000 .000 1 1 1.02000 -25.9758
66 'MOHAVE ' 500.00 1 .000 -196.000 1 1 1.06999 -29.3629
67 'MOHAV1CC' 22.00 2 .000 .000 1 1 1.05000 -21.0424
68 'LUGO ' 500.00 1 .000 .000 1 1 1.05498 -46.0918
69 'SERRANO ' 500.00 1 .000 .000 1 1 1.04128 -50.0799
70 'VALLEY ' 500.00 1 .000 .000 1 1 1.03694 -47.7631
71 'MIRALOMA' 500.00 1 .000 400.000 1 1 1.04087 -49.6814
72 'MIRALOMA' 20.00 2 .000 .000 1 1 1.05000 -45.4439
73 'MIRALOMA' 230.00 1 .000 .000 1 1 1.03821 -50.1272
74 'MESA CAL' 230.00 1 .000 .000 1 1 1.00705 -55.0619
75 'LITEHIPE' 230.00 1 .000 .000 1 1 1.01186 -55.7766
76 'LITEHIPE' 20.00 2 .000 .000 1 1 1.02000 -49.6271
77 'VINCENT ' 500.00 1 1.790 .000 1 1 1.06119 -48.9476
78 'VINCENT ' 230.00 1 .000 -190.000 1 1 .99489 -51.6350
79 'EAGLROCK' 230.00 1 .000 .000 1 1 1.01010 -52.7623
80 'PARDEE ' 230.00 1 .000 .000 1 1 1.00601 -51.6843
81 'PARDEE ' 20.00 2 .000 .000 1 1 1.01000 -39.6019
82 'SYLMAR S' 230.00 1 .000 .000 1 1 1.02073 -48.2577
83 'MIDWAY ' 200.00 1 .000 -130.000 1 1 1.16705 -51.4456
84 'MIDWAY ' 500.00 1 -13.460 -266.390 1 1 1.05934 -48.6077
85 'LOSBANOS' 500.00 1 .000 .000 1 1 1.04926 -49.5300
86 'MOSSLAND' 500.00 1 .000 .000 1 1 1.04638 -49.7948
87 'DIABLO ' 500.00 1 .000 .000 1 1 1.05297 -46.1287
88 'DIABLO1 ' 25.00 2 .000 .000 1 1 .98000 -42.3265
89 'GATES ' 500.00 1 11.960 -265.380 1 1 1.04706 -47.6847
90 'TEVATR ' 500.00 1 3.210 1558.440 1 1 .99815 -38.9958
91 'TEVATR2 ' 20.00 2 .000 .000 1 1 1.00000 -30.7836
92 'OLINDA ' 500.00 1 -.960 13.880 1 1 1.03724 -31.0690
93 'ROUND MT' 500.00 1 -12.820 43.160 1 1 1.03456 -27.9326
94 'TABLE MT' 500.00 1 11.970 -42.210 1 1 1.01342 -32.0705

95 'ROUND MT' 200.00 1 .000 -128.000 1 1 1.12387 -25.1416
96 'ROUND MT' 20.00 2 .000 .000 1 1 1.02000 -15.0806
97 'COTWDPGE' 200.00 1 .000 .000 1 1 1.13614 -30.4897
98 'LOGAN CR' 200.00 1 .000 .000 1 1 1.14016 -34.5852
99 'GLENN ' 200.00 1 .000 .000 1 1 1.14091 -34.2001
100 'CORTINA ' 200.00 1 .000 .000 1 1 1.13097 -34.9758
101 'TEVATR ' 200.00 1 .000 -32.000 1 1 1.12744 -39.6351
102 'TEVATR ' 20.00 2 .000 .000 1 1 1.05000 -35.6868
103 'SYLMARLA' 230.00 1 .000 2146.000 1 1 1.03832 -47.1513
104 'VICTORVL' 500.00 1 .000 .000 1 1 1.05866 -42.4776
105 'VICTORVL' 287.00 1 .000 -108.000 1 1 1.05209 -44.4950
106 'STA B2 ' 287.00 1 .000 .000 1 1 1.03663 -50.7192
107 'STA B1 ' 287.00 1 .000 .000 1 1 1.03663 -50.7192
108 'STA B ' 138.00 1 .000 .000 1 1 1.03256 -51.9028
109 'STA BLD ' 230.00 1 .000 .000 1 1 1.02728 -52.1111
110 'STA F ' 230.00 1 .000 .000 1 1 1.02484 -51.8814
111 'RIVER ' 230.00 1 .000 .000 1 1 1.02362 -51.8463
112 'HAYNES ' 230.00 1 .000 .000 1 1 1.03129 -50.6545
113 'HAYNES3G' 18.00 2 .000 .000 1 1 1.00000 -47.3513
114 'STA G ' 230.00 1 .000 .000 1 1 1.02394 -51.1765
115 'GLENDAL ' 230.00 1 .000 .000 1 1 1.02337 -50.9249
116 'STA E ' 230.00 1 .000 .000 1 1 1.02516 -50.0593
117 'VALLEY ' 230.00 1 .000 .000 1 1 1.02930 -49.0329
118 'RINALDI ' 230.00 1 .000 .000 1 1 1.03402 -47.8412
119 'OWENS G ' 11.50 2 .000 .000 1 1 1.02000 -47.2707
120 'STA E ' 500.00 1 .000 .000 1 1 1.04304 -47.6658
121 'ADELANTO' 500.00 1 .000 912.000 1 1 1.06032 -42.1579
122 'ADELAN&1' 500.00 1 .000 .000 1 1 1.08090 -46.2281
123 'RINALDI ' 500.00 1 .000 -80.000 1 1 1.07212 -45.4836
124 'STA J ' 230.00 1 .000 .000 1 1 1.03112 -48.9159
125 'CASTAIC ' 230.00 1 .000 .000 1 1 1.03195 -47.2926
126 'CASTAI4G' 18.00 2 .000 .000 1 1 1.02000 -45.9828
127 'OLIVE ' 230.00 1 .000 .000 1 1 1.03475 -47.6315
0 /End of bus data, start of Load data
1 BL 1 1 1 100.000 .000 .000 .000 .000 .000
2 BL 1 1 1 3600.000 700.000 .000 .000 .000 .000
5 BL 1 1 1 100.000 .000 .000 .000 .000 .000

6	BL	1	1	1	4400.000	1000.000	.000	.000	.000	.000
7	BL	1	1	1	5000.000	400.000	.000	.000	.000	.000
8	BL	1	1	1	100.000	.000	.000	.000	.000	.000
9	BL	1	1	1	3500.000	500.000	.000	.000	.000	.000
11	BL	1	1	1	2584.000	394.000	.000	.000	.000	.000
12	BL	1	1	1	3200.000	1100.000	.000	.000	.000	.000
13	BL	1	1	1	100.000	.000	.000	.000	.000	.000
14	BL	1	1	1	-44.200	22.000	.000	.000	.000	.000
15	BL	1	1	1	-66.600	-97.000	.000	.000	.000	.000
17	BL	1	1	1	-67.500	160.000	.000	.000	.000	.000
18	BL	1	1	1	3137.000	1681.000	.000	.000	.000	.000
19	BL	1	1	1	100.000	.000	.000	.000	.000	.000
20	BL	1	1	1	160.000	31.250	.000	.000	.000	.000
23	BL	1	1	1	-339.000	-119.000	.000	.000	.000	.000
24	BL	1	1	1	1700.000	300.000	.000	.000	.000	.000
25	BL	1	1	1	-1525.000	-50.000	.000	.000	.000	.000
26	BL	1	1	1	100.000	.000	.000	.000	.000	.000
28	BL	1	1	1	100.000	.000	.000	.000	.000	.000
29	BL	1	1	1	610.000	-414.000	.000	.000	.000	.000
30	BL	1	1	1	33.900	11.900	.000	.000	.000	.000
31	BL	1	1	1	148.000	-7.900	.000	.000	.000	.000
32	BL	1	1	1	255.000	100.000	.000	.000	.000	.000
33	BL	1	1	1	100.000	.000	.000	.000	.000	.000
34	BL	1	1	1	185.000	78.500	.000	.000	.000	.000
35	BL	1	1	1	457.700	81.700	.000	.000	.000	.000
36	BL	1	1	1	141.200	71.400	.000	.000	.000	.000
37	BL	1	1	1	116.100	38.400	.000	.000	.000	.000
38	BL	1	1	1	100.000	.000	.000	.000	.000	.000
39	BL	1	1	1	379.000	-43.000	.000	.000	.000	.000
40	BL	1	1	1	31.600	11.500	.000	.000	.000	.000
42	BL	1	1	1	-62.000	12.800	.000	.000	.000	.000
43	BL	1	1	1	2053.000	907.100	.000	.000	.000	.000
44	BL	1	1	1	100.000	.000	.000	.000	.000	.000
45	BL	1	1	1	2350.000	-127.000	.000	.000	.000	.000
46	BL	1	1	1	100.000	.000	.000	.000	.000	.000
47	BL	1	1	1	100.000	.000	.000	.000	.000	.000
48	BL	1	1	1	840.000	5.000	.000	.000	.000	.000

49	BL	1	1	1	100.000	.000	.000	.000	.000	.000
50	BL	1	1	1	239.000	-56.000	.000	.000	.000	.000
52	BL	1	1	1	139.700	23.800	.000	.000	.000	.000
53	BL	1	1	1	100.000	.000	.000	.000	.000	.000
55	BL	1	1	1	1750.000	-56.000	.000	.000	.000	.000
56	BL	1	1	1	100.000	.000	.000	.000	.000	.000
58	BL	1	1	1	617.000	-69.000	.000	.000	.000	.000
59	BL	1	1	1	793.400	207.000	.000	.000	.000	.000
60	BL	1	1	1	100.000	.000	.000	.000	.000	.000
61	BL	1	1	1	90.000	70.000	.000	.000	.000	.000
62	BL	1	1	1	100.000	.000	.000	.000	.000	.000
63	BL	1	1	1	902.300	-11.400	.000	.000	.000	.000
64	BL	1	1	1	856.000	19.600	.000	.000	.000	.000
65	BL	1	1	1	100.000	.000	.000	.000	.000	.000
67	BL	1	1	1	100.000	.000	.000	.000	.000	.000
68	BL	1	1	1	204.200	-28.200	.000	.000	.000	.000
69	BL	1	1	1	1230.000	72.800	.000	.000	.000	.000
70	BL	1	1	1	406.000	41.000	.000	.000	.000	.000
71	BL	1	1	1	3098.000	1189.000	.000	.000	.000	.000
72	BL	1	1	1	100.000	.000	.000	.000	.000	.000
74	BL	1	1	1	377.400	64.500	.000	.000	.000	.000
75	BL	1	1	1	3191.000	630.000	.000	.000	.000	.000
76	BL	1	1	1	100.000	.000	.000	.000	.000	.000
78	BL	1	1	1	1066.000	-10.800	.000	.000	.000	.000
79	BL	1	1	1	175.000	18.000	.000	.000	.000	.000
80	BL	1	1	1	3118.000	78.000	.000	.000	.000	.000
81	BL	1	1	1	100.000	.000	.000	.000	.000	.000
82	BL	1	1	1	401.000	80.600	.000	.000	.000	.000
83	BL	1	1	1	777.600	32.600	.000	.000	.000	.000
84	BL	1	1	1	55.600	-329.000	.000	.000	.000	.000
85	BL	1	1	1	265.000	14.000	.000	.000	.000	.000
86	BL	1	1	1	40.000	21.500	.000	.000	.000	.000
87	BL	1	1	1	50.000	25.000	.000	.000	.000	.000
88	BL	1	1	1	100.000	.000	.000	.000	.000	.000
89	BL	1	1	1	305.000	-7.600	.000	.000	.000	.000
90	BL	1	1	1	5661.000	3491.000	.000	.000	.000	.000
91	BL	1	1	1	100.000	.000	.000	.000	.000	.000

92 BL 1 1 1 -189.000 61.500 .000 .000 .000 .000
94 BL 1 1 1 -.700 118.500 .000 .000 .000 .000
95 BL 1 1 1 148.000 .000 .000 .000 .000 .000
96 BL 1 1 1 100.000 .000 .000 .000 .000 .000
97 BL 1 1 1 210.400 -77.000 .000 .000 .000 .000
98 BL 1 1 1 8.010 .000 .000 .000 .000 .000
99 BL 1 1 1 27.500 -.100 .000 .000 .000 .000
100 BL 1 1 1 -43.300 20.000 .000 .000 .000 .000
101 BL 1 1 1 884.000 54.800 .000 .000 .000 .000
102 BL 1 1 1 100.000 .000 .000 .000 .000 .000
103 BL 1 1 1 -2771.000 1654.000 .000 .000 .000 .000
105 BL 1 1 1 -129.000 32.200 .000 .000 .000 .000
108 BL 1 1 1 237.200 -63.200 .000 .000 .000 .000
109 BL 1 1 1 138.000 28.000 .000 .000 .000 .000
110 BL 1 1 1 117.000 24.000 .000 .000 .000 .000
111 BL 1 1 1 320.000 65.000 .000 .000 .000 .000
113 BL 1 1 1 100.000 .000 .000 .000 .000 .000
114 BL 1 1 1 121.000 25.000 .000 .000 .000 .000
115 BL 1 1 1 135.000 27.000 .000 .000 .000 .000
116 BL 1 1 1 807.800 132.100 .000 .000 .000 .000
117 BL 1 1 1 205.200 17.600 .000 .000 .000 .000
118 BL 1 1 1 121.000 25.000 .000 .000 .000 .000
119 BL 1 1 1 100.000 .000 .000 .000 .000 .000
121 BL 1 1 1 -1862.000 971.000 .000 .000 .000 .000
124 BL 1 1 1 887.700 -6.200 .000 .000 .000 .000
126 BL 1 1 1 100.000 .000 .000 .000 .000 .000
127 BL 1 1 1 -72.800 -17.000 .000 .000 .000 .000
0 /End of Load data, begin of Generator data
1 1 1120.00 287.54 1330.00 -875.00 1 0 1525.00 0.0030 0.2500 .00000 .00000 1.00000 1 100.0 9999.00 .00
1 2 1120.00 287.54 1330.00 -875.00 1 0 1525.00 0.0030 0.2500 .00000 .00000 1.00000 1 100.0 9999.00 .00
1 3 1120.00 287.54 1330.00 -875.00 1 0 1525.00 0.0030 0.2500 .00000 .00000 1.00000 1 100.0 9999.00 .00
1 4 1120.00 287.54 1330.00 -875.00 1 0 1525.00 0.0030 0.2500 .00000 .00000 1.00000 1 100.0 9999.00 .00

5 1 4450.00 1011.06 4000.00 -4000.00 1 0 9004.00 0.0020 0.1500 .00000 .00000 1.00000 1 100.0
9999.00 .00
8 1 9950.00 1853.96 5780.00 -2000.00 1 0 13000.0 0.0020 0.1610 .00000 .00000 1.00000 1 100.0
9999.00 .00
13 1 5174.76 855.19 2649.00 -1850.00 1 0 5421.00 0.0036 0.2480 .00000 .00000 1.00000 1 100.0
9999.00 .00
19 1 1301.00 431.46 692.00 -711.00 1 0 1199.00 0.0040 0.2870 .00000 .00000 1.00000 1 100.0
9999.00 .00
26 1 2910.00 953.28 1500.00 -1000.00 1 0 3085.00 0.0013 0.1780 .00000 .00000 1.00000 1 100.0
9999.00 .00
28 1 820.00 142.83 300.00 -262.50 1 0 885.00 0.0047 0.2150 .00000 .00000 1.00000 1 100.0
9999.00 .00
28 2 820.00 142.83 300.00 -262.50 1 0 885.00 0.0047 0.2150 .00000 .00000 1.00000 1 100.0
9999.00 .00
33 1 445.00 91.73 9999.00 -9999.00 1 0 832.00 0.0014 0.2600 .00000 .00000 1.00000 1 100.0
9999.00 .00
38 1 1665.00 -31.36 9999.00 -9999.00 1 0 2229.00 0.0040 0.1850 .00000 .00000 1.00000 1 100.0
9999.00 .00
44 1 1780.00 534.59 850.00 -440.00 1 0 1982.00 0.0014 0.2000 .00000 .00000 1.00000 1 100.0
9999.00 .00
46 1 1048.00 -132.91 400.00 -400.00 1 0 1488.00 0.0030 0.1900 .00000 .00000 1.00000 1 100.0
9999.00 .00
47 1 2050.00 464.83 900.00 -900.00 1 0 3000.00 0.0020 0.1900 .00000 .00000 1.00000 1 100.0
9999.00 .00
49 1 962.00 148.78 300.00 -300.00 1 0 2054.00 0.0020 0.2050 .00000 .00000 1.00000 1 100.0
9999.00 .00
53 1 2160.00 -30.48 700.00 -500.00 1 0 2458.00 0.0036 0.2050 .00000 .00000 1.00000 1 100.0
9999.00 .00
5699 1 400.00 61.52 150.00 -150.00 1 0 457.00 0.0030 0.1950 .00000 .00000 1.00000 1 100.0
9999.00 .00
5699 2 400.00 61.52 150.00 -150.00 1 0 457.00 0.0030 0.1950 .00000 .00000 1.00000 1 100.0
9999.00 .00
60 1 880.00 126.03 433.00 -300.00 1 0 1039.00 0.0035 0.2850 .00000 .00000 1.00000 1 100.0
9999.00 .00
60 2 880.00 126.03 433.00 -300.00 1 0 1039.00 0.0035 0.2850 .00000 .00000 1.00000 1 100.0
9999.00 .00

60 3 880.00 126.03 433.00 -300.00 1 0 1039.00 0.0035 0.2850 .00000 .00000 1.00000 1 100.0 9999.00 .00

62 1 1690.00 195.54 700.00 -280.00 1 0 3540.00 0.0019 0.1750 .00000 .00000 1.00000 1 100.0 9999.00 .00

65 1 982.70 -128.76 300.00 -300.00 1 0 2104.00 0.0020 0.3000 .00000 .00000 1.00000 1 100.0 9999.00 .00

67 1 840.00 223.32 350.00 -150.00 1 0 909.00 0.0036 0.2050 .00000 .00000 1.00000 1 100.0 9999.00 .00

67 2 840.00 223.32 350.00 -150.00 1 0 909.00 0.0036 0.2050 .00000 .00000 1.00000 1 100.0 9999.00 .00

72 1 1690.00 593.82 900.00 -400.00 1 0 3000.00 0.0020 0.2900 .00000 .00000 1.00000 1 100.0 9999.00 .00

76 1 3195.00 1032.51 2000.00 -900.00 1 0 9000.00 0.0025 0.1750 .00000 .00000 1.00000 1 100.0 9999.00 .00

81 1 2200.00 393.72 600.00 -600.00 1 0 2500.00 0.0010 0.1800 .00000 .00000 1.00000 1 100.0 9999.00 .00

88 1 765.00 -206.24 330.00 -310.00 1 0 1685.00 0.0030 0.3110 .00000 .00000 1.00000 1 100.0 9999.00 .00

91 1 3467.00 1654.55 2500.00 -1000.00 1 0 6840.00 0.0020 0.1900 .00000 .00000 1.00000 1 100.0 9999.00 .00

96 1 1057.00 25.61 400.00 -400.00 1 0 1022.00 0.0062 0.2630 .00000 .00000 1.00000 1 100.0 9999.00 .00

102 1 594.00 192.36 300.00 -300.00 1 0 895.00 0.0020 0.3000 .00000 .00000 1.00000 1 100.0 9999.00 .00

113 1 325.00 68.27 300.00 -220.00 1 0 540.00 0.0016 0.1850 .00000 .00000 1.00000 1 100.0 9999.00 .00

119 1 110.00 29.08 100.00 -100.00 1 0 113.00 0.0037 0.1500 .00000 .00000 1.00000 1 100.0 9999.00 .00

126 1 200.00 -52.16 268.00 -134.00 1 0 500.00 0.0014 0.1550 .00000 .00000 1.00000 1 100.0 9999.00 .00

0 / End of Generator data, begin of nontransformer branch data

3 2 1 .00200 .02000 .80000 .00 .00 .00 .00000 .00 .00000 .00000 1

6 4 1 .00350 .07000 4.60600 .00 .00 .00 .00000 .00 .00000 .00000 1

6 7 1 .00083 .02390 3.30000 .00 .00 .00 .00000 .00 .00000 .00000 1

7 9 1 .00020 .00820 1.30000 .00 .00 .00 .00000 .00 .00000 .00000 1

7 9 2 .00020 .00820 1.30000 .00 .00 .00 .00000 .00 .00000 .00000 1

9 10 1 .00113 .02069 1.85526 .00 .00 .00 .00000 .00 .00000 .00000 1

9	12 1	.00120	.02316	1.71520	.00	.00	.00	.00000	.00	.00000	.00000	1
9	12 2	.00030	.02000	3.60000	.00	.00	.00	.00000	.00	.00000	.00000	1
9	24 1	.00070	.07400	4.87000	.00	.00	.00	.00000	.00	.00000	.00000	1
11	9 1	.00142	.02258	1.88000	.00	.00	.00	.00000	.00	.00000	.00000	1
11	12 1	.00196	.03304	1.88000	.00	.00	.00	.00000	.00	.00000	.00000	1
11	25 1	.00179	.01405	3.68000	.00	.00	.00	.00000	.00	.00000	.00000	1
14	12 1	.00023	.00451	.33320	.00	.00	2175.00	.00000	.00	.00000	.00000	1
14	12 2	.00020	.00446	.30500	.00	.00	2175.00	.00000	.00	.00000	.00000	1
14	16 1	.00001	.00030	.01434	.00	.00	3450.00	.00000	.00	.00000	.00000	1
14	16 2	.00001	.00030	.01844	.00	.00	3450.00	.00000	.00	.00000	.00000	1
15	12 1	.00063	.01412	1.09756	.00	.00	3450.00	.00000	.00	.00000	.00000	1
15	12 2	.00109	.02408	1.55542	.00	.00	3020.00	.00000	.00	.00000	.00000	1
15	12 3	.00108	.02409	1.55348	.00	.00	3020.00	.00000	.00	.00000	.00000	1
15	21 1	.00101	.00513	1.05130	.00	.00	2000.00	.00000	.00	.00000	.00000	1
15	23 1	.00214	.01664	2.93584	.00	.00	2400.00	.00000	.00	.00000	.00000	1
15	23 2	.00211	.01577	2.95384	.00	.00	2000.00	.00000	.00	.00000	.00000	1
17	18 1	.00006	.00131	.00378	.00	.00	3020.00	.00000	.00	.00000	.00000	1
17	18 2	.00006	.00116	.00332	.00	.00	3020.00	.00000	.00	.00000	.00000	1
22	21 1	.00122	.02373	2.20710	.00	.00	3600.00	.00000	.00	.00000	.00000	1
22	27 1	.00286	.00248	23.91510	.00	.00	1732.00	.00000	.00	.00000	.00000	1
23	21 1	.00084	.00767	.32730	.00	.00	2000.00	.00000	.00	.00000	.00000	1
23	92 1	.00106	.01293	2.75746	.00	.00	.00	.00000	.00	.00000	.00000	1
23	93 1	.00108	.00907	1.28080	.00	.00	1800.00	.00000	.00	.00000	.00000	1
23	93 2	.00104	.00917	1.57146	.00	.00	1800.00	.00000	.00	.00000	.00000	1
30	29 1	.00620	.06730	1.11560	.00	.00	.00	.00000	.00	.00000	.00000	1
30	34 1	.00160	.02260	.38100	.00	.00	.00	.00000	.00	.00000	.00000	1
30	35 1	.00240	.03320	.58490	.00	.00	.00	.00000	.00	.00000	.00000	1
31	32 1	.01080	.09650	.32960	.00	.00	.00	.00000	.00	.00000	.00000	1
35	34 1	.00080	.01060	.20390	.00	.00	.00	.00000	.00	.00000	.00000	1
35	36 1	.00120	.01720	.29870	.00	.00	.00	.00000	.00	.00000	.00000	1
35	37 1	.00520	.06020	1.01000	.00	.00	.00	.00000	.00	.00000	.00000	1
35	37 2	.00490	.05370	.88430	.00	.00	.00	.00000	.00	.00000	.00000	1
35	42 1	.00170	.02250	.39920	.00	.00	.00	.00000	.00	.00000	.00000	1
35	42 2	.00210	.02380	.38450	.00	.00	.00	.00000	.00	.00000	.00000	1
37	36 1	.00340	.03920	.65240	.00	.00	.00	.00000	.00	.00000	.00000	1
37	39 1	.00340	.03740	.62080	.00	.00	.00	.00000	.00	.00000	.00000	1
37	39 2	.00340	.03720	.61820	.00	.00	.00	.00000	.00	.00000	.00000	1

37	40	1	.00960	.08780	1.42650	.00	.00	.00	.00000	.00	.00000	.00000	1
41	50	1	.00480	.04360	.70780	.00	.00	.00	.00000	.00	.00000	.00000	1
42	39	1	.00380	.03400	.58240	.00	.00	.00	.00000	.00	.00000	.00000	1
42	39	2	.00320	.03490	.57220	.00	.00	.00	.00000	.00	.00000	.00000	1
43	42	1	.00180	.02450	.43920	.00	.00	.00	.00000	.00	.00000	.00000	1
43	42	2	.00180	.02450	.43920	.00	.00	.00	.00000	.00	.00000	.00000	1
45	42	1	.00811	.13690	2.43480	.00	.00	.00	.00000	.00	.00000	.00000	1
48	45	1	.00977	.11000	2.00000	.00	.00	.00	.00000	.00	.00000	.00000	1
50	48	1	.00050	.00530	.08820	.00	.00	.00	.00000	.00	.00000	.00000	1
51	57	1	.00180	.03232	3.11294	.00	.00	.00	.00000	.00	.00000	.00000	1
54	50	1	.00179	.01988	2.57600	.00	.00	.00	.00000	.00	.00000	.00000	1
56	5699	1	0	.00001	0	.00	.00	.00	.00000	.00	.00000	.00000	1
57	58	1	.00184	.02689	3.34534	.00	.00	.00	.00000	.00	.00000	.00000	1
57	63	1	.00222	.01600	3.81626	.00	.00	.00	.00000	.00	.00000	.00000	1
59	58	1	.00040	.00960	.90380	.00	.00	.00	.00000	.00	.00000	.00000	1
59	58	2	.00040	.00960	.90380	.00	.00	.00	.00000	.00	.00000	.00000	1
59	64	1	.00259	.02967	2.15300	.00	.00	1800.00	.00000	.00	.00000	.00000	1
59	64	2	.00259	.02967	2.15300	.00	.00	1800.00	.00000	.00	.00000	.00000	1
61	57	1	.00078	.00546	1.39224	.00	.00	.00	.00000	.00	.00000	.00000	1
61	58	1	.00255	.03764	4.72892	.00	.00	.00	.00000	.00	.00000	.00000	1
61	63	1	.00280	.02110	1.01940	.00	.00	1630.00	.00000	.00	.00000	.00000	1
63	68	1	.00193	.02779	4.67120	.00	.00	3600.00	.00000	.00	.00000	.00000	1
63	104	1	.00179	.02524	.53546	.00	.00	.00	.00000	.00	.00000	.00000	1
63	104	2	.00179	.02524	.53546	.00	.00	.00	.00000	.00	.00000	.00000	1
64	70	1	.00042	.00905	.66794	.00	.00	3600.00	.00000	.00	.00000	.00000	1
66	63	1	.00056	.01415	1.04290	.00	.00	3600.00	.00000	.00	.00000	.00000	1
68	66	1	.00190	.03100	4.14020	.00	.00	3600.00	.00000	.00	.00000	.00000	1
68	69	1	.00060	.01280	.94620	.00	.00	3600.00	.00000	.00	.00000	.00000	1
68	71	1	.00028	.00753	.51736	.00	.00	3600.00	.00000	.00	.00000	.00000	1
68	71	2	.00035	.00750	.55360	.00	.00	3600.00	.00000	.00	.00000	.00000	1
68	77	1	.00044	.01125	.82920	.00	.00	3600.00	.00000	.00	.00000	.00000	1
68	77	2	.00044	.01125	.82920	.00	.00	3600.00	.00000	.00	.00000	.00000	1
68	104	1	.00020	.00410	.29620	.00	.00	.00	.00000	.00	.00000	.00000	1
69	70	1	.00040	.00930	.68560	.00	.00	3600.00	.00000	.00	.00000	.00000	1
71	69	1	.00021	.00457	.32336	.00	.00	3600.00	.00000	.00	.00000	.00000	1
73	74	1	.00138	.05399	.15252	.00	.00	2320.00	.00000	.00	.00000	.00000	1
75	74	1	.00110	.01270	.04800	.00	.00	2320.00	.00000	.00	.00000	.00000	1

78	74	1	.00320	.03950	.14400	.00	.00	2320.00	.00000	.00	.00000	.00000	1
79	74	1	.00190	.02580	.09840	.00	.00	2320.00	.00000	.00	.00000	.00000	1
79	80	1	.00845	.07034	.15954	.00	.00	1160.00	.00000	.00	.00000	.00000	1
79	82	1	.00140	.02640	.10200	.00	.00	3070.00	.00000	.00	.00000	.00000	1
80	78	1	.00285	.03649	.12656	.00	.00	2320.00	.00000	.00	.00000	.00000	1
80	78	2	.00138	.03399	.11252	.00	.00	2320.00	.00000	.00	.00000	.00000	1
80	82	1	.00065	.01187	.04672	.00	.00	3070.00	.00000	.00	.00000	.00000	1
80	82	2	.00065	.01187	.04672	.00	.00	3070.00	.00000	.00	.00000	.00000	1
84	77	1	.00125	.00821	1.96874	.00	.00	2134.00	.00000	.00	.00000	.00000	1
84	77	2	.00125	.00815	1.94924	.00	.00	2134.00	.00000	.00	.00000	.00000	1
84	77	3	.00114	.00769	1.60152	.00	.00	2100.00	.00000	.00	.00000	.00000	1
85	84	1	.00153	.01470	.00000	.00	.00	1560.00	.00000	.00	.00000	.00000	1
85	89	1	.00083	.01985	.00000	.00	.00	2450.00	.00000	.00	.00000	.00000	1
86	85	1	.00053	.01297	.00000	.00	.00	2450.00	.00000	.00	.00000	.00000	1
87	84	1	.00087	.02087	1.45710	.00	.00	.00	.00000	.00	.00000	.00000	1
87	84	2	.00087	.02087	1.45710	.00	.00	.00	.00000	.00	.00000	.00000	1
89	84	1	.00074	.00611	2.82404	.00	.00	2450.00	.00000	.00	.00000	.00000	1
89	87	1	.00079	.01937	1.32850	.00	.00	.00	.00000	.00	.00000	.00000	1
90	84	1	.00172	.03757	2.07894	.00	.00	1800.00	.00000	.00	.00000	.00000	1
90	89	1	.00095	.02574	.79756	.00	.00	2450.00	.00000	.00	.00000	.00000	1
92	90	1	.00159	.01110	3.63476	.00	.00	2667.00	.00000	.00	.00000	.00000	1
93	94	1	.00145	.00693	.79438	.00	.00	1800.00	.00000	.00	.00000	.00000	1
93	94	2	.00145	.00693	.79438	.00	.00	1800.00	.00000	.00	.00000	.00000	1
94	90	1	.00098	.01035	.93124	.00	.00	2450.00	.00000	.00	.00000	.00000	1
94	90	2	.00160	.01229	2.28186	.00	.00	2450.00	.00000	.00	.00000	.00000	1
97	95	1	.01113	.06678	.07286	.00	.00	752.00	.00000	.00	.00000	.00000	1
97	95	2	.01050	.06540	.06860	.00	.00	602.00	.00000	.00	.00000	.00000	1
97	95	3	.01105	.06642	.07160	.00	.00	752.00	.00000	.00	.00000	.00000	1
97	98	1	.01668	.11381	.13608	.00	.00	838.00	.00000	.00	.00000	.00000	1
97	99	1	.01382	.09268	.11060	.00	.00	747.00	.00000	.00	.00000	.00000	1
97	100	1	.02482	.16938	.20232	.00	.00	838.00	.00000	.00	.00000	.00000	1
97	101	1	.03903	.27403	.31072	.00	.00	747.00	.00000	.00	.00000	.00000	1
98	101	1	.02235	.16106	.18342	.00	.00	838.00	.00000	.00	.00000	.00000	1
99	101	1	.03058	.20460	.24472	.00	.00	747.00	.00000	.00	.00000	.00000	1
100	101	1	.01480	.10101	.12066	.00	.00	838.00	.00000	.00	.00000	.00000	1
104	123	1	.00083	.01884	1.66668	.00	.00	.00	.00000	.00	.00000	.00000	1
106	105	1	.01070	.07905	.36670	.00	.00	.00	.00000	.00	.00000	.00000	1

107 105 1 .01070 .07905 .36670 .00 .00 .00 .00000 .00 .00000 .00000 1
110 109 1 .00073 .01025 .02558 .00 .00 .00 .00000 .00 .00000 .00000 1
110 109 2 .00073 .01025 .02558 .00 .00 .00 .00000 .00 .00000 .00000 1
110 112 1 .00201 .03074 .06886 .00 .00 .00 .00000 .00 .00000 .00000 1
110 114 1 .00110 .01189 .02514 .00 .00 .00 .00000 .00 .00000 .00000 1
111 110 1 .00037 .00366 .00830 .00 .00 .00 .00000 .00 .00000 .00000 1
111 112 1 .00220 .03422 .07716 .00 .00 .00 .00000 .00 .00000 .00000 1
111 112 2 .00238 .03669 .08284 .00 .00 .00 .00000 .00 .00000 .00000 1
111 114 1 .00055 .00586 .01246 .00 .00 .00 .00000 .00 .00000 .00000 1
112 114 1 .00281 .04296 .09648 .00 .00 .00 .00000 .00 .00000 .00000 1
115 114 1 .00035 .00536 .01204 .00 .00 .00 .00000 .00 .00000 .00000 1
116 114 1 .00119 .01244 .02798 .00 .00 .00 .00000 .00 .00000 .00000 1
116 114 2 .00119 .01244 .02798 .00 .00 .00 .00000 .00 .00000 .00000 1
116 115 1 .00047 .00723 .01624 .00 .00 .00 .00000 .00 .00000 .00000 1
117 116 1 .00128 .00979 .02120 .00 .00 .00 .00000 .00 .00000 .00000 1
118 103 1 .00027 .00393 .00918 .00 .00 .00 .00000 .00 .00000 .00000 1
118 103 2 .00027 .00393 .00918 .00 .00 .00 .00000 .00 .00000 .00000 1
118 103 3 .00027 .00393 .00918 .00 .00 .00 .00000 .00 .00000 .00000 1
118 116 1 .00229 .01583 .03060 .00 .00 .00 .00000 .00 .00000 .00000 1
118 116 2 .00229 .01583 .03060 .00 .00 .00 .00000 .00 .00000 .00000 1
118 117 1 .00138 .01116 .02470 .00 .00 .00 .00000 .00 .00000 .00000 1
118 117 2 .00138 .01116 .02470 .00 .00 .00 .00000 .00 .00000 .00000 1
118 124 1 .00141 .00967 .01940 .00 .00 .00 .00000 .00 .00000 .00000 1
118 124 2 .00141 .00967 .01940 .00 .00 .00 .00000 .00 .00000 .00000 1
118 124 3 .00161 .00971 .01928 .00 .00 .00 .00000 .00 .00000 .00000 1
118 124 4 .00161 .00971 .01928 .00 .00 .00 .00000 .00 .00000 .00000 1
118 127 1 .00029 .00434 .00950 .00 .00 .00 .00000 .00 .00000 .00000 1
121 104 1 .00000 .00159 .12002 .00 .00 .00 .00000 .00 .00000 .00000 1
121 104 2 .00000 .00159 .12002 .00 .00 .00 .00000 .00 .00000 .00000 1
121 120 1 .00082 .01668 1.18802 .00 .00 .00 .00000 .00 .00000 .00000 1
121 122 1 .00074 .01861 1.40264 .00 .00 .00 .00000 .00 .00000 .00000 1
125 103 1 .00226 .03422 .07506 .00 .00 .00 .00000 .00 .00000 .00000 1
125 118 1 .00290 .03800 .08240 .00 .00 .00 .00000 .00 .00000 .00000 1
125 124 1 .00309 .04677 .10080 .00 .00 .00 .00000 .00 .00000 .00000 1
125 127 1 .00221 .03346 .07338 .00 .00 .00 .00000 .00 .00000 .00000 1
0 /End of nontransformer branch data, begin of transformer data
45, 47, 0 , '1 ', 1, 2, 1,.000000, .000000, 2,1

.000000, .015000, 100.00
1.00000, 0.0, .0000, .00, .00, .00, 1
1.0000, 0.0000
55, 54, 0 , '1 ', 1, 2, 1,.000000, .000000, 2,1
.000000, .014600, 100.00
1.00000, 0.0, .0000, .00, .00, .00, 1
1.0000, 0.0000
59, 60, 0 , '1 ', 1, 2, 1,.000000, .000000, 2,1
.000060, .004950, 100.00
1.10610, 0.0, .0000, .00, .00, 3066.00, 1
1.0000, 0.0000
55, 56, 0 , '1 ', 1, 2, 1,.000000, .000000, 2,1
.000000, .017300, 100.00
.95450, 0.0, .0000, .00, .00, .00, 1
1.0000, 0.0000
48, 49, 0 , '1 ', 1, 2, 1,.000000, .000000, 2,1
.000000, .006000, 100.00
1.04350, 0.0, .0000, .00, .00, .00, 1
1.0000, 0.0000
51, 50, 0 , '1 ', 1, 2, 1,.000000, .000000, 2,1
.000000, .011000, 100.00
1.06300, 0.0, .0000, .00, .00, .00, 1
1.0000, 0.0000
51, 50, 0 , '2 ', 1, 2, 1,.000000, .000000, 2,1
.000000, .011000, 100.00
1.06300, 0.0, .0000, .00, .00, .00, 1
1.0000, 0.0000
50, 53, 0 , '1 ', 1, 2, 1,.000000, .000000, 2,1
.000000, .005900, 100.00
1.00000, 0.0, .0000, .00, .00, 3000.00, 1
1.0000, 0.0000
50, 52, 0 , '1 ', 1, 2, 1,.000000, .000000, 2,1
.000280, .013800, 100.00
1.00000, 0.0, .0000, .00, .00, 430.00, 1
1.0000, 0.0000
50, 52, 0 , '2 ', 1, 2, 1,.000000, .000000, 2,1
.000290, .013900, 100.00

1.00000, 0.0, .0000, .00, .00, 430.00, 1
1.0000, 0.0000
61, 62, 0 , '1 ', 1, 2, 1,.000000, .000000, 2,1
.000000, .006660, 100.00
1.08000, 0.0, .0000, .00, .00, 2000.00, 1
1.0000, 0.0000
4, 3, 0 , '1 ', 1, 2, 1,.000000, .000000, 2,1
.000000, .010000, 100.00
1.10000, 0.0, .0000, .00, .00, .00, 1
1.0000, 0.0000
6, 5, 0 , '1 ', 1, 2, 1,.000000, .000000, 2,1
.000000, .001500, 100.00
1.05000, 0.0, .0000, .00, .00, .00, 1
1.0000, 0.0000
2, 1, 0 , '1 ', 1, 2, 1,.000000, .000000, 2,1
.000000, .002000, 100.00
1.00000, 0.0, .0000, .00, .00, .00, 1
1.0000, 0.0000
104, 105, 0 , '1 ', 1, 2, 1,.000000, .000000, 2,1
.000200, .023380, 100.00
.97890, 0.0, .0000, .00, .00, .00, 1
1.0000, 0.0000
43, 44, 0 , '1 ', 1, 2, 1,.000000, .000000, 2,1
.000000, .005200, 100.00
1.02500, 0.0, .0000, .00, .00, .00, 1
1.0000, 0.0000
24, 26, 0 , '1 ', 1, 2, 1,.000000, .000000, 2,1
.000000, .005000, 100.00
1.09000, 0.0, .0000, .00, .00, .00, 1
1.0000, 0.0000
27, 29, 0 , '1 ', 1, 2, 1,.000000, .000000, 2,1
.000000, .007200, 100.00
1.05000, 0.0, .0000, .00, .00, 1500.00, 1
1.0000, 0.0000
7, 8, 0 , '1 ', 1, 2, 1,.000000, .000000, 2,1
.000000, .002500, 100.00
1.06600, 0.0, .0000, .00, .00, .00, 1

1.0000, 0.0000
16, 18, 0 , '1 ', 1, 2, 1,.000000, .000000, 2,1
.000000, .002210, 100.00
1.02340, 0.0, .0000, .00, .00, 2500.00, 1
1.0000, 0.0000
17, 20, 0 , '1 ', 1, 2, 1,.000000, .000000, 2,1
.000890, .029900, 100.00
.98730, 0.0, .0000, .00, .00, 250.00, 1
1.0000, 0.0000
14, 17, 0 , '1 ', 1, 2, 1,.000000, .000000, 2,1
.000200, .011810, 100.00
1.02380, 0.0, .0000, .00, .00, 1008.00, 1
1.0000, 0.0000
14, 17, 0 , '2 ', 1, 2, 1,.000000, .000000, 2,1
.000090, .007350, 100.00
1.02380, 0.0, .0000, .00, .00, 1300.00, 1
1.0000, 0.0000
12, 13, 0 , '1 ', 1, 2, 1,.000000, .000000, 2,1
.000000, .003750, 100.00
1.09770, 0.0, .0000, .00, .00, 5000.00, 1
1.0000, 0.0000
17, 19, 0 , '1 ', 1, 2, 1,.000000, .000000, 2,1
.000000, .010340, 100.00
1.04550, 0.0, .0000, .00, .00, 2000.00, 1
1.0000, 0.0000
96, 95, 0 , '1 ', 1, 2, 1,.000000, .000000, 2,1
.000000, .022810, 100.00
.91740, 0.0, .0000, .00, .00, .00, 1
1.0000, 0.0000
95, 93, 0 , '1 ', 1, 2, 1,.000000, .000000, 2,1
.000100, .017400, 100.00
1.11900, 0.0, .0000, .00, .00, 840.00, 1
1.0000, 0.0000
91, 90, 0 , '1 ', 1, 2, 1,.000000, .000000, 2,1
.000000, .004480, 100.00
.94520, 0.0, .0000, .00, .00, .00, 1
1.0000, 0.0000

102, 101, 0 , '1 ', 1, 2, 1,.000000, .000000, 2,1
.000000, .018150, 100.00
.90910, 0.0, .0000, .00, .00, .00, 1
1.0000, 0.0000
101, 90, 0 , '1 ', 1, 2, 1,.000000, .000000, 2,1
.000200, .012500, 100.00
1.11900, 0.0, .0000, .00, .00, 1120.00, 1
1.0000, 0.0000
83, 84, 0 , '1 ', 1, 2, 1,.000000, .000000, 2,1
.000300, .017400, 100.00
1.11900, 0.0, .0000, .00, .00, 840.00, 1
1.0000, 0.0000
83, 84, 0 , '2 ', 1, 2, 1,.000000, .000000, 2,1
.000200, .011900, 100.00
1.11900, 0.0, .0000, .00, .00, 1120.00, 1
1.0000, 0.0000
87, 88, 0 , '1 ', 1, 2, 1,.000000, .000000, 2,1
.000000, .009800, 100.00
1.05000, 0.0, .0000, .00, .00, .00, 1
1.0000, 0.0000
77, 78, 0 , '1 ', 1, 2, 1,.000000, .000000, 2,1
.000000, .011490, 100.00
1.06310, 0.0, .0000, .00, .00, 1120.00, 1
1.0000, 0.0000
77, 78, 0 , '2 ', 1, 2, 1,.000000, .000000, 2,1
.000000, .011490, 100.00
1.06310, 0.0, .0000, .00, .00, 1120.00, 1
1.0000, 0.0000
77, 78, 0 , '3 ', 1, 2, 1,.000000, .000000, 2,1
.000000, .011490, 100.00
1.06310, 0.0, .0000, .00, .00, 1120.00, 1
1.0000, 0.0000
65, 63, 0 , '1 ', 1, 2, 1,.000000, .000000, 2,1
.000000, .015120, 100.00
.99600, 0.0, .0000, .00, .00, .00, 1
1.0000, 0.0000
66, 67, 0 , '1 ', 1, 2, 1,.000000, .000000, 2,1

.000000, .009800, 100.00
1.05000, 0.0, .0000, .00, .00, .00, 1
1.0000, 0.0000
76, 75, 0 , '1 ', 1, 2, 1,.000000, .000000, 2,1
.000000, .003650, 100.00
.97870, 0.0, .0000, .00, .00, .00, 1
1.0000, 0.0000
72, 71, 0 , '1 ', 1, 2, 1,.000000, .000000, 2,1
.000000, .005160, 100.00
.98430, 0.0, .0000, .00, .00, .00, 1
1.0000, 0.0000
71, 73, 0 , '1 ', 1, 2, 1,.000000, .000000, 2,1
.000000, .005000, 100.00
1.00000, 0.0, .0000, .00, .00, .00, 1
1.0000, 0.0000
107, 108, 0 , '1 ', 1, 2, 1,.000000, .000000, 2,1
.000590, .014910, 100.00
1.00170, 0.0, .0000, .00, .00, .00, 1
1.0000, 0.0000
106, 108, 0 , '1 ', 1, 2, 1,.000000, .000000, 2,1
.000590, .014910, 100.00
1.00170, 0.0, .0000, .00, .00, .00, 1
1.0000, 0.0000
109, 108, 0 , '1 ', 1, 2, 1,.000000, .000000, 2,1
.000300, .013300, 100.00
1.00000, 0.0, .0000, .00, .00, .00, 1
1.0000, 0.0000
109, 108, 0 , '2 ', 1, 2, 1,.000000, .000000, 2,1
.000300, .013400, 100.00
1.00000, 0.0, .0000, .00, .00, .00, 1
1.0000, 0.0000
120, 116, 0 , '1 ', 1, 2, 1,.000000, .000000, 2,1
.000130, .013860, 100.00
1.01060, 0.0, .0000, .00, .00, .00, 1
1.0000, 0.0000
120, 116, 0 , '2 ', 1, 2, 1,.000000, .000000, 2,1
.000130, .013860, 100.00

1.01060, 0.0, .0000, .00, .00, .00, 1
1.0000, 0.0000
122, 118, 0 , '1 ', 1, 2, 1,.000000, .000000, 2,1
.000130, .006930, 100.00
1.05000, 0.0, .0000, .00, .00, .00, 1
1.0000, 0.0000
112, 113, 0 , '1 ', 1, 2, 1,.000000, .000000, 2,1
.000580, .025350, 100.00
1.04910, 0.0, .0000, .00, .00, .00, 1
1.0000, 0.0000
123, 118, 0 , '1 ', 1, 2, 1,.000000, .000000, 2,1
.000260, .013860, 100.00
1.05000, 0.0, .0000, .00, .00, .00, 1
1.0000, 0.0000
118, 119, 0 , '1 ', 1, 2, 1,.000000, .000000, 2,1
.004990, .114730, 100.00
1.04780, 0.0, .0000, .00, .00, .00, 1
1.0000, 0.0000
125, 126, 0 , '1 ', 1, 2, 1,.000000, .000000, 2,1
.000500, .023800, 100.00
1.00000, 0.0, .0000, .00, .00, .00, 1
1.0000, 0.0000
103, 82, 0 , '1 ', 1, 2, 1,.000000, .000000, 2,1
.000000, .001150, 100.00
1.01330, 0.0, .0000, .00, .00, .00, 1
1.0000, 0.0000
81, 80, 0 , '1 ', 1, 2, 1,.000000, .000000, 2,1
.000000, .010260, 100.00
.98710, 0.0, .0000, .00, .00, .00, 1
1.0000, 0.0000
45, 46, 0 , '1 ', 1, 2, 1,.000000, .000000, 2,1
.000000, .012380, 100.00
1.00000, 0.0, .0000, .00, .00, .00, 1
1.0000, 0.0000
37, 38, 0 , '1 ', 1, 2, 1,.000000, .000000, 2,1
.000200, .005800, 100.00
.98550, 0.0, .0000, .00, .00, .00, 1

1.0000, 0.0000
40, 41, 0 , '1 ', 1, 2, 1,.000000, .000000, 2,1
.000000, .019500, 100.00
1.00000, 0.0, .0000, .00, .00, .00, 1
1.0000, 0.0000
30, 31, 0 , '1 ', 1, 2, 1,.000000, .000000, 2,1
.000300, .018100, 100.00
1.00000, 0.0, .0000, .00, .00, .00, 1
1.0000, 0.0000
32, 33, 0 , '1 ', 1, 2, 1,.000000, .000000, 2,1
.000500, .014100, 100.00
1.05880, 0.0, .0000, .00, .00, .00, 1
1.0000, 0.0000
29, 28, 0 , '1 ', 1, 2, 1,.000000, .000000, 2,1
.000000, .004600, 100.00
1.00000, 0.0, .0000, .00, .00, 2000.00, 1
1.0000, 0.0000
0 /End of transformer data, begin of area interchange data
1 0 .000 10.000 ' '
0
0
0
0
0
0
0
0
0
1 'ZONE-001'
0
0

B.2 Dynamic Data

1 'GENROU' 1 4.6 0.04 0.37
0.1 2.95 0 1.825 1.78 0.291
0.44 0.25 0.239 1.3933 4.18/

1	'GENROU'	2	4.6	0.04	0.37
0.1	2.95	0	1.825	1.78	0.291
0.44	0.25	0.239	1.3933	4.18/	
1	'GENROU'	3	4.6	0.04	0.37
0.1	2.95	0	1.825	1.78	0.291
0.44	0.25	0.239	1.3933	4.18/	
1	'GENROU'	4	4.6	0.04	0.37
0.1	2.95	0	1.825	1.78	0.291
0.44	0.25	0.239	1.3933	4.18/	
5	'GENROU'	1	8	0.05	0.2
0.08	4.34	0	0.9	0.6	0.25
0.6	0.15	0.09	2.2	11.0/	
8	'GENROU'	1	7.2	0.043	0.2
0.079	3.46	0	0.638	0.424	0.228
0.424	0.161	0.127	1.9675	7.87/	
13	'GENROU'	1	8	0.03	0.2
0.06	3.67	0	0.93	0.651	0.357
0.651	0.248	0.24	1.39	4.17/	
19	'GENROU'	1	4	0.02	0.2
0.05	3	0	0.89	0.5	0.37
0.5	0.287	0.24	1.39	4.17/	
26	'GENROU'	1	4.78	0.041	0.53
0.067	3.38	0	1.236	1.222	0.22
0.348	0.178	0.128	1.9475	7.79/	
28	'GENROU'	1	4.1	0.033	0.56
0.062	2.32	0	2.07	1.99	0.28
0.49	0.215	0.155	1.8429	6.45/	
28	'GENROU'	2	4.1	0.033	0.56
0.062	2.32	0	2.07	1.99	0.28
0.49	0.215	0.155	1.8429	6.45/	
33	'GENROU'	1	5.21	0.042	1.5
0.042	3.01	0	1.798	1.778	0.324
0.45	0.26	0.193	1.48	5.18/	
38	'GENROU'	1	3.9	0.032	0.49
0.062	2.82	0	1.64	1.57	0.24
0.43	0.185	0.13	1.9225	7.69/	

```
44          'GENROU'    1       4.7     0.031   0.67
        0.061       2.88    0       1.99    1.9     0.245
        0.42        0.2     0.15    1.9057      6.67/
46          'GENROU'    1       4       0.032   0.52
        0.063       2.61    0       1.81    1.73    0.245
        0.51        0.19    0.14    1.785       7.14/
47          'GENROU'    1       4.5     0.04    0.5
        0.06        2.45    0       1.7     1.65    0.25
        0.5         0.19    0.14    1.785       7.14/
49          'GENROU'    1       3.8     0.031   0.49
        0.058       2.63    0       1.67    0.61    0.26
        0.453       0.205   0.145   1.9714      6.90/
53          'GENROU'    1       8.4     0.035   0.46
        0.07        3.42    0       1.76    1.58    0.285
        0.485       0.205   0.155   1.8429      6.45/
60          'GENROU'    1       8.2     0.033   0.48
        0.055       3.83    0       1.98    1.85    0.375
        0.567       0.285   0.225   1.48        4.44/
60          'GENROU'    2       8.2     0.033   0.48
        0.055       3.83    0       1.98    1.85    0.375
        0.567       0.285   0.225   1.48        4.44/
60          'GENROU'    3       8.2     0.033   0.48
        0.055       3.83    0       1.98    1.85    0.375
        0.567       0.285   0.225   1.48        4.44/
62          'GENROU'    1       4.2     0.032   0.6
        0.066       3.59    0       1.76    1.68    0.22
        0.4         0.175   0.13    1.9225      7.69/
65          'GENROU'    1       7.8     0.06    0.2
        0.11        6.07    0       0.75    0.53    0.32
        0.53        0.3     0.215   1.55        4.65/
67          'GENROU'    1       8.4     0.035   0.46
        0.07        3.49    0       1.76    1.58    0.285
        0.485       0.205   0.155   1.8429      6.45/
67          'GENROU'    2       8.4     0.035   0.46
        0.07        3.49    0       1.76    1.58    0.285
        0.485       0.205   0.155   1.8429      6.45/
```

```
72          'GENROU'    1       8       0.05    1.5
            0.06        2.75    0       1.95    1.87    0.34
            1           0.29    0.24    1.39        4.17/
76          'GENROU'    1       5.3     0.035   0.5
            0.077       2.82    0       1.62    1.57    0.245
            0.376       0.175   0.095   2.106       10.53/
81          'GENROU'    1       4.3     0.032   0.43
            0.066       3.03    0       1.79    1.715   0.22
            0.44        0.18    0.135   1.8525      7.41/
88          'GENROU'    1       6.12    0.052   1.5
            0.144       3.46    0       2.129   2.074   0.467
            1.27        0.311   0.25    1.3333      4.00/
91          'GENROU'    1       4.5     0.04    0.5
            0.06        3.82    0       1.7     1.65    0.25
            0.5         0.19    0.14    1.785       7.14/
96          'GENROU'    1       4       0.051   0.2
            0.033       4.39    0       1.05    0.67    0.32
            0.67        0.263   0.14    1.785       7.14/
102         'GENROU'    1       7.8     0.06    0.2
            0.11        4.16    0       0.75    0.53    0.32
            0.53        0.3     0.215   1.55        4.65/
113         'GENROU'    1       4.8     0.037   0.5
            0.075       4.13    0       1.7     1.62    0.256
            0.41        0.185   0.155   1.8429      6.45/
119         'GENROU'    1       7.4     0.03    0.2
            0.16        3.8     0       0.619   0.365   0.238
            0.365       0.15    0.14    1.785       7.14/
126         'GENROU'    1       9.8     0.028   0.2
            0.16        6.41    0       0.995   0.568   0.195
            0.568       0.155   0.089   2.24        11.2/
5699        'GENROU'    1       3.9     0.032   0.54
            0.062       2.64    0       1.86    1.78    0.25
            0.453       0.195   0.145   1.9714      6.90/
5699        'GENROU'    2       3.9     0.032   0.54
            0.062       2.64    0       1.86    1.78    0.25
            0.453       0.195   0.145   1.9714      6.90/
```

```
1         'EXST1'   1         0.02      99        -99
          0         0.02      200       0.08      9999      -9999
          0         0.015     1.0/
1         'EXST1'   2         0.02      99        -99
          0         0.02      200       0.08      9999      -9999
          0         0.015     1.0/
1         'EXST1'   3         0.02      99        -99
          0         0.02      200       0.08      9999      -9999
          0         0.015     1.0/
1         'EXST1'   4         0.02      99        -99
          0         0.02      200       0.08      9999      -9999
          0         0.015     1.0/
5         'EXST1'   1         0.02      99        -99
          0         0.02      145       0.02      9999      -9999
          0         0.01      1.5/
19        'EXST1'   1         0.02      99        -99
          0         0.02      200       0.16      9999      -9999
          0         0.026     1.0/
26        'EXST1'   1         0.02      99        -99
          0         0.02      195       0.13      9999      -9999
          0         0.02      1.0/
28        'EXST1'   1         0.02      99        -99
          0         0.02      200       0.36      9999      -9999
          0         0.03      1.0/
28        'EXST1'   2         0.02      99        -99
          0         0.02      200       0.36      9999      -9999
          0         0.03      1.0/
33        'EXST1'   1         0.02      99        -99
          0         0.02      200       0.1       9999      -9999
          0         0.012     1.0/
38        'EXST1'   1         0.02      99        -99
          1         10        250       0.02      9999      -9999
          0         0.01      1.0/
53        'EXST1'   1         0.02      99        -99
          0         0.02      200       0.02      9999      -9999
          0         0.01      1.0/
```

```
62          'EXST1'     1           0.02        99          -99
    1           10          300         0.02        9999        -9999
    0           0.01        1.0/

65          'EXST1'     1           0.02        99          -99
    0           0.02        200         0.02        9999        -9999
    0           0.01        1.20/

67          'EXST1'     1           0.02        99          -99
    0           0.02        200         0.02        9999        -9999
    0           0.01        1.0/

67          'EXST1'     2           0.02        99          -99
    0           0.02        200         0.02        9999        -9999
    0           0.01        1.0/

72          'EXST1'     1           0.02        99          -99
    0           0.02        200         0.19        9999        -9999
    0           0.015       1.00/

81          'EXST1'     1           0.02        99          -99
    0           0.02        250         0.2         9999        -9999
    0           0.035       1.75/

88          'EXST1'     1           0.02        99          -99
    0.02        0.02        400         0.02        9999        -9999
    0           0.01        1.0/

102         'EXST1'     1           0.02        99          -99
    0           0.02        200         0.02        9999        -9999
    0           0.01        1.20/

119         'EXST1'     1           0.02        99          -99
    0           0.02        200         0.16        9999        -9999
    0           0.015       1.0/
```

126		'EXST1'	1	0.02	99	-99
	0	0.02	300	0.16	9999	-9999
	0	0.01	1.0/			
1		'ST2CUT'	1	4	0	0
	0	10	0	0.1	0	1
	1	0.2	0.01	0	0	0
	0	0.05	-0.05	0	0.0/	
1		'ST2CUT'	2	4	0	0
	0	10	0	0.1	0	1
	1	0.2	0.01	0	0	0
	0	0.05	-0.05	0	0.0/	
1		'ST2CUT'	3	4	0	0
	0	10	0	0.1	0	1
	1	0.2	0.01	0	0	0
	0	0.05	-0.05	0	0.0/	
1		'ST2CUT'	4	4	0	0
	0	10	0	0.1	0	1
	1	0.2	0.01	0	0	0
	0	0.05	-0.05	0	0.0/	
5		'ST2CUT'	1	4	0	0
	0	-3.5	0	0	0	1
	1	0	3	0.08	0.027	0.08
	0.027	0.1	-0.1	0	0.0/	
8		'ST2CUT'	1	3	0	0
	0	-0.06	0	0	0	29.5
	29.5	1.5	0.15	1.5	0.15	0
	0	0.09	-0.09	0	0.0/	
8		'ESDC2A'	1	0.02	40	0.1
	0.02	0	3	-3	0	0.57
	0.05	1.2	0	4.5	0.3	3.375
	1.0/					
13		'ST2CUT'	4	1	0	0
	0	-0.04	0	0	0	29.5
	29.5	1.5	0.15	1.5	0.15	0
	0	0.09	-0.09	0	0.0/	

```
13          'ESDC2A'        1       0.02    40      0.06
        0.02        0       3       -3      0       0.13
        0.05        1.3     0       4.5     0.3     3.375
        1.0/
19          'ST2CUT'        1       1       0       0
        0       10      0       0       0       3
        3       0.15    0.05    0.15    0.05    0.15
        0.05    0.05    -0.05   0       0.0/
26          'ST2CUT'        1       1       0       0
        0       3       0       0.03    0       20
        20      6.72    0.672   0       0       0
        0       0.1     -0.1    0       0.0/
28          'ST2CUT'        1       1       0       0
        0       10      0       0       0       3
        3       0.15    0.05    0.15    0.05    0.15
        0.05    0.05    -0.05   0       0.0/
28          'ST2CUT'        2       1       0       0
        0       10      0       0       0       3
        3       0.15    0.05    0.15    0.05    0.15
        0.05    0.05    -0.05   0       0.0/
33          'ST2CUT'        1       1       0       0
        0       1.2     0       0.03    0       30
        30      0.4     0.05    0.4     0.05    0
        0       0.04    -0.04   0       0.0/
38          'ST2CUT'        1       1       0       0
        0       8.08    0       0.03    0       10
        10      0.15    0.05    0.15    0.05    0
        0       0.05    -0.05   0       0.0/
44          'ST2CUT'        1       1       0       0
        0       3       0       0       0       10
        10      0.3     0.03    0.3     0.03    0
        0       0.1     -0.1    0       0.0/
44          'ESST3A'        1       0.02    0.2     -0.2
        7.2     1       4       200     0       99
        -99     1       4.35    0.243   8.4     0.01
        0.005   6.36    20      0.6     99      0.00/
```

```
46          'ST2CUT'        1       2       0       0
        0       5.5     0       0.03    0       10
        10      0.4     0.04    0       0       0
        0       0.05    -0.05   0       0.0/
46          'ESST3A'        1       0.02    0.2     -0.2
        8.2     1       5       200     0       99
        -99     1       3.56    0.335   5.01    0.01
        0.0077  5.6     3.75    0.4     99      0.00/
47          'ST2CUT'        1       2       0       0
        0       0       0       0.025   0       0.016
        0.016   0.26    0.026   0.26    0.026   0
        0       0.1     -0.1    0       0.0/
47          'ESDC2A'        1       0.02    200     0.05
        0.02    0       3       -3      0       0.512
        0.07    1.3     0       5.31    0.5     3.9825
        1.049/
49          'ST2CUT'        1       2       0       0
        0       0       0       0       0       30
        30      0.23    0.025   0.23    0.025   0
        0       0.06    -0.06   0       0.0/
49          'ESDC2A'        1       0.02    50      0.02
        0.02    0       3       -3      0       0.642
        0.103   0.994   0       3.46    0.356   2.595
        1.0/
53          'ST2CUT'        1       1       0       0
        0       10      0       0       0       3
        3       0.15    0.05    0.15    0.05    0.15
        0.05    0.05    -0.05   0       0.0/
60          'ST2CUT'        1       1       0       0
        0       10      0       0       0       3
        3       0.15    0.05    0.15    0.05    0.15
        0.05    0.05    -0.05   0       0.0/
60          'ST2CUT'        2       1       0       0
        0       10      0       0       0       3
        3       0.15    0.05    0.15    0.05    0.15
        0.05    0.05    -0.05   0       0.0/
```

```
60          'ST2CUT'        3       1       0       0
    0           10          0       0       0       3
    3           0.15        0.05    0.15    0.05    0.15
    0.05        0.05        -0.05   0       0.0/
60          'ESST3A'        1       0.02    0.2     -0.2
    6.8         1           5       200     0       99
    -99         1           3.77    0.124   4.52    0.01
    0.005       6.77        0       0.4     99      0.00/
60          'ESST3A'        2       0.02    0.2     -0.2
    6.8         1           5       200     0       99
    -99         1           3.77    0.124   4.52    0.01
    0.005       6.77        0       0.4     99      0.00/
60          'ESST3A'        3       0.02    0.2     -0.2
    6.8         1           5       200     0       99
    -99         1           3.77    0.124   4.52    0.01
    0.005       6.77        0       0.4     99      0.00/
62          'ST2CUT'        1       1       0       0
    0           10          0       0       0       3
    3           0.15        0.05    0.15    0.05    0.15
    0.05        0.05        -0.05   0       0.0/
65          'ST2CUT'        1       1       0       0
    0           10          0       0       0       3
    3           0.15        0.05    0.15    0.05    0.15
    0.05        0.05        -0.05   0       0.0/
67          'ST2CUT'        1       2       0       0
    0           5           0       0.029   0       2.4
    2.4         0.144       0.04    0.377   0.105   0
    0           0.05        -0.05   0       0.0/
67          'ST2CUT'        2       2       0       0
    0           5           0       0.029   0       2.4
    2.4         0.144       0.04    0.377   0.105   0
    0           0.05        -0.05   0       0.0/
72          'ST2CUT'        1       2       0       0
    0           0.5         0       0.042   0       10
    10          1           0.08    1.7     0.08    0
    0           0.05        -0.05   0       0.0/
```

76 'ST2CUT' 1 3 0 0
0 0 0 0 0 29.5
29.5 1.5 0.15 1.5 0.15 0
0 0.09 -0.09 0 0.0/
76 'ESDC2A' 1 0.02 40 0.05
0.02 0 3 -3 0 0.6
0.07 1.3 0 3.76 0.32 2.82
1.0/
81 'ST2CUT' 1 1 0 0
0 10 0 0 0 3
3 0.15 0.05 0.15 0.05 0.15
0.05 0.05 -0.05 0 0.0/
88 'ST2CUT' 1 1 0 0
0 10 0 0 0 3
3 0.15 0.05 0.15 0.05 0.15
0.05 0.05 -0.05 0 0.0/
91 'ST2CUT' 1 4 0 0
0 0 0 0 0 29.5
29.5 1.5 0.15 1.5 0.15 0
0 0.09 -0.09 0 0.0/
91 'ESDC2A' 1 0.02 200 0.05
0.02 0 3 -3 0 0.512
0.07 1.3 0 5.31 0.5 3.9825
1.049/
96 'ST2CUT' 1 3 0 0
0 0 0 0 0 29.5
29.5 1.5 0.15 1.5 0.15 0
0 0.09 -0.09 0 0.0/
96 'ESDC2A' 1 0.02 183 0.06
0.02 0 2 -2 0 0.5
0.05 1 0 3.5 0.54 2.625
1.0/
102 'ST2CUT' 1 1 0 0
0 10 0 0 0 3
3 0.15 0.05 0.15 0.05 0.15
0.05 0.05 -0.05 0 0.0/

113 'ST2CUT' 1 3 0 0
0 0 0 0.03 0 1.5
1.5 0.375 12 0 0 0
0 0.05 -0.05 0 0.0/
113 'ESDC2A' 1 0.02 40 0.2
0.02 0 2 -2 0 0.545
0.09 1 0 4.13 0.41 3.0975
1.0/
119 'ST2CUT' 1 1 0 0
0 10 0 0 0 3
3 0.15 0.05 0.15 0.05 0.15
0.05 0.05 -0.05 0 0.0/
126 'ST2CUT' 1 2 0 0
0 0 0 0 0 15
15 0 0.053 0 0.053 0
0 0.05 -0.05 0 0.0/
5699 'ST2CUT' 1 1 0 0
0 5 0 0 0 10
10 0.3 0.03 0.3 0.03 0
0 0.1 -0.1 0 0.0/
5699 'ST2CUT' 2 1 0 0
0 5 0 0 0 10
10 0.3 0.03 0.3 0.03 0
0 0.1 -0.1 0 0.0/
5699 'ESST3A' 1 0.02 0.2 -0.2
8 1 5 200 0 99
-99 1 3.67 0.435 4.48 0.01
0.0098 2.86 3.33 0.4 99 0.00/
5699 'ESST3A' 2 0.02 0.2 -0.2
8 1 5 200 0 99
-99 1 3.67 0.435 4.48 0.01
0.0098 2.86 3.33 0.4 99 0.00/

Vita

Dawei Fan received his B.S. and M.S. degrees in power system and its automation both from Wuhan University, China, in 1999 and 2002, respectively. He joined Virginia Tech in 2004 to pursue a PhD degree in the Bradley Department of Electrical and Computer Engineering. His research interests focus on wide area measurements and their applications in power systems.